UAB
Universitat Autònoma de Barcelona

Deciphering the role of LEF1 in the pathogenesis of chronic lymphocytic leukemia

Judith Mateos Jaimez

ADVERTIMENT. L'accés als continguts d'aquesta tesi queda condicionat a l'acceptació de les condicions d'ús establertes per la següent llicència Creative Commons:  https://creativecommons.org/licenses/?lang=ca

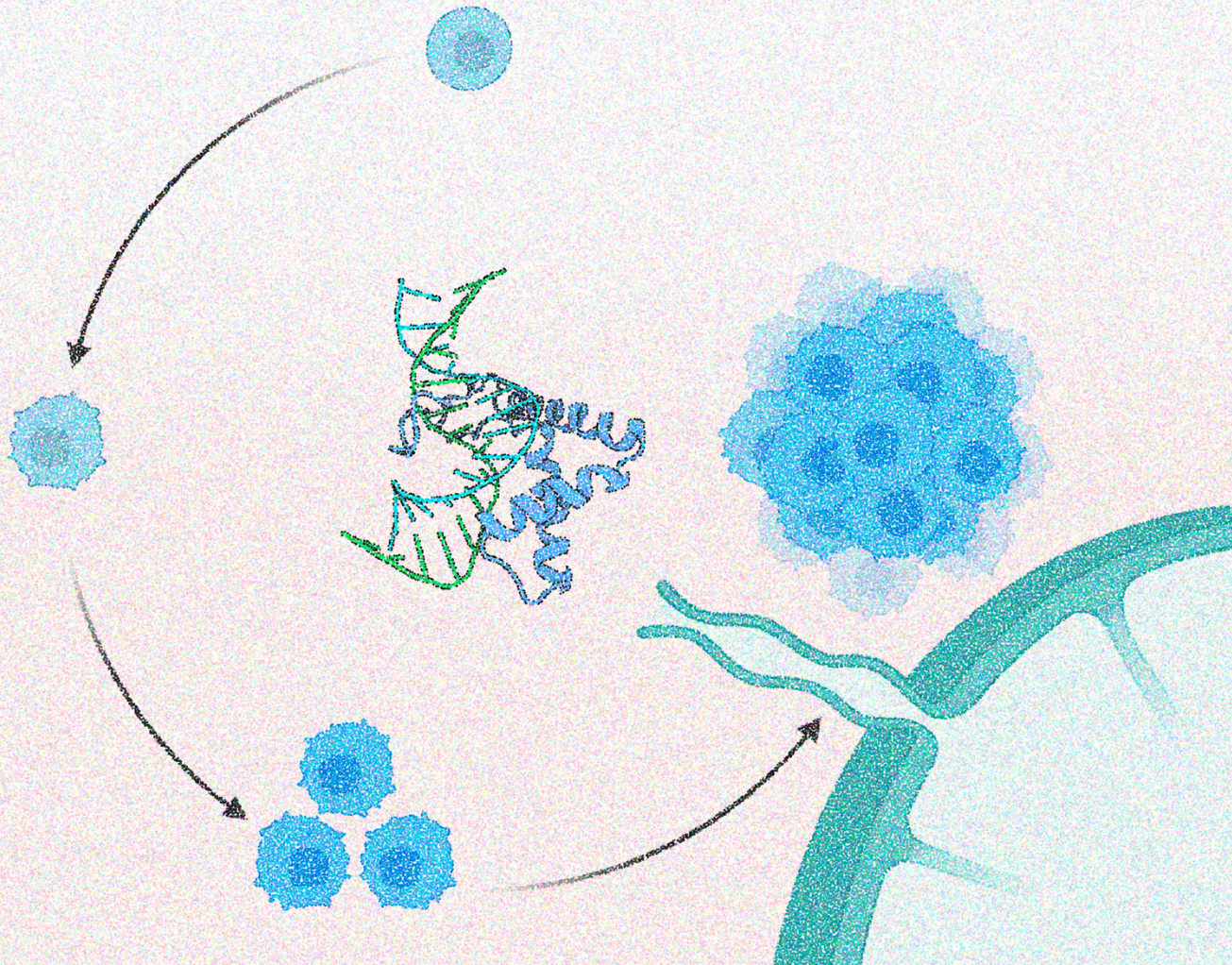
ADVERTENCIA. El acceso a los contenidos de esta tesis queda condicionado a la aceptación de las condiciones de uso establecidas por la siguiente licencia Creative Commons:  https://creativecommons.org/licenses/?lang=es

WARNING. The access to the contents of this doctoral thesis it is limited to the acceptance of the use conditions set by the following Creative Commons license:  https://creativecommons.org/licenses/?lang=en

Doctoral thesis

Deciphering the role of LEF1 in the pathogenesis of chronic lymphocytic leukemia

Judith Mateos Jaimez



Doctoral program in Biochemistry, Molecular Biology and Biomedicine
Universitat Autònoma de Barcelona (UAB)

Deciphering the role of LEF1 in the pathogenesis of chronic lymphocytic leukemia

Doctoral thesis presented by:

Judith Mateos Jaimez

Biomedical Epigenomics
Institut d'Investigacions Biomèdiques August Pi i Sunyer (IDIBAPS)

Judith Mateos Jaimez
PhD candidate

José Ignacio Martín Subero
Thesis supervisor

Alba Maiques Diaz
Thesis supervisor

Ibane Abasolo Olaortua
Thesis tutor

Barcelona, 2024

This doctoral thesis was supported by a pre-doctoral fellowship from “La Caixa” Foundation (LCF/BQ/DR20/11790011). The work presented here was funded by Fundació La Marató de TV3 (201924-30) and was developed at the Centre Esther Koplowitz (CEK) of Barcelona.

A mis padres, hermana y Ferran
Mi sol, luna y estrella

Caminante, no hay camino,
se hace camino al andar.
Antonio Machado

Cuando creíamos que teníamos todas las respuestas,
de pronto, cambiaron todas las preguntas.
Mario Benedetti

Abstract

Chronic lymphocytic leukemia (CLL) is an incurable disease caused by the expansion of CD5+ mature B cells in peripheral blood (PB), lymph nodes (LN) and bone marrow. CLL is the most frequent adult leukemia in Western countries and is a genetically and clinically very heterogeneous. Despite intensive research, the molecular mechanisms leading to CLL development and evolution remain incomplete. Moreover, although the genome, transcriptome and epigenome of CLL have been described, the role of transcription factors in CLL pathogenesis remains poorly understood. In this context, LEF1 is a CLL-specific transcription factor *de novo* expressed in all phases of the disease, from premalignant conditions to aggressive variants, and its binding motif is present in regulatory elements becoming active in CLL. Remarkably, LEF1 is expressed in almost all patient-derived CLL cells, while it is lost in CLL cell lines or mouse models. Therefore, the global aim of this doctoral thesis was to develop methods that would allow to perform *in vitro* functional studies using primary CLL cells, and apply these methodologies to elucidate the oncogenic role of LEF1 in CLL pathogenesis.

In **Study 1**, I characterized the effects of a new *in vitro* system, based on MM1 murine stromal cells expressing human CD40L and secreting human BAFF and IL-21, in patient-derived CLL cells. Remarkably, CLL cells stimulated with the MM1 cell culture system, acquired an activated and proliferative phenotype and transcriptome, reminiscent of LN-derived CLL cells. Furthermore, it maintained primary CLL cells with good viability for longer time in culture. This enabled the development of molecular biology techniques, such as a robust electroporation-based CRISPR-Cas9 gene editing method, which was optimized to induce gene knockdowns not only in patient-derived CLL cells but also in cells from mantle cell lymphoma, a related disease.

Then, in **Study 2**, I applied all these new functional approaches to decipher the mechanism of action of LEF1 in CLL initiation and development. Through comprehensive functional analyses in patient-derived CLL samples, I uncovered that LEF1 can induce transcriptional changes promoting both quiescence and proliferation in CLL, distinct roles modulated by disease context. LEF1 function is controlled by a two-fold mechanism: protein abundance and alternative splicing. Low protein levels contribute to the steady-state phase of the disease by targeting genes involved in cell survival, adhesion/migration and lymphocyte activation. As LEF1 protein increases, it adds a proliferative push to CLL cells since it targets, in addition, genes involved in cell cycle progression and proliferation. Interestingly, I found that higher LEF1 protein levels are present specifically in U-CLL samples, the most aggressive subtype of the disease, driven by a higher LEF1 protein stability. In parallel, in response to the proliferative signals coming from the tumor microenvironment in the LN, CLL cells switch isoform expression and promote the exclusion of exon 6. I identified that LEF1 exon 6 inclusion is favored in PB cells and drives a quiescence transcriptional profile, while exon 6 skipping predominates in actively proliferating cells and induces cell cycle progression.

In summary, this doctoral thesis provides significant insights into the role of LEF1 in the pathogenesis of CLL. As LEF1 mediates both cell survival and proliferation in CLL, it may represent an attractive therapeutic target suitable for the entire clinical spectrum of CLL, including both indolent and progressive forms of the disease.

Resumen

La leucemia linfocítica crónica (LLC) es una enfermedad incurable causada por la expansión de células B maduras CD5+ en sangre periférica (SP), ganglios linfáticos (GL) y medula ósea. La LLC es la leucemia de adultos más frecuente en los países occidentales y es genéticamente y clínicamente muy heterogénea. A pesar de una intensiva investigación, los mecanismos moleculares causantes del desarrollo y evolución de la LLC no están claramente identificados. Además, el rol de los factores de transcripción en la patogénesis de la LLC está muy poco entendido. En este contexto, LEF1 es un factor de transcripción expresado *de novo* en todas las fases de la enfermedad, desde condiciones premalignas a variantes más agresivas, y su motivo de unión está presente en elementos reguladores que se activan en la LLC. LEF1 se expresa en las células de pacientes, mientras que se pierde en líneas celulares o modelos murinos de LLC. Por ello, el objetivo principal de esta tesis doctoral era desarrollar modelos que permitieran realizar estudios funcionales *in vitro* con células primarias de LLC, y aplicar esta metodología para elucidar el rol oncogénico de LEF1 en la patogénesis de la LLC.

En el **Estudio 1**, caracterícé los efectos de un nuevo sistema de cultivo *in vitro*, basado en células estromales de origen murino, que expresan CD40L humano y secretan BAFF y IL-21 humanos, en células de LLC de pacientes. Con este sistema, las células de LLC adquirieron un fenotipo y transcriptoma de activación y proliferación, similares a las células de LLC obtenidas de GL. Además, este sistema mantuvo las células primarias de LLC con buena viabilidad durante más tiempo en cultivo. Esto permitió el desarrollo de técnicas de biología molecular, como el método de edición génica CRISPR-Cas9 por electroporación, que fue optimizado para reducir la expresión de genes diana en células derivadas de paciente de LLC y también de linfoma de células del manto, una enfermedad parecida a la LLC.

En el **Estudio 2**, apliqué todos estos avances funcionales para descifrar el rol de LEF1 en el inicio y desarrollo de la LLC. A través de análisis funcionales integrales en muestras de LLC de pacientes, descubrí que LEF1 puede inducir quiescencia y proliferación en LLC, según el contexto de la enfermedad. La función de LEF1 se controla por un mecanismo dual: abundancia de proteína y *splicing* alternativo. Bajos niveles de proteína contribuyen a una fase estable de la enfermedad, regulando la expresión de genes relacionados con supervivencia celular, adhesión/migración y activación de linfocitos. Cuando la proteína de LEF1 aumenta, añade un empuje proliferativo a las células de LLC ya que regula, además, la expresión de genes involucrados en la progresión del ciclo celular y proliferación. Interesantemente, encontré que los niveles de proteína LEF1 son más elevados en las muestras de U-CLL, el subtipo más agresivo de la enfermedad, por un mecanismo de mayor estabilidad de la proteína. En paralelo, en respuesta a estímulos proliferativos del microambiente tumoral en el GL, las células de LLC cambian la expresión de las isoformas de LEF1, promoviendo la exclusión del exón 6. Identifiqué que la inclusión del exón 6 ocurre, principalmente, en las células de SP y promueve un perfil transcripcional quiescente, mientras que la exclusión del exón 6 en las isoformas de LEF1 predomina en células que están activamente proliferando e induce progresión del ciclo celular.

En definitiva, esta tesis doctoral aporta detalles importantes sobre el rol de LEF1 en la patogénesis de la LLC. Puesto que LEF1 regula la supervivencia y proliferación de las células de LLC, podría representar una diana terapéutica atractiva para todo el espectro de LLC.

Resum

La leucèmia limfocítica crònica (LLC) és una malaltia incurable causada per l'expansió de cèl·lules B madures CD5+ en sang perifèrica (SP), ganglis limfàtics (GL) i medul·la òssia. És la leucèmia d'adults més freqüent als països occidentals i és genèticament i clínicament molt heterogènia. Malgrat la intensiva investigació realitzada, els mecanismes moleculars causants del desenvolupament i evolució de la LLC no estan clarament identificats. És més, el rol dels factors de transcripció en la patogènesi de la LLC roman molt poc entès. En aquest context, LEF1 és un factor de transcripció expressat *de novo* en totes les fases de la malaltia, des de condiciones premalignes a variants més agressives, i el seu motiu d'unió és present als elements reguladors que s'activen en la LLC. LEF1 s'expressa en les cèl·lules de pacient, però es perd en línies cel·lulars o models de ratolí de LLC. Per això, l'objectiu principal d'aquesta tesi doctoral era desenvolupar models que permetin realitzar estudis funcionals *in vitro* amb cèl·lules primàries de LLC, i aplicar aquesta metodologia per elucidar el rol oncogènic de LEF1 en la patogènesi de la LLC.

A l'**Estudi 1**, vaig caracteritzar els efectes d'un nou sistema de cultiu *in vitro*, basat en cèl·lules estromals d'origen murí que expressen CD40L humà i secreten BAFF i IL-21 humans, en cèl·lules de LLC de pacients. Amb aquest sistema, les cèl·lules de LLC van adquirir un fenotip i transcriptoma d'activació i proliferació, semblant al de les cèl·lules de LLC obtingudes del GL. A més a més, aquest sistema va mantenir les cèl·lules primàries de LLC amb bona viabilitat durant més temps en cultiu. Això va permetre el desenvolupament de tècniques de biologia molecular, com el mètode d'edició gènica CRISPR-Cas9 per electroporació, per reduir l'expressió de gens diana en cèl·lules de pacients de LLC i també del limfoma de cèl·lules del mantell, una malaltia semblant a la LLC.

A l'**Estudi 2**, vaig aplicar aquests avenços per desxifrar el rol de LEF1 a l'inici i evolució de la LLC. A partir d'anàlisis funcionals integrals en mostres de LLC de

pacients, vaig descobrir que LEF1 pot induir quiescència i proliferació a les cèl·lules de LLC, segons el context de la malaltia. La funció de LEF1 es controla per un mecanisme dual: abundància de la proteïna i *splicing* alternatiu. Nivells baixos de la proteïna contribueixen a una fase estable de la malaltia, regulant l'expressió de gens relacionats amb supervivència cel·lular, adhesió/migració i activació dels limfòcits. Quan la proteïna de LEF1 augmenta, afegeix un impuls proliferatiu a les cèl·lules de LLC ja que regula, addicionalment, l'expressió de gens involucrats en la progressió del cicle cel·lular i proliferació. Interessantment, vaig trobar que els nivells de proteïna de LEF1 són més elevats en les mostres de U-CLL, el subtipus més agressiu de la malaltia, per un mecanisme de més estabilitat de la proteïna. En paral·lel, en resposta a estímuls proliferatius del microambient tumoral en el GL, les cèl·lules de LLC canvien l'expressió de les isoformes de LEF1, promovent l'exclusió de l'exó 6. Vaig identificar que la inclusió de l'exó 6 té lloc a SP i promou un perfil transcripcional quiescent, mentre que l'exclusió de l'exó 6 en les isoformes de LEF1 predomina en les cèl·lules que estan activament proliferant i indueix la progressió del cicle cel·lular.

En definitiva, aquesta tesi doctoral aporta detalls importants sobre el rol de LEF1 en la patogènesi de LLC. Donat que LEF1 regula la supervivencia i proliferación de les cèl·lules de LLC, podria representar una diana terapèutica atraciva per tot l'espectre de LLC.

Table of contents

List of abbreviations **5**

Introduction **11**

1. Chronic lymphocytic leukemia 13
   1.1. Epidemiological and clinical features 13
   1.2. Immunoglobulin genes and the germinal center reaction 15
   1.3. Cell of origin and CLL subtypes 18
      1.3.1. Immunogenetic subtypes 19
      1.3.2. Epigenetic subtypes 21
      1.3.3. Transcriptomics 24
   1.4. Pathophysiology of CLL 24
      1.4.1. Tumor microenvironment 25
      1.4.2. BCR signaling 28
      1.4.3. Genomic abnormalities 32
      1.4.4. Epigenomic abnormalities 34
         1.4.4.1. Introduction to the epigenetic layers 34
         1.4.4.2. Regulatory chromatin landscape 38
         1.4.4.3. TF networks drive the altered CLL epigenome 40
2. Lymphoid-Enhancer Factor 1 (LEF1) 42
   2.1. WNT signaling 42
      2.1.1. Canonical WNT signaling 43
      2.1.2. Non-canonical WNT signaling 43
   2.2. The TCF/LEF family 44
   2.3. Role of LEF1 in normal hematopoiesis 47
   2.4. Role of LEF1 in cancer 48
   2.5. Role of LEF1 in CLL 49
3. *In vitro* an *in vivo* modeling of CLL to study disease pathogenesis 53
   3.1. CLL cell lines 54
   3.2. Mouse models 55
      3.2.1. Genetically engineered mouse models 55
      3.2.2. Xenograft mouse models 57
   3.3. Primary CLL cells 58
      3.1.1. *In vitro* culture with MM1 stromal cells 60

Aims **63**

Material and methods **67**

1. Cell culture 69
2. Flow cytometry 71
3. CUT&RUN 73
4. CUT&Tag 75
5. DNA extraction 76
6. CRISPR interference 76
8. TIDE analysis of gene editing 79
9. RNA extraction 80
10. Expression analysis/RT-qPCR 80
11. Plasmids 81
12. Lentiviral infection 82
13. Microarrays data 83
14. RNA-sequencing and data analysis 84
15. Inhibition of protein synthesis and proteasome degradation 85
16. Protein extraction and western blot 85
17. Total and nuclear immunoprecipitation 86
18. Mass spectrometry (mass-spec) 87
19. Statistical analyses 92

Results **93**

Study 1: Characterization of a new in vitro culture system to develop CRISPR-based gene inactivating methods for primary CLL cells *95*

Part 1: Characterization of the phenotypic and transcriptional effects of MM1 on primary CLL cells 97

1. Introduction 97
2. Results 98
   2.1. CLL immunophenotypic changes induced by with the *in vitro* system 98
   2.2. CLL transcriptional changes with the *in vitro* system 101
3. Conclusions 103

Part 2: Development of CRISPR-Cas9-based gene inactivation strategies for primary CLL cells 104

1. Introduction 104

2. Results....106
2.1. Selection of dCas9-repressor plasmid in CLL and MCL cell lines....106
2.3. Test of CRISPRi technology in cell lines....110
2.4. Test of CRISPRi in primary CLL cells....112
2.5. Optimization of classic CRISPR-Cas9 in CLL....113
3. Conclusions....124

Study 2: Defining the role of LEF1 in CLL origin and pathogenesis....125
1. Introduction....127
2. Results....127
2.1. LEF1 mRNA and protein levels in CLL....128
2.2. LEF1 stability in CLL cells....131
2.3. Genome-wide distribution of LEF1 binding sites in CLL....136
2.4. Proliferation of CLL cells modulate the protein levels of LEF1....143
2.6. The LEF1 interactome of CLL cells....147
2.7. *LEF1* exon 6 skipping in proliferative CLL cells....153
2.8. Effects of overexpressing different LEF1 isoforms in CLL cell lines....156
3. Conclusions....161

Discussion....163

1. *In vitro* modeling of CLL to study disease pathogenesis....165
2. The role of LEF1 protein abundance in CLL....170
3. The role of alternative isoforms of LEF1 in CLL proliferation....177
4. Dual role of LEF1 in CLL....179

General conclusions....183

References....187

Appendix....209

Acknowledgments....215

List of abbreviations

A

AML: Acute myeloid leukemia

APC: Adenomatous polyposis coli

ATAC-seq: Assay for Transposase-Accessible Chromatin using Sequencing

B

B-ALL: B-cell acute lymphoblastic leukemia

BCL2: B-cell leukemia/lymphoma 2

BCR: B-cell receptor

BM: Bone marrow

BMSC: Bone marrow-derived stromal cell

BTKi: Bruton tyrosine kinase inhibitor

C

CDC5L gene: Cell division cycle 5-like gene

ChIP-seq: Chromatin immunoprecipitation followed by next-generation sequencing

CHX: Cycloheximide

CLL: Chronic lymphocytic leukemia

cMCL: Conventional mantle cell lymphoma

CRC: Colorectal cancer

CRD: Context dependent regulatory domain

CRISPR: Clustered regularly interspace short palindromic repeats

CRISPRi: CRISPR interference

crRNA: CRISPR RNA

CSR: Class-switch recombination

D

dCas9: dead/deactivated Cas9

DE: Differentially expressed (genes)

Del: Deletion

dnLEF1: Dominant negative LEF1 isoform

DUB: Deubiquitinase

E

EBV: Epstein-Barr virus

F

FCR: Fludarabine, cyclophosphamide and rituximab

FISH: Fluorescent *in situ* hybridization

G

GC: Germinal center

GCBC: Germinal center B cell

GEP: Gene expression profiling

gRNA: Guide RNA

Gro/TLE: Groucho/transducin-like enhancer of split

GSEA: Gene set enrichment analysis

GSK-3β: Glycogen synthase kinase-3 β

H

HDR: Homology-directed repair

HMG: High-mobility group

HSC: Hematopoietic stem cells

I

i-CLL: intermediate CLL

Ig: Immunoglobulin

IGH: immunoglobulin heavy-chain

IGHV: immunoglobulin heavy-chain variable region

IGK/L: immunoglobulin light-chain

IHQ: Immunohistochemistry

IL: Interleukin

Indel: Insertion/deletion

K

KD: Knockdown

KO: Knockout

KRAB: Krüppel-associated box

L

LEF1: Lymphoid Enhancer Factor 1

LEF1-Δexon 6 isoforms: LEF1 isoforms lacking exon 6

LEF1-FL: LEF1 full-length

LEF1-I5: LEF1 isoform 5

LEF1-I6: LEF1 isoform 6

LN: Lymph node

Log2FC: Log2-transformed fold change

M

m-CLL: Memory B cell-like CLL

M-CLL: Mutated CLL

MBC: Memory B cell

MBL: Monoclonal B-cell lymphocytosis

MCL: Mantle cell lymphoma

MDSC: Myeloid-derived suppressor cells

ΔMFI: Difference in Median Fluorescence Intensity

MFIR: Median Fluorescence Intensity Ratio

N

n-CLL: Naive B cell-like CLL

NBC: Naive B cell

NES: Normalized Enrichment Score

NGS: Next-generation sequencing

NHEJ: Non-homologous end joining

NLC: Nurse-like cell

NLS: Nuclear localization signal

nnMCL: Non-nodal MCL

NTC: Non-targeting control

P

PB: Peripheral blood

PBMC: Peripheral blood mononuclear cell

PC: Plasma cell

PCA: Principal component analysis

PCP: Planar cell polarity

PDX: Patient-derived xenograft

PLC: Phospholipase-C

Pol II: RNA polymerase II

PTM: Post-translational modification

R

RNA-seq: RNA sequencing

RT: Room temperature

S

SFFV: Spleen focus-forming virus

sgRNA: Single-guided RNA

SHM: Somatic hypermutation

sIg: Surface immunoglobulin

sIgM: Surface IgM

T

TCL1: T-cell leukemia/lymphoma 1

TCRα: T-cell receptor α-chain

$T_{cytotoxic}$: Cytotoxic T cells

TF: Transcription factor

TGF-β: Transforming growth factor β

T_{helper}: Helper T cells

TLR: Toll-like receptor

TME: Tumor microenvironment

tracRNA: Tracer RNA

T_{reg}: Regulatory T cells

TSS: Transcription start site

TTFT: Time-to-first-treatment

U

U-CLL: Unmutated CLL

UCOE: Ubiquitous chromatin opening element

USP10: Ubiquitin-specific peptidase 10

W

WNT: Wingless-related integration site

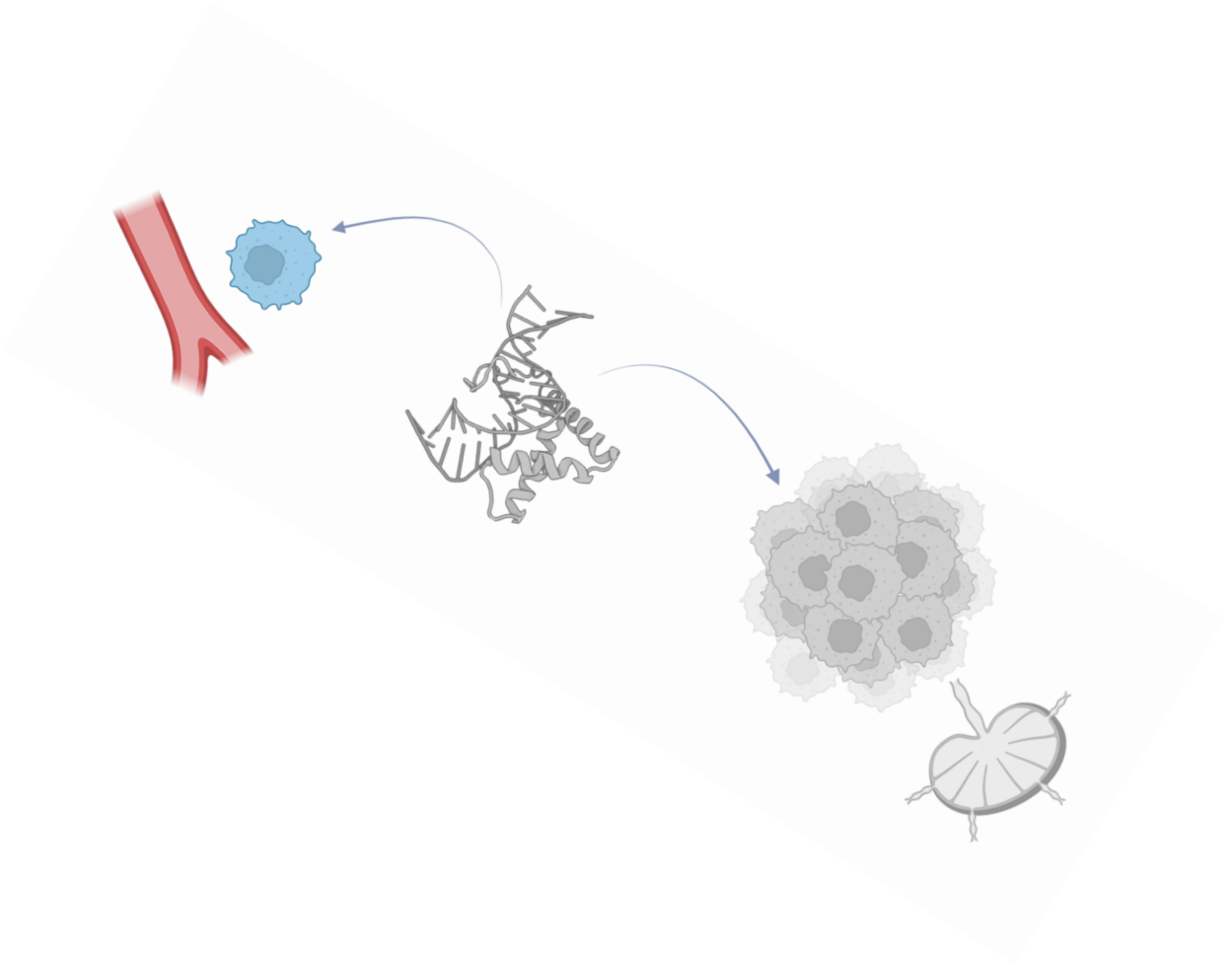
WRE: WNT response element

WT: Wildtype

Z

ZNF: Zinc finger protein

Introduction



1. Chronic lymphocytic leukemia

1.1. Epidemiological and clinical features

Chronic lymphocytic leukemia (CLL) is a neoplasm of mature small B-lymphocytes involving peripheral blood, bone marrow and secondary lymphoid tissues (lymph nodes and spleen) (1). CLL represents the most frequent adult leukemia in western countries, with an annual incidence rate of 4.6 cases per 100,000 population (statistics from the US National Cancer Institute Surveillance, Epidemiology, and End Results Program, NIH SEER, 2016-2020). In fact, CLL accounts for a 1% of all new cancers diagnosed in the United States each year. Remarkably, the incidence of CLL is incredibly low in eastern Asian countries such as Japan (2). The risk of developing CLL is two-times higher for men than for women (6.8 per 100,000 men and 3.5 per 100,000 women), and increases with age (median age at diagnosis ranges from 70 to 72 years) (NIH SEER).

Diagnosis of CLL requires a monoclonal B-cell count higher than $5x10^9$/L, with the morphology and immunophenotype of CLL in peripheral blood (PB). Flow cytometry demonstration of the typical CLL immunophenotype is crucial for diagnosis as it distinguishes CLL from other lymphoproliferative disorders (3,4). It is based on the expression, in malignant B cells, of CD5, CD19, $CD20^{dim}$, $CD22^{dim}$, CD23, $CD43^{bright}$, $CD45^{dim}$, dim to negative CD79b, $CD81^{dim}$, CD200, and dim monoclonal surface immunoglobulin (sIg^{dim})(4,5). All cases of CLL are preceded by monoclonal B-cell lymphocytosis (MBL), a premalignant condition defined as < $5x10^9$/L clonal B-cells in the absence of other signs of a lymphoproliferative disorder (6). The majority of cases of MBL have the immunophenotype of CLL. MBL can be categorized as either low or high count based on whether the B-cell count is below or above $0.5x10^9$/L, respectively (**Figure 1**). Low-count MBL can be detected in 5 % of adults over 40 years old but very rarely progresses to CLL, yet it persists over time. In contrast, high-count MBL progresses to CLL requiring therapy at a rate

of 1 to 2% per year. Several typical CLL driver gene mutations have been reported in high-count MBL even years before the transition to CLL. Such mutations have been detected in CD34+ cells from patients with CLL, suggesting that these aberrations may be implicated in CLL onset (7).

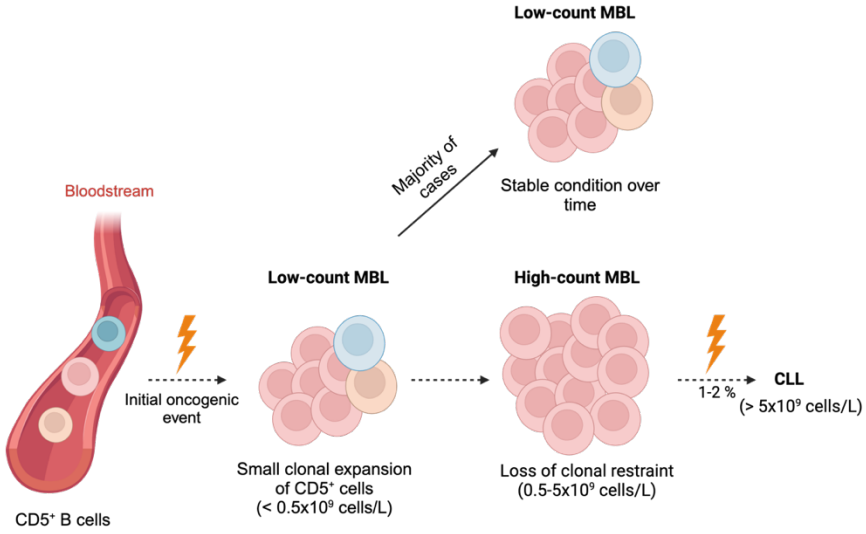


Figure 1. Model for progression from MBL to CLL. Evolution from low-count MBL to high-count MBL-and subsequently CLL-occurs in a stepwise fashion with gradual acquisition of high-risk genetic abnormalities. In high-count MBL and CLL, there is a loss of oligoclonality, alluding to different antigenic pressures shaping the clonal repertoire and the role of microenvironment in disease progression. The majority of low-count MBL remain stable over time and do not progress to high-count MBL. Created with Biorender.com.

CLL is an extremely heterogeneous disease that shows a wide spectrum of biological and clinical manifestations (8). About one-third of patients will never require treatment. In another one-third of patients, there is an indolent phase followed by progression, and in the final one-third, the condition is aggressive since the diagnosis, with these patients requiring immediate treatment and having frequent relapses. In a 5–10% of cases, the disease evolves into an aggressive diffuse large B cell lymphoma with dismal outcome, known as Richter syndrome (9).

Patients with CLL are only treated when becoming symptomatic, based on earlier studies that showed no survival advantage to early intervention (10,11). Thus, in the early stage asymptomatic CLL patients, irrespective of disease risk category, the standard of care is clinical observation ("wait and watch" approach). Once the disease progresses, the first-line treatment varies depending on the age and physical condition of the patient as well as the presence of high-risk features (12), such as *TP53* abnormality and IGHV mutation. Young fit patients (<65 or no co-morbidities) are typically treated with chemotherapy (fludarabine and cyclosphophamide) combined with anti-CD20 monoclonal antibody (rituximab, obinutuzumab), known as the FCR regimen (13,14) or with a covalent Bruton tyrosine kinase (BTK) inhibitor (ibrutinib, acalabrutinib). Older or unfit patients (>65 years) can be treated with ibrutinib, lower-intensity chemotherapy combined with anti-CD20 monoclonal antibody (bendamustine with rituximab) or an anti-CD20 regime in combination with B-cell leukemia/lymphoma 2 (BCL2) inhibitor (venetoclax) (15). When high-risk features are present, older unfit patients do not receive chemotherapy, only novel targeted agents.

Novel agents targeting CD20, B cell receptor signaling pathway (BTK) and BCL2 have improved outcomes and prolonged survival especially in patients with high-risk features that do not respond well to chemotherapy, and in elderly frail patients, which typically are not fit enough to receive chemotherapy (14). Despite all the progress made in the clinical management and treatment of the disease, CLL is still considered incurable and, thus, further biological research is needed to fully understand its variable course and heterogeneous behavior.

1.2. Immunoglobulin genes and the germinal center reaction

B cells and T cells are key players of the adaptive immune system in mammals. B cells are responsible for the humoral response, as they secrete antigen-specific antibodies that allow the removal of a certain pathogen by T cells and

macrophages. These antibodies are essentially a secreted form of a B-cell receptor (BCR). In fact, B cells can be identified by the presence of a unique BCR in their surface, which defines the antigen specificity of the cell. In humans, B cells originate and develop in the bone marrow (BM) and undergo selection and maturation in secondary lymphoid organs. Processes such as B-cell maturation, survival and fate decision are tightly regulated by the BCR expressed in B cells (16).

The BCR is composed of a membrane-bound immunoglobulin (Ig) for antigen recognition and the heterodimer Igα (CD79a)/Igβ (CD79b) that functions as the intracellular signaling entity (17). Igs are heterodimeric proteins composed of two heavy and two light chains (**Figure 2**). They can be separated functionally into variable domains that bind antigens and constant domains that specify effector functions such as activation of complement or binding to Fc receptors.

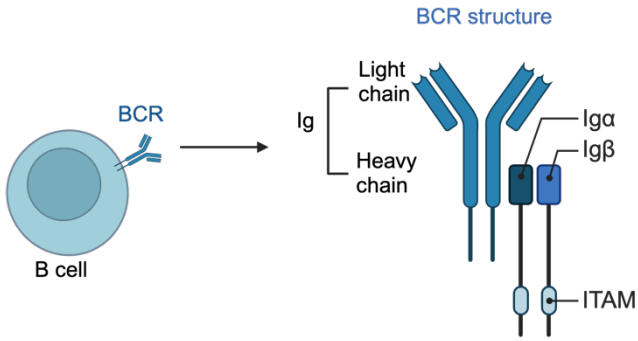


Figure 2. BCR structure. BCR is composed of a membrane bound immunoglobulin (Ig), usually IgM and IgD, and the heterodimer Igα/Igβ. The Ig is formed by two heavy and two light chains. Created with Biorender.com.

During B-cell development in the BM, the immunoglobulin heavy-chain (IGH) and light-chain (IGK and IGL) variable loci undergo somatic recombination to generate a vast array of antigen-specific BCRs. As a result of this, a functional BCR is expressed on the surface of any naive B cell (NBC) (18). Then, the NBC leaves the BM to recirculate through secondary lymphoid organs such as lymph nodes (LN) or spleen, where it will encounter the cognate antigen and become activated (**Figure**

3). Upon antigen binding, B cells congregate and interact with T cells forming follicles, which will drive the initial B-cell proliferation and the induction of the germinal center (GC) responses. Basically, the GC is a transient specialized structure within secondary lymphoid organs in which responding B cells undergo rapid proliferation and somatic hypermutation (SHM) to allow selection for increased antigen affinity (affinity maturation). The initial densely packed replicative B cells form the GC dark zone, where the SHM occurs. The SHM introduces mutations in the heavy and light chain genes of the BCR at a rate of up to 10^{-3} per base pair per cycle, leading to the expression of a BCR Ig with unique immunogenetic and functional characteristics. GC B cells (GCBC) transit from the dark zone to the light zone after having divided a determined number of times (19).

In the light zone, GCBC are selected based on their affinity for the encountered antigen, through their interaction with follicular dendritic cells and follicular T helper cells. During this process, B cells that recognize autoantigens or have disadvantageous mutations caused by the SHM are removed (negative selection), while there is a positive selection of the B cells with the BCR showing the highest affinity towards the external antigen. Eventually, light-zone GCBC can also migrate back to the dark-zone for further rounds of SHM to reach higher antigenic affinity (18,19). Finally, this selected BCR may undergo Ig class-switch recombination (CSR), a process in which the constant region of the IGH is changed to allow altered effector function while maintaining antigen specificity. After affinity maturation, B cells can differentiate antibody secreting plasma cells (PC) or memory B cells (MBC), to build an immunological memory for future antigen recalls (18,19).

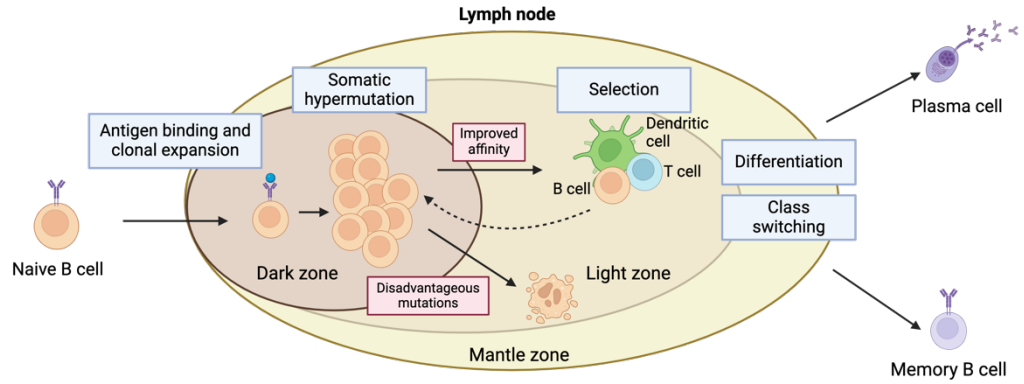


Figure 3. Germinal center reaction in the LN. Naive B cells will encounter their cognate antigen in the secondary lymphoid organs, such as LN. Upon antigen binding and T-cell stimulation, B cells will experience clonal expansion and affinity maturation through somatic hypermutation and/or class switch recombination processes to become terminally differentiated into PC secreting antibodies or MBC. Created with Biorender.com.

BCR is also present in the cell surface of malignant B cells. Given that B-cell neoplasms arise from the transformation of a single B cell, BCR IG gene rearrangements are ideal clonal markers as they will be identical in all neoplastic cells derived from a certain B cell. Moreover, the rearranged Ig sequence also serves as a cell maturation marker, since its configuration is linked to specific B-cell developmental stages. Remarkably, in CLL, the load of SHM within the rearranged IG heavy-chain variable region (IGHV) can be used as a surrogate marker of the cell of origin and it holds prognostic value with marked clinical implications (20).

1.3. Cell of origin and CLL subtypes

The cell of origin of CLL is still controversial. To date, no consensus has been reached regarding the normal cellular counterpart of CLL cells even though several B-cell types have been proposed (21,22). What is clear is that all CLL cases show a common surface phenotype of activated lymphocytes, which is highly similar to the surface phenotype of antigen-experienced B cells (23,24). Consistent with the

concept that CLL are antigen-experienced cells is the uniform expression of CD27, a marker for antigen-experienced MBC (22). The identification of the cellular origin of CLL is essential to elucidate the pathobiology of this disease. For this reason, several immunogenetic, transcriptomic and epigenetic profiling studies have defined several CLL subtypes, which have shed light on the possible origin of CLL.

1.3.1. Immunogenetic subtypes

CLL can be globally classified into two major molecular subtypes based on the level of SHM in the IGHV locus (also known as mutational IGHV status), which basically reflects whether CLL cells are derived from a GC-experienced B cell or not. This different origin will be partially associated with the subsequent acquisition of genomic, epigenomic alterations and the behavior of the disease (as will be discussed in the next sections). CLL with no or limited SHM are called unmutated IGHV (unmutated CLL, U-CLL) and originate from B cells that have not passed through the germinal center. U-CLL show a more aggressive behavior and shorter survival from diagnosis than those with mutated IGHV locus (mutated CLL, M-CLL) (**Figure 4**), which have passed and matured through the germinal center and present a more benign clinical course (25,26). The clinical cut-off of a ≥98% identity to germline IGHV sequence is routinely used to dichotomize CLL patients into mutated (<98 % identity) or unmutated (≥98%) groups (27). The clinical value of the IGHV mutational status, at the prognostic and predictive level, has been further accentuated by the observation that U-CLL patients have poorer responses to chemoimmunotherapy such as FCR than M-CLL (28–30). In this line, ERIC guideline recommends the assessment of IGHV status prior to therapy (20).

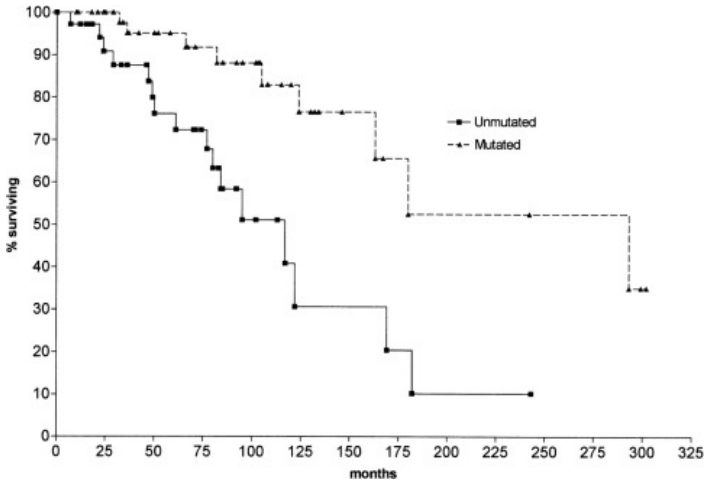


Figure 4. Overall survival (%) of CLL patients according to IGHV mutational status. Kaplan-Meier survival curve comparing stage A CLL patients with mutated and unmutated IGHV genes. Median survival for U-CLL: 95 months; median survival for M-CLL: 293 months. The difference is significant at the P = 0.0008 level (log-rank test). Retrieved from Hamblin, 1999 (26).

Immunogenetic studies have also revealed that one-third of unrelated CLL patients carry (quasi)identical or "stereotyped" BCR IGs, suggesting the role of antigen selection in the clonal expansion of CLL (31,32). Patients assigned to the same subset have similar biological features and clinical course, often differing from other patients within the same SHM category (33). In total, 19 major stereotyped subsets have been proposed. The majority of CLL cases with stereotyped BCRs correspond to U-CLL, but some of them can also be found in M-CLL. For instance, steoreotyped subset #4 is the largest subset of M-CLL and it is associated with an indolent disease, enriched in young patient and long time-to-first treatment (TTFT) (34).

Apart from the different clinical outcome and enrichment in stereotyped subsets, at the biological level, U-CLL have a higher responsiveness to IgM stimulation (more sIgM levels) (35) and, consequently, show a more activated phenotype than M-CLL (**Figure 5**). In fact, differential expression of activation markers are useful clinical predictors of outcome. For example, ZAP-70 and CD38

are more usually detected on U-CLL than M-CLL (36,37). The higher BCR signaling capacity clearly influences on the tumor survival and growth (33,38). Furthermore, U-CLL derive from an antigen-experienced B cell that has not undergone the germinal center reaction, where there is a negative selection of B cells recognizing autoantigens as well as an increased affinity/specificity of the BCR. In consequence, U-CLL cells may recognize autoantigens and polyantigens more often than M-CLL cells (23,39). Finally, U-CLL are also more enriched in somatic mutations and cytogenetic aberrations than M-CLL.

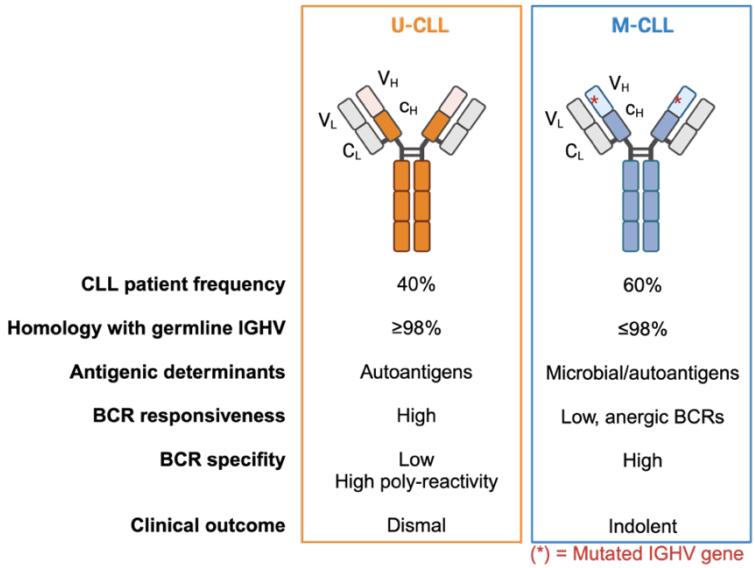


Figure 5. Characteristics of U-CLL and M-CLL patient subsets. CLL patients can be classified into two main subsets (U-CLL or M-CLL), characterized by a different level of somatic hypermutations, BCR responsiveness, antigenic determinants and clinical outcome. Adapted from Ten Hacken, 2019 (33).

1.3.2. Epigenetic subtypes

DNA methylation is an epigenetic mark involving the covalent transfer of a methyl group onto a cytosine. The majority of DNA methylation occurs on cytosines that precede a guanine nucleotide or CpG sites. Initially, it was just considered a repressive mark, as it regulates gene expression by recruiting proteins involved in

gene repression or by inhibiting the binding of transcription factors to DNA. However, at present, it has been demonstrated that its function is broader and depends on the genomic context where methylated CpGs are present. During normal B cell differentiation, the DNA methylome is extensively modified, where each differentiation stage shows a specific epigenetic fingerprint (40,41). In this line, genome-wide DNA methylation analyses in CLL samples have identified three epigenetic subtypes or "epitypes" associated with normal B cell differentiation: naive B cell-like (n-CLL), memory B cell-like (m-CLL) and intermediate-CLL (i-CLL) (**Figure 6**). Notably, these three epigenetic subtypes can be used to infer the putative cell of origin as well as to shape the clinical outcome of a given patient.

There is a clear overlap between the immunogenetic and epigenetic subgroups (**Figure 6**). First, m-CLL is composed by M-CLL, being epigenetically more similar to memory, GC-experienced B cells. Second, n-CLL subgroup includes U-CLL, with a signature more similar to naive, pre-germinal center B lymphocytes. Finally, i-CLL shows an intermediate methylation profile, between naive-like and memory-like, and a moderate SHM, suggesting that it may derive from a MBC that has been selected early to exit the GC reaction (42). These subsets have different usage of IGHV genes, stereotypes and genomic aberrations (43). For example, i-CLL carry moderate IGHV levels with bias toward light-chain usage, with 50 % of cases expressing IGLV3-21 gene (44). Moreover, more than a third (38 %) of i-CLL cases carry a mutation, known as R110, induced by SHM in the IGLV3-21 gene, which changes the glycine at position 110 to an arginine(45). The R110 mutation triggers an aberrant BCR-BCR interaction, inducing a constant BCR signaling in CLL cells. The presence of mutated IGHV genes and the R110 due to SHM in i-CLL further support the concept that i-CLL derive from a GC-experienced B cell.

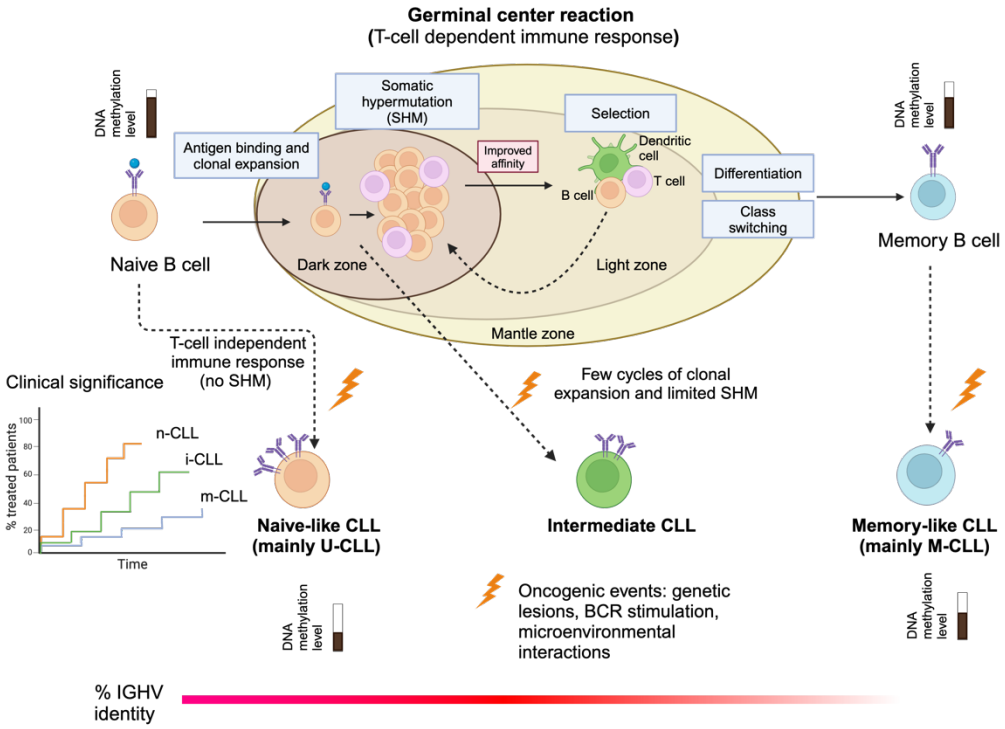


Figure 6. CLL cell of origin according to epigenetic changes. DNA methylation patterns reflects both cell of origin and proliferative history of the tumor cells. The normal B cell differentiation entails widespread DNA methylation with a high degree of demethylation occurring during GC reaction, which is recovered in MBC. Upon malignant transformation cells retain the methylation specific of their cell of origin, and develop a new oncogenic profile. Three epigenetic subtypes of CLL have been identified: naive-like, memory-like, and intermediate. Naive-like CLLs have higher methylation heterogeneity than memory-like CLLs. These three epigenetic subtypes have different clinical outcomes. The illustrated curves of TTFT are representative of different studies. Adapted from Nadeu, 2020 (46).

The three epigenetic subtypes also differ in the TTFT and overall survival, with prognostic value in multivariate analyses including other classical parameters as IGHV mutational status (47–49). Several studies have confirmed that n-CLL have poorer prognosis and shorter TTFT, followed by i-CLL with intermediate prognosis and, finally, m-CLL with better prognosis and longer TTFT. Of note, i-CLL cases can be further divided into two prognostic groups depending on the presence/absence of IGLV3-21^{R110} mutation (45,50). IGLV3-21^{R110} i-CLL cases are more aggressive and behave as n-CLL/U-CLL while i-CLL lacking IGLV3-21^{R110} mirror m-CLL/M-CLL.

1.3.3. Transcriptomics

Initial gene expression profiling (GEP) revealed that both U-CLL and M-CLL cells have similar gene expression signatures, highly different from normal B cells (51,52). Further transcriptomic analyses of CLL and normal B cell subsets showed that CLL cells are more similar to mature CD5+ B cells than to any other type of mature B cell (21). The transcriptome of human mature CD5+ B cells is distinct form conventional NBC and MBC. In humans, CD5 is expressed on up to 60-75 % of B cells in the umbilical cord blood. A decrease is seen in the PB of adults where CD5+ B cells represent about 5-30 % of the circulating B cells. It is expressed in a subset of regulatory B cells and in a minor subset of pre-naive, naive mature and MBC (22). The majority of CD5+ B cells are pre-naive or naive and use unmutated IGHV genes and have stereotyped IGHV genes rearrangements. However, there is a small fraction CD5+ CD27+ B cells (1 % of total B cells in PB) that carry mutated IGHV genes. According to this study, CD5+ B cells could be the cell of origin of this leukemia. U-CLL would derive from CD5+ CD27- pre-GC B cells while M-CLL would arise from CD5+ CD27+ post-GC B cells. Nonetheless, CD5 expression in CLL cells could just occur as a response to their activated phenotype, suggesting that CLL could derive from CD5- B cells instead (23).

Overall, the immunogenetic, epigenetic and transcriptomic studies highlight that the cell of origin for U-CLL and M-CLL is different, with U-CLL deriving from a GC-independent mature B cell and M-CLL originating from a GC-experienced B cell. In addition, immunogenetic and epigenetic classifications also revealed the relevant implication of the BCR IG in the disease pathophysiology.

1.4. Pathophysiology of CLL

The pathogenic factors that play a key role in defining the biological features of CLL cells, as well as the clinical aggressiveness of the disease, are divided into: extrinsic factors, coming from direct microenvironmental interactions of CLL cells;

and intrinsic factors, mainly genomic and epigenomic alterations of CLL cells (53). Both extrinsic and intrinsic factors influence on the characteristic BCR signaling of CLL cells, which is crucial for survival, growth and proliferation of the malignant B cells (54). Given that CLL is a prime example of a malignancy extremely dependent on microenvironmental stimuli, extrinsic factors will be introduced first.

1.4.1. Tumor microenvironment

Historically, CLL has been considered a disease with an inherent defect in apoptosis, as slowly proliferating CLL cells accumulate in PB due to reduced cell death (38). Consistent with this view, the majority of PB CLL cells are arrested in G0/G1 (52). However, *in vivo* labeling studies using deuterated water revealed that CLL is a dynamic condition, with CLL cells that multiplied and died at variable rates (55). Subsequent *in vivo* labeling studies identified LN as the anatomical site harboring the largest fraction of newly born CLL cells, while BM did not seem to be a major proliferation site (56).

CLL cells are extremely dependent on signals coming from the microenvironment for proliferation and survival (57). CLL cells recirculate between LN where they actively proliferate, and the PB where they become quiescent (58). In the LN, CLL interact with the complex microenvironment and proliferate in distinct tissue areas known as “pseudofollicles”, or proliferation centers (55,59,60). Despite the global quiescent phenotype of CLL cells in PB, there is a spectrum of proliferative and quiescent CLL cells in PB based on the protein levels of CXCR4 and CD5 (57). Circulating CLL cells expressing CXCR4 low CD5 high have recently emigrated from LN to PB and are enriched in proliferative cells (or cells that have recently proliferated, known as proliferative fraction) (**Figure 7**). As CLL cells spend more time in PB, they become more quiescent leading to downregulation of CD5 and increased surface expression of CXCR4, which are primed to return to the LN (**Figure 7**). This resting fraction (CXCR4 high CD5 low) is enriched in older, less vital cells that need to either immigrate back to the LN or die (58,61).

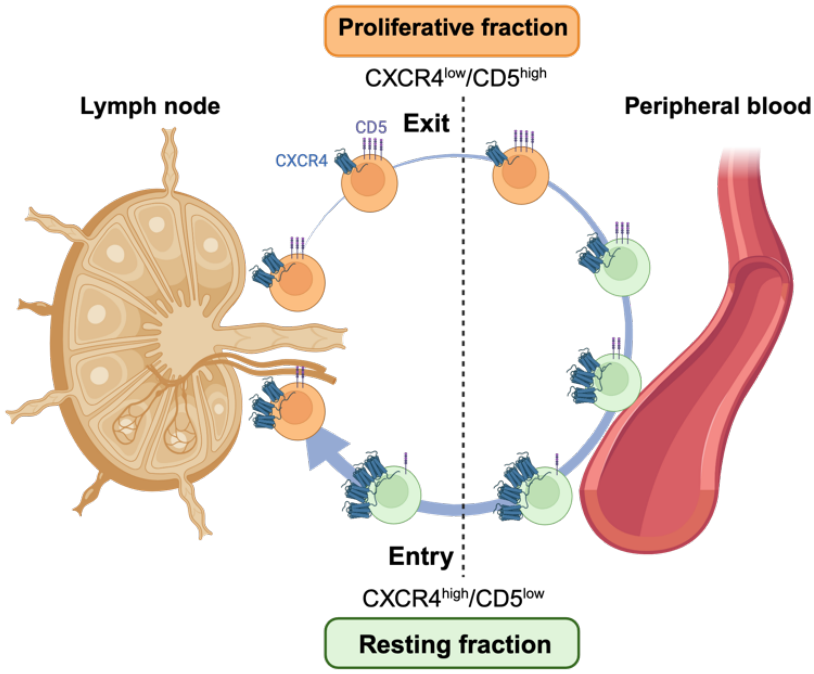


Figure 7. CLL recirculation between lymph node and peripheral blood. Spectrum of circulating CLL illustrating the proliferative fraction enriched in LN emigrants versus the resting fraction enriched in LN immigrants. CXCR4 high CD5 low are in a resting state in PB. When these cells enter the LN, CD5 is upregulated and CXCR4 is internalized. Then, CXCR4 low CD5 high cells are released from the LN and migrate into PB. Eventually, these cells become more quiescent with a decrease in CD5 levels and renewed surface expression of CD5. Adapted from Haselager, 2020 (57).

In the LN, CLL cells are in intimate contact with the extracellular matrix and accessory cells, such as monocyte-derived nurse-like cells (NLC), T cells and stromal cells (mesenchymal and follicular dendritic cells) that conform the tumor microenvironment (TME)(62–64) (**Figure 8**). Continuous crosstalk of CLL cells with these cell populations from the TME affect the function of both parties (65,66). One example is the T-cell compartment, since in CLL can exert pro-tumor as well as anti-CLL cytotoxic activity (67). Recruited CD4+ helper T cells (T_{helper} cells) within proliferation centers provide tumor support through CD40/CD40L co-stimulation and cytokine signaling (68,69) (**Figure 8**). In PB of patients, T-cell numbers are skewed towards cytotoxic CD8+ T-cell ($T_{cytotoxic}$ cells) and effector subpopulation

(70). Both CD4+ and CD8+ T-cell subpopulations show functional defects and increased markers of chronic activation and exhaustion, such as PD-1, contributing to inhibited effector function (71,72). In addition, patients with CLL also have increased levels of regulatory T cells (T_{reg}), an immunosuppressive subset of T cells that inhibit anti-tumor T-cell responses (73). Therefore, CLL cells are able to instruct the TME by inducing a supportive role from exhausted T_{helper} and $T_{cytotoxic}$ cells while causing an accumulation of T_{reg} cells to prevent anti-tumor effector functions. As a result, there is an immunosuppressive environment surrounding CLL cells that favors immune evasion and promotes tumor progression (66). In line with this, spontaneous regression of the disease without treatment has been associated with a reversal of T-cell exhaustion features and increased T-cell proliferation in patients, suggesting the importance of the T-cell compartment in controlling (74).

Similarly, myeloid cells in CLL play both tumor-supportive and immunosuppressive roles (**Figure 8**). These cells include NLC and myeloid-derived suppressor cells (MDSC). Interestingly, NLC were first described by Burger et al. in 2000, as they observed that, *in vitro*, a fraction of CD14+ cells (monocytes) from patients with CLL differentiated into large, round, adherent cells that attracted leukemic cells and protected them from undergoing apoptosis *ex vivo*. When removed from these adherent cells, CLL cells experienced a rapid decline in viability. Subsequent studies identified abundant cells with the morphology and phenotype of NLCs in secondary lymphoid tissues of patients with CLL, suggesting they promote CLL survival *in vivo* as well (75). NLC are known to secrete chemokines, such as CXCL12 that binds to CXCR4 in CLL cells, that aid migration and homing of CLL cells into protective niches of the LN (76,77). Moreover, NLC secrete anti-apoptotic cytokines (e.g., BAFF, APRIL) promoting CLL survival (63,78,79). On the other hand, MDSC suppress T-cell effector function and promote T_{reg} differentiation (80).

In summary, the TME favors CLL migration and homing as well as proliferation of the malignant cells through diverse receptors including BCR, Toll-like receptors (TLR) and CD40. Reciprocally, CLL cells release cytokines including interleukin (IL)-10 (81), chemokines like CCL2 (69) and extracellular vesicles (82) that recruit and alter the microenvironmental cells, inducing a tumor-supportive niche (**Figure 8**).

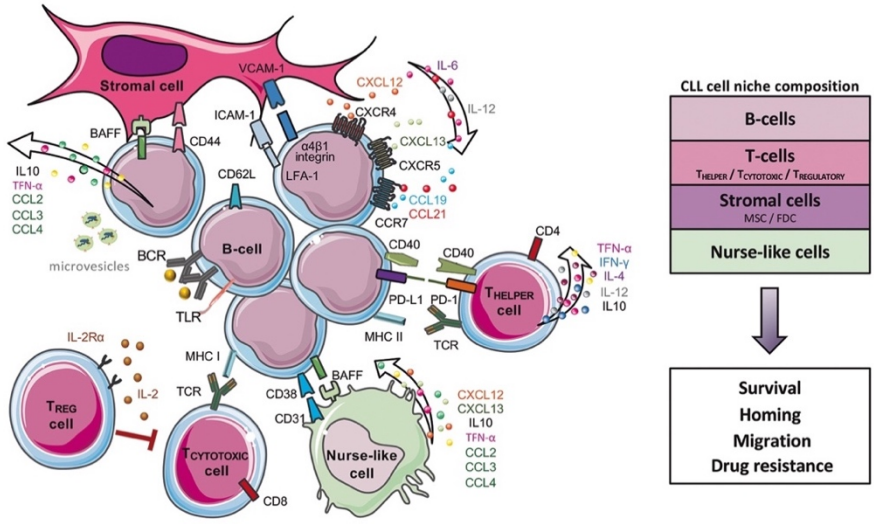


Figure 8. The CLL microenvironment. Communication between CLL and stromal cells, NLC and T cells is established and maintained by direct contacts, chemokine/cytokine receptors, adhesion molecules and ligand-receptor interactions. CLL cells migrate to tissues attracted by the chemokines secreted from nurse-like cells and stromal cells. The presence of environmental and/or self-antigens in the niches may trigger BCR and TLRs (Toll like receptors pathway) activation, which amplify the responsiveness of CLL cells to the signals and factors that are provided by its microenvironment. Retrieved from Delgado, 2020 (43).

1.4.2. BCR signaling

BCR signaling is a major determinant of CLL pathogenesis (1,83). Actually, the introduction of therapeutic agents blocking BCR signaling in CLL cells, such as BTKi (e.g., ibrutinib), has remarkably changed the management of CLL, allowing for treatment without chemotherapy. Treatment of patients with ibrutinib leads to lymphocytosis due to efflux of CLL cells from the proliferative LN compartment into

the PB, thereby depriving CLL cells from microenvironmental signals and halting disease progression.

The lymphatic tissues are the principal site of BCR activation for malignant B cells, where they find a spectrum of (auto)antigens, spanning from microbial foreign and autologous molecules, that will activate the BCR signaling in a ligand-dependent manner (83,84)(**Figure 9**). Additionally, BCR activation can also occur in a ligand-independent manner ("tonic BCR signaling") (85,86), as a consequence of CLL polyreactive BCRs binding themselves (homotypic interaction) as well as oncogenic mutations within the BCR pathway components (**Figure 9**). Interestingly, and contrary to other lymphoid neoplasms, activating mutations in BCR pathway are uncommon in CLL, suggesting the role of antigenic triggering in disease pathogenesis (83). At a functional level, the BCR engagement in CLL activates a complex cascade of intracellular signaling molecules, including upstream kinases LYN, SYK, BTK and PI3K (83), which transduce signals to calcium signaling modulators, cytoskeletal activators (87) and downstream effectors, including AKT and ERK kinases and the NF-κB pathway (88), which act on nuclear transcription factors leading to the production of chemokines (CCL3 and CCL4), and upregulation of anti-apoptotic proteins of the BCL2 family like MCL1 (89). This cascade of signaling events promote B cell survival and proliferation as well as the recruitment of lymphocytes and monocytes with the secretion of CCL3/4 chemokines (90,91).

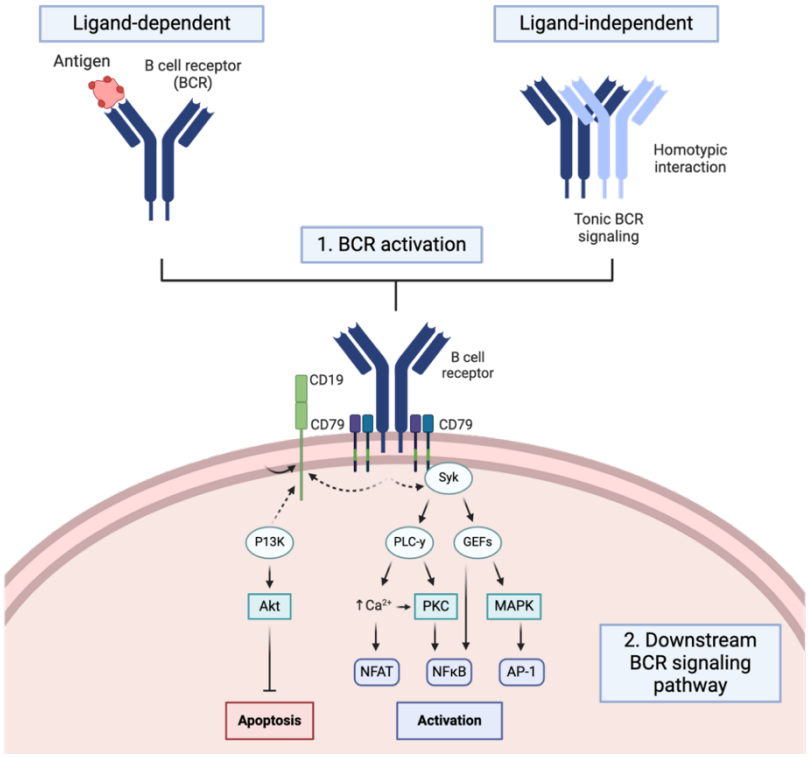


Figure 9. Upstream and downstream BCR signaling pathway. BCR activation can occur in a ligand-dependent (extrinsic antigen) or ligand-independent manner (homotypic interaction between different BCRs). Upon BCR activation, there is a signaling cascade that engages BTK, PI3Ks (including PI3Kδ), NF-κB, PI3K, NF-AT, MAP kinase, and RAS signaling pathways, leading to cell survival and proliferation. Created with Biorender.com.

CLL is highly heterogeneous and the outcome of BCR signaling ranges from enhanced B cell activation/proliferation to B cell anergy (84,92) (**Figure 10**). In fact, the BCR signaling capacity strongly depends on the mutational status of the IGHV genes (83,93). Anergy, which is defined by a failure to respond to BCR-mediated stimuli, is one of the mechanisms of the immune system to silence autoreactive B cells upon recognition of self-antigens (92). It is a state of BCR desensitization induced by chronic binding of antigen *in vivo* with high-affinity that results in unresponsiveness when cells are stimulated with antigen *in vitro* (33). M-CLL cells are thought to be selected and expanded by high-affinity binding to restricted set of antigenic epitopes that either occur infrequently as they are

external antigens (e.g., to β-(1,6)-glucan, an antigen from yeasts and rheumatoid factors)(94,95) or induce anergy due to high-affinity/avidity (83). Consequently, M-CLL present a weak response to BCR engagement associated with low proliferation and indolent disease (96). In contrast, U-CLL patients express polyreactive low-affinity BCRs that are less specific and recognize a variety of environmental and auto-antigens (e.g., vimentin, myosin or lipoproteins) present in the TME (97–99). Thus, low-affinity BCR binding occurs more frequently in U-CLL, which would lead to increased BCR signaling that is related to higher ZAP-70 expression (100). In fact, ZAP-70 kinase, which can be used as a surrogate marker for U-CLL (101) and therefore acts as a factor of poor prognosis (102). Mechanistically, ZAP-70 interacts with CD79B and enhances BCR signaling (103,104) and also enhances migration toward chemokines and response to survival stimuli from microenvironment (105). In short, not only U-CLL cells have higher capacity for homing to the LN compartment in response to chemokines, but they also are more responsive to BCR activation, which is linked to higher proliferation and more aggressive disease (33,92).

As mentioned before, CLL-BCRs can also signal in the absence of an external antigen, in autonomous manner, by interactions between individual BCRs through the recognition of conserved epitopes within specific regions of the immunoglobulin heavy and light chains (85,106). The autonomous signaling activity of the CLL-BCRs has been described to be essential for leukemia development in the Eμ-TCL1 mouse model of aggressive U-CLL (107).

All in all, both antigen-dependent and antigen-independent BCR signaling have been described in CLL, and CLL cells can receive both continuous and intermittent BCR signals that may facilitate proliferation (83). Indeed, ligand-dependent and tonic BCR signaling might not be mutually exclusive. CLL clones could originate as antigen-dependent, but evolve to become more autonomous (57).

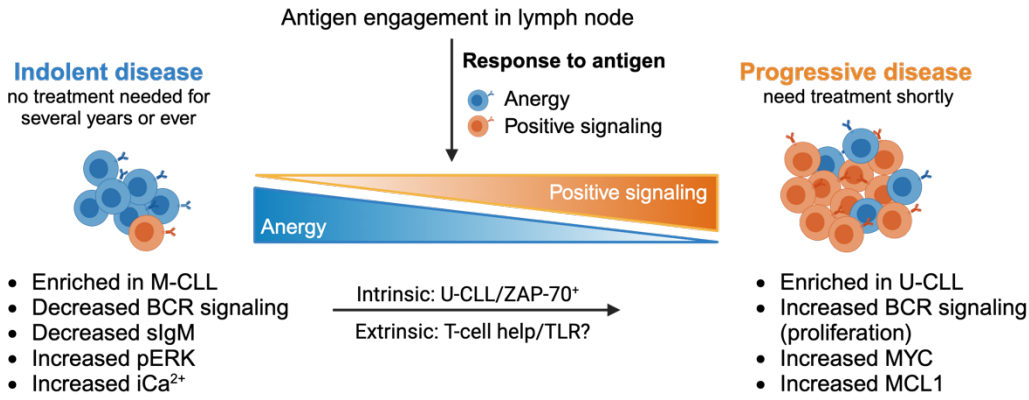


Figure 10. Variable BCR signaling responses influence clinical outcome. Antigen engagement may induce anergy or positive signaling in CLL. The balance between these two different responses is determine by intrinsic and extrinsic factors. A temporary imprint (markers) of the two different responses in tissues (LN) can be detected in circulating CLL cells. Adapted from Packham, 2014 (92).

1.4.3. Genomic abnormalities

Fluorescent in situ hybridization (FISH) identifies chromosomal aberrations in more than 80% of patients with CLL (108). The most frequent aberrations are deletion in chromosome 13q14.3 (del(13q)), del(11q), del(17p) and trisomy 12 (109). Del(13q) is the most common chromosomal alteration, present in approximately 50% of patients, and is associated with favorable prognosis. Within this deleted region is the DLEU2–mir-15-16 cluster, which negatively regulates the expression of proteins that can inhibit apoptosis (110). Consequently, upon loss of 13q14 region, there is an imbalance in the regulation of the apoptotic process that contributes to CLL immortality. Del(17p) is found in 7% of patients and is associated with loss of the tumor suppressor gene *TP53* (111), whereas del(11q) is found in 18% of patients and is often associated with alterations in *ATM*, which is involved in DNA repair (112). Thus, del(17p) and del(11q) are associated with adverse clinical outcome (108,113). Finally, trisomy 12 is found in 16% of patients with CLL and is associated with high frequency of *NOTCH1* mutation. Interestingly, trisomy 12 defines a subgroup of CLL with more

frequent atypical morphological and immunophenotypic features and intermediate prognosis (114).

On average, CLL tumors accumulate around 2,500 somatic mutations (43,46). However, the mutational landscape of the disease is highly heterogeneous. Next-generation sequencing (NGS) approaches using large cohort of patients have identified few recurrent mutated genes that are present in 5-20% of the patients, such as *SF3B1*, *ATM1*, *TP53*, *NOTCH1* and *BIRC3* (115–117). These more common driver genes are followed by a long tail of genes mutated at low frequencies (<2% of tumors) (**Figure 11**), suggesting the lack of a common genetic driver in CLL.

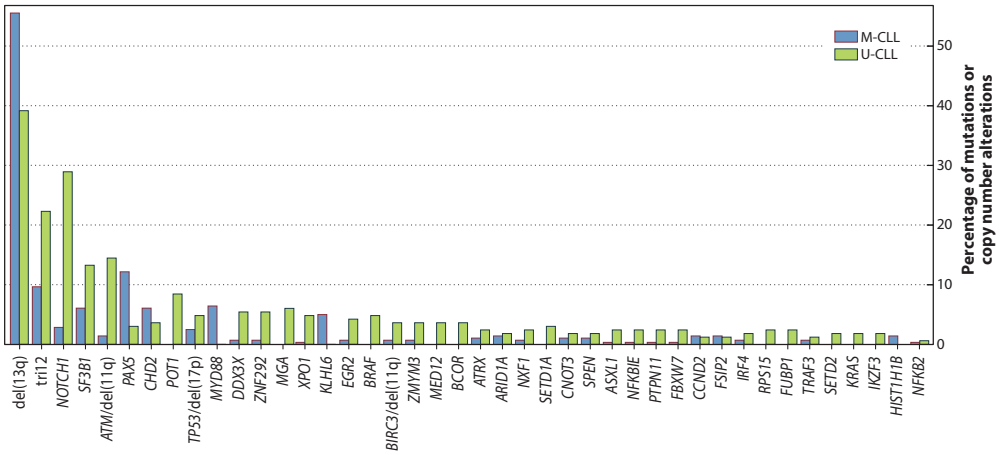


Figure 11. Driver genes in CLL. Mutation frequency of CLL drivers according to the IGHV status. Most driver genes are mutated in both subtypes but at different frequencies, with only a small subset of genes being subtype specific. Adapted from Nadeu, 2020(46).

Many of these genes appear to have higher frequency mutations in U-CLL tumors (**Figure 11**). Interestingly, most mutations can be grouped into small number of cellular pathways (43), including DNA damage response (*ATM*, *TP53*, and *POT1*), NOTCH1 signaling (*NOTCH1* and *FBXW7*), RNA splicing and metabolism (*SF3B1*, *XPO1*, *DDX3X*, and *RPS15*), NF-κB signaling (*BIRC3*, NF*KB2*, *NFKBIE*, *TRAF3*, and *TRAF2*), BCR and TLR signaling (*EGR2*, *BCOR*, *MYD88*, *TLR2*, *IKZF3*, *KRAS* and *NRAS*), and chromatin modifiers (*CHD2*, *SETD2*, *KMT2D*, *ASXL1*). While the

prognostic value of the highly frequent mutations has been demonstrated, the precise role and clinical impact of many of these mutations remain to be elucidated.

Finally, the subclonal architecture of CLL has been shown to be important for the clinical outcome of patients (116,118). NGS has revealed that subclonal mutations (those present in only a fraction of tumor cells) can be detected for all driver genes and are associated with rapid progression and poor outcome (119). In this line, clonal aberrations, which are mostly structural abnormalities (e.g., trisomy 12, del(13q)) generally correspond to earlier driving events, while subclonal mutations in driver genes (e.g., *SF3B1, POT1, NOTCH1*) are acquired later over the course of the disease (118). All in all, CLL samples carry relatively few genetic aberrations compared with other adult cancers (120), and some patients have an aggressive disease despite being classified as "low risk" based on genetic markers, indicating that non-genetic factors are relevant for CLL etiology and outcome.

1.4.4. Epigenomic abnormalities

CLL cells undergo a widespread epigenetic reconfiguration. Epigenetics encodes a variety of molecular features that regulate gene expression output without changing the underlying DNA sequence. So far, four major epigenetic layers have been described, which are DNA methylation, histone post-translational modifications, chromatin accessibility and 3D structure of the genome (121) (**Figure 13**). The interplay between these epigenetics layers is crucial to give rise to consistent transcriptional programs necessary for all cellular processes.

1.4.4.1. Introduction to the epigenetic layers

DNA is tightly packed to fit into the microscopic space of the nucleus with the help of specialized proteins, known as histones (122). Histones pack the DNA into nucleosomes, which constitute the primary functional unit of the chromatin. Indeed, the local configuration of the nucleosomes distinguishes two different

states of the chromatin. A condensed state of the chromatin, known as heterochromatin, is less accessible and transcriptionally silent, and an open state, known as euchromatin, is characteristic of actively transcribed genes (**Figure 13**).

Histone proteins are dynamic structures that influence DNA-templated processes such as chromatin compaction, nucleosome dynamics and transcription (123). To achieve this wide spectrum of functions, histones are decorated by a variety of post-translational modifications (PTMs), referred to as epigenetic marks (**Figure 13**). Histone PTMs are present in both the terminal tails of histone and their globular core domains (124), and include methylation, acetylation, phosphorylation, ubiquitylation and sumoylation, among others (125). These different types of PTM exert their functions in DNA-templated processes via direct activation/inhibition of transcription, or indirectly, by inducing the binding of an effector protein or chromatin remodeling complex (126).

Chromatin immunoprecipitation followed by next-generation sequencing (ChIP-seq) (127) has been instrumental in demonstrating that specific genomic regions, such as active promoters and enhancers, are enriched in particular patterns of histone modifications (123). For example, the H3K27 acetylation (H3K27ac) marks active regulatory regions that end up being enhancers if H3K4 monomethylation (H3K4me1) is present as well, or promoters if H3K4 trimethylation (H3K4me3) is present instead. Other histone marks are related to silencing and heterochromatin like H3K27me3 or H3K9me3, whereas others are linked to transcriptional elongation such as H3K36me3. The combination of different histone proteins and their PTMs allows the segmentation of the genome into chromatin states (128)(**Figure 12**), which are informative about the underlying genomic function (129,130).

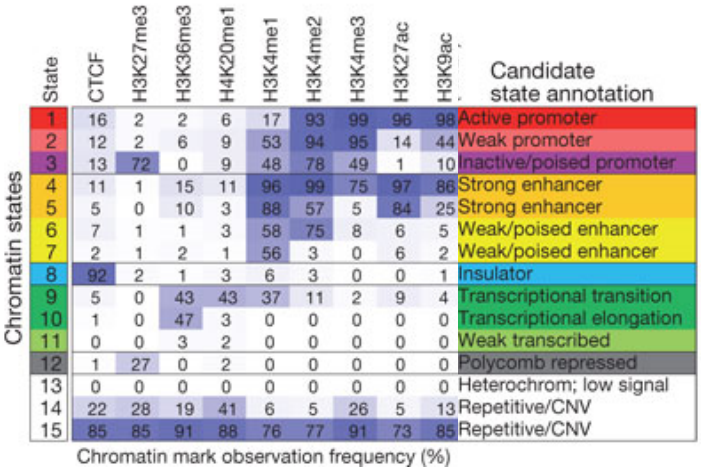


Figure 12. Chromatin states definition. Emission table with the frequency of each chromatin marks used to defined each chromatin state by multivariate Hidden Markow model (HMM). Adapted from Ernst, 2011 (130).

Chromatin accessibility refers to the extent to which nuclear complexes can physically contact with chromatin. Accessible chromatin is the fraction of the genome that permits the binding of regulatory elements, such as transcription factors (TF), to the DNA to regulate gene expression (131) (**Figure 13**). It is regulated by histone modifications in the first place that can induce increased/decreased chromatin compaction by modulating nucleosome affinity for active chromatin remodelers (ATP-driven remodeling enzymes). Genome-wide chromatin accessibility can be measured by several methods, but the Assay for Transposase-Accessible Chromatin using Sequencing (ATAC-seq) is currently the most widely used (132). Open/accessible chromatin in enhancers and promoters is necessary for the regulation of gene transcription (131). However, poised enhancer and promoters related to silent genes are usually open, indicating that accessible chromatin is needed but not sufficient for enhancer or promoter activity (133–135). Therefore, active chromatin depends on open chromatin as well as the presence of certain histone modifications (H3K27ac).

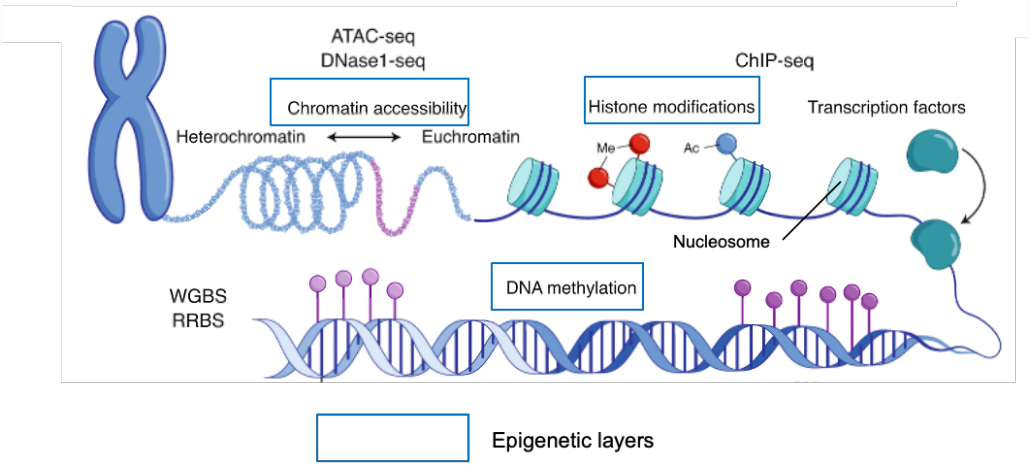


Figure 13. Genome organization. Overview of the different epigenetic layers as well as the corresponding techniques to study them. WGBS, whole-genome bisulfite sequencing, for DNA methylation; ChIP-seq for histone and transcription factors: ATAC-seq for chromatin accessibility. Adapted from Scherer, 2021 (136).

There is a clear interplay and cooperation between epigenetic layers/modifiers and TFs to accomplish gene regulation (137,138). TFs are proteins that recognize and bind cis-regulatory regions (promoters and enhancers) at their TF binding sites (i.e., a specific DNA sequence) to regulate transcription in a time and context-dependent manner. TFs can act as "activators" or "repressors" of gene expression depending on which chromatin region they are binding to as well as the interacting partners (co-activators or co-repressors). The majority of TFs require an accessible, or at least partially open, chromatin to bind the DNA, which is, first, regulated by the action of epigenetic modifiers such as the ATP-driven remodeling enzymes (139)(**Figure 13**). Nonetheless, a certain class of TFs, the so-called pioneer TFs, have the ability to engage with nucleosome-bound chromatin independently of other factors. Pioneer TFs are believed to be the first factors to engage with target chromatin regions and associate with compact chromatin to facilitate the binding of other additional factors and local epigenetic modifications (140,141). For instance, EBF1 has been proposed to act as a pioneer TF of early B-cell differentiation (142), as it is able to induce epigenetic changes, by increasing chromatin accessibility and recruiting other chromatin modifiers enzymes and

others TFs, to induce locus activation of B-cell specific genes. In addition, EBF1 and PAX5 collaborate to repress alternative cell fates (silencing of T-cell genes) and lock B cells into the B-lineage fate (143).

Although TF binding and profiling has been traditionally performed with ChIP-seq, the CUT&RUN technique is being used more and more these days. CUT&RUN is considerably similar to ChIP-seq, with the differences that 1) just a very low number of cells is required to carry out the protocol (500,000 cells) and 2) no chromatin-protein crosslinking is needed (144). Furthermore, the CUT&RUN technique can also be used to assess histone modifications in the chromatin in a very efficient way.

1.4.4.2. Regulatory chromatin landscape

Even though initial studies dealing with epigenomic regulation in CLL have focused almost exclusively on DNA methylation, recent technological advances made possible to map chromatin landscapes in large cohorts of CLL patients (135,145–148). The CLL epigenome was defined after the integration of the of whole-genome maps of the DNA methylome, six histone modifications with non-overlapping functions (e.g., H3K4me3, H3K4me1, H3K27ac, H3K36me3, H3K9me3 and H3K27me3), chromatin accessibility, 3D chromatin architecture, transcriptome and genome in seven representative CLL cases (135,149). The combination of the different histone modifications allowed the generation of a chromatin state model specific for B cells using chromHMM (**Figure 14A**).

The integration of the multiple epigenetic layers revealed that CLL cases showed a variable number of active regulatory regions, with some of them being already modulated during normal B cell differentiation while others were acquired *de novo* (**Figure 14B**). The variability of active regions was larger in U-CLL than M-CLL, and U-CLL carried a significantly larger number of accessible and active sites than M-CLL, two features that could be linked to the more aggressive behavior of

this subtype. In addition, there was a set of active regions that related CLL (as a whole or subtype-specific) to a variety of combinatorial patterns in NBC, GCBC, MBC and PC. For instance, U-CLL cells, despite being derived from GC-unexperienced cells, acquired chromatin features of proliferative GCBCs, which could be associated to the higher proliferation of U-CLLs when compared to M-CLLs. This suggests U-CLLs hijack some epigenetic mechanisms associated with the normal B-cell proliferative mechanisms. Finally, and more importantly, CLLs, as a whole and subtype-specific, also reconfigured their chromatin landscape independently of B-cell differentiation. Remarkably, *de novo* chromatin alterations in CLL as a whole were enriched in active regulatory regions (with increased H3K27ac and increased chromatin accessibility). The majority of these regions corresponded to active enhancers or super-enhancers (135) that regulate the expression of genes, such as *LEF1, CTLA4, FMOD* and *TCF4*, known to be involved in CLL pathogenesis (150). These newly active regions (N=498) were enriched in the TF binding motif of members of the NFAT, FOX and TCF/LEF families (135) (**Figure 14C**), which appear to be orchestrating this *de novo* epigenetic dysregulation. Importantly, other independent studies in CLL have also reported that regulatory regions with increased H3K27ac are enriched in the binding sites of the same TF families (147,148).

In summary, this pattern of *de novo* chromatin activation is shared between U-CLL and M-CLLs, and therefore, seems to be a signature of CLLness, which contrasts with the genetic heterogeneity observed in CLL patients. This finding indicates that CLL evolution is linked to *de novo* chromatin programming, from inactive regions in normal B cells to active enhancers in CLL, and suggests that this onco-epigenetic process mediated by specific TFs is an early essential event during leukemogenesis.

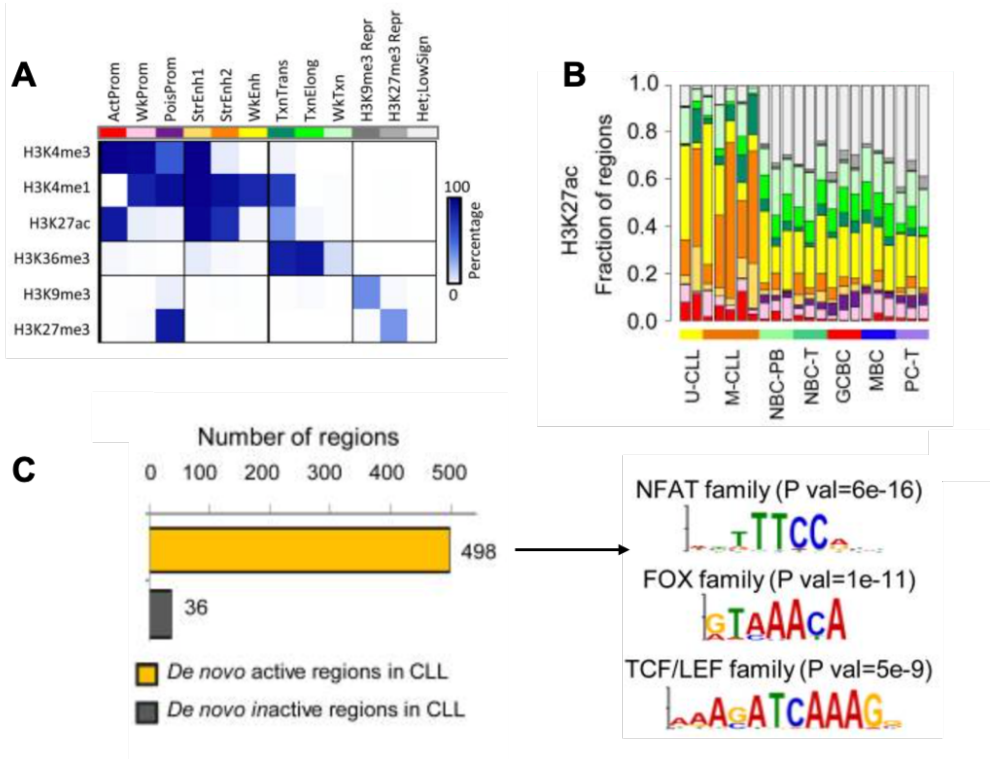


Figure 14. The CLL reference epigenome. A) Emission of the generated chromatin state model. ActProm, Active Promoter; WkProm, Weak Promoter; PoisProm, poised Promoter; StrEnh1, Strong Enhancer 1; StrEnh2, Strong Enhancer 2; WkEnh, Weak Enhancer; Txn_Trans, Transcription Transition; Txn_Elong, Transcription Elongation; Wk_Txn, Weak Transcription; H3K9me3_Repr, H3K9me3 Repressed; H3K27me3_Repr, H3K27me3 Repressed; Het;LowSign, Heterochromatin;Low Signal. B) Distribution of the different chromatin states in CLL and B cell at regions with de novo H3K27ac increase in CLL. C) Binding motifs of NFAT, FOX and TCF/LEF transcription family members, which are highly enriched in the accessible loci of the *de novo* active region (N=498). Adapted from Beekman, 2018 (135).

1.4.4.3. TF networks drive the altered CLL epigenome

As mentioned before, several independent studies have pinpointed similar TFs candidates as potential drivers of the unique CLL activation of regulatory regions, including NFAT, TCF/LEF1, and FOX TF families. Interestingly, some single variant polymorphisms (SNPs) that associate with higher risk of CLL development showed an increased binding affinity for these TF families (151).

Notably, *de novo* altered chromatin accessibility in U-CLL or M-CLL (subtype-specific) was associated with markedly different TF motifs. Interestingly, regions gaining accessibility in U-CLL were enriched in binding motifs of IRF, STAT1/2, AP-1, FOXP1, and GFI1 and TCF/LEF TF (135). Many of these TFs are involved in cell cycle regulation and, some of them, are operative in proliferative B cell subpopulations, suggesting again that U-CLL may exploit specific molecular mechanisms present in normal B cell subpopulations to achieve higher proliferation.

The exact role of these TFs in disease progression remains unclear, even though several functional studies have demonstrated the functional and therapeutic potential in CLL of some of the TFs involved in the epigenetic reprogramming of CLL (49,152,153). One example is LEF1, from the TCF/LEF TF family, whose binding motif is not only present in the unique activation signature of CLL as a whole but also in U-CLL specific *de novo* open chromatin regions. LEF1 is a hallmark of CLL and the definition of its role in CLL initiation and progression has been the main focus of this doctoral thesis.

2. Lymphoid-Enhancer Factor 1 (LEF1)

LEF1 is *de novo* expressed in almost all CLL cells and, as described before, its binding motifs are present in the *de novo* active regulatory regions associated with in CLL as a whole and in U-CLL. LEF1 is a TF that belongs to the TCF/LEF family of the high-mobility group (HMG) of TFs, which are key mediators of the Wingless-related integration site (WNT) signaling pathway in metazoans (154,155). Activation of this pathway causes the translocation of β-catenin into the nucleus, where it forms complexes with any member of the TCF/LEF family and activates the transcription of WNT-dependent genes.

2.1. WNT signaling

The WNT signaling pathway activity is tightly regulated in time and space and it is fundamental for mammalian embryonic development as well as adult tissue homeostasis (156). WNT signaling refers to a diverse collection of signals triggered by WNT ligand–receptor interactions that direct cell behavior in multiple ways: cell polarity, movement, proliferation, differentiation, survival and self-renewal. It is not surprising, then, that deregulation of WNT pathway is implicated in tumorigenesis and progression of multiple neoplasms, such as for instance colorectal cancer and CLL (157).

WNT signaling is divided into two major pathways: a canonical pathway involving β-catenin (β-catenin-dependent) and a non-canonical pathway that is β-catenin-independent. The canonical WNT pathway mainly controls cell proliferation, whereas the non-canonical WNT pathway regulates cell polarity and migration, and the two main pathways form a network of mutual regulation (157). WNT ligands that activate the canonical WNT signaling are different from those activating the non-canonical one (158,159).

2.1.1. Canonical WNT signaling

This pathway is activated upon the binding of extracellular WNT ligands glycoproteins (WNT-1, WNT-3, WNT-3a, WNT-8b, WNT-10b and WNT-16) to membrane receptors (Frizzled and LRP5/6) by autocrine/paracrine methods (158). Ligand binding triggers destabilization of the AXIN/glycogen synthase kinase-3 β (GSK-3β)/adenomatous polyposis coli (APC) destruction complex, which, in the absence of WNT ligand, is responsible for β-catenin degradation by proteasome. Consequently, cytoplasmic β-catenin accumulates and is transported to the nucleus (160), where it binds TCF/LEF TFs to activate the transcription of target genes involved in cell proliferation, survival and differentiation, such as *MYC* and *CCND1* (**Figure 15**).

In the absence of WNT ligands, β-catenin is captured by the destruction complex and degraded through the proteasome in the cytoplasm. Under these conditions, TCF/LEFs act as transcriptional repressors of WNT/β-catenin target genes by interacting with the Groucho/transducin-like enhancer of split (Gro/TLE) repressor family (161). On the contrary, upon WNT signaling activation, β-catenin physically displaces Groucho from TCF/LEFs and transiently converts these proteins into activators of WNT-target genes.

2.1.2. Non-canonical WNT signaling

Compared to the canonical pathway, much less is known regarding the non-canonical WNT signaling, which can be further subdivided into the WNT/Planar Cell Polarity (PCP) and WNT/Calcium (157,162)(**Figure 15**). Non-canonical WNT ligands (WNT4, WNT5a, WNT5b and WNT11A) bind to Frizzled receptor as well as a variety of several co-receptors with a cysteine-rich binding domain (e.g., ROR1/2, RYK and CTHRC1) (163). In the WNT/PCP pathway, WNT ligands lead to the activation of small GTPases such as Rac1 and Rho that, along with their effectors, remodel the actin cytoskeleton. This controls cell polarity as well as cell migration.

Finally, in the WNT/Calcium, ligand binding triggers the activation of phospholipase-C (PLC), resulting in higher calcium levels inside the cell and leads to the transcription of *NFAT* genes.

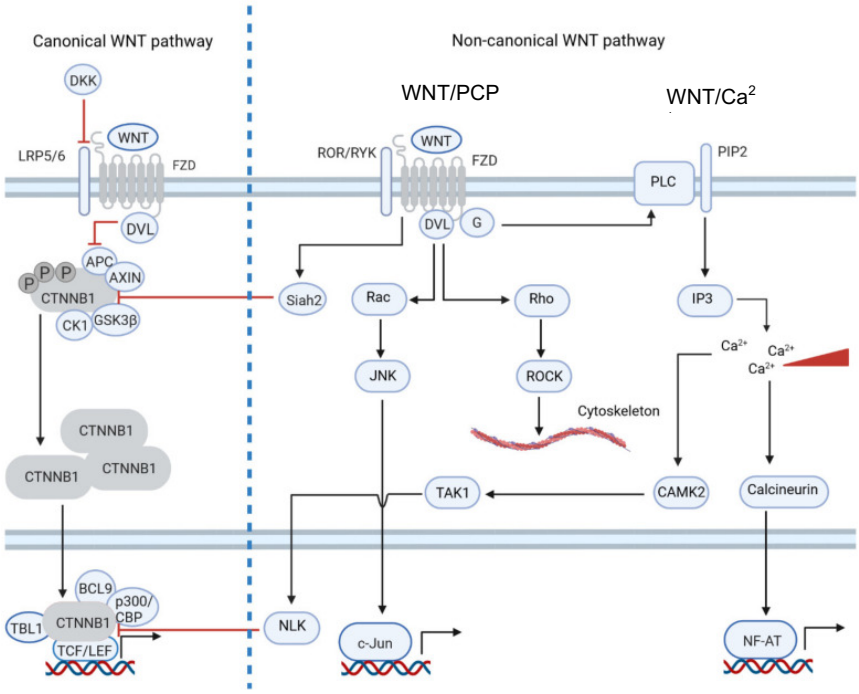


Figure 15. WNT signaling pathways. Canonical and non-canonical (WNT/PCP and WNT/Calcium). WNT pathways are usually activated by different set of WNT ligands and Frizzled (FZD) receptors. Retrieved from Urbanek, 2022 (164).

2.2. The TCF/LEF family

The TCF/LEF family is composed of four members: TCF7, LEF1, TCF7L1 and TCF7L2. The full-length isoforms of these members contain several functional domains, which are highly conserved in various metazoan organisms. These conserved domains are HMG-box DNA-binding domain, nuclear localization signal (NLS) and N-terminal β-catenin-binding domain (**Figure 16**). TCF/LEFs bind DNA by a monomeric HMG box domain found near the C-terminal region that recognizes the consensus sequence 5′-ACATCAAAG-3′, also called the WNT response element (WRE) (165), present in numerous regulatory regions (promoters and enhancers)

(166,167). TCF/LEFs interact with both co-repressor and activator complexes, being β-catenin probably the most potent activator identified (168). Binding to β-catenin is mediated through a conserved N-terminal motif. In the case of LEF1 TF, it also contains a context-dependent regulatory domain (CRD) that participates in WNT-independent activation of certain genes such as the T-cell receptor α-chain (TCRα) gene, which is (167,169) essential for the expression of TCRα in developing thymocytes. In addition, TCF/LEFs are also known as architectural TFs, as their own binding to the minor groove of the DNA causes a strong bend in the DNA with a specific angle, and exert functions independently of WNT/β-catenin signaling by interacting with cofactors such as ALY, ETS, TFE-3 and Sp1 (170). For example, LEF1 has been shown to bind the TCRα enhancer and induce a sharp bend in DNA *in vitro*, which, in turn, facilitates interaction of ETS and RUNX family of TFs that bind to sequences flanking the LEF1 site (167,171).

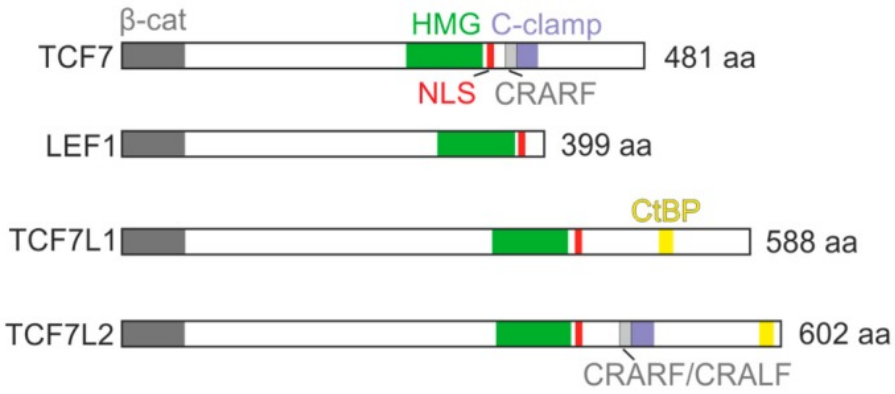


Figure 16. Functional domains of TCF/LEF Ts. The diagrams show the position of conserved functional domains in the TCF/LEF family members encoded by Ensembl database transcripts ENST00000395029 (encodes human TCF7), ENST00000265165 (LEF1), ENST00000282111 (TCF7L1), ENST00000627217 (TCF7L2). β-cat, β-catenin-binding domain (gray); HMG DNA-binding domain (green); NLS (red); C-clamp DNA-binding motif (blue); CtBP, the domain mediating interaction with the C-terminal binding protein (yellow). Retrieved from Hrckulak, 2016 (154).

TCF/LEFs proteins display common structural features and are often expressed in overlapping patterns, denoting their redundancy (e.g., LEF1 and

TCF7) (154). However, individual family members also display unique features. For instance, TCF7L1 behaves mainly as a repressor and LEF1 as an activator, while TCF7 and TCF7L2 display dual transcriptional effects depending on the cellular context (172). In addition, TCF/LEF factors display complex expression patterns to increase diversity from a single gene in a very context-specific manner, by means of tissue-specific enhancers, alternative promoters, alternative exon cassette splicing and alternative splicing sites (173). Thus, there is a myriad of protein variants that can be expressed depending on cell states and cell types. In human and mouse cells, there are two promoters that produce *LEF1* mRNA (**Figure 17**). The first promoter drives the expression of the full-length (FL) LEF1 isoform (44 kDa) that interacts with β-catenin and respond to WNT signaling (174). In contrast, the second alternative promoter, located in the second intron of LEF1 gene, drives the expression of an isoform lacking β-catenin domain, which has been described as a dominant negative LEF1 (dnLEF1) isoform (32 kDa) as it cannot activate WNT target genes due to the lack of interaction with β-catenin (175) (Figure 17). These two isoforms were first described in colon cancer, where cancer cells predominantly express high levels of LEF1-FL isoform, while downregulating the expression of dominant negative isoform (176).

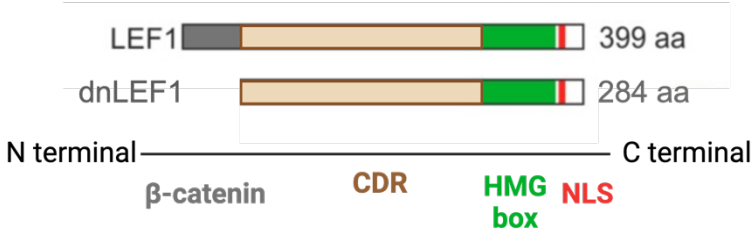


Figure 17. LEF1 isoforms. The diagram shows the position of conserved functional domains in LEF1-FL and dnLEF1 isoforms. The dnLEF1 isoform lacks -catenin-binding domain (gray) but shares with the LEF1-FL the context-dependent regulatory domain (CDR), DNA binding domain (HMG box, green) and the nuclear localization signal (NLS, red). Adapted from Hrckulak, 2016(154).

2.3. Role of LEF1 in normal hematopoiesis

Different studies have described the WNT-β-catenin-TCF/LEF signaling cascade in the context of lymphopoiesis and/or hematopoiesis (177,178). In fact, it has been shown that WNT/β-catenin pathway is essential for maintenance, activation and proliferation of normal hematopoietic stem cells (HSCs) (179,180). However, specific functions of LEF1, apart from WNT signaling, have also been reported. For example, in human CD34+ hematopoietic progenitor cells, inhibition of LEF1 but not of β-catenin, impaired proliferation and survival mechanisms in these cells, supporting the β-catenin–independent function of LEF1 in early human myelopoiesis (181)

LEF1 is required for the early development B and T/NK lymphocytes (**Figure 18**). In the T cells, LEF1 and TCF1 control T-cell maturity and T-cell lineage commitment processes (182,183). T cell differentiation is severely impaired in fetal thymic organ cultures from mice carrying inactivation of *Lef1* and *Tcf7* genes, but not in cultures from mice carrying single loss of one of these genes alone (184). This indicates that LEF1 and TCF1 play an important, and partially redundant, role in T cell differentiation. Some these actions are β-catenin independent, as the interaction between TCF1/LEF1 with RUNX3 is required for silencing of *Cd4* gene in mice, leading to the formation of CD8+ T cells in the thymus (185,186). Furthermore, LEF1 and TCF1 positively regulate the immunosuppressive functions T_{reg} cells by inducing the expression of the signature genes, such as *Ikzf4* (187). Both LEF1 and TCF1 are expressed at varying levels during T cell differentiation within the thymus and in mature peripheral T cells in mice (184). Similarly, in humans, LEF1 is expressed in all types of mature of T lymphocytes, being especially high in naive CD4+ T cells (both T_{helper} and T_{reg}) (data from The Human Protein Atlas).

The role of LEF1 in the development of B cells has been less examined than in T cells (**Figure 18**). LEF1 expression is restricted to B-cell precursors, with

expression turned off at later stages of B lineage development, being totally absent in mature B cells (152). Mice lacking LEF1 have reduced numbers of pro-B and pre-B cells (188). The loss of LEF1 leads to reduced proliferation and increased apoptosis of pro-B cells caused by elevated levels of *Fas* transcription.

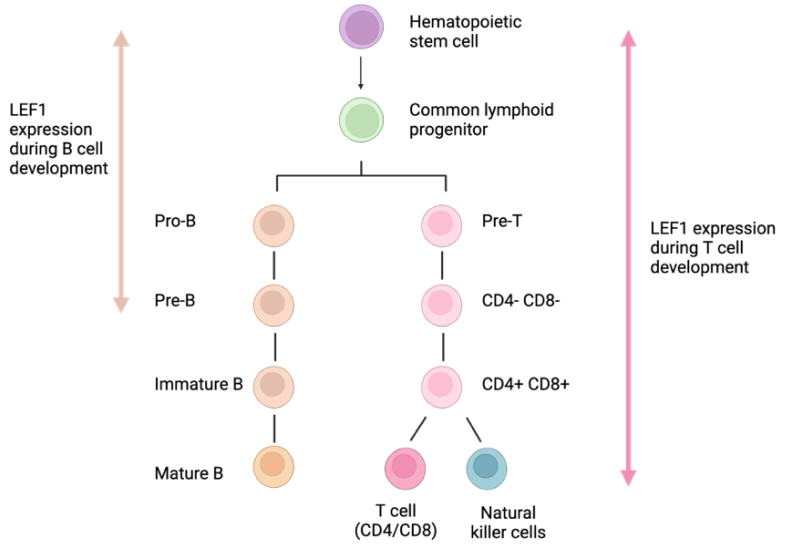


Figure 18. LEF1 expression during B and T-cell development. Lymphocytes develop from HSC via common lymphoid progenitor. *LEF1* is present during all the stages of T-cell development as well as mature T cells or natural killer cells. On the contrary, *LEF1* is switched off in immature B cells and no longer present in any type of mature B cell. Created with Biorender.com

2.4. Role of LEF1 in cancer

WNT pathway deregulation and malfunction is observed in a variety of cancers, including leukemia, lymphoma, lung adenocarcinoma, prostate cancer and colorectal cancer (CRC) (152,176,189,190). In the case of CRC, the activation canonical WNT pathway, by increased translocation of β-catenin into the nucleus, is critical in the transformation of the malignant cells (191,192). In addition, LEF1 is aberrantly expressed in CRC cells while it is not expressed in the normal intestine (176). Interestingly, CRC cells express LEF-FL but not the dnLEF1 isoform, suggesting the dependence on WNT/β-catenin pathway for its oncogenic role.

Knockdown of *LEF1* decreased the growth of subcutaneous CRC xenograft (193). Furthermore, LEF1 remodels the cytoskeleton of CRC cells, controlling the epithelial/mesenchymal-transition, that is linked to cancer invasion and metastasis (194). In general, LEF1 expression is associated with an unfavorable outcome in solid cancers (195).

High levels of LEF1 are detected in several hematological malignancies, such as Burkitt lymphoma, chronic lymphocytic leukemia (CLL) (152), B-cell acute lymphoblastic leukemia (B-ALL) (196), acute myeloid leukemia (AML) (197) and acute promyelocytic leukemia (198). Keeping in line with this, mice transplanted with murine HSCs retrovirally transduced to overexpress LEF1-FL isoform developed B-ALL and AML, without the need to co-express other oncogenic factors in this model (199). *In vitro* studies showed a pro-survival effect of LEF1 in the AML1-*ETO*–positive leukemic cell line (200) and CLL cells (152). In addition, the prognostic significance of LEF1 expression depends on the disease. Higher LEF1 expression is linked to a better prognosis in AML patients (201), while it is associated to unfavorable prognosis in CLL (202,203) and adult B-ALL (196).

Taken together, all these reports indicate that LEF1 is involved in the early oncogenesis or progression of both solid and hematological cancers.

2.5. Role of LEF1 in CLL

The canonical and non-canonical WNT pathways have been described to play a significant role in the development of CLL (157). CLL is known for its overexpression of several WNT ligands, receptors and effector transcription factors (164). Regarding the non-canonical pathway, CLL cells overexpress the ROR1 receptor (**Figure 19A**) (204) and show a high expression of its ligand, *WNT-5a*, which is linked to poor prognosis (157) (**Figure 19B**). In fact, *WNT-5a* mRNA levels are useful to distinguish patients with worse outcome within the prognostically favorable M-CLL subgroup (205). In terms of canonical WNT pathway, high levels

of *WNT3*, the most overexpressed WNT ligand in CLL, are associated to good prognosis (206). Moreover, *WNT3* declines with disease progression. Finally, LEF1 and TCF4 (*ITF2*) are two downstream effectors of canonical WNT pathway overexpressed in CLL (164). Finally, high *LEF1* mRNA levels seem to be linked to an unfavorable outcome (**Figure 19C**) (202,203), associating high levels of *LEF1* with the U-CLL subtype. These results are controversial, since other studies have not encountered any differences in *LEF1* expression levels between U-CLL and M-CLL cases (207,208).

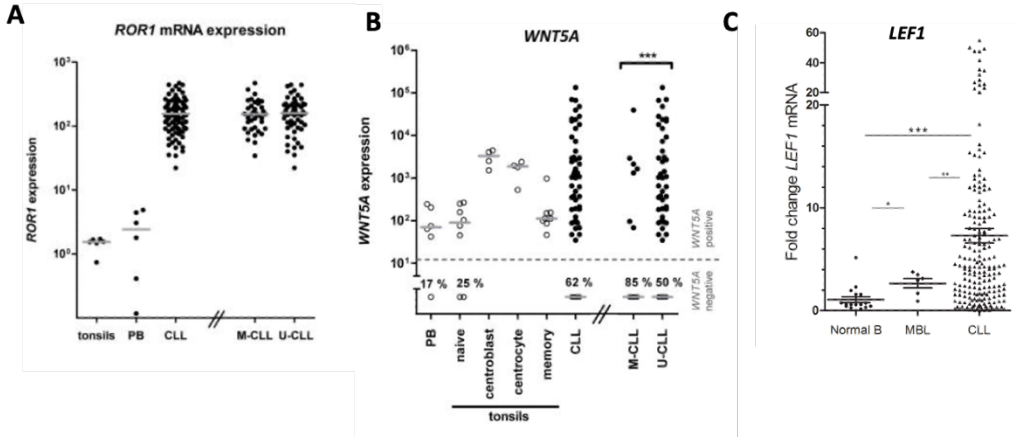


Figure 19. WNT-associated genes deregulated in CLL. A) *ROR1* mRNA is uniformly overexpressed in all CLL, regardless of the IGHV mutational status, when compared to healthy PB and tonsillar B cells. B) *WNT5A* signals via *ROR1*. Relative expression of *WNT5A* mRNA in untreated CLL samples and in non-malignant B cells from tonsil or PB. C) Relative expression of *LEF1* mRNA in untreated CLL patients, MBL and normal B cells. Retrieved from Janovská, 2016 (205) and Wu, 2016 (203).

Despite all the biological and clinical heterogeneity occurring in CLL, LEF1 expression is a unifying characteristic (hallmark) of all prognostic groups. Overall, *LEF1* shows a stable gene expression across samples independently of the IGHV status (207,208). However, cases with trisomy 12 have been reported to express significantly lower levels of *LEF1* (207). As it was mentioned before, LEF1 is required in the early phases of B-cell development, but there is virtually no expression of *LEF1* in any type of normal mature B cells (152,163,188). In contrast, LEF1 expression is also high in premalignant MBL state as well as CLL, where LEF1

has a pro-survival role (152)(**Figure 19**). Assessment of LEF1 protein expression by immunohistochemistry (IHQ) determined that the majority of CLL cases expressed LEF1 (sensitivity > 70 %), which positively correlated with ZAP-70 levels (209,210). For this reason, LEF1 expression in CLL can be used as a differential diagnostic marker in CLL (150), as it is very useful to distinguish atypical cases of CLL from other B-cell chronic lymphoproliferative disorders that do not express LEF1.

While there is no expression of LEF1 in B cells, Gutierrez and colleagues reported that the levels of β-catenin levels were similar between B and CLL cells. In keeping with this finding, two other independent studies reported strong LEF1 nuclear signal in CLL samples with a remarkable absence of β-catenin staining in the nucleus of CLL cells (209,211), suggesting that the oncogenic action of LEF1 in the DNA of CLL cells might be β-catenin-independent. In fact, LEF1 can function as an architectural context-dependent TF and, subsequently, interact with alternative coactivator factors, such as intracellular NOTCH and ALY (212,213).

There are no genetic alterations in *LEF1* gene that could be responsible for its high expression or increased activity in CLL. On the contrary, the cause of LEF1 expression seems to be the *de novo* activation of the gene promoter, which is silenced in normal B cells (214). The drivers of this promoter activation are currently unknown. The downstream effects of *de novo* LEF1 expression in CLL are partly known. On the one hand, the LEF1 DNA binding motif was significantly enriched in the *de novo* epigenetic signature present in all CLLs, indicating the possible role of LEF1 as an oncogenic TF driving the chromatin reprogramming necessary for the leukemia initiation (135). On the other hand, little is known about the target genes of LEF1 in CLL. One candidate gene regulated by LEF1 in the CLL context is the cylindromatosis gene (*CYLD*) (215). Low *CYLD* expression is associated with U-CLL status and shorter overall survival. In this context, LEF1 acts as a transcriptional repressor of CYLD (216), which contrasts with the possible role

of transcriptional activator of newly active regulatory regions of CLL. CYLD is a deubiquitinating enzyme that regulates cell death (necrosis/necroptosis) and proliferation. Defect in its tumor suppressor activity has been implied in several cancers, including CLL (217). In this line, LEF1 knockdown in CLL cells led to higher CYLD levels and an increased sensitivity to necroptosis (215). This suggests that the necrotic signaling in CLL can be blocked by the action of LEF1.

In conclusion, the presence of LEF1 in the epigenetic signature of CLLness along with its pro-survival role in CLL cells suggest that LEF1 is an early pathogenic event in CLL. Further research is needed to uncover the direct role and mechanism of action of LEF1 (activator/repressor of transcription) in the chromatin of CLL cells, as well as its implications in the course of the disease. However, there are very few functional studies studying in depth the role of LEF1 in CLL due to the lack of appropriate CLL models *in vitro* and *in vivo*, which will be introduced in the following section.

3. *In vitro* an *in vivo* modeling of CLL to study disease pathogenesis

Functional studies in CLL have faced many obstacles because of the difficulties to genetically manipulate primary CLL cells and the lack of patient-derived cell lines or xenografts (218). Indeed, primary leukemic cells and the few existing cell lines are essential for the *in vitro* investigation of biological and molecular features of CLL (**Figure 20**). However, a number of major biological questions and the complete validation of new drugs need to be approached by using animal models (i.e., pre-clinical modeling *in vivo*). For years, due to the lack of known driver genetic lesions in contrast with other blood cancers, no CLL animal models could be generated (219). Currently, *in vivo* experiments are performed in transgenic or xenograft mouse models (**Figure 20**).

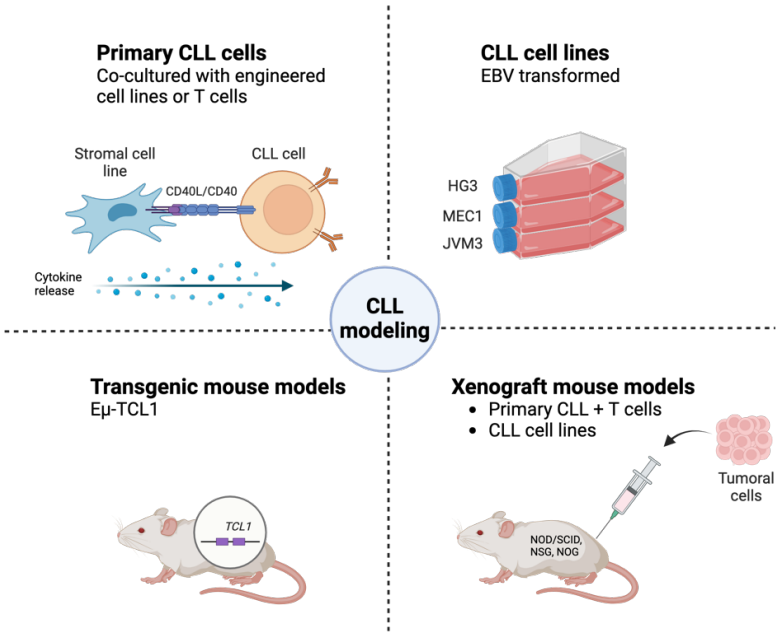


Figure 20. CLL modeling in vitro and in vivo. Patient-derived CLL cell lines can be used *in vitro* with the help of feeder stromal cells, engineered to express human T-cell factors and cytokines. Alternatively, cell lines derived from patients can be used. However, all of them are transformed with Epstein-Barr virus (EBV). For *in vivo* experiments, transgenic mouse models, displaying CLL cytogenetic aberrations or TCL1 oncogene overexpression, display a similar disease to advanced CLL. Xenograft models are generated through the injection of primary CLL + T cells or cell lines. Created with Biorender. Com.

3.1. CLL cell lines

Cell lines represent quick, easy to use and non-expensive methods to work with many cancer types. Unlike many other hematopoietic malignancies, there is a limited number of CLL cell lines (220). Failures in establishing CLL cell lines are well known, and all the existing CLL cell lines are either derived from Epstein-Barr virus (EBV)-seropositive patients or were established by *in vitro* EBV infection. EBV is not involved in the etiology of CLL, since generally CLL cells do not carry the EBV genome, but is needed to generate CLL cell lines by conferring patient-derived CLL cells the ability to proliferate indefinitely in the absence of the TME (220–222). The resistance of primary CLL cells to viral transformation and immortalization by EBV has been defined as the major reason for the lack of representative immortalized cell lines that accurately reflect the disease (223,224). In others words, while CLL cells express the virus receptor CD21 and can be infected, CLL cells usually do not transform to cell lines, due to a restricted expression of the EBV-encoded genes that does not induce proliferation (225–227).

In addition to EBV infection, CLL cell lines represent more aggressive forms of the disease (228). The few established cell lines have molecular features of high-risk (e.g., *TP53* mutations), unmutated IGHV genes and lack many primary features associated with clinical CLL (220,228,229). Although there are some cell lines (e.g., MEC1, MEC2 and JVM3) with mutated IGHV genes, they are derived from CLL patients with prolymphocytic transformation (230). The most well characterized CLL cell line, MEC1, bears mutated *TP53* as well (230). Therefore, these cell lines may not be very useful to study the initial events driving CLL pathogenesis as well as more indolent behavior of the disease.

Remarkably, most of the CLL cell lines (HG3, MEC1 and JVM3) do not recapitulate the chromatin activation signature of CLL, which is believed to be involved in the early leukemogenesis. Thus, at the chromatin level, they are

completely distinct from primary CLL cells. In addition, transformed and highly proliferative cell lines do not require microenvironmental stimuli to proliferate as primary CLL do. Consequently, the effects of different microenvironmental stimuli cannot be studied on them. In this line, in contrast to primary CLL cells, CLL cell lines have zero or very low expression levels of LEF1. Hence, CLL cells lines are poor representatives of the biological heterogeneity of CLL and might not be good models to assess the drivers of CLL origin, like in the case of LEF1, whose role in CLL seems to be influenced by microenvironmental stimuli.

3.2. Mouse models

3.2.1. Genetically engineered mouse models

Several mouse models mimicking genetic lesions found in CLL (13q14 deletion) and transgenic for genes overexpressed in the disease (e.g., *TCL1, APRIL, BCL2 x traf2dn, ROR1*) have been generated (218,219). The most used *in vivo* model of CLL is the T-cell leukemia/lymphoma 1 (Eμ-TCL1) transgenic mice (231). The Eμ-TCL1 is generated through engineering of *TCL1* oncogene under the control of the IGHV promoter-IgH-Eμ enhancer, thus overexpressing the human *TCL1* gene in all mouse B cells (**Figure 21**). Although *TCL1* is overexpressed in a subset of U-CLL cases with poor prognosis (232) and functions as an activator of NF-κB signaling (233,234), it is not a recurrent CLL genetic lesion and, consequently, the model does not reflect the genetic landscape of human CLLs. Eμ-TCL1 mice develop B220+ CD5+ lymphoproliferation at 100% penetrance by 2 months of age, with clonal overt disease by approximately 13-15 months. BCRs of TCL1 mice resemble those of aggressive human disease, with unmutated IGHV rearrangements, stereotypy and autoantigen/microbial recognition (219). Intriguingly, the leukemic cells from Eμ-TCL1 mouse model do not express Lef1 (personal communication from Dr. Martina Seiffert).

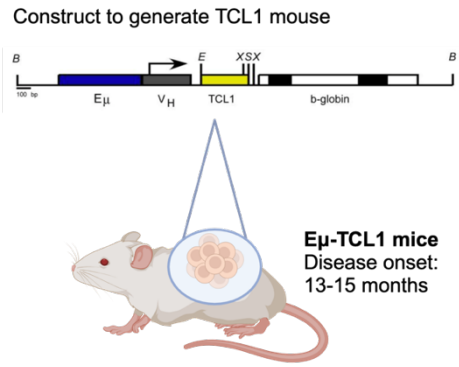


Figure 21. Generation of Eμ-TCL1 mouse model. Construct image was retrieved from Bichi, 2002.

All the previous mentioned mouse models present several limitations (235). First, the lymphoproliferative disorders develop late in life, which makes extremely cumbersome to test in reasonable time the effects of drugs or immunotherapeutic strategies. Second, the B-lymphoproliferations occurring in these models represent a more aggressive form of CLL, as all of them have expression of unmutated stereotypic BCRs, indicating a role of antigen in the expansion of the CLL clone. Third, the variable penetrance of the phenotype, with 100 % in the Eμ-TCL1, 50 % in 13q14 deletion and 5 % in ROR1 transgenic mice (235). The different tumor incidence highlights that the different genetic aberrations predispose to, but are not sufficient *per se*, for the malignant transformation of B cells (219). Similar results have been obtained when inducing knock in/knockout by CRISPR-Cas9 in genes recurrently mutated or deleted in CLL patients (236–238). In these new models, the onset of disease occurs late in life and the overt disease is highly aggressive as well, with variable penetrance (<40 %). Again, the low tumor penetrance suggests something else is needed for the malignant transformation of B cells, such as the tumor microenvironment and epigenetic dysregulation (219). In conclusion, new mouse models are expensive, time consuming and may not adequately reproduce the biological features of CLL,

including the absence of *Lef1* expression in the leukemic cells (personal communication from Dr. Elisa Ten Hacken).

3.2.2. Xenograft mouse models

In a xenograft model, human tumor cell or cell lines are transplanted into immunocompromised mice. To date, numerous attempts to xenograft primary CLL from PB have had no or very limited success compared with other B-cell malignancies (218). Initial efforts to xenotransplant human primary CLL cells were hampered due to the lack of mice immunodeficient enough to avoid the rejection of human cells. Then, the scenario changed because of the use of more severely immunodeficient animals (NOD/SCID and NSG mice), lacking mature B and T cells, with a highly restricted ability to reject xenogeneic cells (239,240). Even though U-CLL samples engrafted better than M-CLL, the proliferation of CLL cell population was not observed until expansion of patient-derived T cells (241–243). For this reason, to improve CLL engraftment, PB-derived CLL cells were co-injected with activated autologous CD4+ T cells (242). Nevertheless, the utility of xenografted mice was limited due to the short life span of recipient animals (4-12 weeks upon CLL injection)(219), which died due to an infiltration of human T cells into the liver, indicating a graft-vs-host disease (242). This somewhat limits the application of xenograft mice, as the death of mice was not due to tumor progression but an immunologic response from transplanted human T cells against the recipient mouse.

As an alternative, xenograft mice from CLL cell lines have been widely used (218). The key limitation of this model is that CLL-derived cell lines are EBV-transformed, which can drive proliferation independently of oncogenic mechanisms active in human CLL. In addition, CLL cell lines engage partially with murine microenvironmental component, given the incomplete homology between human/murine receptor-ligand pairs.

In summary, CLL mouse models are more complex than cell lines and allow the (limited) study microenvironmental interactions. However, both models represent a more aggressive form of the disease that is not reflecting the tremendous interpatient heterogeneity found in real life. Moreover, they lack LEF1 expression, which is one of the most specific CLL markers par excellence. The alternative (and last) option to overcome these limitations is the use of patient-derived CLL cells *in vitro*.

3.3. Primary CLL cells

CLL cells are extremely dependent on signaling coming from the microenvironment for survival and proliferation (244). Actually, CLL cells undergo rapid apoptosis when cultured *in vitro*, suggesting that a favorable *in vivo* microenvironment is required. To solve this, multiple *in vitro* systems for CLL have been developed to recreate the microenvironment (**Figure 22**). Among the most widely used and relevant systems are the bone marrow-derived stromal cell (BMSC) and NLC co-culture systems (245). The first BMSC and NLC systems showed an increased cell viability as well as a larger size in CLL cells (78,246). These beneficial effects were caused by direct cell-cell interaction, since CLL cells that were in the same media as stromal cells but not in contact with them, had no survival advantage. Although stromal co-culture systems induce pro-survival signaling and up-regulate anti-apoptotic proteins just by direct cell-cell contact, these systems are not sufficient to induce CLL proliferation *in vitro*.

Surprisingly, and contrary to *in vivo* data, ligation of the BCR on CLL cells using anti-IgM induces no or low proliferation *in vitro* (247,248). There is a considerable variability in response to anti-IgM *in vitro*, as most of BCR-responders were U-CLLs (248,249). Similarly, the addition of TLR stimulation via CpG-ODN induced a greater activated phenotype in U-CLLs cells than M-CLLs (250,251).

In addition to activation of the BCR and TLR signaling pathways, it has been shown that CLL proliferation highly depends on T-cell derived factors and cytokines (252) (**Figure 22**). Indeed, *in vitro* CLL cells virtually never divide spontaneously until they are provided with factors produced by T_{helper} cells (253,254), some of which are:

- CD40L: membrane molecule from T_{helper} cells that binds to CD40 receptor in CLL cells. It provides B cells with the T_{helper} signals needed for activation, differentiation and prevention of apoptosis (255,256). In CLL cells, its binding results in enhanced activation of NF-κB and increased cell viability of CLL. The pro-survival effect is more potent when the ligand is displayed on the cell membrane of the supportive cell line (257). Even though CD40L induces activation of CLL cells, it is not enough to promote proliferation in CLL cells.
- IL-4: it is secreted by T_{helper} cells and supports the *in vitro* survival of CLL cells by itself, but without inducing their division, as it relies on pre-activating the CD40 pathway (258). Thus, a combination of CD40L and IL4 usually induces a weak proliferation in CLL cells (259,260), which can be increased in U-CLLs with the addition of CpG-ODN (261).
- IL-21: it is typically secreted by follicular dendritic T_{helper} cells. This cytokine strongly potentiates CD40L/IL4 stimulation (262) and induces higher proliferation of CLL cells in an antigen independent manner (253,263). However, IL-21 can show a pro-apoptotic effect in quiescent CLL cells (263) and other B-lymphomas (264).

In response to a combination of these factors, CLL cells regain their activated phenotype, increased proliferation and increased cellular adhesion to stromal cells (252). These factors can be added in soluble form to CLL cells alone or in co-culture with stromal cells. However, the effects are even better when supportive stromal

cell lines are genetically engineered to express T-cell factors and anti-apoptotic cytokines like BAFF and APRIL (265,266).

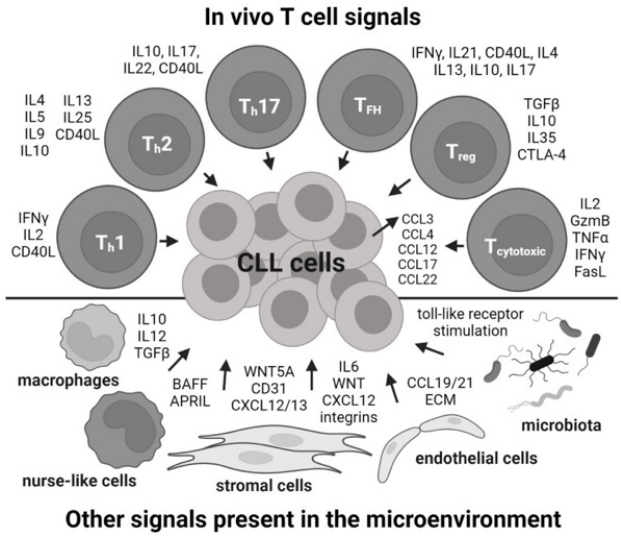


Figure 22. Microenvironmental signals provided by several T-cell subsets and other cell types in immune niches. Retrieved from Hoferkova, 2022.

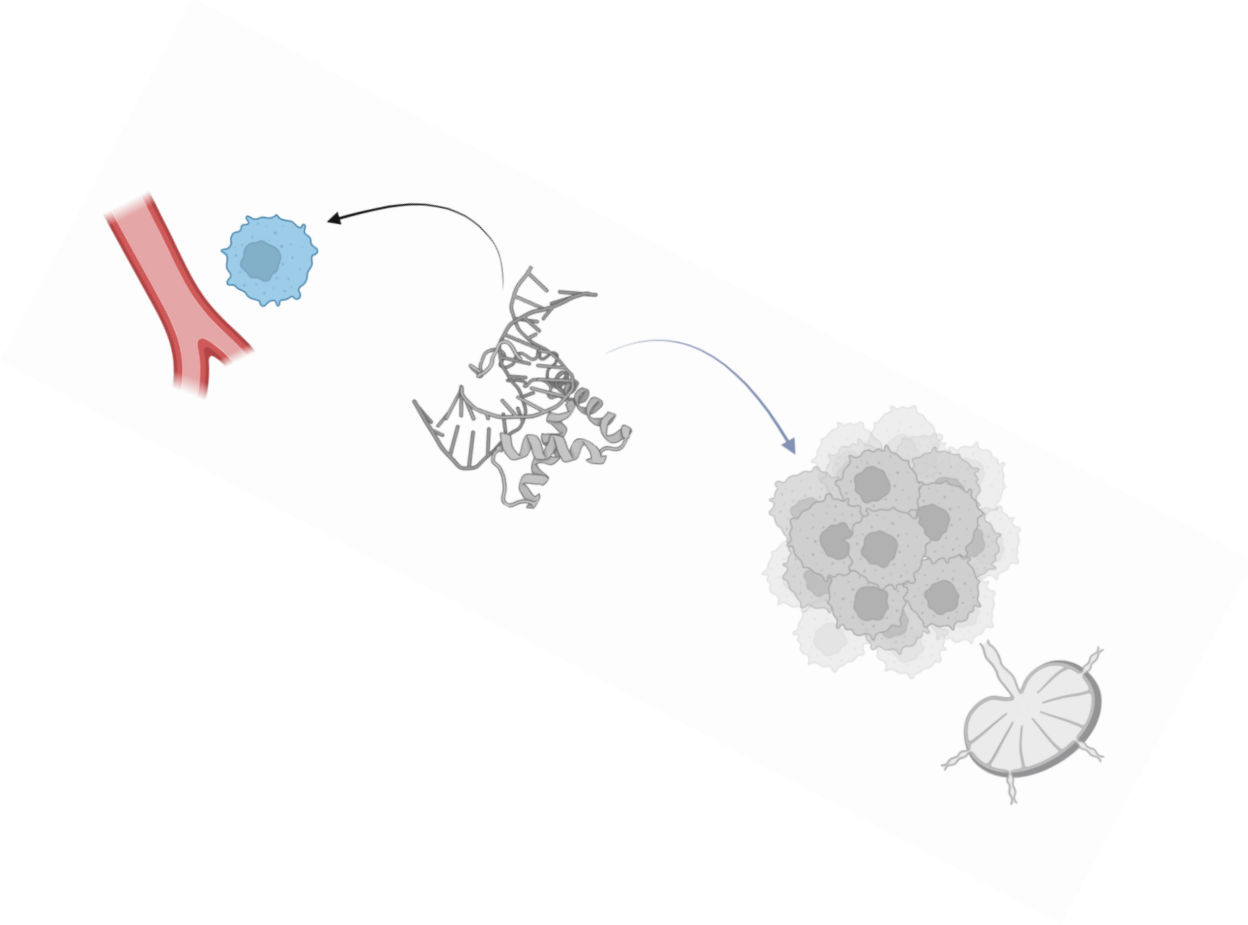
In conclusion, primary CLL cells seem to represent the most suitable model to study CLL biological and clinical heterogeneity and present high levels of LEF1. Nonetheless, CLL cells are challenging to manipulate *in vitro* and require the use of more sophisticated co-culture systems to sustain CLL viability and proliferation. Additionally, primary CLL cells are difficult to transfect and have a number of limited divisions *in vitro*, thus limiting studies at both gene and protein levels (266).

3.1.1. *In vitro* culture with MM1 stromal cells

Attempts to infect primary CLL cells using retro- and lentivirus vectors for gene transfer have been unsuccessful for decades, limited by low transfection efficacy (<1%) and substantial toxicity, which have made downstream analyses impossible (267). To overcome these limitations, Mangolini and coworkers developed a method to effectively infect primary neoplastic human B cells using engineered forms of viral envelopes derived from the gammaretrovrius family (266), which had been demonstrated to effectively transduce normal tonsillar B

cells (265). In addition, the authors established a cell culture system that induced a vigorous proliferation of CLL cells *ex vivo* to facilitate the transduction with retroviruses. The cell culture system was based in murine BMSC expressing human CD40L and secreting human BAFF and IL-21. The combination of these new viral vectors along with MM1 stromal cells permitted gene transfer with high transduction efficacy and minimal toxicity (266). Moreover, this *in vitro* system maintained patient-derived CLL cells with overall good viability for weeks. In the majority of the experiments carried out during this doctoral thesis to investigate the role of LEF1 in CLL, I used primary CLL cells seeded with this MM1 cell line.

Aims

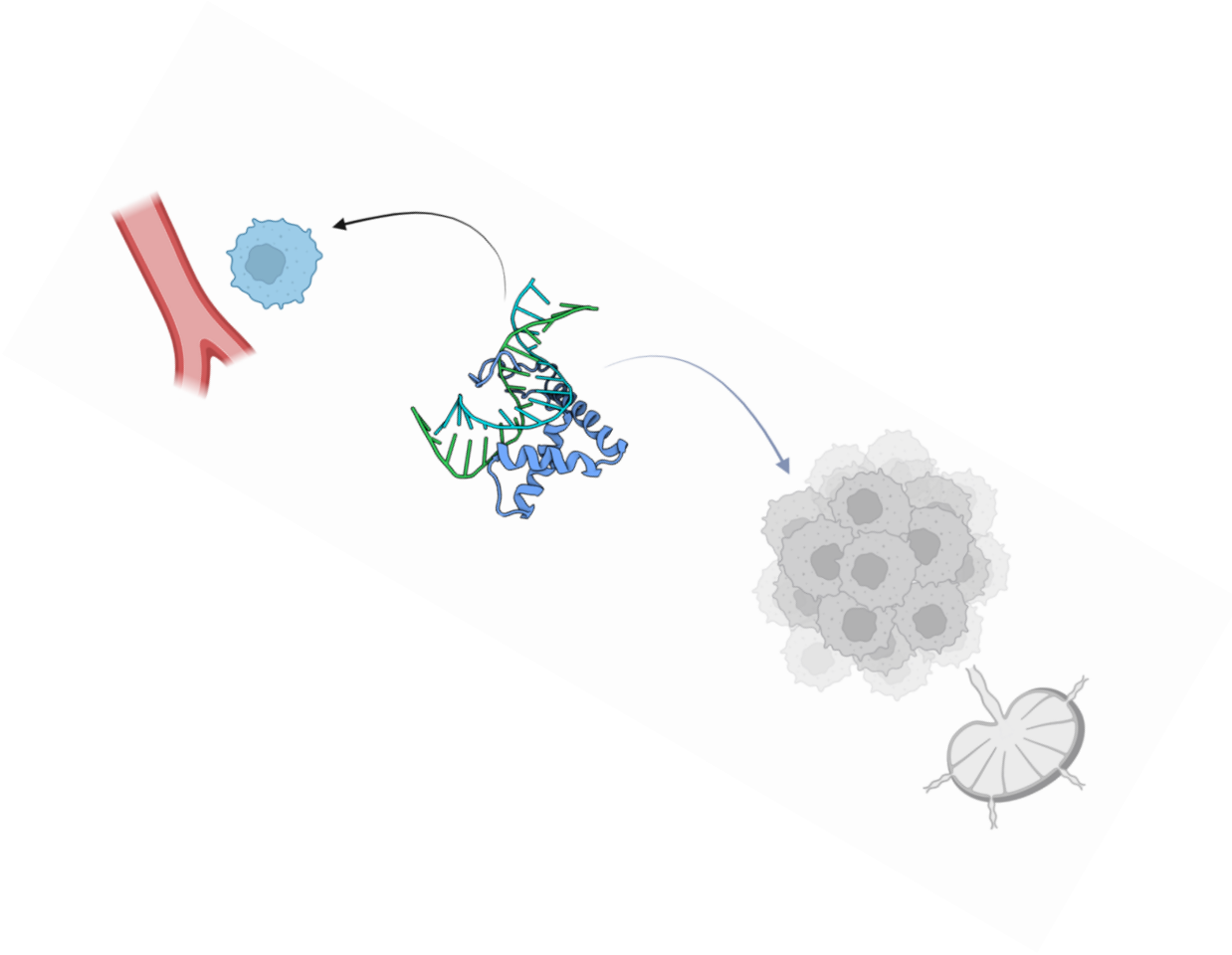


CLL is a genetically and clinically heterogeneous disease. Despite intensive research, the molecular mechanisms leading to CLL development and evolution remain incomplete. This is in part due to the inherent complexity of the disease, but also to the scarcity of suitable experimental models and the difficulties in performing functional experiments in patient samples. Additionally, although the genome, transcriptome and epigenome of CLL has been described, the role of transcription factors in CLL pathogenesis remains poorly understood. In this context, LEF1 is a CLL-specific transcription factor *de novo* expressed in all phases of the disease, from premalignant conditions to aggressive variants, and its binding motif is present in regulatory elements becoming active in CLL. Due to these facts, this thesis is based on the hypothesis that LEF1 is an early and key driver of CLL development. Therefore, the global aim of this doctoral thesis is to develop methods to functionally study primary CLL cells and apply these methodologies to elucidate the oncogenic role of the LEF1 transcription factor in CLL.

This global aim is divided into three specific aims, which are associated with the two results chapters of my thesis:

1. To characterize the phenotypic and transcriptional effects induced by a new cell culture system in patient-derived CLL cells (Study 1).
2. To develop a CRISPR/Cas9-based approach allowing gene inactivation in primary patient samples (Study 1).
3. To decipher the mechanisms of action and pathogenic role of *de novo* LEF1 expression in CLL (Study 2).

Material and methods



1. Cell culture

Healthy T/B cells and MBLs

PB mononuclear cells (PBMCs) were obtained from healthy donor buffy coats provided by Banc de Sang i Teixits (Barcelona, Spain) after Ficoll-Paque gradient separation (GE Healthcare). The PBMCs white layer was, then, purified for T and B cells. T cells were enriched by negative selection with the RosetteSep™ Human T Cell Enrichment Cocktail (STEM in the majority of the experiments of this doctoral thesis CELL technologies,). T cells were activated with anti-CD3/CD28 beads (ThermoFisher Scientific, Waltham, MA, USA) at a bead-to-cell ratio of 1:1 and cultured for 4 days at a density of $1x10^6$ cells/ml in Advanced Roswell Park Memorial Institute (RPMI) 1640 medium supplemented with 10% FBS, 1% penicillin/streptomycin (Gibco-ThermoFisher Scientific), 30 U/ml IL-2 (Miltenyi Biotec, Bergisch Gladbach, Germany) at 37 °C in a humidified incubator (5% CO2 and 95% atmosphere).

B cells were purified using $CD19^+$ magnetic beads and LS columns (Miltenyi Biotec) and purity > 98% was verified by flow cytometry.

In the case of MBL samples, PBMCs were obtained after Ficoll-Paque gradient separation from donors, but B cell fraction was not purified. PBMCs were cryopreserved with 10% DMSO (Sigma-Aldrich, St. Louis, MO, USA) and stored in liquid nitrogen until use at IDIBAPS Biobank. Patients' characteristics from MBL samples are described in **Appendix Table 2**.

Patients' samples (primary CLL) and MM1 feeder cells

Untreated CLL patients' samples were obtained from PB mononuclear cells from the Hematopathology collection registered at the Biobank (Hospital Clínic-IDIBAPS; R121004-094). All samples contained > 70 % of tumor content. Clinical

and biological characteristics of the patients are shown in **Appendix Table 1, 3 and 4**. The enrolled patients gave informed consent for scientific study following the International Cancer Genome Consortium (ICGC) guidelines and the ICGC Ethics and Policy committee (Consortium, 2010). This study was approved by the clinical research ethics committee of the Hospital Clinic of Barcelona. After thawing cells in primary CLL media, the cell suspension was centrifuged at 300 x g for 6 min and the supernatant was discarded. Then, CLL cells were resuspended at a concentration of $5x10^6$ cells/ml and cells were added to a 12-well plate of MM1 feeder cells (1 ml of CLL cells/1 well of MM1) in Advanced Roswell Park Memorial Institute medium (Advanced RPMI-1640) with GlutaMAX containing 10% FBS (Gibco), 1% penicillin/streptomycin (Gibco), 25 mM HEPES and 7 μM 2-Mercaptoethanol and kept at 37°C in a humidified incubator (5% CO_2 and 95% atmosphere). After 2-3 days, CLL cells were counted and seeded $1x10^6$ cells/well into a new 12-well plate of stroma. Passages of CLL cells occurred every 2 days.

MM1 feeder cells (murine bone marrow-derived stromal cell line)(266) were cultured in MEM Alpha+GlutaMAX medium (ThermoFisher Scientific) supplemented with 10% FBS, 10% horse serum (Sigma-Aldrich), 10 μM 2-Mercaptoethanol and 1% penicillin/streptomycin. $3x10^5$ feeder cells were seeded in a 12 multi-well plate coated with 0.1% gelatin 24 hours before the addition of primary CLL cells.

Cell lines

Lenti-X 293 T cell line (kindly given by Dr. Ingo Ringshausen, University College London (UCL), London, UK) was cultured in Dulbecco's modified Eagle's medium (DMEM, Invitrogen) containing 10% FBS, 1% penicillin/streptomycin and 1 mM GlutaMAX (Gibco). CLL cell lines HG3 and MEC1 (all kind gifts from Dr. Lluís Hernández, IDIBAPS, Barcelona, Spain) were cultured Roswell Park Memorial Institute medium (RPMI-1640) with GlutaMAX containing 10% FBS and 1% penicillin/streptomycin. Cell lines were kept at 37 °C in a humidified incubator (5%

CO_2 and 95% atmosphere). All cell lines used in this study were confirmed to be free from mycoplasma contamination with EZ-PCR Mycoplasma Detection Kit (Biological Industries).

2. Flow cytometry

Cells were washed with FACS buffer (PBS + 2% FBS) and centrifuged at 2000 rpm for 3 min. Cell surface antigens were stained at 4°C for 20 min using a mixture of fluorophore-conjugated antibodies. When intracellular or transcription factor staining was needed, cells were fixed and permeabilized using the eBioscience Foxp3/Transcription Factor Staining Buffer Set (ThermoFisher Scientific). After extracellular staining cells were washed with FACS buffer and 0.5 ml of fixation/permeabilization buffer was added to each tube. Then, cells were incubated in dark conditions for 30 min at room temperature (RT). After cells had been fixed and permeabilized, they were washed with 2 ml of permeabilization buffer (2000 rpm for 3 min at RT). Next, intracellular staining was performed by adding the conjugated primary antibody (**Table 1**) recognizing the intracellular protein of interest in the cells and incubating it for 30 min at 4°C. Finally, cells were washed with 2 ml of permeabilization buffer (2000 rpm for 3 min at RT). LEF1 levels were assessed in PB-derived healthy T, B, MBL and CLL cells (day 0) as well as after *in vitro* stimulation in T, B and CLL cells (day 4 in T cells and day 6 in B and CLL cells).

Samples were acquired on a LSR II Fortessa 4L cell analyzer (BD Biosciences) and analyzed using FlowJo v10 software (BD Biosciences). In the case of cell lines, FACS cell sorting was performed using the FACS Aria SORP (BD Biosciences) by the expression of reporter proteins (EGFP, mCherry or BFP); and, for primary samples, CLL cells were sorted by aqua- CD19+/CD5+ at day 0 (from the PB cryotube) and day 6 after co-culture with MM1 cells.

Antibody	Conjugate	Clone	Staining	Dilution	Company
Anti human CD19	APC	SJ25C1	Extracellular	1:100	BD Biosciences, San Jose, CA, USA
Anti human CD20	FITC	2H7	Extracellular	1:10	BD Biosciences
Anti human CD20	PB	2H7	Extracellular	1:100	BioLegend
Anti human CD5	PE	L17F12	Extracellular	1:200	BD Biosciences
Anti-human CXCR4	PE	12G5	Extracellular	1:100	BD Biosciences
Anti-human CD38	APC	HIT2	Extracellular	1:100	BD Biosciences
Anti human CD3	FITC	7D6	Extracellular	1:50	ThermoFisher
Anti human LEF1	AF647	EPR2029Y	Intracellular	1:5000	Abcam
Anti human Ki67	PE	SolA15	Intracellular	1:20000	Invitrogen

Table 1. Primary antibodies used for flow cytometry experiments.

Cell viability and cell proliferation

Cell death was analyzed using LIVE/DEAD Fixable Aqua Dead Cell Stain (1:300, ThermoFisher Scientific) and, for some experiments, a combination of annexin V-FITC (1:100, Invitrogen) with 7-AAD (1:1000, Sigma-Aldrich).

Cell proliferation was assessed with Ki67 staining (1:20,000) as well as with CellTrace Violet or CFSE Cell Proliferation Kit (ThermoFisher Scientific, #C34571 and #C34554). For the staining with CellTrace (Violet or CFSE), NTC and LEF1 CRISPR-edited CLL cells were washed twice with warm PBS and resuspended with PBS at a concentration of $10x10^6$ cells/ml. Then, 0.5 μM of CellTrace Violet/CFSE was added to the cells. After 10 min incubation at 37°C in dark conditions, the staining was stopped by adding an equal amount of 100% warm FBS for 10 min at RT. Finally, cells were washed twice. CellTrace Violet/CFSE was followed by flow cytometry at the right after the staining and 3-6 days later.

3. CUT&RUN

Chromatin Immunoprecipitation, Cleavage Under Targets & Release Using Nuclease (CUT&RUN) was performed following the standard protocol (144) with some modifications. After 6 days in culture, CLL cells were carefully separated from MM1 cells and centrifuged at 600 x g for 3 min at RT. 0.5 million CLL cells were used per condition. Briefly, 0.5 million cells were resuspended in 100 µl/sample of RT Wash Buffer and centrifuged at 600 x g for 3 min at RT. After two washes, cells, resuspended in 100 µl/sample of Wash Buffer, were conjugated with 10 µl/sample of activated Concanavalin-coated magnetic beads (#BP531, Bangs Laboratories) after 10-min incubation at RT. Binding of antibodies was done overnight with 50 µl of antibody buffer (containing a final concentration of 0.01% of digitonin) and an antibody dilution of 1:50. Antibodies used were anti-LEF1 (ab137872, Abcam)/anti-BRD4 (#13-2003, EpiCypher)/anti-RNA Polymerase II (#2629S, Cell Signaling Technologies), against our protein of interest, and anti-rabbit IgG (#12-370, Merck Millipore) as a control. On the next day, beads were washed three times with 250 µl of cold Digitonin-wash buffer. Binding of pAG-Mnase was done for 2 hours at 4°C on the nutator, in 150 µl of Digitonin-wash buffer (containing 0.05% of digitonin) and 700 ng/ml of the pAG-MNase protein (kindly shared with us by Dr Manuel Serrano, IRB, Barcelona). To start chromatin digestion freshly prepared 0.1M $CaCl_2$ was added to each sample, mixed by pipetting and incubated for 30 min on ice. To stop the reaction 100 µl of Stop Buffer was used, followed by 30 min incubation at 37ºC with gentle mixing. Samples were placed on a magnet stand to remove the beads, and supernatant containing the digested chromatin was transferred to a new tube and incubated with 2 µl SDS 10 % and 2.5 µl proteinase K 20 mg/ml for 1 h at 50°C to degrade proteins and increase the DNA purity of the sample. Finally, DNA was extracted with phenol-chloroform (ThermoFisher Scientific).

Libraries were done following Nan Liu's protocol (268) with the NEBNext Ultra II DNA library preparation kit (#E7645S, Illumina) and were sequenced with Illumina NextSeq 500, High output v2.5 kit generating 75-bp paired-end sequences. The quality of the sequencing data was checked using FastQC (v0.11.9). The detailed step-by-step protocol for library preparation can be found in protocol.io (DOI: **dx.doi.org/10.17504/protocols.io.bagaibse**).

CUT&RUN data analysis

Processing of the sequenced library data was done using the R package *cutruntools2.0* (269), using default parameters and the option of keeping 120 bp fragments. Peak calling was done using MACS2 (v2.2.6), on deduplicated reads, using the IgG as control. A cut-off of 0.01 false discovery rate was used as a threshold and paired-end was taken into account. Peaks located in sexual chromosomes were filtered out. Then, motif enrichment analysis of LEF1 peaks were performed in a window of +/- 200 bp around peak summits using Centrimo with default parameters (270).

Genomic annotation of peaks was done using R package *ChIPseeker* (v1.38.0)(271). Transcript promoter regions were defined as those 2000 bp upstream to 500 downstream of transcription start sites.

Enrichment of CUT&RUN peaks in specific genomic locations (Promoters, Exons, Introns and Distal intergenic regions) was assessed with Chi-square tests. First, we defined a background collection of regions by binning the hg38 genome into 250-bp bins. Next, we compared the proportions of annotations between CUT&RUN peaks and genomic bins from different genomic elements using the full genome of bins as background. All tests were adjusted for multiple testing using FDR and odds ratios were used as a measure of enrichment.

Gene set overrepresentation analyses of genes mapping to CUT&RUN peaks were performed with R packages *goseq* (v1.54.0). First, the genes mapping to peaks were kept if they were protein-coding and expressed (> 1 TPM) in our CLL samples (unstimulated and sitmulated) RNA-seq data. Next, GSEA were performed using Gene Ontology and Reactome databases from MsigDB (272) accessed using the R package *msigdbr* (v7.5.1). We used as background all protein coding genes (excluding sex- or MT-chromosome genes) and corrected the data within *goseq* for gene length to account for bias due to differential detection of CUT&RUN peaks. Gene sets with less than 15 or more than 1,000 genes were filtered out from the results. Gene sets were considered significant at FDR < 0.05 and odds ratio > 1.5.

4. CUT&Tag

Cleavage Under Targets and Tagmentation (CUT&Tag) was performed with CUT&Tag-IT Assay Kit (#53160, Active Motif, Carlbad, CA, USA) as described in the kit's protocol. After 6 days in culture, CLL cells were carefully separated from MM1 cells and centrifuged at 600 x g for 3 min at RT. Initially, 0.1 million cells were incubated overnight with Concanavalin A beads along with 1 µL of the primary antibodies: IgG rabbit (#12-370, Merck Millipore) as a control, H3K4me3 (#39060, Active Motif), H3K4me1 (#C15410194, Diagenode), H3K27me3 (#39157, Active Motif), H3K27ac (#C15410196, Diagenode). Following the secondary anti-rabbit antibody incubation (1:100), tagmentation was carried out at 37 °C using protein-A-Tn5. To terminate the tagmentation process, a mixture of EDTA, SDS, and proteinase K was added, and the reaction was incubated at 55 °C. Subsequently, DNA extraction and ethanol purification were performed followed by PCR amplification and barcoding using the CUT&Tag-IT Assay Kit, facilitating the identification and differentiation of the DNA fragments. Processing of CUT&Tag data (and peak calling) was performed as previously indicated with the CUT&RUN data.

5. DNA extraction

DNA purification was performed with phenol-chloroform and phase lock gel eppendorfs. Basically, phenol:chloroform:isoamyl (Sigma-Aldrich) was added to the samples with digested chromatin (1 volume P:C:I/1 volume sample, v:v) and it was mixed thoroughly. Then, samples were centrifuged for 5 min at 13,000 rpm. Gel from phase lock eppendorfs separated DNA from the dense phenol-chloroform. After that, chloroform:isoamyl (Sigma-Aldrich) was added to the DNA (v:v) in the phase lock gel eppendorfs and, again, mixed well by pipetting up and down. Samples were centrifuged for 5 min at 13,000 rpm. DNA, from the liquid phase, was precipitated overnight with 2 μg glycogen and 100% ethanol. On the next day, samples were centrifuged at 13,000 rpm for 10 min at 4°C. Supernatant was removed and DNA was washed with 100% ethanol by centrifuging at 13,000 rpm for 5 min at 4°C. DNA pellet was air-dried for 5-10 min and, afterwards, resuspended in nuclease-free water. Quantification of DNA was carried out with Qubit Fluorometer according to manufacturer's instructions (ThermoFisher Scientific).

6. CRISPR interference

A two-vector system was used to perform CRISPR interference (CRISPRi) to silence target genes in CLL and MCL cell lines (HG3, MEC1, Z138 and JVM2). First, cell lines were transduced with a lentiviral vector encoding for dCas9-KRAB repressor domain (see Part 2 of the Study 1, in the results, for the optimization and selection of dCas9 vectors). Then, they were sorted to obtain cell lines stably expressing dCas9-KRAB repressor, which were, subsequently, transduced with a lentiviral vector encoding for a sgRNA against the target gene of interest. Cells expressing sgRNA were either selected with puromycin or GFP+ depending on the vector used for sgRNA expression. In the case of sgRNA vector with puromycin resistance gene, cell lines were selected with 3 μg/ml for 48 hours. The level of gene

expression downregulation after CRISPRi was determined by real time-quantitative PCR (RT-PCR) or western blot.

Most of the sgRNA sequences (5'-3'), listed below (**Table 2**), were designed with Off-Spotter tool from Thomas Jefferson University (273).

Target gene	Name	sgRNA sequence	Source
-	NTC	AAAATAGCAGTAAACTCAAC	Brunello library
UBE4A	*UBE4A*	GCACTTCAGGCTCTGGTAAGAC	Weissman lab https://weissman.wi.mit.edu
MYC	*MYC*	GCTGTAGTAATTCCAGCGAG	Fulco et al, 2016
LEF1	*LEF1* sg1	GCCGAGCCGACCCACCGCAA	Off-Spotter
LEF1	*LEF1* sg2	GAGGCGCTTTATCGGGTCTTC	Off-Spotter
LEF1	*LEF1* sg3	GAGCCGGGCACTAGTCCTGCA	Off-Spotter
LEF1	*LEF1* sg4	GACCCTTGAGTTACCCCTCTG	Off-Spotter
LEF1	*LEF1* sg5	GAACTCTGCGCCACGGACGA	Off-Spotter

Table 2. sgRNA sequences used for CRISPRi.

7. Electroporation-based CRISPR-Cas9

All the details in the optimization of CRISPR-Cas9 protocol are described in in the Part 2 of Study 1. Guide RNAs (gRNAs), IDT Electroporation Enhancer 100 µM (#1075915) and Cas9 62 µM (#1081058) were purchased from Integrated DNA Technologies (IDT). Briefly, gRNA was composed by the annealing of crRNA and tracrRNA-ATTO550/ATTO488 (#1075928 and #10007810, IDT). Crispr RNA (crRNA) and tracer RNA (tracrRNA) were mixed at equimolar concentrations in a sterile microcentrifuge tube to a final concentration of 44 µM, heated at 95°C for 5 min and cooled down at RT (15-25°C). Electroporation transfection was performed on the Neon Transfection System (ThermoFisher Scientific). Prior to transfection 0.5 µl gRNA (40 µM), 2 µl IDT Electroporation enhancer (10.8 µM) and 0.5 µl Cas9 (36 µM) were mixed and incubated for 20 min at RT to allow the formation of the ribonucleoprotein complex (RNP). For double gRNAs transfection experiments, 0.5

µl g*CD19* (36 µM), 0.5 µl *CCND2* g1, 2 µl IDT Electroporation enhancer (10.8 µM) and 1 µl Cas9 (36 µM) were mixed and incubated for 20 min at RT. Final molar ratio of RNP complexes is 1:1 gRNA:Cas9. These volumes of gRNA, Cas9 and electroporation enhancer can be used in the range of 0.3-1·10^6 cells.

Primary cells were counted, washed with PBS and resuspended in Buffer R from the Neon Electroporation System kit (10 µl of Buffer R per 1x10^6 cells) (**Figure 23**). Then, 1x10^6cells in 10 µl of Buffer R were added to the RNP complex and electroporated in the Neon system with the 10-ul pipette tip. Electroporated cells were immediately transferred to a pre-warmed 12-well plate coated with MM1 cells and maintained until day 4 or 8 after electroporation.

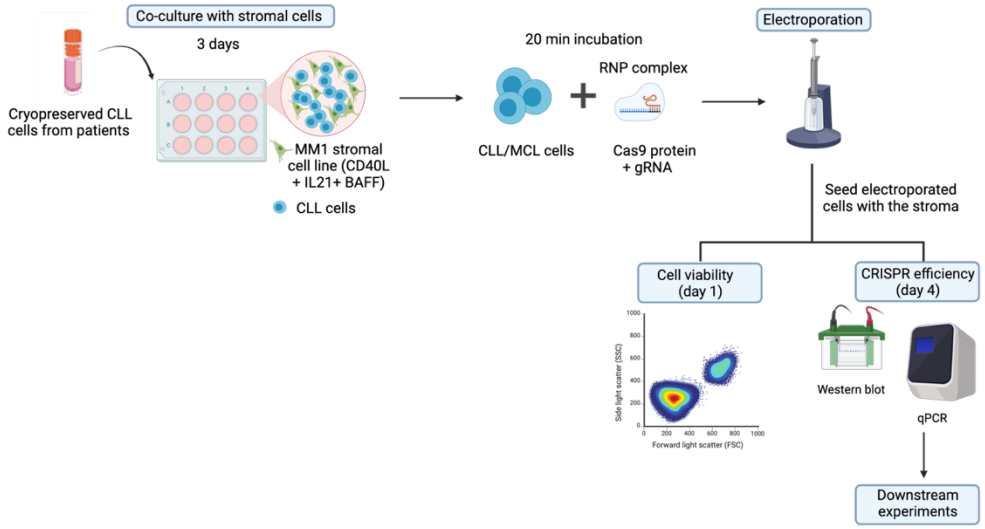


Figure 23. Schematic representation of electroporation-based CRISPR-Cas9 protocol. Adapted from Mateos-Jaimez, 2023 (274).

The sequences (5'-3') of the gRNAs (**Table 3**) used for each target gene were:

Target gene	Name	gRNA sequence	Source
OR2H1	Negative control	GATGGCCTTTGACCGATACG	Brunello library
-	Non-targeting control (NTC)	AAAATAGCAGTAAACTCAAC	Brunello library
CD19	*CD19*	CGAGGAACCTCTAGTGGTGA	Wu, 2018 (275)
CCND1	*CCND1* g1	CGTGCCTCCGTAGGTCTGCG	Brunello library
CCND1	*CCDN1* g2	GTGTTCAATGAAATCGTGCG	Brunello library
CCND2	*CCND2* g1	ATGTGCTCAATGAAGTCATG	Brunello library
CCND2	*CCDN2* g2	CACTTGAAGTAGGAGCACTG	Brunello library
LEF1	*LEF1* g1	TCAGGAGCCCTACCACGACA	IDT
LEF1	*LEF1* g2	GCAGTCAAATAAAGTGCCCG	Brunello library
MYC	*MYC* gRNA	CTTCGGGGAGACAACGACGG	Brunello library
USP10	*USP10* gRNA	ACTGACCAAAATCAGCCCCG	Brunello library

Table 3. gRNA sequences used for electroporation-based CRISPR-Cas9 protocol.

8. TIDE analysis of gene editing

Genomic DNA from NTC and *CD19*-edited CLL and MCL cells was collected at day 2, 4 and 8 after transfection and extracted using the QuickExtract™ DNA Extraction Solution (Lucigen, #QE0905T). A PCR from the extracted DNA using the Kapa HiFi HotStart Ready Mix (Roche #7958927001) was carried out with primer pairs spanning the targets sites at the *CD19* gene. Amplified DNA was subsequently Sanger sequenced. Edited and control sequences were then analyzed using the TIDE analysis tool (276) to determine the percentage of insertion/deletion (indel) mutations found in the DNA edited pools. The designed primers are listed below (5'-3'):

CD19 forward: GCAGACACCCATGGTTGAGTG

CD19 reverse: CAGCGTTATCTCCCTCTGTGGA

9. RNA extraction

RNA purification was performed with TRIzol (ThemoFisher Scientific) and phase lock gel eppendorfs. Cell pellets were resuspended and homogenized with 0.5-1 ml TRIzol. After 5-min incubation, the lysates were passed 20 times through a needle with a syringe 20G. Next, 0.2 ml of chloroform:isoamyl was added per 1 ml of TRIzol reagent. After mixing properly, samples were incubated for 3 min at RT and centrifuged for 15 min at 12,000 x g at 4°C. Following centrifugation, the mixtures separated into a lower red phase (phenol-chloroform), an interphase, and a colorless upper aqueous phase (RNA). The aqueous phase was transferred to a new tube and RNA was precipitated by mixing with glycogen (10 μg) and isopropanol (Sigma-Aldrich)(0.5 ml per 1 ml TRIzol used). Samples were incubated overnight at -20°C. Next, samples were centrifuged for 10 min at 12,000 x g at 4°C. Supernatant was removed and RNA pellet was washed twice with 75% ethanol (1 ml ethanol per 1 ml of TRIzol) by centrifuging for 10 min at 8,000 x g at 4°C. RNA pellets were air-dryed for 5-10 min and resuspended in nuclease-free water. Finally, RNA concentration and A260/A280 ratio > 1.8 from samples was assessed with NanoDrop (ThermoFisher Scientific).

10. Expression analysis/RT-qPCR

Complementary DNA (cDNA) was obtained from 1 μg RNA by using the qScriptTM cDNA SuperMix kit (QuantaBio). Quantitative reverse-transcription polymerase chain reaction (RT-qPCR) was performed on cDNA using the fast SYBR reagents and the CFX96 Touch Real-Time PCR Detection System (Biorad). Target gene (*CCND2 and UBE3A*) expression levels were normalized to *GAPDH* and values

are represented as fold change relative to control using the ΔΔCt method. The human designed primers are listed below (5'-3'):

CCND2 forward: CCTCCAAACTCAAAGAGACCAG

CCND2 reverse: TTCCACTTCAACTTCCCCAG

UBE4A forward: CAGCTGGAAAGCCTCAAATC

UBE4A reverse: GGCATTTGCAAAAGTGTCCT

GAPDH forward: CAAGATCATCAGCAATGCCT

GAPDH reverse: AGGGATGATGTTCTGGAGAG

11. Plasmids

CRISPR interference

2nd generation of lentiviral vectors for dCas9 and single guide RNA (sgRNA) expression were purchased from Addgene repository. Vector used for dCas9 expression was pLV-dCas9-KRAB-PGK-HygR (#83890) and vectors used for sgRNA expression were named lentiGuide-Puro (#52963) and pAW12.lentiguide.GFP (#104374). The reference number of these three vectors can be used to retrieve further information about them.

LEF1 isoforms overexpression

For overexpression of LEF1 isoforms FL, I6 and I5 in HG3 and MEC1 cell lines, 3rd generation lentiviral vectors were constructed and packaged by VectorBuilder (Chicago, IL, US). Each vector had a different reporter gene to differentiate the three isoforms by flow cytometry (**Table 4**). Reporter genes (*EGFP*, *mCherry* and *BFP*) were located before the CDS of *LEF1* isoform to avoid the addition of T2A peptide at the C-terminal of *LEF1* transcripts.

Overexpression vector	Vector name in VectorBuilder	Vector ID in VectorBuilder
Stuffer (control vector)	pLV[Exp]-Puro-EF1A>mCherry	VB900084-0158zxv
EGFP-LEF1-FL	pLV[Exp]-EF1A>EGFP(ns):T2A:hLEF1[NM_016269.5]	VB231212-1090ave
mCherry-LEF1-I6	pLV[Exp]-EF1A>mCherry(ns):T2A:hLEF1[NM_001130714.3]	VB231212-1488vqd
BFP-LEF1-I5	pLV[Exp]-EF1A>TagBFP2(ns):T2A:hLEF1[NM_001130713.3]	VB231212-1487qmy

Table 4. LEF1 overexpression vectors.

The vectors ID can be used to retrieve all detailed information about the vectors on vectorbuilder.com.

12. Lentiviral infection

CRISPR interference

2nd generation lentiviral packaging plasmids p8.91 and VSV-G (kindly given by Dr. Pedro Jares, IDIBAPS, Barcelona) were used as follow: 2 µg p8.91 (gag-pol), 1 µg VSV-G (envelope) and 4 µg of dCas9-ZIM3 vector were used to transfect 10 cm^2 dish of Lenti-X 293T (confluence 70%), after mixing with 1 ml of Opti-MEM media (Invitrogen) and 21 µl of polyethylenimine (Polysciences) and 30 min incubation at RT. Cell media was changed on the next morning and, after 24h, the virus supernatant was filtered through a 0.45 µM filter (Merck Millipore). If needed, media was replenished and harvested again at 24 h later. For lentiviral transduction, $1–2 \times 10^6$ target cells were resuspended with 4 ml of viral supernatant and infected by centrifugation (900 × g, 30 min at 37 °C) with the addition of 10 µg/ml Polybrene (Merck Millipore) in 6-well plates. Viral supernatant was replaced after 6 h of incubation by centrifuging target cells (400 x g, 5 min at RT) and adding fresh media. Cells were maintained in the incubator, at 37 °C with 5% CO_2 for 3–4 days before analyzing by FACS. Transduction efficiency

was assessed by flow cytometry measuring reporter protein mCherry expression. Cells were sorted and, after initial expansion, they underwent a second round of lentiviral infection to express sgRNA vectors. After 3-4 days of infection, double positive cells, containing dCas9-mCherry and sgRNA-GFP vectors, were analyzed and followed up by flow cytometry.

LEF1 isoforms overexpression

3rd generation lentiviral packaging plasmids RRE, Rev and VSV-G (kind gift from Dr. Sonia Guedan, IDIBAPS, Barcelona) were used as follows: 7.5 µg RRE (gag-pol), 7.5 µg Rev (gag-pol), 3.5 µg VSV-G (envelope), and 9 µg of LEF1 overexpression vector were used to transfect each 10 cm^2 dish of Lenti-X 293T. Transfection and lentiviral infection of target cells was performed as described before.

13. Microarrays data

Gene expression levels

Microarray-based gene expression data from MBL (N=46) and CLL (N=411) cases generated from a previous study (41) were used to assess and compare gene expression levels of LEF1 and CDC5L between M-CLL (N=264) and U-CLL (N=147) (t-test or Wilcoxon depending on the normal distribution of the data). Gene expression levels (rma) were represented in boxplots with *ggplot2* R package (v3.3.5) (277).

Time-to-first treatment analysis-

To analyze the prognostic differences, patients were categorized into two groups based on a cut-off of the continuous variable (*CDC5L*/*CELF2* mRNA levels) defined by R package *maxstat* (278). Then, TTFT variable was analyzed according to the Kaplan-Meier method with the R package *survival* (279) and p-values were calculated by the long-rank test.

14. RNA-sequencing and data analysis

Stimulated (day 6 in culture with MM1 cells) and unstimulated (day 0, from the cryotube) CLL cells were sorted by CD19 expression and RNA was extracted. Similarly, RNA from NTC and LEF1-edited primary CLL cells (sorted at day 4 post-CRISPR) was extracted as well. Cell lines with LEF1 overexpression and control vectors (n=2 replicates per isoform/cell line) were sorted by reporter protein expression at day 6 after infection and RNA was extracted as indicated before. The resultant RNA was assayed for quantity and quality using Qubit RNA HS Assay (Life Technologies).

Total RNA strand-specific RNA libraries were prepared using 200 ng of total RNA with the Stranded RNA Prep Ligation kit with RiboZero Plus (Illumina) following manufacturer's recommendations and sequenced on a NextSeq 2000 (Illumina; 2 × 50 bp, aiming at >40 millions of paired-end reads/sample). Ribosomal RNA reads were filtered out using SortMeRNA (v4.3.2), using all rRNA databases provided by the tool (280). Non-ribosomal reads were trimmed using trimmomatic (v0.39) (281). Quality control of the original and trimmed FASTQ files was performed using FastQC (v0.11.9). Gene-level counts (GRCh38.p13, Ensembl release 105) were calculated using kallisto (v0.46.1)(282) and tximport (v1.22.0).

Principal component analyses (PCAs) from RNA-sequencing (RNA-seq) data were performed using the *prcomp* function (*Stats* package) in R software.

Differential gene expression analysis

Differential expression was conducted using R package *DESeq2* (version 1.30.1) (283). Shrinkage of effect size was performed using the apeglm method (284). For cell lines, adjusted p-value (Q) <0.01 and absolute log2-transformed fold change (log2FC) >0.5 were used to identify differentially expressed genes (DEGs).

For primary CLL samples, p-value (Q) <0.01 was used to identify DEGs. Heatmaps of selected genes were generated using *ComplexHeatmap* package (v2.6.2) (285).

Gene set enrichment analysis

Gene set enrichment analyses (GSEAs) were conducted with GSEA software (v4.1.0)(286), using the pre-ranked modality and log2FC results obtained from DESeq2 as input data. Hallmark gene sets, the C2 curated gene sets, the C3 motif gene sets, the C5 gene ontology gene sets (Molecular Signature Database v7.5), and custom gene sets were used. Significant enriched pathways, with false discovery rate (FDR) < 0.05 or 0.01 were represented in bar plots.

15. Inhibition of protein synthesis and proteasome degradation

After 6 days in culture, CLL cells were carefully separated from MM1 and resuspended with primary CLL media at 10^6 cells/ml. CLL were left untreated (DMSO vehicle) or exposed to 50 µM cycloheximide (CHX, #M7449, Sigma-Aldrich), 5 µM MG-132 (#239765, Sigma-Aldrich) and a combination of both drugs for 4, 8 and 12h. After the treatment, cells were collected for protein extraction.

16. Protein extraction and western blot

For total protein extraction, sorted CLL cells from day 0 and day 6, as well as unsorted CLL cells from day 6, were lysed with RIPA buffer (50 mM HEPES pH 7.6, 1 mM EDTA, 0.7% Na deoxycholate, 1% NP-40, 0.5 M LiCl) complemented with protease inhibitors (Complete EDTA-free tablets, Roche). For subcellular fractionation experiments, lysates were prepared using a Subcellular Protein Fractionation Kit for Cells, according to manufacturer's instructions (Pierce). A total of 15-20 µg protein was separated by SDS-PAGE gel electrophoresis using 9 % poly-acrylamide gels, blotted to nitrocellulose membranes (ThermoFisher Scientific), and probed with the indicated primary antibodies diluted in 5 % BSA in TBS-T (**Table 5**).

Antibody	Clone	Reference	Dilution	Company
Anti-LEF1	EPR2029Y	ab137872	1:1000	Abcam
Anti-LEF1	B-6	sc-374522	1:200	Santa Cruz Biotechnology (SCBT)
Anti-CDC5L	2136C1a	sc-81220	1:200	SCBT
Anti-USP10	C-7	sc-365828	1:200	SCBT
Anti-cyclin D1	E3P5S	1675506	1:1000	Cell Signaling
Anti-cyclin D2	D52F9	3741	1:1000	Cell Signaling
Anti-β-catenin	D10A8	8480	1:500	Cell Signaling
Anti-cMYC	D84C12	5605	1:1000	Cell Signaling
Anti-β-actin	C-4	MAB1501	1:5000	Sigma-Aldrich
Anti-vinculin	hVIN-1	V9131	1:5000	Sigma-Aldrich

Table 5. Primary antibodies used for western blotting.

For visualization, the membranes were incubated with IRDye800CW goat-anti-rabbit or goat-anti-mouse IgG antibodies (1:5000, LI-COR, #925-32211 and 925-32210) for 1 hour at RT and then scanned with an Odyssey DLX Imaging System (LiCor). PageRuler Plus Prestained Protein Ladder (ThermoFisher Scientific) was used as molecular weight marker. Protein levels were quantified by ImageJ (NIH, MD, USA).

17. Total and nuclear immunoprecipitation

Total and nuclear immunoprecipitation (IP) were carried out in primary CLL cells and cell lines (HG3 and MEC1). All primary samples used for these experiments had been maintained for 6 days in culture with MM1 stromal cell line prior the immunoprecipitation experiments.

For co-IP of whole cell extracts, cells were lysed in TNN Buffer (50 mM Tris-HCl (pH 7.5), 100 mM NaCl, 5 mM EDTA, 0.5% Nonidet P-40, 6.25 mM NaF, 20 mM β-glycerophosphate, 1 mM DTT, 1x Protease Inhibitor Cocktail (Roche) and 1:10,000 benzonase (Sigma-Aldrich) and lysate was incubated overnight with the appropriate antibody, LEF1 (ab137872, Abcam) or IgG control (#12-370, Merck

Millopore), pre-bound to Protein G-Sepharose (Sigma-Aldrich). Immune complexes were pulled down and washed three times with TNN buffer, eluted with LDS Sample Buffer 1X (ThermoFisher Scientific), boiled at 70°C for 10 min (to separate antibodies from beads) and separated by SDS-PAGE.

For co-IP of nuclear protein extracts, the Nuclear Extraction Protocol (Invitrogen) was used. Briefly, cells were lysed in hypotonic buffer (20 mM Tris-HCL, pH7.4, 10 mM NaCl, 3 mM MgCl2 containing 1x Protease Inhibitor Cocktail (Roche) and 10% NP40 was added followed by centrifugation for 10 min at 3000 rpm at 4°C. The nuclear fraction pellet was resuspended in cell extraction buffer (Invitrogen) (complemented with 6.25 mM NaF, 20 mM β-glycerophosphate, 1 mM DTT, 1x Protease Inhibitor Cocktail (Roche) and 1:10,000 benzonase) for 30 min on ice with vortexing at 10-min intervals, followed by centrifugation for 30 min at 14,000 x g at 4°C. The nuclear fraction supernatant was used for IP, as described above. In this case, the magnetic beads used in IP were washed three times with PBS and prepared for mass-specrometry. Afterwards, for validation of LEF1 interactors partner, beads used in IP were washed three times with TNN buffer, eluted with LDS Sample Buffer 1X (ThermoFisher Scientific), boiled at 70°C for 10 min (to separate antibodies from beads) and separated by SDS-PAGE.

18. Mass spectrometry (mass-spec)

Sample preparation

Beads used in immunoprecipitation were cleaned three times with 500 µl of 200 mM ammonium bicarbonate and 60 µl of 6 M Urea / 200 mM ammonium bicarbonate were added. Samples were then reduced with dithiothreitol (30 nmol, 37°C, 60 min), alkylated in the dark with iodoacetamide (60 nmol, 25°C, 30 min) and diluted to 1M urea with 200 mM ammonium bicarbonate for trypsin digestion (1 µg, 37°C, 8h, #V5113, Promega).

After digestion, peptide mix was acidified with formic acid and desalted with a MicroSpin C18 column (The Nest Group, Inc) prior to LC-MS/MS analysis.

Data dependent acquisition (for LEF1 partners identification)

Samples were analyzed using an LTQ-Orbitrap Fusion Lumos mass spectrometer (ThermoFisher Scientific) coupled to an EASY-nLC 1200 (ThermoFisher Scientific). Peptides were loaded directly onto the analytical column and were separated by reversed-phase chromatography using a 50-cm column with an inner diameter of 75 μm, packed with 2 μm C18 particles.

Chromatographic gradients started at 95% buffer A and 5% buffer B with a flow rate of 300 nl/min and gradually increased to 25% buffer B and 75% A in 52 min and then to 40% buffer B and 60% A in 8 min. After each analysis, the column was washed for 10 min with 100% buffer B. Buffer A: 0.1% formic acid in water. Buffer B: 0.1% formic acid in 80% acetonitrile.

The mass spectrometer was operated in positive ionization mode with nanospray voltage set at 2.4 kV and source temperature at 305°C. The acquisition was performed in data-dependent adquisition (DDA) mode and full MS scans with 1 micro scans at resolution of 120,000 were used over a mass range of m/z 350-1400 with detection in the Orbitrap mass analyzer. Auto gain control (AGC) was set to 'standard' and injection time to 'auto'. In each cycle of data-dependent acquisition analysis, following each survey scan, the most intense ions above a threshold ion count of 10000 were selected for fragmentation. The number of selected precursor ions for fragmentation was determined by the "Top Speed" acquisition algorithm and a dynamic exclusion of 60 seconds. Fragment ion spectra were produced via high-energy collision dissociation (HCD) at normalized collision energy of 28% and they were acquired in the ion trap mass analyzer. AGC and injection time were set to 'Standard' and 'Dynamic', respectively and isolation window of 1.4 m/z was used.

Digested bovine serum albumin (#P8108S, New England Biolab) was analyzed between each sample to avoid sample carryover and to assure stability of the instrument and QCloud (287) has been used to control instrument longitudinal performance during the project.

Acquired spectra were analyzed using the Proteome Discoverer software suite (v2.5, ThermoFisher Scientific) and the Mascot search engine (v2.6, Matrix Science)(288). The data were searches against a Swiss-Prot human database (as in April 2023, 20422 entries) plus Q9UJU2-5, Q9UJU2-6, D6RAB1, D6RIV1 and a list of common contaminants (289) and all the corresponding decoy entries. For peptide identification a precursor ion mass tolerance of 7 ppm was used for MS1 level, trypsin was chosen as enzyme and up to three missed cleavages were allowed. The fragment ion mass tolerance was set to 0.5 Da for MS2 spectra. Ubiquitinylation of Lysines, phosphorylation of Serine, Threonine and Tyrosine, Oxidation of methionine and N-terminal protein acetylation were used as variable whereas carbamidomethylation on cysteines was set as a fixed modification. FDR in peptide identification was set to a maximum of 1%.

Parallel reaction monitoring (PRM) acquisition (for LEF1 isoforms identification)

Samples were analyzed using an LTQ-Orbitrap Fusion Lumos mass spectrometer (ThermoFisher Scientific) coupled to an EASY-nLC 1200 (ThermoFisher Scientific). Peptides were loaded directly onto the analytical column and were separated by reversed-phase chromatography using a 50-cm column with an inner diameter of 75 µm, packed with 2 µm C18 particles.

Chromatographic gradients started at 95% buffer A and 5% buffer B with a flow rate of 300 nl/min and gradually increased to 25% buffer B and 75% A in 52 min and then to 40% buffer B and 60% A in 8 min. After each analysis, the column was washed for 10 min with 100% buffer B. Buffer A: 0.1% formic acid in water. Buffer B: 0.1% formic acid in 80% acetonitrile. The mass spectrometer was

operated in positive ionization mode with nanospray voltage set at 2.4 kV and source temperature at 305°C.

A full MS scans with 1 micro scan at resolution of 30,000 were used over a mass range of m/z) 350-1400 with detection in the Orbitrap mass analyzer. A PRM (parallel reaction monitoring method was used for data acquisition with a quadrupole isolation window set to 1.4 m/z and MSMS scans over a mass range of m/z 300-2000, with detection in the Orbitrap at resolution of 60,000. MSMS fragmentation was performed using HCD at 30 NCE, the AGC was set to 1e5 and maximum injection time of 118 ms. Peptide masses (m/z) were defined in the mass list table (**Table 6**) for further fragmentation.

Skyline software (290)(v23.1.1.318) was used to generate the libraries (output of the data dependent acquisition searches) and extract the fragment areas of each peptide.

Peptide	Protein name	m/z	z	Note
EKLQESASGGKR	Q9UJU2-6 (I6)	430.5651	3	Unique peptide for I6
SSFPTCK	Q9UJU2-6 (I6)	413.6918	2	Unique peptide for I6
FSHHMIPGPPGPHTTGIPHPAIVTPQVK_z3	Q9UJU2 (FL)	984.1885	3	Unique peptide for FL z3
FSHHMIPGPPGPHTTGIPHPAIVTPQVK_z4	Q9UJU2 (FL)	738.3932	4	Unique peptide for FL z4
FSHHMIPGPPGPHTTGIPHPAIVTPQVK_Mox-z4	Q9UJU2 (FL)	742.3919	4	Unique peptide for FL z4 Methionine Oxidated
IFAEISHPEEEGDLADIK	Q9UJU2-5 (I5), Q9UJU2 (FL), Q9UJU2-6 (I6)	1006.9942	2	Common peptide for FL, I5 and I6
EHPDDGKHPDGGLYNK	Q9UJU2-5 (I5); Q9UJU2 (FL); Q9UJU2-6 (I6)	889.9083	2	Common peptide for FL, I5 and I6

Table 6. Peptide masses (m/z) defined in the PRM method for further fragmentation.

Mass-spec analysis

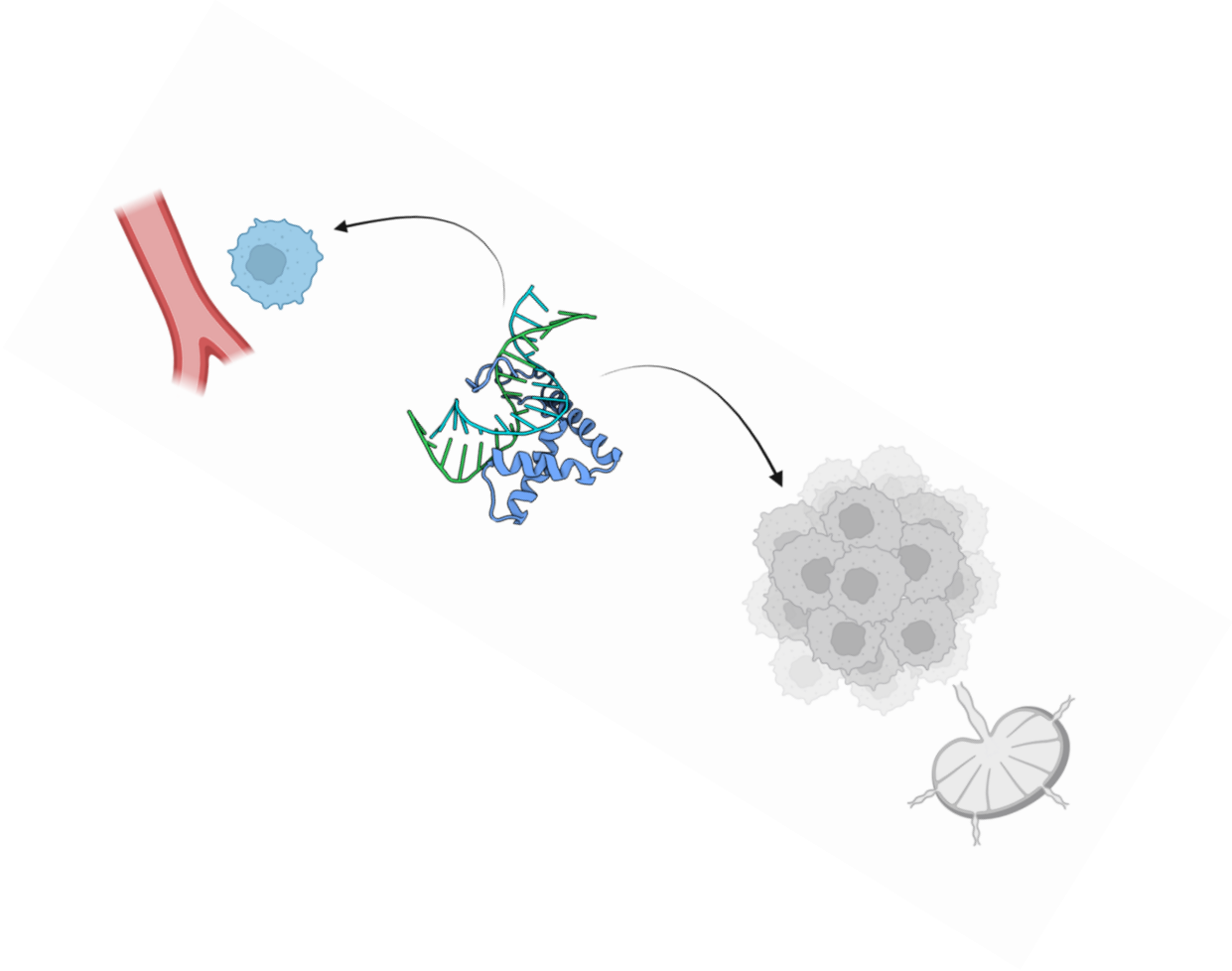
Protein/peptide identification in CLL samples was performed using the Proteome Discoverer software (v2.5). Peptides were filtered based on FDR and only peptides showing an FDR lower than 5% were retained. The final list of LEF1 interacting proteins was manually cleaned by excluding any protein that had < 2 peptides in the LEF1-immunoprecipitated conditions, potential contaminants (based on the www.crapome.org list), or those showing a log2FC < 10 abundance comparing LEF1 versus IgG control. To identify bona-fide interactors only those proteins

independently identified in the 2 U-CLL and 2 M-CLL cases studies were kept. Protein-Protein Interaction Networks and functional enrichment analysis of LEF1 interactors of each CLL subtype was performed with STRING database (291). Finally, DNA binding interactors were selected if present in at least two different references (292–295).

19. Statistical analyses

Data analyses were performed using GraphPad Prism 9.4.1 (GraphPad Software, La Jolla, USA). Unpaired or Paired Student's t-test was used to compare two groups in all experiments as indicated. Shapiro-Wilk test was used to test for normal distribution. In case of non-normal distribution, Wilcoxon or Mann Whitney U test were used. Statistical annotations were denoted with asterisks as follows: ****P <0.0001, ***P < 0.001, **P < 0.01, *P < 0.05, and not significant (ns) P > 0.05.

Results



Study 1: Characterization of a new *in vitro* culture system to develop CRISPR-based gene inactivating methods for primary CLL cells

The results derived from this Study 1 (part 2) have been published:

Mateos-Jaimez J*, Mangolini M*, Vidal A, Kulis M, Colomer D, Campo E, et al. Robust CRISPR-Cas9 Genetic Editing of Primary Chronic Lymphocytic Leukemia and Mantle Cell Lymphoma Cells. Hemasphere. 2023 Jun;7(6):e909 (PMID: 37304935).

Part 1: Characterization of the phenotypic and transcriptional effects of MM1 on primary CLL cells

1. Introduction

To overcome the extreme dependence of primary CLL cells on microenvironmental stimuli for survival and proliferation *ex vivo,* I co-cultured them with the MM1 cell line. MM1 cells are murine bone marrow-derived stromal cells that were engineered to express human CD40L at the membrane, and secrete BAFF and IL-21 (266). As the co-culture of CLL cells with MM1 cells is a relatively new *in vitro* system, the specific goal of this first part of the study was to define the phenotypic and transcriptional changes in CLL cells after being co-cultured with MM1 cells, to determine to which extent they resemble LN-derived cells. According to Mangolini et al., MM1 cells generate a cell culture system reminiscent of a LN environment that induces vigorous proliferation of CLL cells (266). LN-derived CLL cells show a distinct phenotype from PB-derived cells, which can be assessed by different expression of markers associated with lymphocyte activation and co-stimulation (CD69, CD86 and CD5) along with markers of adhesion and migration (CD38, CD49d and CXCR4) (296). Thus, 10 cases of CLL (5 U-CLL and 5 M-CLL) were thawed and cultured with MM1 cells for 6 days. Subsequently, phenotypic (by FACS) and transcriptomic analysis (by RNA-seq) were carried out (**Figure 24**). First, CLL cells were stained with CD19, CD5, CD69, CD86, CD38, CD49D and CXCR4 at day 0 (unstimulated), day 3 and day 6 in culture to assess immunophenotypic changes. In addition, cell viability was assessed with L/D Aqua dye and cell proliferation with CFSE and Ki67 at the indicated time-points. Second, at day 0 and day 6, RNA was extracted from CD19+ sorted cells and RNA-seq was performed to define the transcriptional changes associated with the co-culture of CLL cells.

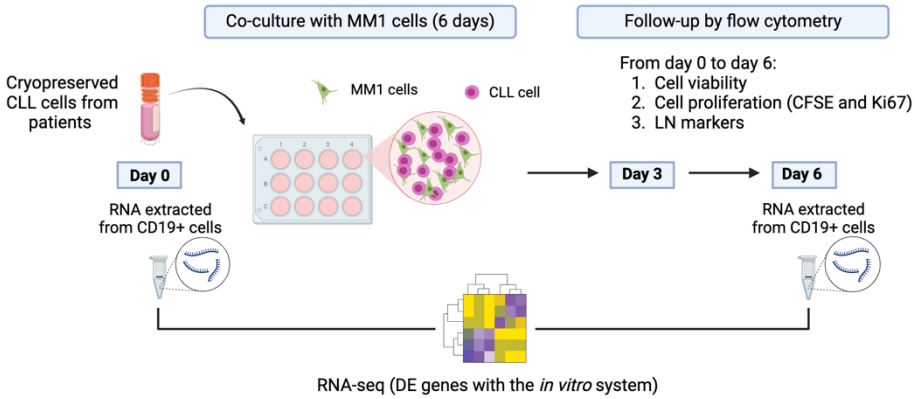


Figure 24. Schematic representation of the systematic characterization of the effects of MM1 in primary CLL cells at the immunophenotypic and transcriptomic level before and after stimulation. Created with Biorender.com.

2. Results

2.1. CLL immunophenotypic changes induced by with the *in vitro* system

Initial follow-up of primary CLL cells showed a significant decrease in cell viability after being in culture for 3 and 6 days, especially in the M-CLL subgroup (**Figure 25A**). CLL cells were maintained for 3 days with the same MM1 cells and, then, they were seeded into a new plate of stromal cells until day 6 (**Figure 25B**). Interestingly, when passages of CLL cells occurred every 2 days, no differences in cell viability were found between day 0 and day 6, indicating cell death was occurring as a consequence of the excessive accumulation of CLL cells. Moreover, the CLL fraction (CD19+/CD5+) from the cryotubes grew over time in culture (**Figure 25C**), while the number of T cells (CD3+ or CD19-/CD5+) present at day 0 decreased. This *in vitro* system enriched the tumor content present in culture and maintained CLL cells with good viability (> 70%).

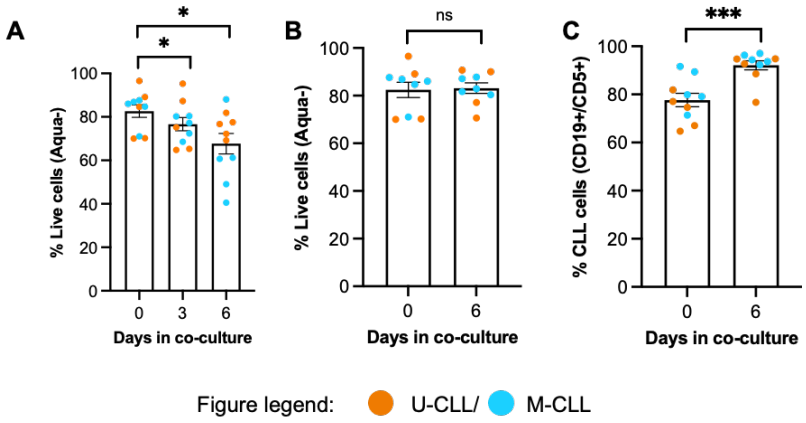


Figure 25. A-B) Bar plots represent the percentage (mean ± SEM) of live cells (Aqua-) at day 0, 3 and 6. C) Percentage of CLL cells (CD19+ and CD5+) present in at day 0 (cryotube: unstimulated cells) and day 6 (co-culture: stimulated cells). Orange dots represent U-CLL and blue dots M-CLL subtypes. Unpaired t-test was performed in all three figures.

Changes in CD5, CD69, CD86, CD38 and CXCR4 expression levels in stimulated versus unstimulated CLL cells were compared to those occurring in PB versus LN-derived cells (296). Stimulated CLL cells (day 3 and day 6) showed an increase in lymphocyte activation markers such as CD69 and CD86 as in LN-derived cells. However, CD5 levels were reduced even though they are normally augmented in the LN (**Figure 26A-C**). Similarly, CD38, a marker of lymphocyte adhesion, escalated in stimulated cells like in LN-derived cells (**Figure 26D**). Finally, CXCR4, a marker of cell migration typically downregulated in LN, showed a significant downregulation in the protein levels of stimulated CLL cells (**Figure 26E**). Apart from the immunophenotypic markers, the activation of CLL cells in culture was also observed by the considerable increase in size from day 0 to day 6 (**Figure 26F**).

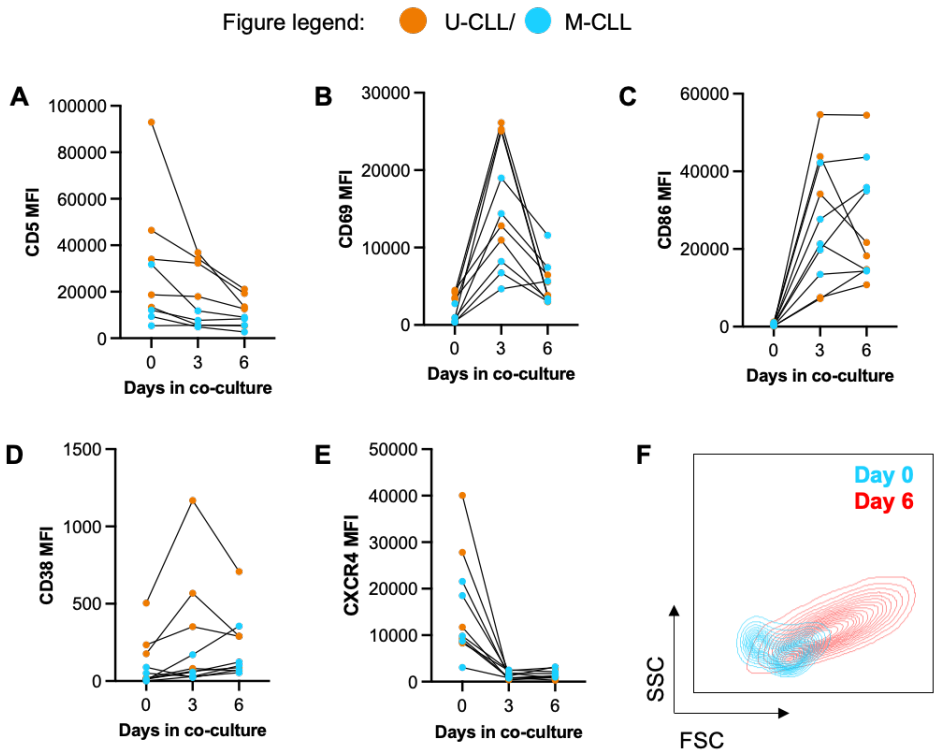


Figure 26. Before-after plots represent the median fluorescence intensity (MFI) of surface markers in CLL cells at day 0, 3, 6 in culture with MM1 cells for A) CD5 B) CD69 C) CD86 D) CD48 and E) CXCR4 F) FSC vs SCC dot plots of a representative CLL case at day 0 (unstimulated) and day 6 (stimulated).

Ki67 expression was very low or even absent at day 0 as CLL cells, derived from PB cryotubes were in a quiescent state (**Figure 27A**). Nonetheless, at day 3 in culture, some CLL cells were activated and ready to proliferate (20% Ki67+). At day 6, almost all CLL cells in culture were proliferating (> 80% Ki67+ cells). These dynamic changes in cell proliferation were also confirmed with the gradual loss of CFSE staining at day 3 and 6 (**Figure 27B-C**). In all cases studied, CLL cells had undergone at least two cycles of cell division by day 6 (**Figure 27D**). In summary, the *in vitro* system induces a strong proliferation of CLL cells, which acquire a similar pattern of the surface markers present in LN-derived CLL cells.

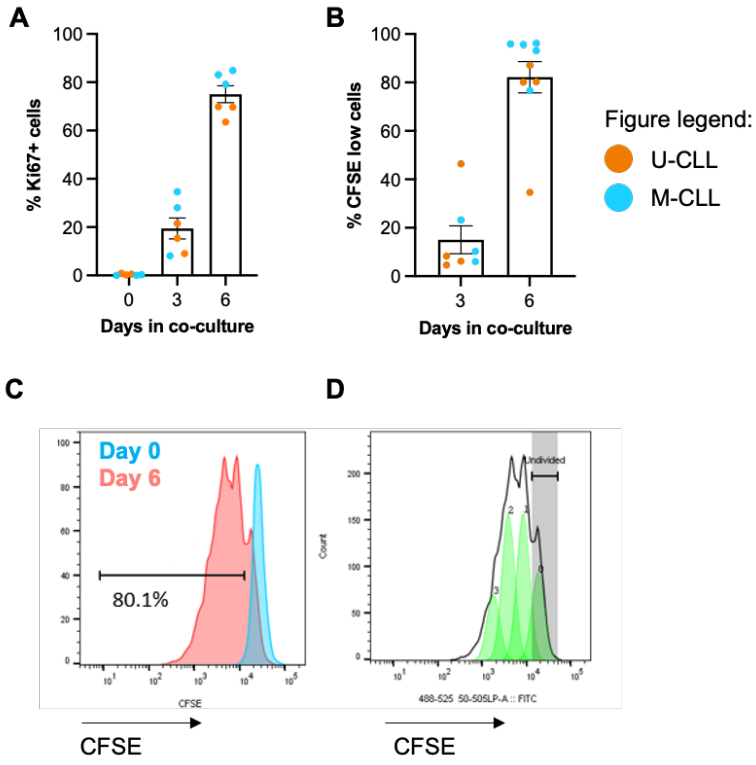


Figure 27. A) Bar plot represents the percentage of Ki67 CLL cells at day 0, 3, 6 in culture. B) Bar plot represents the percentage of CFSE low CLL cells at day 3 and 6 in culture. C) Histogram depicts CFSE staining in CLL cells at day 0 (unstimulated cells) and day 6 (stimulated CLL cells). D) Quantification of CLL proliferation (number of divisions) with Proliferation FlowJo tool under the histogram generated from CFSE staining.

2.2. CLL transcriptional changes with the *in vitro* system

Principal component analysis (PCA) of the RNA-seq data, from paired CLL cells at day 0 (unstimulated) and day 6 (stimulated), showed that unstimulated CLL cells used in this study clustered together with previously profiled CLL cells (135) (**Figure 28A**). However, PC2 separated very clearly stimulated CLL cells from the cluster of unstimulated CLL samples and normal B cells, suggesting the profound impact of the *in vitro* system on the transcriptome of CLL (**Figure 28A**). Differential gene expression analysis revealed 3212 upregulated and 2054 downregulated genes (log2FC > 1/-1, p-adj < 0.01) in stimulated CLL cells compared to unstimulated CLL cells. Interestingly, GSEA showed that the upregulated genes in

stimulated CLL cells were enriched in pathways related to increased cell proliferation (E2F, MYC targets and G2/M), metabolic reprogramming (OXPHOS, mTORC1) and DNA repair (**Figure 28B-C**). In addition, the malignant B cells LN signature ("LN upregulated") described by Saba and colleagues is positively enriched in stimulated CLL samples (297) (**Figure 28C**).

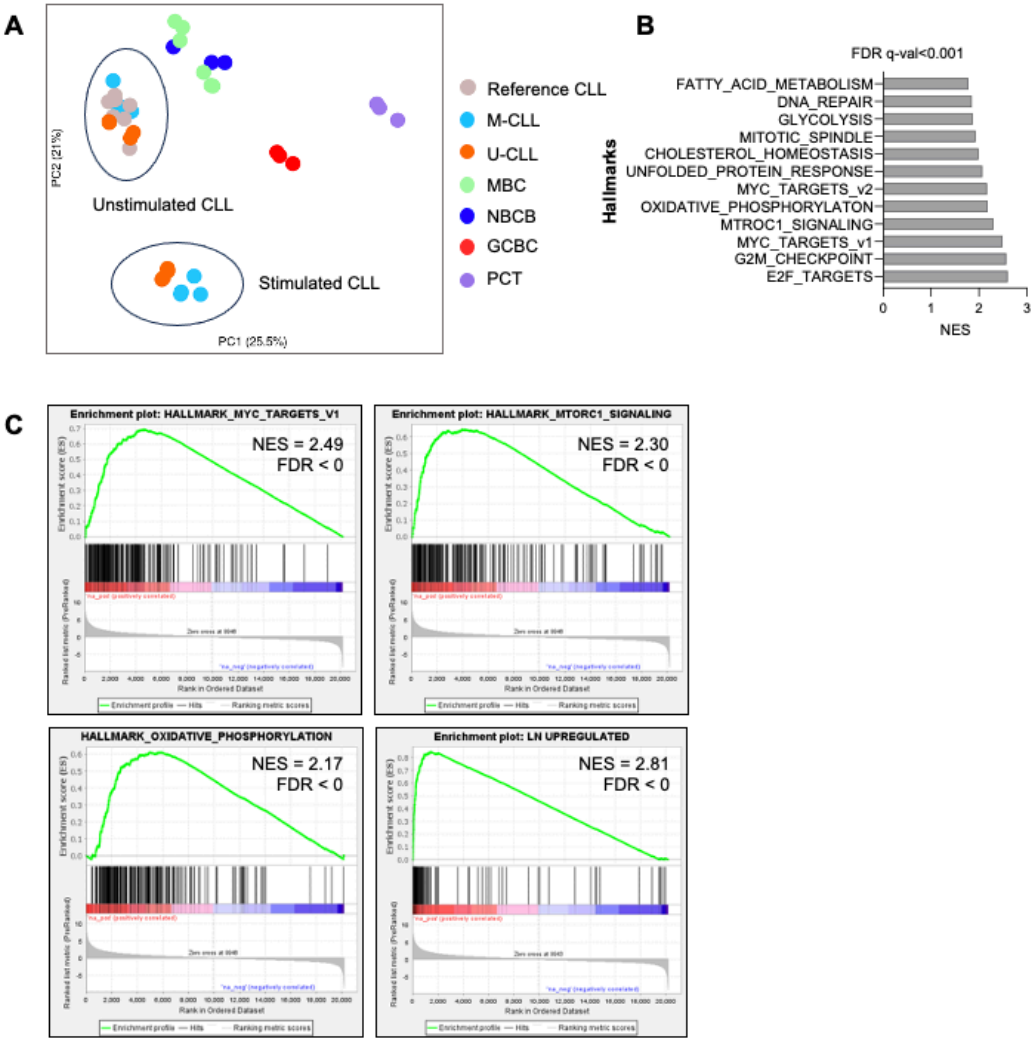


Figure 28. A) PCA for the RNA-seq data of unstimulated and stimulated CLL cells along with other normal B cells and CLL sequenced from another independent study (135). B) Significant pathways (FDR q-val < 0.001) from the upregulated genes in the stimulated CLL cells (GSEA analysis, Hallmark database). C) Representative plots of the top positively enriched pathways in stimulated CLL cells from Hallmark database and curated (297).

Interestingly, in a previous study, CLL proliferation was quantified by the expression levels of E2F and c-MYC targets, which were considerably higher in the LN samples (298). These results overlap with the results observed in stimulated CLL cells and, thus, it is another layer of evidence indicating that the MM1 *in vitro* system mimics LN microenvironment by inducing a vigorous proliferative response at the phenotypic level (higher Ki67 levels) and transcriptomic (increased E2F and MYC targets). Therefore, this model is useful to understand the proliferative fraction of CLL cells *in vitro*. This is much needed at present as almost all studies using primary CLL samples are based in PB-derived cells, which are in a quiescent state and may not reflect accurately the role of certain driver genes in CLL progression. For this reason, with this new *in vitro* system, it is possible to develop new molecular tools, such as gene editing, in patient-derived material to investigate the oncogenic mechanisms driving CLL.

3. Conclusions

The MM1 cell line constitutes a good cell culture system that mimics a LN microenvironment and allows to perform *in vitro* studies with primary CLL cells:

1. CLL cells are expanded while autologous T cells present in the initial sample are lost over time. At day 6 after culture, most of the cells are proliferative (>80%) and have overall good viability.
2. Stimulated cells express LN-like surface markers and partially recapitulate the transcriptional changes occurring in LN.

Part 2: Development of CRISPR-Cas9-based gene inactivation strategies for primary CLL cells

1. Introduction

The specific goal of this second part was to develop a gene inactivation method suitable to study the molecular mechanisms underlying CLL using primary cells, such as the role of LEF1 in these malignant cells. Currently, clustered regularly interspace short palindromic repeats (CRISPR) and their associated protein 9 (Cas9) are the most effective, efficient and accurate method of gene editing/inactivation tool in living cells (299). It is based on a Cas9 nuclease, which binds and cuts DNA, and a guide RNA sequence, which directs the Cas9 to its target. The double-breaks introduced at the DNA by the Cas9 can be repaired by non-homologous end joining (NHEJ) and homology-directed repair (HDR). NHEJ is exploited to inactivate gene function, while HDR is exploited to insert or repair specific mutations or DNA fragments. These modifications at the DNA level are irreversible. A single cell harboring those mutations can be used to establish a new cell line, thereby creating a CRISPR-induced knockout (KO) clone. However, the successful derivation of KO clones can be technically challenging, depending on the cell type, the interconal heterogeneity and incomplete target ablation (300). For instance, primary CLL cells are impossible to grow as single clones, since they are very dependent on the interaction with each other and feeder cells for their survival *in vitro*.

An alternative modality of CRISPR-Cas9 editing is to rewrite the epigenetic landscape to alter gene expression without changing the underlying DNA sequence (301) (**Figure 29**). One example is CRISPR interference (CRISPRi), which is a novel method for specific gene knockdown (KD). It is based on a catalytically inactive enzyme, called dead Cas9 (dCas9), fused to a repressor construct that, upon binding to the DNA, increases the heterochromatic H3K9me3 mark and induces the

packaging of the chromatin, blocking the transcription of target genes. Therefore, the silencing occurs within the gene's native context, just by modifying the chromatin and 3D structure. In this line, programmable epigenome editing is reversible, and does not require DNA breaks, effectively bypassing the cellular toxicity associated with gene editing (301). This protocol typically relies on the expression of two vectors in the target cell. First, a dCas9-expressing plasmid is stably transduced using lentiviruses into the target cells. Following selection for dCas9 expression, cells are transduced with a plasmid encoding for the gRNA. Typically, the gRNAs are located surrounding the transcription start site (TSS) to silence gene promoters but they can be located at distal enhancers as well. Both plasmids contain reporter genes (antibiotic resistance or fluorescent genes) that allow the selection of a pool of cells containing the dCas9 and the gRNA, where the target gene will be silenced. Therefore, single clones are not needed, allowing the use of this technique in primary CLL cells.

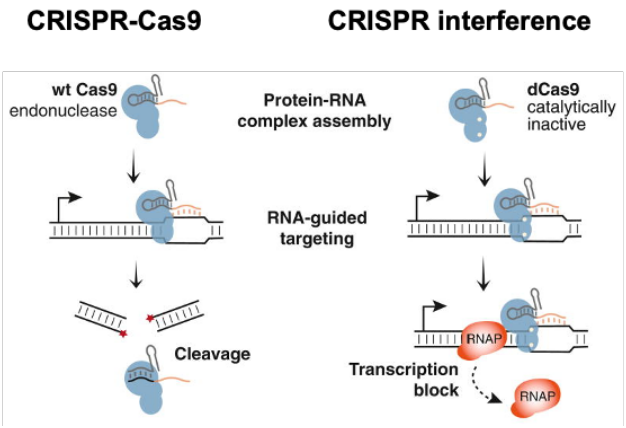


Figure 29. Gene inactivation strategies based on CRISPR-Cas9 technology. Comparison of classic CRISPR-Cas9 gene editing versus CRISPRi. Adapted from Qi, 2013 (302).

Given that primary CLL cells are limited and difficult to genetically manipulate *in vitro*, CRISPRi protocol was first optimized in cell lines. Cell lines used were derived from CLL, such as HG3 and MEC1; mantle cell lymphoma (MCL, another mature B-cell neoplasm with considerable similarities to CLL), like Z138

and JVM2, and human erythroid progenitors, K562, which has been widely used for CRISPRi experiments.

2. Results

2.1. Selection of dCas9-repressor plasmid in CLL and MCL cell lines

Vector 1

Krüppel-associated box-containing zinc finger proteins (KRAB-ZFPs) constitute the largest class of transcriptional repressors. The KRAB repressor domain promotes the recruitment of heterochromatin-inducing factors and complexes. Almost all approaches of CRISPRi use the KRAB domain from KOX1 (ZNF10). Thus, I lentivirally transduced K562 (CT+), HG3, MEC1, Z138 and JVM2 cells with pHR-SFFV-dCas9-BFP-KRAB (dCas9-KRAB-BFP) vector to induce the stable expression of dCas9-KRAB (303).

To assess the cell infection efficiency, at day 3 after lentiviral infection, I determined the percentage of dCas9-KRAB-BFP+ cells by flow cytometry. Surprisingly, infection efficiencies were dramatically low for all the malignant lymphoid cell lines (< 5 BFP+ cells) with the exception of the positive control K562 (> 60 % BFP+ cells) (**Figure 30A-B**). Notably, BFP+ cells declined over time in CLL and MCL cell lines (**Figure 30C**). After multiple rounds of lentiviral infections with dCas9-KRAB vector and I obtained similar results. Therefore, I reached the conclusion that our vector was being lost due to a possible epigenetic silencing of the dCas9 promoter.

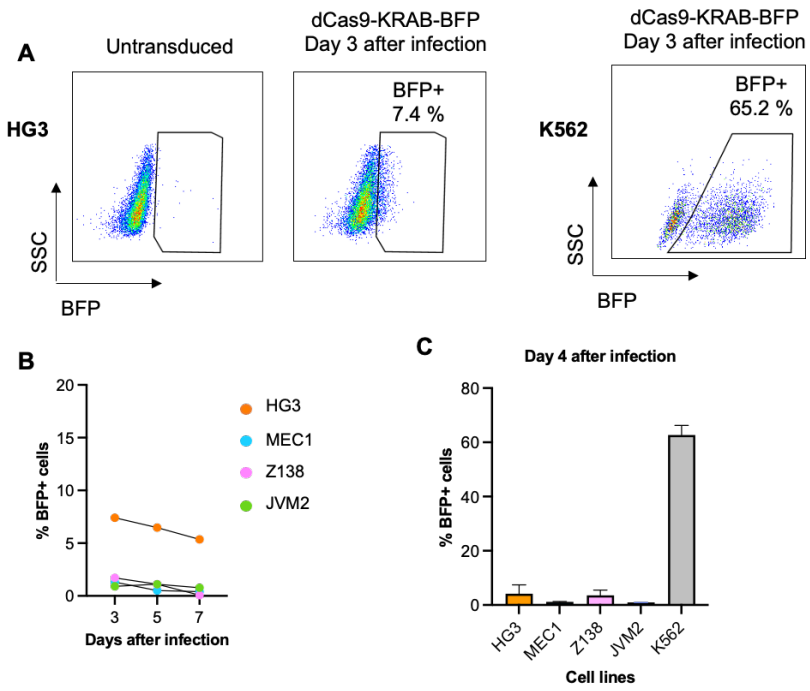


Figure 30. A) Representative flow cytometry images of transduction efficiency with dCas9-KRAB-BFP vector (day 3 after infection) in HG3 and K562 (CT+) cell line. B) Before and after plots represent the evolution of BFP+ cells at day 3, 5 and 7 after infection. Each cell line is represented with a different color. C) Percentage of BFP+ cells at day 4 after infection in the 5 cell lines tested (n=3/cell line, mean ± SEM).

Lentiviral vectors remain subject to a certain degree of silencing and are influenced by the site of integration within the genome (304). In addition, immune cells have a strong epigenetic defense against foreign DNA and, thus, they can silence the expression of the transgene. The vector used for dCas9 expression had the spleen focus-forming virus (SFFV) promoter, which is a potent viral promoter but its utility can be hindered by the transcriptional silencing (305). To counteract the silencing of transgene expression, ubiquitous chromatin opening elements (UCOEs) are used (304). UCOEs, consist of a methylation-free CpG island, that promote a transcriptionally-permissive environment and, consequently, are defined by their ability to consistently confer stable, site of integration-independent transgene expression (306,307). Taking all this information into account, I decided to use an alternative vector with the UCOE sequence to avoid the silencing of the

dCas9; and a second one, with a human promoter for dCas9 expression that should not be susceptible to silencing.

Vector 2

The second vector used for dCas9 expression was pHR-UCOE-SFFV-dCas9-mCherry-ZIM3-KRAB (dCas9-ZIM3-mCherry), which contained two differences compared to the first vector (dCas9-KRAB-BFP). First, the UCOE sequence upstream the SFFV promoter to avoid the loss of dCas9 expression. Second, the KRAB domain was from ZIM3 protein, which is stronger and more potent than KOX1 KRAB (308). In this case, the percentage of infected cell lines, containing dCas9-ZIM3-mCherry vector, was significantly higher than with dCas9-KRAB-BFP (**Figure 31A-B**). Infected cell lines were sorted and mCherry+ cells were followed over time (day 2 and 10 post-sorting). Remarkably, after the initial loss of positive cells after sorting, mCherry+ cells were maintained in all cell lines (malignant B cells and K562) (**Figure 31C**). Thus, using this vector I managed to establish cell lines with stable expression of dCas9-ZIM3-KRAB.

Vector 3

The third vector used for dCas9 expression was pLV-dCas9-KRAB-PGK-HygR (dCas9-KRAB-HygR). The promoter used for dCas9-KRAB expression was human the constitutive Ubiquitin C (UbC) promoter. Unlike the other two vectors, dCas9-KRAB-HygR vector contained a Hygromycin resistance gene for the selection of cells containing the vector (309). Cell lines (HG3, MEC1, Z138, JVM2 and K562) were transduced with lentivirus containing dCas9-KRAB-HygR. At day 3 after infection, cells were selected with Hygromycin B (varying concentration depending on the cell line, range 200-500 μg/ml) for 7 days.

Finally, dCas9 expression was validated in cell lines selected with mCherry+ (vector 2: dCas9-ZIM3-mCherry) and Hygromycin B (vector 3: dCas9-KRAB-HygR)

by western blotting (**Figure 31D-E**). Strikingly, dCas9 levels were considerably higher with dCas9-ZIM3-KRAB vector (**Figure 31D**). In fact, dCas9 was expressed at minimal levels with dCas9-KRAB-HygR even in the K562 (**Figure 31E**), which showed a dramatic decrease compared to K562 containing dCas-ZIM3-mCherry.

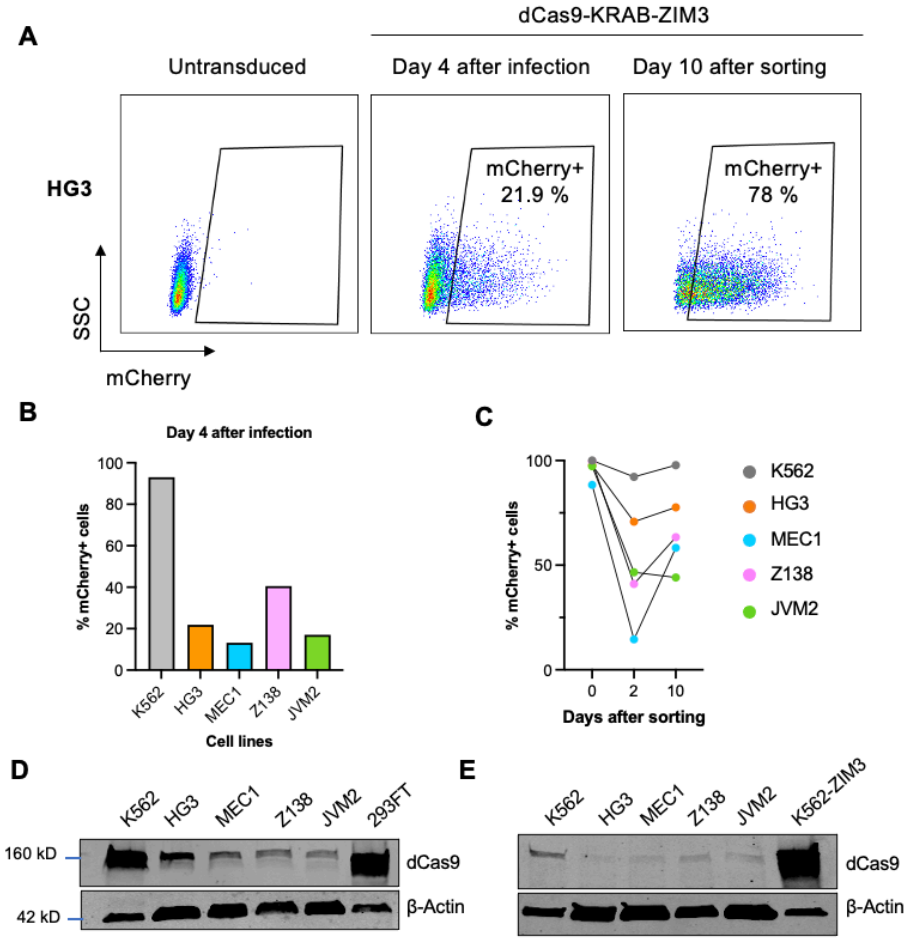


Figure 31. A) Representative flow cytometry images of transduction efficiency with dCas9-KRAB-ZIM3-mCherry vector (day 4 after infection) and 10 days after sorting by mCherry+ in HG3 cell line. B) Percentage of mCherry+ cells at day 4 after infection in the 5 cell lines tested. C) Before and after plots represent the evolution of mCherry+ cells at day 0, 2 and 10 after sorting. Each cell line is represented with a different color. D & E) dCas9 immunoblot of all cell lines transduced with D) vector dCas9-ZIM3-mCherry and E) vector dCas9-KRAB-HygR. D) Transfected 293FT cells with dCas9-ZIM3 vector were used as a positive control for dCas9 expression. E) K562 containing dCas9-ZIM3-mCherry (K562-ZIM3) was used as positive control of dCas9 expression. β-Actin was used as loading control.

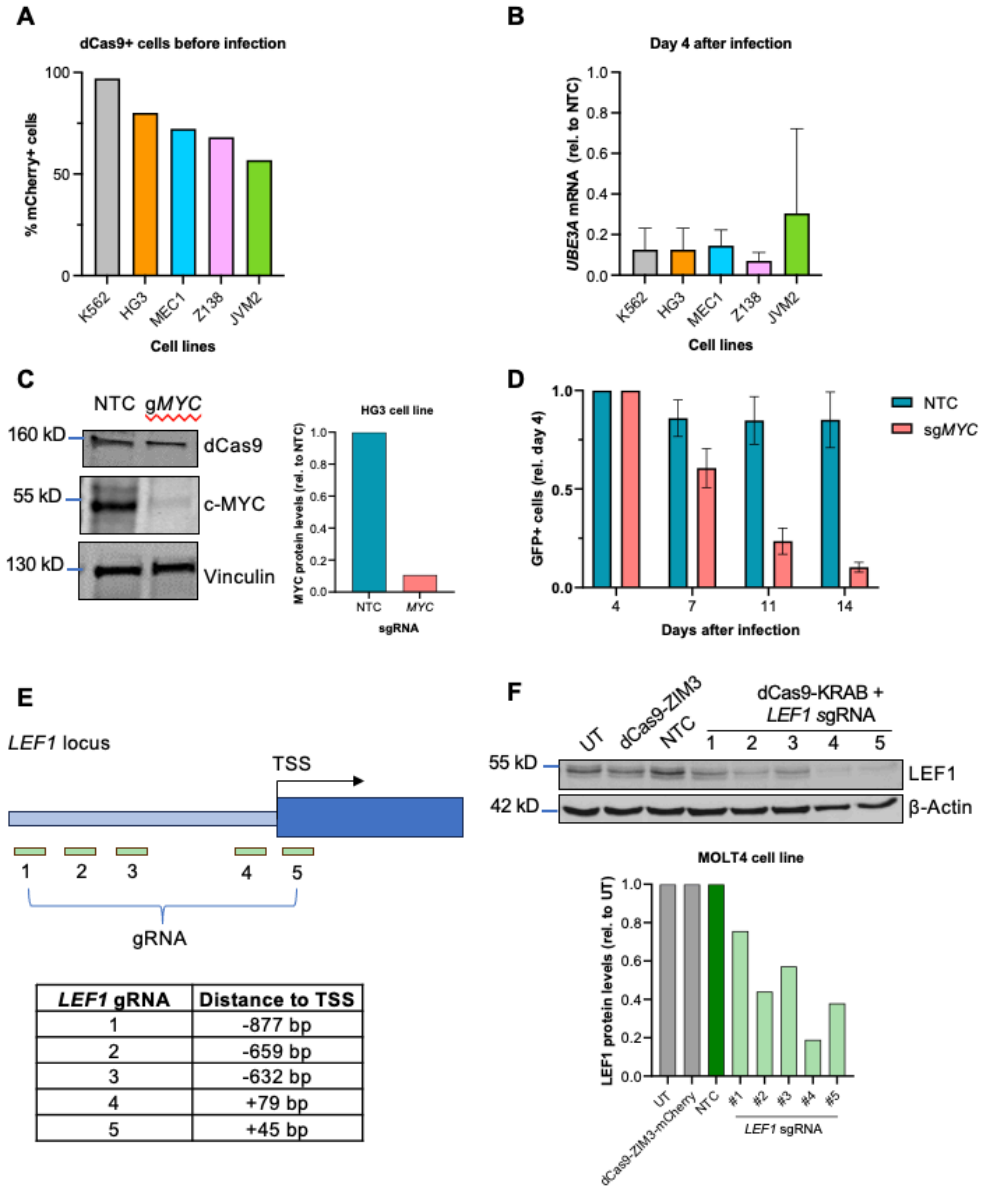
In summary, viral promoters, such as CMV or SFFV, confer higher expression levels of the desired transgene than mammalian promoters like UbC or PGK (310). However, viral promoters can be silenced in certain cell types and require the inclusion of UCOE sequence within the vector for the proper expression of the transgene (304). As the expression levels of dCas9 were crucial for the efficacy of the CRISPRi system, I decided to use dCas9-ZIM3-mCherry, with the SFFV promoter and UCOE sequence, for the optimization of CRISPRi experiments in cell lines and primary cells.

2.3. Test of CRISPRi technology in cell lines

CLL and MCL cell lines, stably expressing dCas9-ZIM3-mCherry vector, were sorted again to enrich the mCherry+ population and were expanded (**Figure 32A**). Then, cells were transduced with a second lentiviral vector, encoding for sgRNA against the target genes. Given that none of these cell lines express *LEF1*, I used two alternative positive controls: *UBE3A*, encoding for a non-essential cell surface protein in all these cell lines; and, in HG3 cell line, *MYC*, an essential gene for cell proliferation that would display a phenotypic effect upon downregulation in cells. In addition, a NTC sequence was used as a negative control. These three sgRNAs would serve later as positive and negative controls for CRISPRi in primary CLL cells.

The vector used was pAW12.lentiguide.GFP with human U6 promoter for sgRNA expression and *EGFP* reporter gene to detect infected cells (311). Expression levels (mRNA or protein) of *UBE3A* and *MYC* were assessed after 10 days of infection. The downregulation effect, assessed by q-PCR or western blot, was around 80% in all cell lines tested (**Figure 32B-C**). Moreover, *MYC*-silenced HG3 cells demonstrated a significant decrease in cell count compared to NTC cells (**Figure 32C-D**), showing the expected phenotypic effect of downregulating a key gene involved in cell proliferation control. Furthermore, I designed five sgRNA against *LEF1* gene located in different sites of *LEF1* promoter to use in primary CLL cells. According to CRISPRi developers, the sgRNA that work best in CRISPRi are

located in a distance of -50 to + 300 bp from TSS (**Figure 32E**). I first tested these five sgRNA in a T-cell acute lymphoblastic leukemia cell line (MOLT4) that expresses high levels of LEF1. As with the other cell lines, MOLT4 was first transduced with dCas9-ZIM3-mCherry vector followed by infection with sgRNA vector. After 10 days, LEF1 protein levels showed a considerable decrease (60-80%), especially, in sgRNA #4 and 5, which were the ones closest to the TSS (**Figure 32F**).



LEF1 gRNA	Distance to TSS
1	-877 bp
2	-659 bp
3	-632 bp
4	+79 bp
5	+45 bp

Figure 32. A) Percentage of dCas9-ZIM3-mCherry+ cells before infection with sgRNA vector. B) *UBE3A* mRNA levels (relative to NTC) after CRISPRi in K563, HG3, MEC1, Z138 and JVM2 cell lines. C) c-MYC protein levels at day 10 after CRISPR. NTC and *MYC*-silenced cells express the same levels of dCas9. Vinculin was used as a loading control. Bar plot on the right shows the quantification of the western blot. D) Proportion of GFP+ cells containing NTC or *MYC* sgRNA vectors for 14 days after infection (n=3, mean ± SEM). E) Schematic representation of *LEF1* sgRNA distribution across *LEF1* promoter. F) LEF1 protein levels after CRISPRi with the different *LEF1* sgRNAs. Bar plot shows the quantification of the western blot.

2.4. Test of CRISPRi in primary CLL cells

Primary CLL cells were first transduced with the lentiviral vector dCas9-ZIM3-mCherry and, 72 hours later, with sgRNA-GFP vector following the spin infection protocol from Mangolini and colleagues (266). Remarkably, CLL cells (n=4) were successfully infected with the sgRNA vector but were resistant to transduction with dCas9-ZIM3-mCherry large plasmid (> 14 kb) (**Figure 33A**). Lentiviruses encoding for dCas9-ZIM3-mCherry were concentrated 10 and 100 times with lenti-X concentrator to evaluate whether cell infection efficiency could be improved. Despite all the attempts, the results were exactly the same: dCas9-ZIM3 was not entering into the primary cells (**Figure 33B**). Consequently, primary CLL cells showed no expression of dCas9 (**Figure 33C**).

CLL and normal B cells are well known for their resistance to most gene transfer methods (267). This major obstacle seemed to be solved with Mangolini's protocol with the elaboration of new packaging plasmids to specifically transduce B cells (normal and malignant) with lentivirus and retrovirus. Nonetheless, this approach seems to be limited by the size of the transgene plasmid, since I was not able to express dCas9-ZIM3 (> 14 kb) in primary cells but could express efficiently the sgRNA vector (10 kb). In this line, the efficiency of a CRISPR system depends on the efficacy with which it can be introduced into and expressed within the target cell. Here, the CRISPRi would not work due to the lack of dCas9-ZIM3 expression. Therefore, I had to move onto an alternative method to transduce primary CLL cells for gene inactivation, and electroporation CRISPR-based gene editing was the technique of choice.

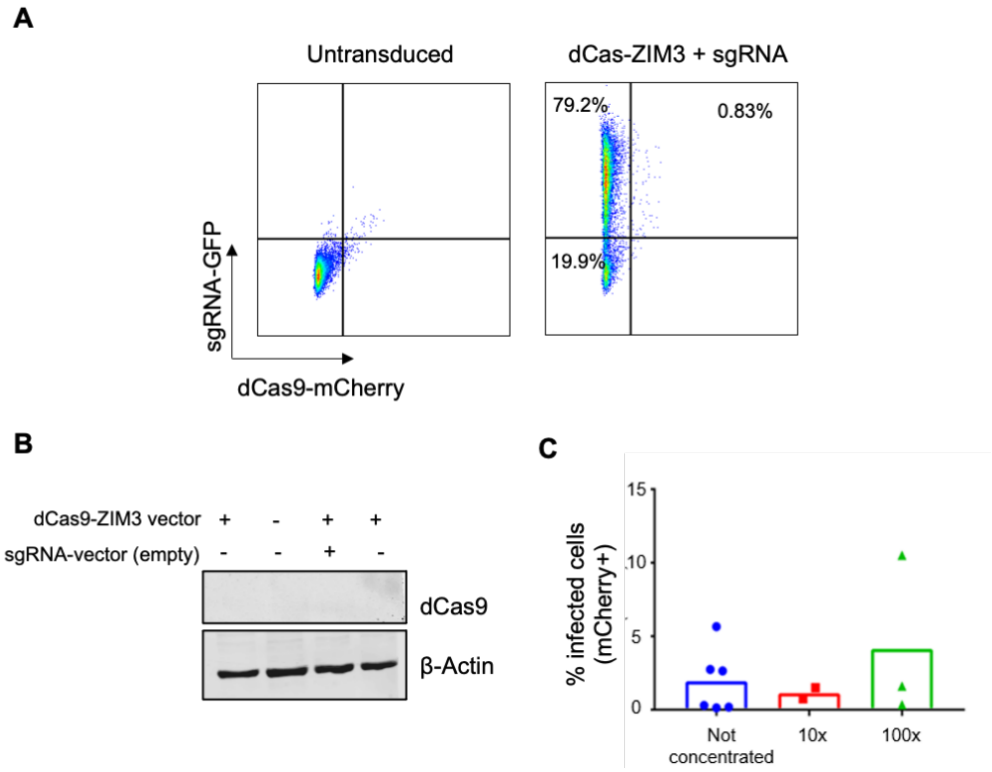


Figure 33. A) Representative flow cytometry image of transduction efficiency in a primary CLL case with dCas9-ZIM3-mCherry and sgRNA-GFP vectors to perform CRISPRi. B) Percentage of mCherry+ cells (containing dCas9-ZIM3-mCherry vector) after three infection conditions: no concentration of lentivirus, 10- and 100-times concentration with lenti-X concentrator. C) Expression of dCas9 in different infection conditions tested in primary samples. β-Actin was used as loading control.

2.5. Optimization of classic CRISPR-Cas9 in CLL

The results shown in section 2.5 have been already published in the June 2023 issue of the journal Hemasphere: **Mateos-Jaimez J***, Mangolini M*, Vidal A, Kulis M, Colomer D, Campo E, Ringshausen I, Martin-Subero JI, Maiques-Diaz A. Robust CRISPR-Cas9 Genetic Editing of Primary Chronic Lymphocytic Leukemia and Mantle Cell Lymphoma Cells. Hemasphere. 2023 Jun 7;7(6):e909. doi: 10.1097/HS9.0000000000000909. PMID: 37304935; PMCID: PMC10249715.

Introduction

For this experimental part, I used primary CLL and MCL cells to optimize CRISPR conditions. Although my doctoral thesis has been focused only on CLL, I included MCL in the optimization because of the considerable clinico-biological overlap between CLL and MCL. Among the similarities, functional studies using primary cells in both diseases have been limited by the difficulty of growing CLL and MCL malignant cells *in vitro*, as well as their resistance to most gene transfer/transfection methods. CLL and MCL are two mature neoplasms characterized by the accumulation of mature CD5+ B cells in PB, LN and bone marrow (312). Both neoplasms have two major subtypes that depend on the level of mutation of IGHV genes that are associated to clinical outcome. U-CLL and conventional MCL (cMCL, also IGHV unmutated) have a more aggressive behavior M-CLL and non-nodal MCL (nnMCL, which is also IGHV mutated). Finally, the use of gene editing tools in these malignant B cells is still elusive.

In the previous section, I described that it was impossible to perform CRISPRi in primary malignant B cells since these cells could not be lentivirally transduced with the dCas9-KRAB vector. For this reason, I changed the transfection method and the gene inactivation system to electroporation-based classic CRISPR-Cas9. Electroporation generates pores in the membranes of cells that allows the entrance of Cas9 protein together with the gRNA. As mentioned before, the major drawback of classic CRISPR-Cas9 editing in CLL cells is that it is impossible to grow single clone Kos for our gene of interest (e.g., *LEF1*). Thus, when working with this methodology, I will be able to evaluate the effects on a pool containing both gene KO and wildtype (WT) cells, where the global effect studied is similar to a gene KD.

Optimization of electroporation conditions

Every cell type requires slightly different electroporation conditions (depending on the cell size and sensitivity, among others) that must be determined

experimentally. In addition, electric field strength and pulse duration are key parameters to maximize transfection efficiency and maintain cell viability (313). An excessive pulse in terms of voltage, duration or number (repetitions of pulses) can cause a decrease in cell viability following electroporation. Thus, the objective of this part was to define the most optimal conditions for inducing gene inactivation in a highly efficient manner with no significant effects in cell viability. As an initial proof of concept, the CD19 pan-B cell marker was targeted since it is highly expressed in both CLL and MCL cells. In this line, I decided to assess the effect of 1) cell size (unstimulated versus stimulated cells) and 2) voltage and pulse duration in *CD19* downregulation. Unstimulated CLL cells from PB and paired stimulated cells (3 days in culture with MM1) were electroporated with three different conditions in the Neon Electroporation System to allow the entrance of Cas9 protein with *CD19* gRNA in the cells:

1. 1350 Volts, 30 ms, 1 pulse
2. 1400 Volts, 20 ms, 3 pulses
3. 1600 Volts, 10 ms, 3 pulses

To assess electroporation efficiency, the gRNA was labeled with a fluorescent tracer (ATTO550). Cell viability, measured 24 hours after electroporation, demonstrated a remarkable low percentage of dead cells in unstimulated and stimulated CLL cells, with the exception of 1400 V condition in stimulated CLL and MCL cells, which showed lower viability (**Figure 34A-B**). In addition, unstimulated CLL cells showed less than 60% of ATTO550+ cells (containing the gRNA) in all three conditions tested, while all stimulated cells had more than 80% of ATTO550+(**Figure 34C-D**). However, the greater difference was seen in the very low ATTO550 mean fluorescence intensity ratio (MFIR) detected in unstimulated cells compared to the stimulated cells (**Figure 34E-F**), which indicates that less Cas9-RNP complex is entering per cell. This observation directly correlated with the lower global efficiency observed in CD19 editing and

downregulation in unstimulated cells. In fact, it was observed less than 10% reduction of CD19+ in all unstimulated cases and conditions, whereas, in stimulated cells, it was achieved a reduction in CD19+ of more than 80% (with 1400 V and 1600 V electroporation conditions) (**Figure 34G-H**).

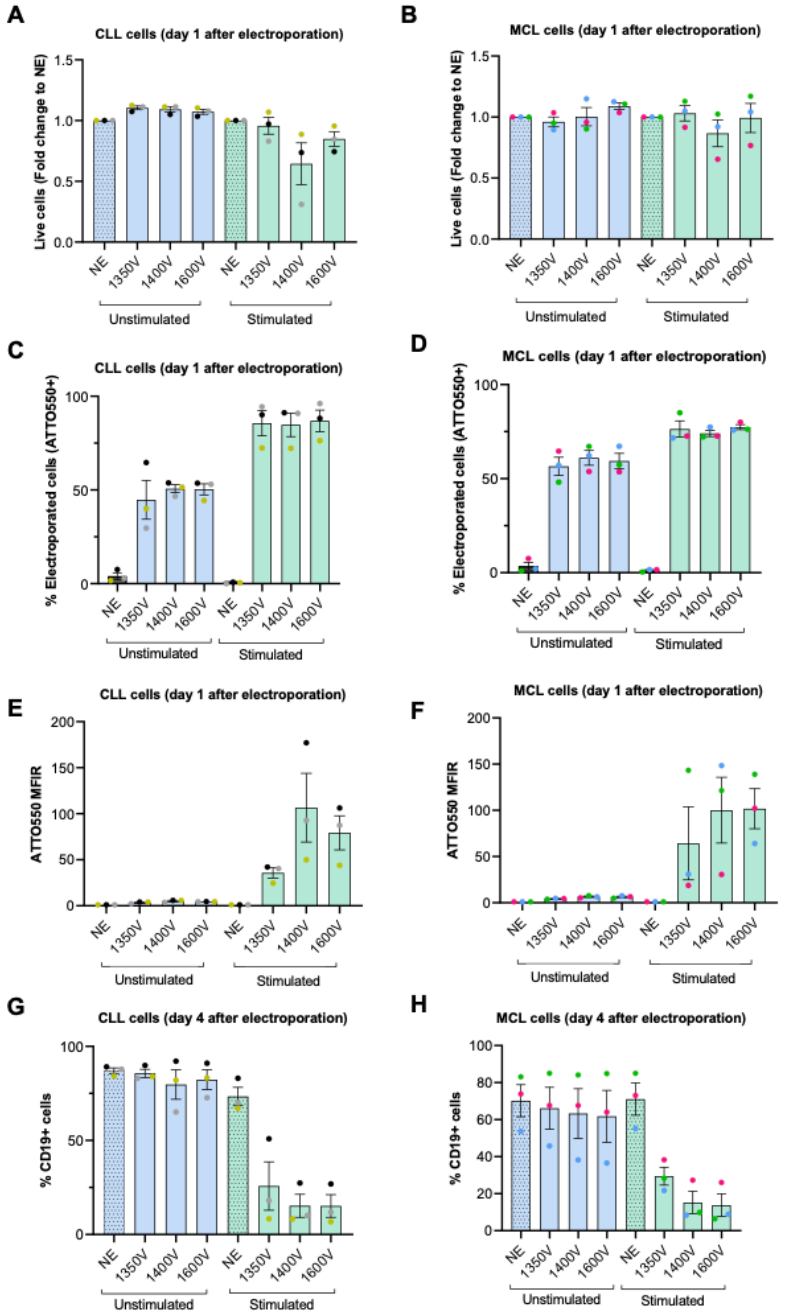


Figure 34. Optimization of the CRISPR-Cas9 protocol. A-B) Percentage of live cells (Aqua-), mean ± SEM, in electroporated with the indicated conditions versus non-electroporated (NE) cells in A) 3 CLL and B) 3 MCL samples. C-D) Bar graphs show the percentage of electroporated cells (ATTO550+), mean ± SEM, in the live population of C) 3 CLL and D) 3 MCL samples. E-F) Bar graphs show the ATTO550+ MFIR ± SEM in the live population of E) 3 CLL and F) 3 MCL samples. G-H) Bar graphs show the percentage of CD19+ cells in the indicated conditions at day 4 after electroporation in G) 3 CLL and F) 3 MCL samples. Each color represents a different case.

In summary, stimulated malignant cells showed greater electroporation efficiency, which resulted in a more efficient gene editing, than unstimulated cells. Therefore, cell size matters considerably for the electroporation efficiency. Regarding the three electroporation conditions, 1350 V resulted in less reduction of CD19+ compared to 1400 V and 1600 V. Moreover, 1400 V pulses were of higher duration (30 ms), which induced higher cell death in primary CLL cells. Therefore, the balance between highly efficient electroporation and editing efficiency and good cell viability was accomplished with condition 3 (1600 V 10 ms 3 pulses) in stimulated cells, and therefore these conditions was used for further experiments using stimulated CLL/MCL cells.

CD19 KD in primary CLL and MCL cells

Cryopreserved CLL and MCL cells, isolated from PB cells, were expanded for 3 days *in vitro* and subsequently electroporated with optimized conditions (1600 V 10 ms 3 pulses). As previously observed, at day 1 after electroporation, no significant effects on cell viability were detected in electroporated cells compared to non-electroporated cells (**Figure 35A, D**). High transfection efficiency was accomplished with over 90% of cells containing the gRNA labeled with fluorescent tracer (**Figure 35A, D**). Lower levels of CD19 expression were already evident at day 2 after electroporation (**Figure 35B, E**). By day 4, CD19 levels were downregulated by more than 90% in all CLL samples tested (n=8), and by 75% in MCL samples (n=4) (**Figure 35C, F**).

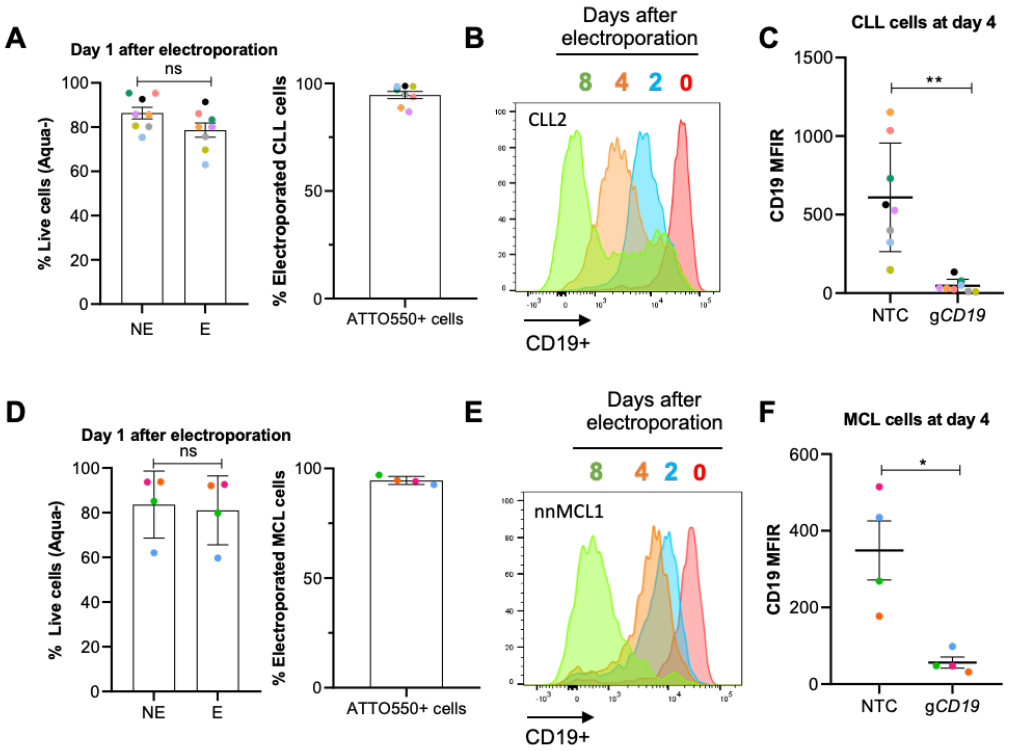


Figure 35. Efficient CRISPR-Cas9 editing of primary malignant B cells. A & D) Left bar graphs represent the percentage of live cells (Aqua−) ± SEM in electroporated (E) vs non electroporated (NE) cells in A) CLL (n=8) and D) MCL samples (n=4). Right bar graphs show the percentage of electroporated cells (ATTO550+) ± SEM in the live population. Unpaired t test. B & E) Histogram shows CD19 protein levels assessed by flow cytometry at day 0, 2, 4, and 8 after electroporation in 1 exemplary sample of B) CLL or E) MCL. C & F) Box plot on the right represents CD19 MFIR value in NTC and g*CD19*-electroporated cells at day 4 after electroporation in C) CLL and F) MCL samples. Paired t test. Each color represents a different case.

These low protein levels were maintained over time (**Figure 36A-B**). I performed amplicon sequencing to measure the percentage of CD19 alleles with an insertion/deletion (indel) mutation induced by the Cas9-gRNA and observed 64% and 65% of mean allele editing in CLL (n=3) and MCL (n=3), respectively. No changes on the proportion of allele editing were found over time (**Figure 36C-D**). In summary, I have developed a method for the transient transfection of the Cas9-gRNA complex into patient-derived malignant B cells, without inducing cell death and with highly efficient gene editing and protein depletion.

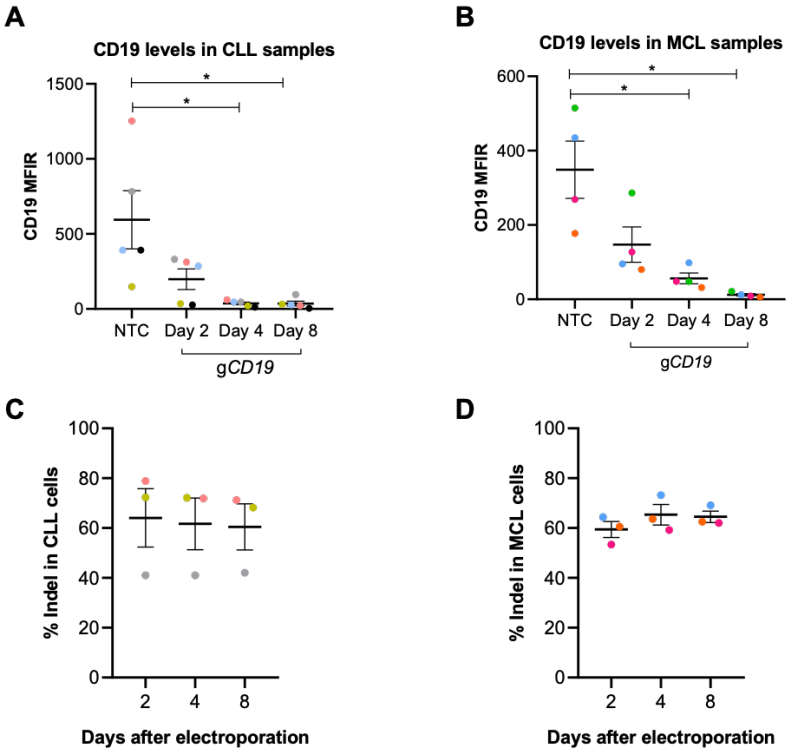


Figure 36. *CD19* gene editing in CLL and MCL primary cells. A-B) CD19 MFIR values of NTC and *CD19*-edited cells at day 2, 4 and 8 after electroporation in CLL (n=5). C-D) Percentage of indels in D) CLL (n=3) and E) MCL (n=3) samples. Each color represents a different case of CLL/MCL. Paired t-test.

CCND1/2 KD in primary CLL and MCL cells

For further validation of the electroporation-based CRISPR-Cas9 protocol in malignant B cells, we decided to target 2 important cell cycle regulatory proteins respectively involved in CLL and MCL pathogenesis, cyclin D1 (*CCND1*) and cyclin D2 (*CCND2*), to study downstream effects of the depletion of these proteins. Cyclin D1 overexpression is a hallmark of MCL development (312), while cyclin D2 is upregulated in CLL cells, particularly at the proliferation centers in lymph nodes (314,315). Concordantly, cyclin D2 becomes highly expressed in CLL cells exposed to the pro-proliferative stimuli of the *in vitro* culture system (MM1 cells) (**Figure 37A**). *CCND2* was downregulated by using 2 independent gRNAs in 8 primary CLL cases (3 U-CLL and 5 M-CLL, see **Appendix Table 1A** for patients' characteristics).

At day 4, cyclin D2 levels were 70% reduced at the mRNA and protein level (**Figure 37B-C**). Remarkably, cyclin D2 depletion had a major impact on cell proliferation on both U-CLL and M-CLL cases, as, by day 2, there was a mean cell growth reduction of 62% and 50% with each gRNA used (**Figure 37D**), without significant impact on cell viability (**Figure 37E**).

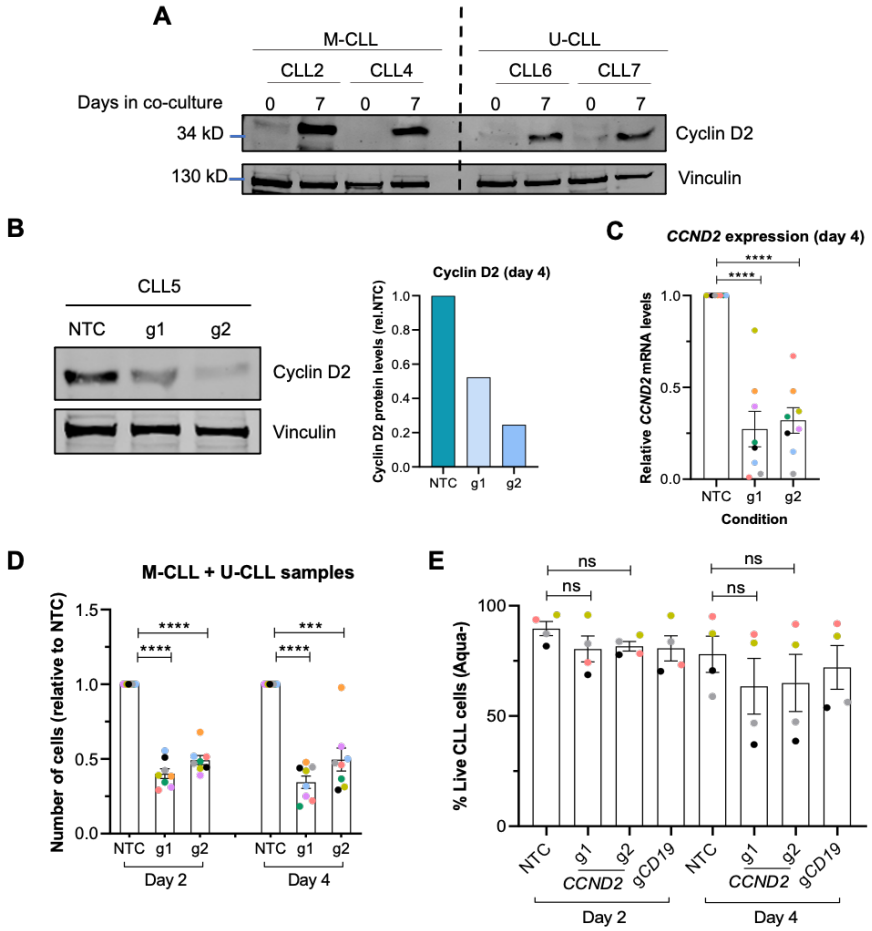


Figure 37. *CCND2* gene editing in CLL primary cells. A) Western blot shows cyclin D2 protein levels before and after co-culture with MM1 cells for 7 days in CLL cells (2 U-CLL and 2 M-CLL). B) Cyclin D2 protein levels at day 4 in one representative case of CLL upon electroporation. Bar plot shows ImageJ protein quantification normalized with NTC. C) Bar plot shows the relative levels of *CCND2* mRNA ± SEM in NTC and *CCND2* g1/g2-electroporated CLL cells at day 4 after electroporation (n=8). Unpaired t-test. D) Bar plot displays the relative cell number of NTC and *CCND2* g1/g2-electroporated CLL cells at day 2 and day 4 after electroporation ± SEM (n=8). Unpaired t test. E) Percentage of live cells (Aqua-) ± SEM at day 2 and day 4 in NTC and *CCND2* g1/g2 or *CD19* gRNA-electroporated CLL cells (n=8). Each color represents a different case of CLL/MCL.

In parallel, the *CCND1* gene was targeted with 2 independent gRNAs in 4 MCL primary cases (2 cMCL and 2 nnMCL, see **Appendix Table 1B** for patient characteristics). At day 4, a 65% decrease in cyclin D1 protein levels was found with both gRNAs (**Figure 38A-C**).

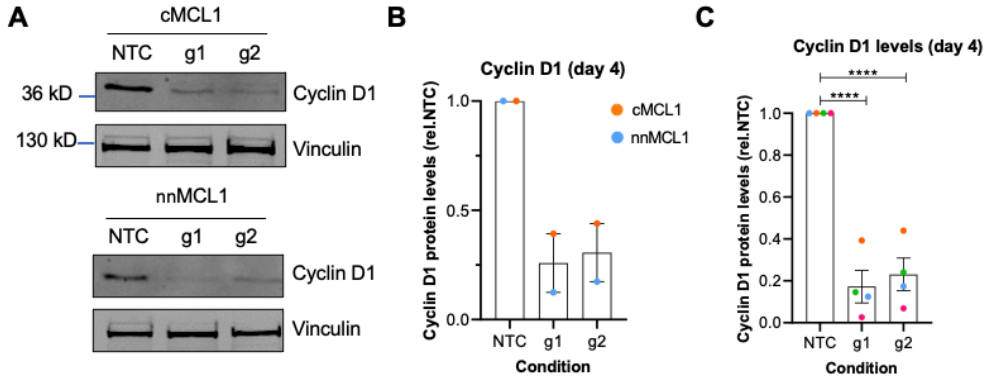


Figure 38. *CCND1* gene editing in MCL primary cells. A) Protein levels of cyclin D1 at day 4 in NTC and *CCND1* g1/g2-electroporated cells in 1 case of cMCL and nnMCL. B) Bar plot shows ImageJ protein quantification ± SEM normalized with NTC in cMCL (orange) and nnMCL (blue). C) Bar plot shows ImageJ protein quantification of cyclin D1 levels normalized with NTC of 4 independent MCL cases. Unpaired t-test.

Notably, upon cyclin D1 depletion, cell viability was not significantly affected (**Figure 39A**), while cell proliferation was reduced in cMCL cases (n=2) but not in nnMCL cases (n=2) (**Figure 39B-C**). Despite the small sample size, this observation suggests that the contribution of cyclin D1 to cell proliferation may differ between the 2 MCL clinico-biological subtypes and reinforces the importance of studying the pathobiology of MCL with primary cells, which preserve the diversity of cMCL and nnMCL cases.

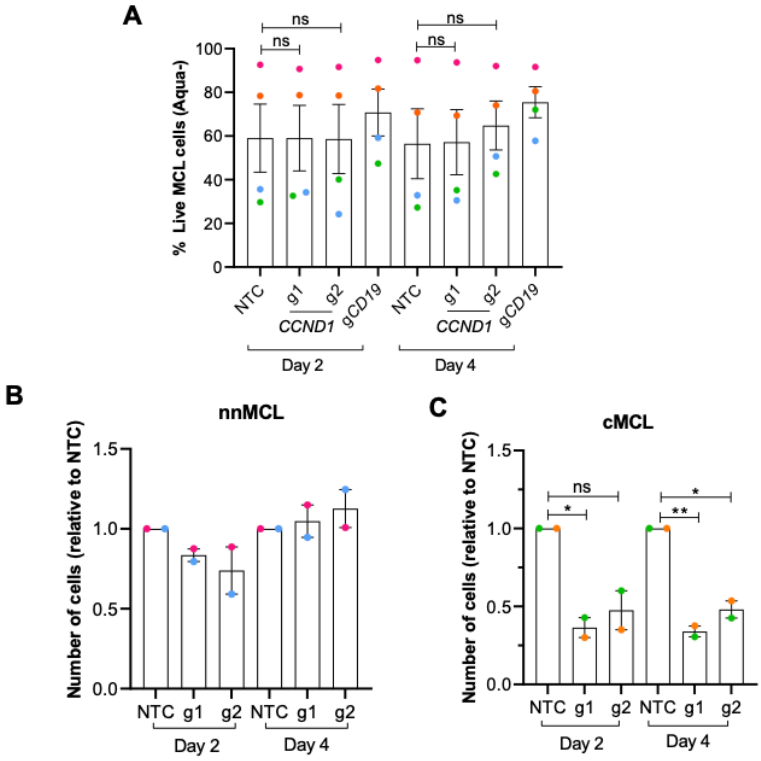


Figure 39. Effects of *CCND1* gene editing in MCL primary cells. A) Bar plot shows percentage of live cells ± SEM at day 2 and day 4 in NTC and *CCND1* g1/g2 or g*CD19*-electroporated MCL cells (n=4). Paired t-test B-C) Bar plot displays the relative cell number in NTC and *CCND1* g1/g2-electroporated cells in B) nnMCL cells and C) cMCL at day 2 and day 4 after electroporation ± SEM (n = 4). Unpaired t test. Each color represents a different case.

Dual gene editing in CLL cells

As an additional technical development, I wondered if I could edit efficiently two or more genes at the same time in primary CLL cells. To test the efficacy of simultaneous electroporation, *CD19* and *CCND2* gRNAs were combined with Cas9 protein and electroporated into CLL cells (n = 2). At day 1 after electroporation, cell viability was maintained and 60 % of the cell population contained both gRNAs, each labeled with a different fluorescent tracer (**Figure 40A-B**). Then, at day 4 after electroporation, CLL cells were sorted by CD19- and a western blot was performed to assess CD19 and cyclin D2 levels in these cells (**Figure 40C**). I achieved an almost

complete depletion of both CD19 and cyclin D2 proteins (**Figure 40D**). Importantly, such levels of protein depletion were similar to those obtained with single gRNAs, suggesting that dual gene targeting is feasible and highly effective in primary CLL cells. This protocol paves the way to design more biologically relevant experiments using primary malignant B cells, such as the role of LEF1 in CLL.

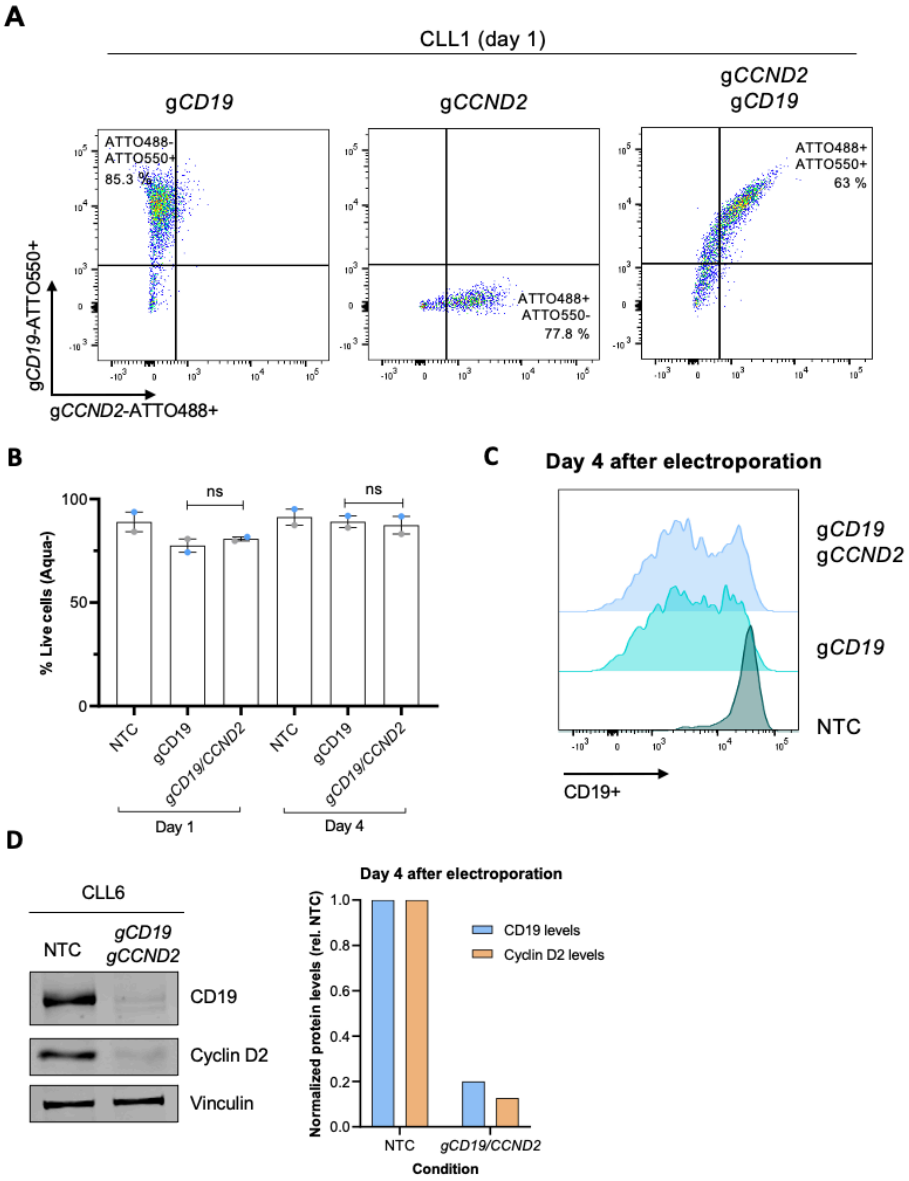


Figure 40. Dual editing of *CD19* and *CCND2* genes in CLL cells. A) FACS plots show the percentage of electroporated cells with one single gRNA (containing g*CD19*-ATTO550 or g*CCND2*-ATTO488) and two gRNA (g*CD19*-ATTO550 + g*CCND2*-ATTO488) in CLL1. B) Bar graphs show the percentage of live cells (Aqua-) ± SEM in electroporated cells with the indicated conditions. C) Western blot shows CD19 and cyclin D2 protein levels in NTC or double-edited CLL cells, sorted by CD19- in CLL6. Bar plot shows ImageJ protein quantification normalized with NTC for CD19 levels (orange) and Cyclin D2 (blue). D) Histogram displays CD19 protein levels assessed by flow cytometry at day 4 in NTC, single edited g*CD19* cells and double edited g*CD19*-g*CCND2* in sample CLL6.

3. Conclusions

Regarding the gene inactivation strategies studied in this section:

1. CRISPRi is as efficient as CRISPR-Cas9 in downregulating gene expression in cell lines.
2. Viral promoters for dCas9 expression are the strongest, but they should include the UCOE sequence to avoid its silencing within the target cells, especially in cell lines from B-cell origin, which tend to silence foreign DNA.
3. Primary CLL cells are resistant to gene transfer methods. In fact, large plasmids, such as dCas9-ZIM3-KRAB (14 kb), cannot enter the CLL cells. Therefore, I did not manage to perform CRISPRi in primary CLL cells.
4. Electroporation-based CRISPR-Cas9 methodology provides a robust and efficient method for gene editing in primary human malignant B cells:
    a. Proliferation of CLL cells seems to be key for a successful gene editing. Unlike stimulated CLL cells, unstimulated cells are not receptive to electroporation/editing of target genes.
    b. More than one gene can be targeted simultaneously, with a protein depletion that is maintained after cell division.
    c. Gene editing occurs in some CLLs of the total cell population. As it is not possible to grow single KO clones from patient-derived cells, the resultant effect of CRISPR-Cas9 editing in a pool, with a mix of WT and KO cells, is a KD.

Study 2: Defining the role of LEF1 in CLL origin and pathogenesis

The results derived from this Study 2 are completely unpublished. The manuscript is under preparation

1. Introduction

LEF1 is a pivotal TF that regulates cell proliferation and survival. Although it has a critical role in lymphopoiesis (188), LEF1 is not expressed in any type of normal mature B cells (51,316). In contrast, LEF1 expression is very high in CLL and the premalignant state preceding it, MBL. Overall, LEF1 shows a stable gene expression across samples independently of the IGHV status (207,208). However, cases trisomy 12 have been reported to express significantly lower levels of LEF1 (207). There are few studies investigating the role of LEF1 in CLL (152), probably due to the lack of LEF1 expression in the widely used CLL cell lines and mouse models, along with the difficulty of manipulating patient-derived CLL *ex vivo*.

The specific aim of this study was to uncover how LEF1 contributes to CLL pathogenesis and clinical behavior. To achieve this, I used the LN-mimicking *in vitro* system for growing CLL *ex vivo*, which has been defined in Study 1, and applied several cell biology and molecular biology techniques, such as electroporation-based CRISPR-Cas9 editing of *LEF1* gene, in patient-derived CLL cells.

2. Results

I initially validated the protein expression of LEF1 in CLL cells after being co-cultured with MM1 cells (**Figure 41**). Notably, LEF1 expression was enriched in the nuclear fraction of both unstimulated and stimulated CLL cells. Interestingly, upon culture with MM1 cells, the fraction of LEF1 protein bound to chromatin increased, suggesting an increased transcriptional activity of LEF1 under proliferative conditions. Thus, I could proceed to deepen into the mechanistic role of LEF1 in primary CLL cells seeded with MM1 cells.

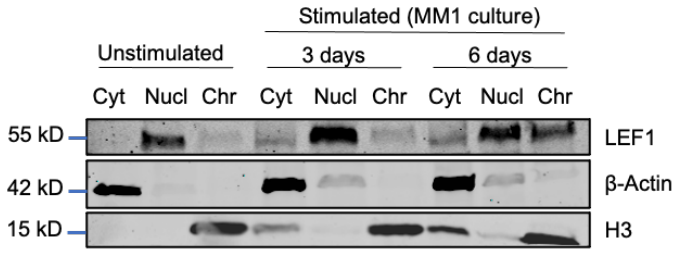


Figure 41. LEF1 expression in cellular fractions of unstimulated and stimulated CLL cells. LEF1 protein levels were assessed by western blot in CLL cells before (unstimulated) and after being cultured for 3 and 6 days (stimulated) in cytoplasmic (cyt), nuclear (nucl) and chromatin-bound protein fraction (chr). β-Actin was used as cytoplasmic loading control and histone 3 (H3) as a chromatin-bound protein loading control.

2.1. LEF1 mRNA and protein levels in CLL

LEF1 expression was first studied at the mRNA level in PB-derived samples of MBL (n=46), M-CLL (n=264) and U-CLL (n=147) (**Figure 42A**). As indicated in some articles of the literature, there were no differences in the mRNA levels between U-CLL and M-CLL. In addition, *LEF1* mRNA levels in MBL were similar to those in CLL cells, reinforcing the idea of LEF1 as an early driver in CLL pathogenesis. Then, LEF1 expression was assessed at the protein level by intracellular flow cytometry in normal B cells as negative control (n=3), MBL (n=13), M-CLL (n=15) and U-CLL (n=16) derived from PB samples (**Figure 42B-C**). Surprisingly, the LEF1 protein levels were variable depending on diagnosis (MBL/CLL) and IGHV subtype (M/U-CLL), and did not correlate with the homogeneous *LEF1* mRNA levels (**Figure 42C**). MBL had the lowest LEF1 protein levels compared to CLL. Strikingly, LEF1 protein levels were significantly higher in U-CLL ($p\text{-val} < 0.001$). Furthermore, when classifying these CLL cases by epigenetic subtypes, levels were higher in n-CLL (all harboring an unmutated IGHV gene) together with i-CLL with unmutated IGHV, while the lowest levels were observed in m-CLL (i.e., all IGHV mutated) and i-CLL with mutated IGHV. These observations suggest that the difference in LEF1 protein levels is directly associated to the IGHV status and, thus, may be modulated depending on whether the cell of origin of the CLL clone has experienced or not the GC reaction. (**Figure 42D**).

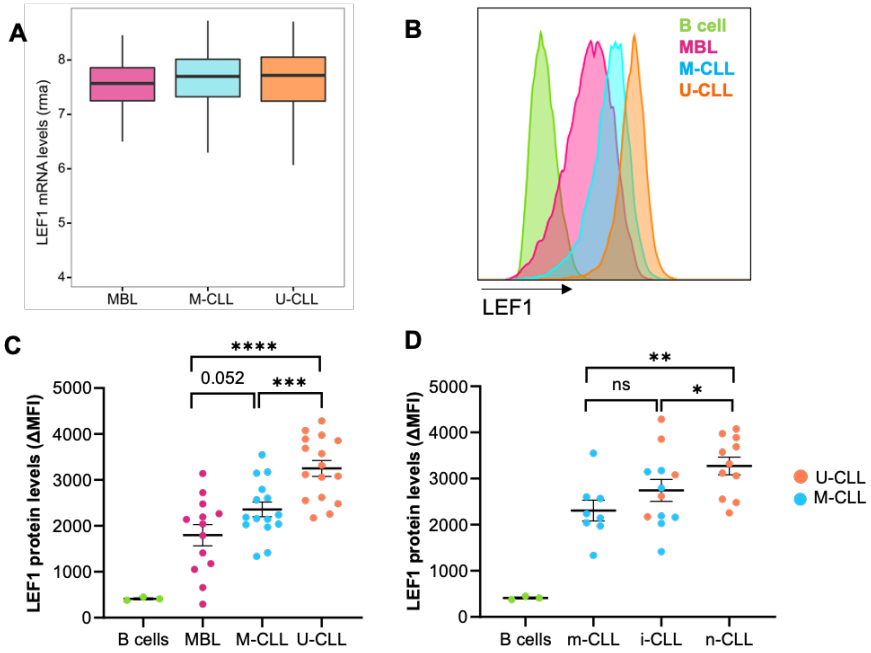


Figure 42. LEF1 mRNA and protein levels in MBL and CLL samples. A) Box plot shows the *LEF1* gene expression level measured by microarray data (rma) in MBL (n=46), M-CLL (n=264) and U-CLL (n=147) samples. Wilcoxon test. B) Representative histogram plot of LEF1 protein intracellular staining in B cells, MBL, M-CLL and U-CLL samples. C) LEF1 protein levels measured by intracellular flow cytometry in B cells (n=3), MBL (n=13), M-CLL (n=15) and U-CLL (n=16) samples. Unpaired t-test. D) LEF1 protein levels depending on the epigenetic subtype of CLL cells. Unpaired t-test.

I also explored whether the percentage of IGHV identity correlated with LEF1 protein levels. Neither U-CLL nor M-CLL cases showed a correlation between the percentage of IGHV identity and LEF1 protein levels (**Figure 43A-B**). Hence, the higher LEF1 levels observed in U-CLL reinforce the concept that LEF1 levels reflect their different cell of origin rather than the degree of GC experience, measured by the level of somatic hypermutation occurring in the cells. Next, I wanted to determine if LEF1 protein levels were associated to CLL prognosis. For survival analysis, patients were divided into high- and low-LEF1 subgroups by LEF1 protein level cut-off defined by the maxstat pipeline. Globally, TTFT was much shorter in the high-LEF1 subgroup than in the low-LEF1 subgroup (median TTFT: LEF1 high, 0.4 years, LEF1 low, 9.9 years, p-val = 0.0017) (**Figure 43C**). Remarkably, the high-

LEF1 group was mostly constituted by U-CLL cases, while, in the low-LEF1 almost all CLLs were IGHV mutated (Fisher's test, p-val<0.01) (**Figure 43C**). These results raised the question of whether higher protein levels of LEF1 are linked to the cell of origin (IGHV status) or aggressiveness of CLL, because all U-CLL profiled were aggressive with rapid progression (TTFT < 1 year) while most of the M-CLL were indolent (untreated or TTFT > 7 years). For this reason, I assessed LEF1 protein levels in aggressive M-CLL cases that were treated rapidly upon diagnosis (TTFT < 1 year) and U-CLLs with a more indolent course (TTFT > 6 years). Notably, these indolent U-CLL cases still had significantly higher protein levels than aggressive M-CLLs (**Figure 43D**). Therefore, these findings denote that higher LEF1 protein abundance is a marker of the U-CLL subtype, regardless of the individual course of the disease in individual cases.

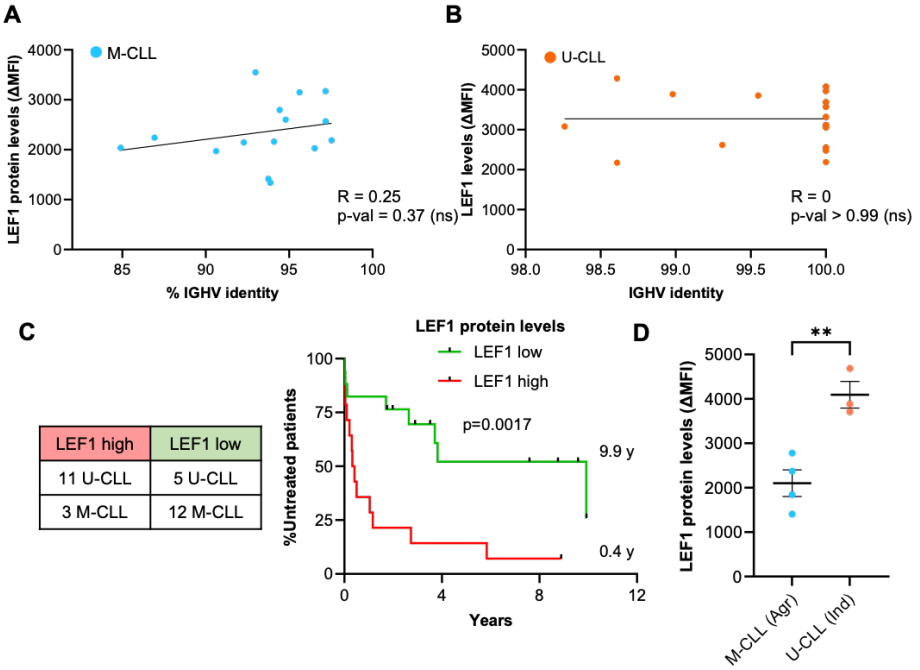


Figure 43. LEF1 protein levels correlation to IGHV identity and prognosis. A-B) Correlation between the % of IGHV identity and LEF1 protein levels in A) M-CLL cases (n=15) and B) U-CLL cases (n=16). C) Kaplan-Meyer curves show the percentage of untreated patients over time (years) in high (red) or low LEF1 protein (green) groups. The table on the left shows the composition of each group in terms of M-CLL and U-CLL cases. D) LEF1 protein levels measured by intracellular flow cytometry in aggressive (agr) M-CLL with TTFT < 1 year (n=4) and indolent (ind) U-CLL with TTFT > 6 years (n=3).

2.2. LEF1 stability in CLL cells

I next sought to study which was the cause of higher LEF1 protein levels observed in the U-CLL subtype. Given that there were no differences at the mRNA levels of U-CLL and M-CLL, I hypothesized that similar protein levels of LEF1 would be produced in both CLL subgroups. In consequence, the final differences in protein abundance that I was observing could be linked to different protein stability in U-CLL and M-CLL. To investigate this, 6 U-CLL and 6 M-CLL were treated with a protein synthesis inhibitor, CHX (50 μM), for 12 hours. Total protein was extracted at 0, 4, 8 and 12 hours after CHX treatment and western blot was performed to assess the level of protein expression at the indicated time-points (**Figure 44A**). Remarkably, LEF1 levels were considerably more stable in U-CLLs compared to M-CLLs. For instance, after 8 hours of protein synthesis inhibition, LEF1 protein was only reduced by a 20% in U-CLL cells, while it decreased a 60% in M-CLL cells (**Figure 44A, C**). This phenotype was rescued by treating cells with the proteasome inhibitor MG-132 (5 μM), observing a restoration of LEF1 levels in all CLL cells, especially in U-CLL samples (**Figure 44B**).

Finally, I wondered whether the increased protein stability in U-CLL was specific for LEF1 or a global phenomenon. To test whether this was the case, β-catenin protein levels analyzed after CHX treatment alone or in combination with MG-132 proteasome inhibition (**Figure 44B**). In this case, β-catenin was degraded at the same rate in both CLL subgroups (N=2/subgroup) and protein degradation was blocked when adding MG-132 (**Figure 44D**). Altogether, these results indicate that the higher LEF1 protein levels observed in U-CLL are caused by an impaired LEF1 proteasomal degradation in cells from this CLL subtype.

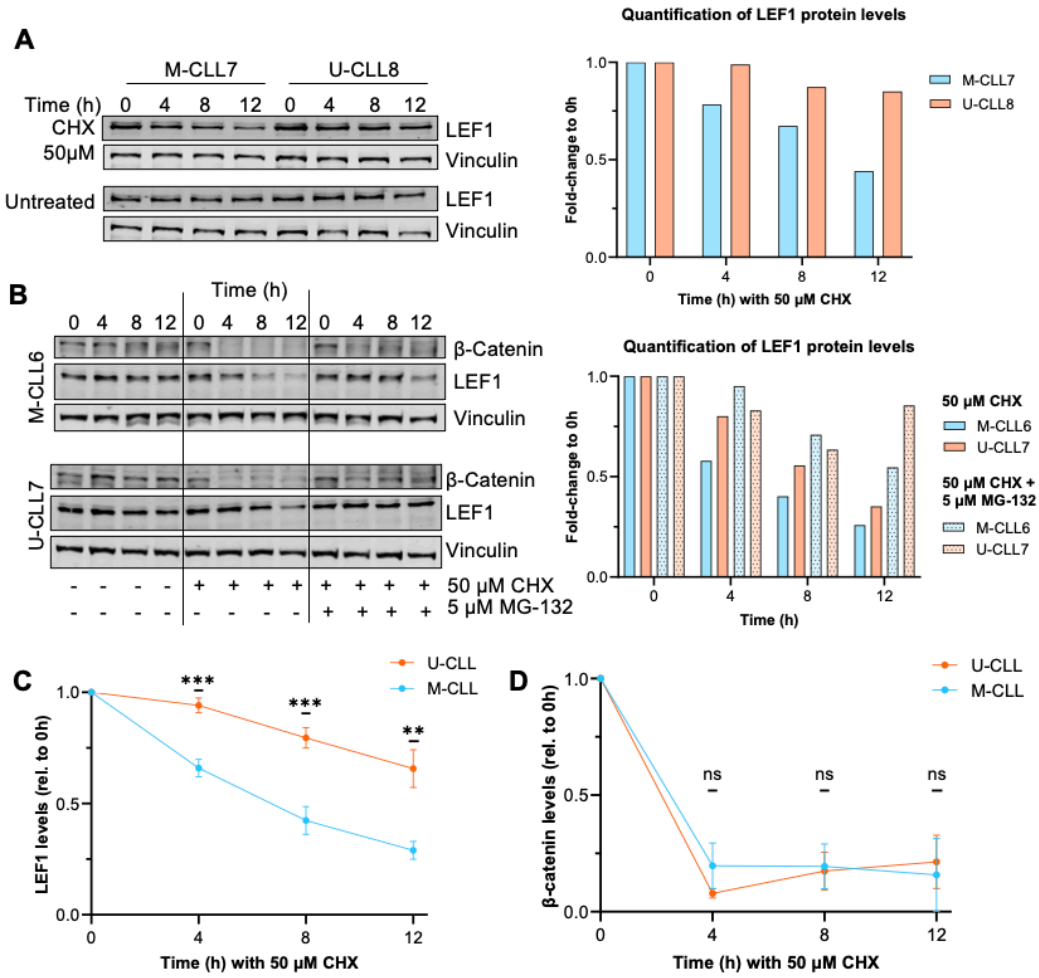


Figure 44. LEF1 and β-catenin stability in CLL cells. A) Western blot shows LEF1 protein levels before and after 4,8 and 12 hours of treatment with 50 μM CHX in one M-CLL and one U-CLL case. Bar plot shows the western blot normalization and quantification of LEF1 protein levels. B) Western blot shows LEF1 and β-catenin protein levels before and after 4,8 and 12 hours of treatment with 50 μM CHX or with 50 μM CHX and 5 μM MG-132 in one M-CLL and one U-CLL case. Bar plot shows the western blot normalization and quantification of LEF1 and β -catenin protein levels. C) XY graph represents LEF1 protein levels upon treatment with CHX in 6 U-CLL and 6 M-CLL (mean ± SEM). D) XY graph represents β -catenin protein levels upon treatment with CHX in 2 U-CLL and 2 M-CLL (mean ± SEM).

2.2.1. Mechanism behind LEF1 protein stability

Ubiquitination is a protein post-translational protein modification that rules cellular protein degradation through the proteasome. Deubiquitinases (DUBs) have been shown to remove ubiquitin, reverting the degradation of the target protein (317). Ubiquitin-specific peptidase 10 (USP10) belongs to the DUBs family and has been defined to act on β-catenin (318,319) as well as TCF4 (320), two well-known interactors of LEF1 and members of the same family. Therefore, I hypothesized that USP10 could be interacting with LEF1 to avoid its degradation specifically in U-CLL cells. To test the validity of this hypothesis, I first performed a total IP of LEF1 in 2 U-CLL and 2 M-CLL samples. Remarkably, these experiments showed that LEF1 was interacting with USP10 in both CLL subtypes (**Figure 45A**). However, the amount of USP10 protein precipitated together with LEF1 was higher in U-CLL samples. Consequently, I downregulated *USP10* with CRISPR-Cas9 in 2 U-CLL and 2 M-CLL cases to evaluate if there was any effect on LEF1 protein levels. After 3 days of *USP10* CRISPR-Cas9, there were no significant differences in LEF1 protein levels between NTC and *USP10*-edited cells (**Figure 45B**). In fact, U-CLL cells with reduced levels of USP10 had a slight increase in LEF1 protein, which could be a transcriptional response to the diminished protein stability caused by USP10 depletion.

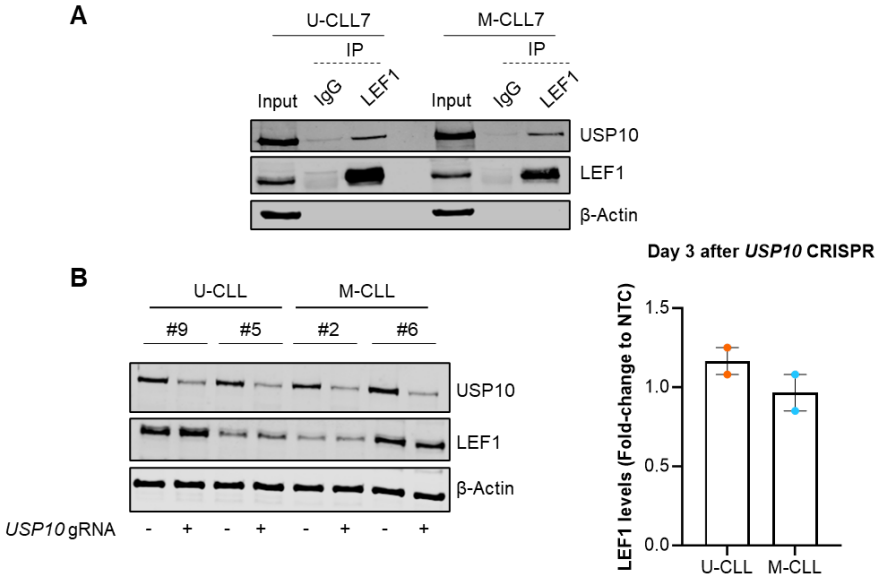


Figure 45. LEF1 interaction with USP10 protein. A) Total IP using *LEF1* and IgG antibodies in CLL samples shows the interaction of LEF1 with USP10 in both CLL subtypes (n=2/subtype). B) Western blot shows LEF1 and USP10 protein levels in NTC and *USP10* gRNA after 3 days of CRISPR in 2 independent cases of U-CLL and M-CLL. β-Actin was used as a loading control. Bar plot on the right displays the western blot quantification of LEF1 in USP10 KD samples relative to NTC cells (mean ± SEM).

Thus, *USP10*-edited and NTC cells, at day 3 after CRISPR, were treated with 100 μM CHX for 8 hours to block protein synthesis and avoid possible compensatory mechanisms. However, the reduction in LEF1 after treatment assessed by western blot was similar between NTC and *USP10*-edited cells in U-CLLs (**Figure 46A**). In contrast, upon treatment, *USP10*-edited M-CLLs showed the expected behavior with lower LEF1 protein compared to NTC cells (**Figure 46A-B**). These results suggest that USP10 was clearly regulating LEF1 protein stability in M-CLL. On the contrary, U-CLL showed no effect in LEF1 protein stability after the downregulation of *USP10*. This could be simply explained by the fact that the higher accumulation of LEF1 protein in U-CLL cells would need more time, after *USP10* knock-down, to display a decrease in LEF1 protein levels.

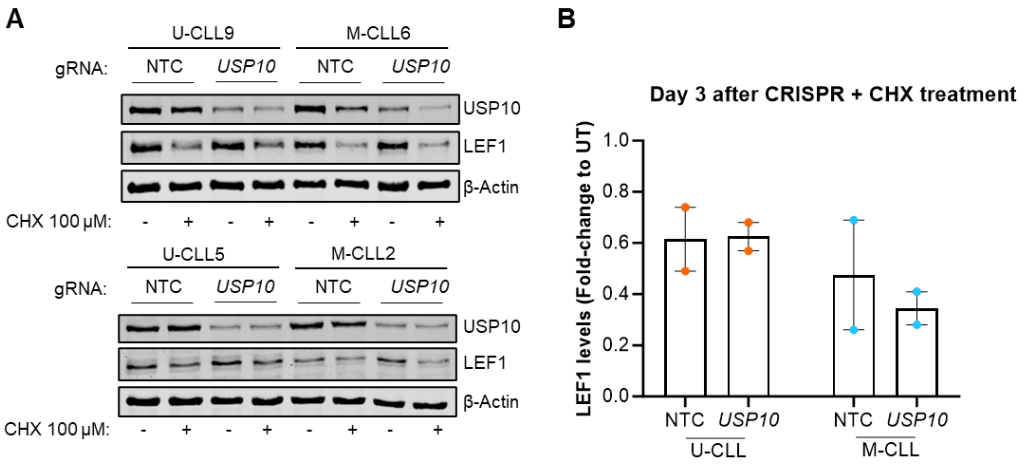


Figure 46. LEF1 levels after *USP10* downregulation and CHX treatment. A) Western blots show LEF1 and USP10 protein levels in NTC and *USP10* gRNA after 3 days of CRISPR and 8 hours of CHX treatment in 2 independent cases of U-CLL and M-CLL. β-Actin was used as a loading control. B) Bar plot displays the western blot quantification of LEF1 in NTC and *USP10* KD samples relative to untreated (UT) cells (mean ± SEM).

For this reason, NTC and *USP10*-edited cells were maintained in culture until day 6 after CRISPR editing. At this time-point, I observed a considerable increase in the basal levels of LEF1 protein in *USP10*-edited cells versus NTC cells in U-CLL samples (**Figure 47A-B**). In contrast, M-CLL with *USP10* downregulation showed a decrease in LEF1 protein levels at basal state, which were even more magnified when treating with CHX (**Figure 47A-C**). In summary, these data suggest that, as compared to M-CLL, U-CLL cells have additional mechanisms, besides interaction with USP10, to secure LEF1 protein levels.

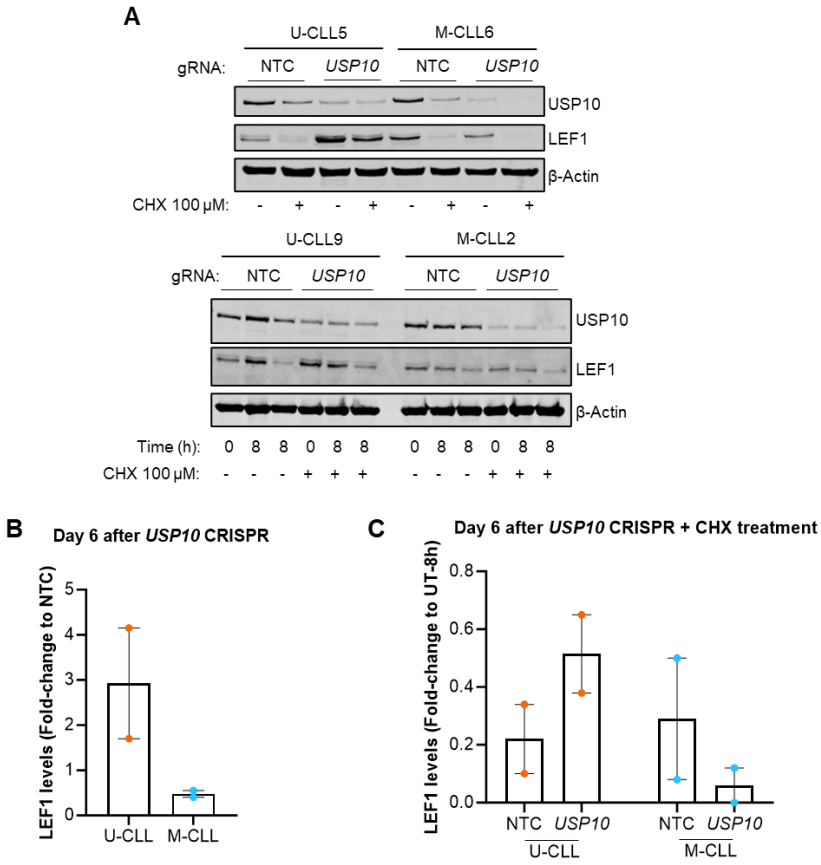


Figure 47. LEF1 levels after *USP10* downregulation and CHX treatment at day 6 after CRISPR. A) Western blots show LEF1 and USP10 protein levels in NTC and *USP10* gRNA after 6 days of CRISPR and 8 hours of CHX treatment in 2 independent cases of U-CLL and M-CLL. β-Actin was used as a loading control. B) Bar plot displays the western blot quantification of LEF1 in *USP10* KD cells relative to NTC cells (under untreated conditions). C) Bar plot displays the western blot quantification of LEF1 in NTC and *USP10* KD samples relative to untreated (UT) cells (mean ± SEM).

2.3. Genome-wide distribution of LEF1 binding sites in CLL

As I observed significantly higher LEF1 protein abundance in U-CLL cells, I wanted to determine whether LEF1 was playing different roles in M-CLL and U-CLL. I identified the genome-wide LEF1 binding sites by CUT&RUN in primary CLL cells (n=4/subtype), which had been expanded with MM1 cells for 6 days and had high viability and high CLL purity (CD20+CD5+ > 90%) (**Figure 48A-B**). I specifically

selected cases with significantly different LEF1 protein levels to be able to properly compare between both IGHV subtypes (**Figure 48C**).

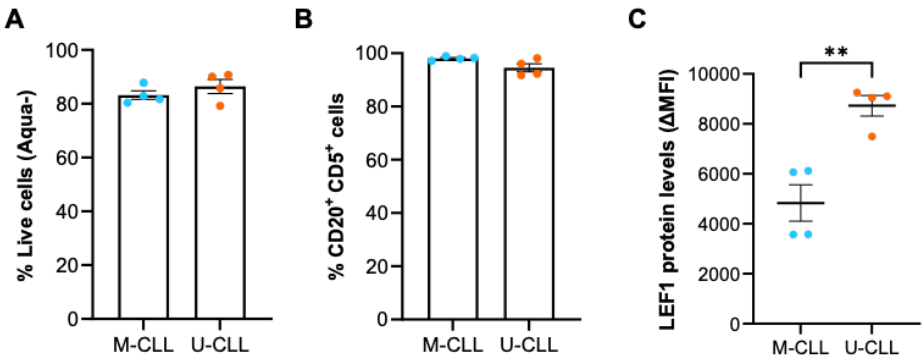


Figure 48. LEF1 CUT&RUN in primary CLL cells. A) Percentage of live cells (Aqua-) in the U-CLL and M-CLL samples prior to CUT&RUN technique (n=4 CLL/subtype). B) Percentage of leukemic cells (CD20+ CD5+) in the M-CLL and U-CLL samples prior to CUT&RUN technique (n=4 CLL/subtype). C) LEF1 protein levels in primary samples used for CUT&RUN technique (n=4 CLL/subtype). Unpaired t-test.

The result of these experiments led to a 2.7-fold more LEF1 peaks in U-CLL than in M-CLL cells: I found 17,843 total number of peaks in U-CLL and 6,518 for M-CLL (**Figure 49A**). Motif analysis revealed a significant enrichment of the TCF/LEF binding motif at the peak summit in all samples, indicating LEF1 was binding directly to DNA in both subtypes (**Figure 49C**). Global LEF1 binding distribution was also considerably similar between M-CLL and U-CLL, and I observed LEF1 peaks were significantly enriched in intronic regions, suggesting that LEF1 was preferentially binding to potential intragenic regulatory regions. (**Figure 49B**). This feature was even more evident when comparing the genome-wide binding of BRD4 and RNA polymerase II (Pol II), assessed by CUT&RUN in the same cases (n=2/subtype). As expected, BRD4 and Pol II binding was biased towards promoters. Hence, it seems that LEF1 is a TF with a preferential binding to enhancers, located in intronic regions. Interestingly, the overlap of LEF1 peaks in M-CLL and U-CLL revealed that although most of M-CLL peaks were also found in U-CLL (n=5,777 peaks), a 68% of the LEF1 binding sites identified in U-CLL cells were unique (n=12,059 peaks) (**Figure 49C**). To understand the differential LEF1

peaks identified, I first analyzed the chromatin accessibility and activity of those regions in PB unstimulated primary samples (by ATAC-seq and H3K27ac ChIP-seq data from Beekman, 2018 (135), n=104). I observed that LEF1 specific peaks in U-CLL were located at regions that had significantly more accessibility and higher H3K27ac in PB U-CLL cells. This indicates LEF1 is binding to regions that are already differentially open and active in U-CLLs (**Figure 49D-E**).

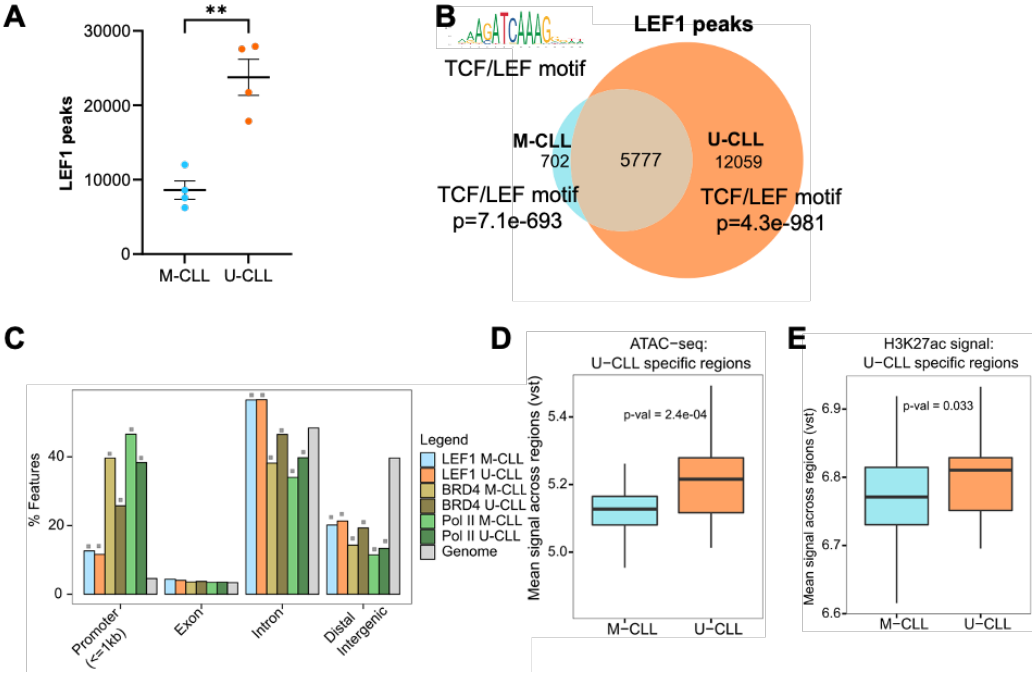


Figure 49. LEF1 CUT&RUN in primary CLL cells. A) Number of LEF1 peaks obtained in U-CLL and M-CLL samples (n=4/subtype). Unpaired t-test. B) Distribution of LEF1, BRD4 and Pol II peaks (and genome used as background) over promoter, exon, intron or distal intergenic regions. Square shape above the bar shows significant enrichment in the region compared to genome (OR >1, Chi-squared test). D&E) Box plot represent the D) accessible regions and E) active regions (H3K27ac) in chromatin in M-CLL and U-CLL samples (n=104). Wilcoxon test.

Finally, to characterize the chromatin modifications associated to LEF1 binding sites in proliferative CLL cells, I performed a comprehensive chromatin characterization of one U-CLL after 6 days of *in vitro* expansion LEF1 peaks at promoters associated with high H3K4me3, while intragenic and intergenic LEF1 peaks present high H3K4me1 levels, and all regions showed moderate H3K27ac

levels. However, no association between LEF1 peaks and H3K27me3 (heterochromatic mark) signal was observed (**Figure 50**). In short, these results indicate that LEF1 is binding to open and active regulatory regions at U-CLL cells, suggesting it contributes to maintain a chromatin environment that may positively contribute to the gene expression of its target genes.

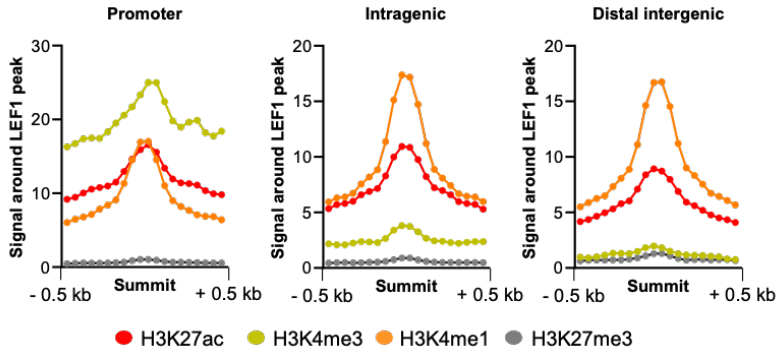


Figure 50. Histones marks around summit of LEF1 peaks located in distal intergenic, gene body (intron and exon) and promoter in one representative U-CLL case.

To identify LEF1 targets genes, U-CLL and M-CLL peaks were annotated to the nearest gene genes using *ChIPseeker* R package (271). I restricted the analysis to those peaks located at promoters and gene bodies, which very likely regulate the expression of the gene within which they are located, and discarded those located at distal intergenic regions (25%), in which their target gene is less obvious. As a result of the peak annotation, I identified twice more LEF1 target genes in U-CLL (n=6,614) than in M-CLL (n=3,192). Despite these differences, the total number of U-CLL genes (n=6,614) was lower than expected, given that the initial number of peaks identified in these cells was much higher (n=17,843), suggesting that several peaks corresponded to the same gene. The overlap between LEF1 target genes in U-CLL and M-CLL demonstrated, in a similar way to the peak comparison, that almost all M-CLL genes were also found in U-CLL, and that a 51.2 % of LEF1 target genes were U-CLL specific (**Figure 51A**). In addition, as LEF1 peaks were mostly located in active chromatin regions, I discarded all the annotated genes that were not expressed in CLL cells (TPM < 1 in RNA-seq from CLL cells before and after MM1

co-culture, data from Study 1) and kept all the protein-coding genes for gene ontology analyses (U-CLL=4,303/M-CLL=2,176). I identified that LEF1 target genes common to U-CLL/M-CLL were involved in a "CLLness"-related functions, such as BCR/TLR/IL/Rho signaling, which controls how cells respond to microenvironmental signals and survival such as *CD86*, a late activation marker of lymphocytes (**Figure 51B-C**). On the contrary, U-CLL specific target genes were linked to cell cycle progression and proliferation mechanisms (**Figure 51B, D**), such as *CCND2*, which is upregulated in proliferative CLL cells either in lymph nodes (314) or in co-culture with the MM1 stromal cells (274).

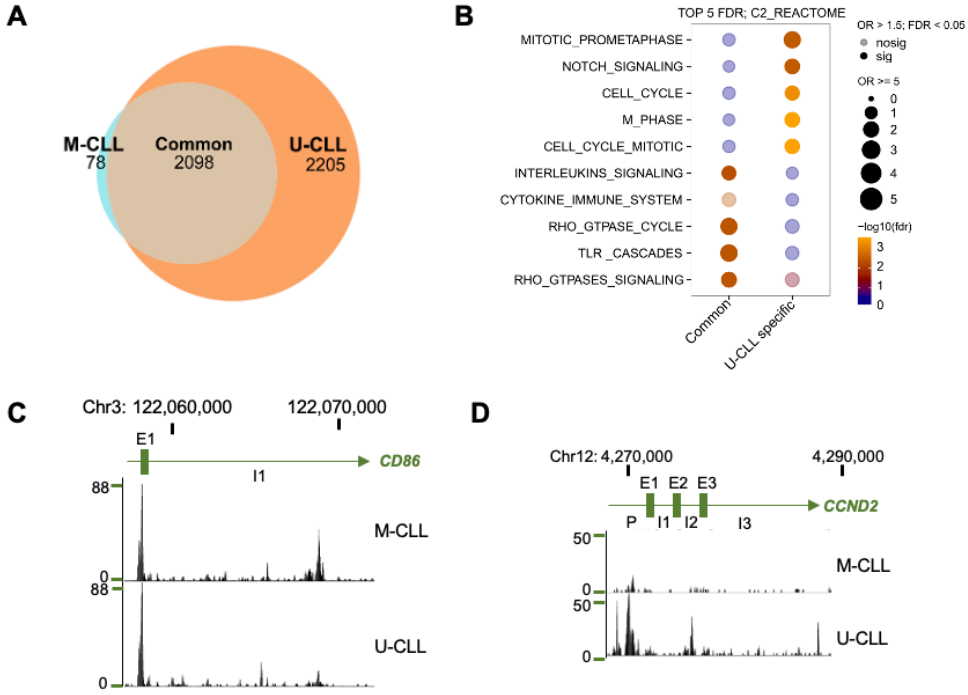


Figure 51. LEF1 target genes in primary CLL cells. A) Overlap of LEF1 peak-associated genes in M-CLL and U-CLL samples (n=4/subtype). B) Gene pathway enrichment analysis for LEF1 target genes common in CLL and specific for U-CLL (FDR < 0.05). C-D) Representative UCSC plot of LEF1 peaks obtained with CUT&RUN in C) a common CLL target gene, *CD86* and D) a U-CLL specific target gene, *CCND2,* in a representative M-CLL and U-CLL case.

Given that LEF1 is highly expressed in normal T cells (182), I wondered whether the specific U-CLL signature associated to cell proliferation was exclusive for U-CLL cells or it was somehow related to the role of LEF1 in T cells. To answer this, LEF1 CUT&RUN was also performed in healthy T cells derived from PB stimulated with IL-2 and anti-CD3/CD28 beads *in vitro* (n=3). Intracellular staining determined that stimulated T cells had LEF1 protein levels similar to M-CLL cells and, consequently, the number of peaks (n=7,100) obtained was similar to M-CLL (n=6,518) (**Figure 52A-B**). The overlap of peaks between U-CLL, M-CLL and T-cell revealed that still 59 % of the peaks were U-CLL specific and are neither shared with M-CLL nor T-cells (**Figure 52C**). Moreover, there were common peaks in CLLs not shared by T cells and 50 % of T-cell LEF1 peaks were also specific for T-cells. I annotated these T-cell peaks to genes (n=2,326) following the previously described criteria and, interestingly, only a 16% of the total number of genes were T-cell specific, while the rest were shared with all the CLLs (**Figure 52D**). In conclusion, I identified that in U-CLL cells 38% of genes (n=1,618) showed a LEF1 peak that was specific for the U-CLL subgroup. Gene ontology analyses revealed that common genes between 1) CLL and T cells and 2) U-CLL specific genes were significantly enriched in certain pathways, whereas no enrichment was found in T-cell specific or CLL-specific genes (**Figure 52E**). Common CLL/T-cell genes were enriched in pathways related to immune signaling and microenvironmental stimuli (e.g., interleukin, TLR, cytokine) and lymphocyte migration and activation cascades such as *CTLA4* (**Figure 52F**). This suggests that LEF1 could be involved in the regulation of T-cell related factors since CTLA4 induces inhibitory effects in T cells. On the other hand, U-CLL specific genes were related to cell cycle progression and proliferation, such as *E2F3*, where LEF1 was binding to enhancers located within intragenic regions (**Figure 52G**). Therefore, this comparison including also T cells further confirms that LEF1 binds to genes involved in cell cycle progression exclusively in U-CLL cases.

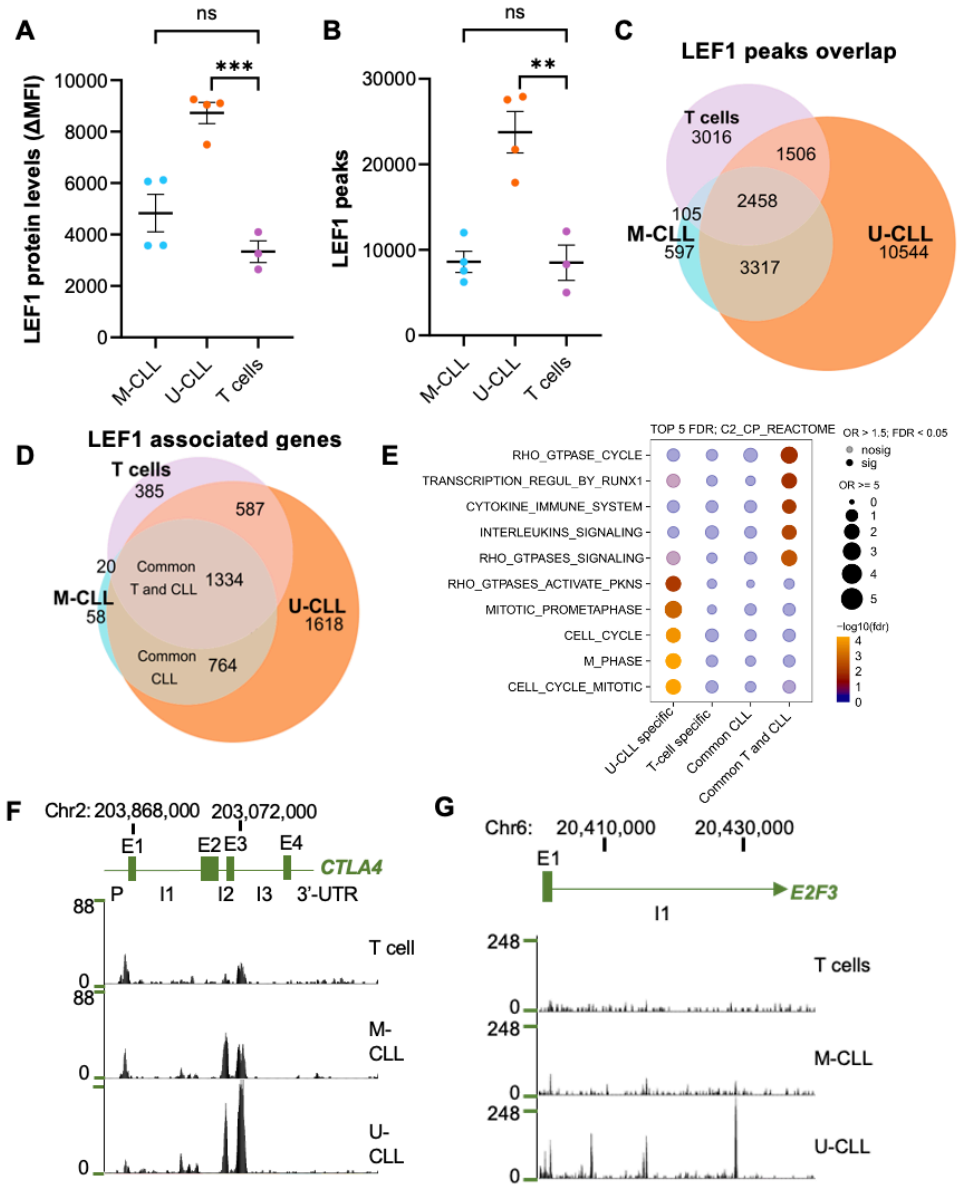


Figure 52. LEF1 CUT&RUN in primary CLL and T cells. A) Protein levels of LEF1 found in M-CLL (n=4), U-CLL (n=4) and T cells (n=3) prior to CUT&RUN technique. Unpaired t-test. B) Number of peaks related to LEF1 after CUT&RUN. Unpaired t-test. C) Overlap of LEF1 peaks in M-CLL, U-CLL T cells samples. D) Overlap of LEF1 associated genes in these M-CLL, U-CLL T cells samples. E) Gene pathway enrichment analysis for LEF1 target genes common in CLL/CLL and T cells and specific for U-CLL or T cells (FDR < 0.05). F-G) Representative UCSC plot of LEF1 peaks obtained with CUT&RUN in F) a common T-cell and CLL target gene, *CTLA4* and G) a U-CLL specific target gene, *E2F3*, in 1 T cell, 1 M-CLL and 1 U-CLL.

2.4. Proliferation of CLL cells modulate the protein levels of LEF1

Given that LEF1 appeared to be regulating genes involved in lymphocyte activation and proliferation in CLL cells, which mainly occur in the LN, I wondered if LEF1 protein levels could be increased in LN. CLL cells from PB can be separated into proliferative or resting fractions depending on the levels of CXCR4 and CD5 (**Figure 53A**). Remarkably, LEF1 protein levels were significantly higher in the proliferative (CXCR4 low CD5 high) than in the resting fraction (CXCR4 high CD5 low), independently of the IGHV status (**Figure 53B**). In other words, LEF1 protein was increased in those CLL cells that had just exited the LN, suggesting that LEF1 levels increased upon LN-stimuli. In line with this finding, LEF1 protein levels also increased in *in vitro* stimulated CLL cells with MM1 stromal cells (**Figure 53C**). Even though LEF1 levels were increased in both CLL subtypes, proliferative U-CLLs still showed higher protein abundance (**Figure 53D**), similar to what was reported in unstimulated cells. As shown previously (Study 1), CLL cells became gradually activated and proliferative upon co-culture with MM1 cells (**Figure 53E**). At day 3 after culture, just a few of cells were proliferating (Ki67+ = 20 %) and exhibited higher LEF1 protein levels than non-proliferating cells (Ki67-) (**Figure 53F**). Thus, LEF1 protein levels are rapidly increased in response to LN-stimulation, particularly in those cells that become proliferative.

To further understand if there was a direct relationship between LEF1 protein levels and CLL proliferation, CRISPR-Cas9 *MYC* KD was induced in stimulated U-CLL cells (upon day 6 in culture). As expected, Ki67 levels were significantly decreased as *MYC* KD blocked cell proliferation (**Figure 53G**). Strikingly, LEF1 protein levels were also reduced in *MYC* KD cells compared to NTC (**Figure 53H**). In summary, all these results indicate LEF1 protein levels are modulated by the proliferation state of U-CLL cells.

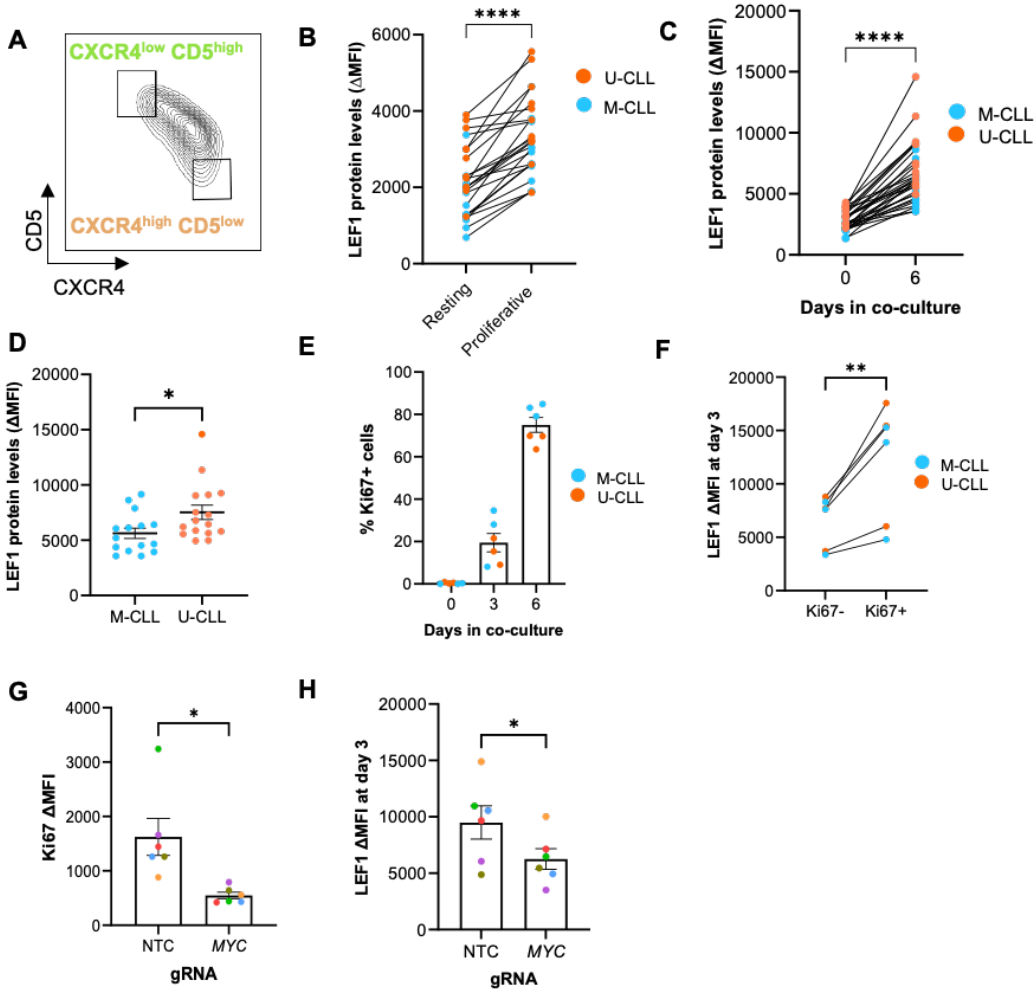


Figure 53. LEF1 protein levels in proliferative CLL cells. A) Density plot shows the proliferative (CXCR4 low CD5 high) and resting (CXCR4 high CD5 low) populations in a CLL sample from PB. B) LEF1 protein levels in the resting and proliferating fraction of CLL samples (n=15/subtype). Paired t-test. C) LEF1 protein levels in unstimulated (day 0) and stimulated (day 6 in culture with MM1) CLL samples (15 M-CLL and 16 U-CLL). Wilcoxon matched signed rank test. D) LEF1 protein levels in stimulated M-CLL (n=15) and U-CLL (n=16) samples. Mann Whitney test. E) Percentage of Ki67+ CLL cells over time in culture (day 0, 3 and 6). F) LEF1 protein levels at day 3 in Ki67- and Ki67+ CLL cells. Paired t-test. G) Ki67 levels in NTC and *MYC*-edited cells at day 3 after electroporation. Wilcoxon matched signed rank test. H) LEF1 levels in NTC and *MYC*-edited cells at day 3 after electroporation. Paired t-test.

2.5. LEF1 plays a direct role in CLL proliferation

Following the previous findings, I aimed to study if the increased LEF1 protein levels in LN were just correlative or were indicating a direct role of LEF1 in the proliferation of CLL cells. To do so, *LEF1* KD was induced by CRISPR-Cas9 in primary CLL samples (3 U-CLL and 3 M-CLL) with two independent sgRNA to avoid off-target effects (**Figure 54A**). At day 4 after CRISPR-Cas9, when LEF1 protein levels were reduced by an 80% compared to NTC cells (**Figure 54B**), RNA-seq from *LEF1* KD and NTC cells was performed. Gene expression analysis showed very few differentially expressed genes between *LEF1* KD and NTC cells, since 1) most of the differences captured were caused by the huge interpatient heterogeneity and 2) I was working with a bulk population with some *LEF1*-edited cells as well as non-edited. Because of this, I used less stringent criteria to define differentially expressed genes between *LEF1* KD and NTC cells. Pairwise analysis of all 6 patient samples identified 420 differentially expressed genes of which 178 were upregulated and 242 were downregulated (applying a cut-off of p-val < 0.01) (**Figure 54C**). GSEA indicated that CLL cells with decreased levels of LEF1 showed a downregulation of cell cycle genes (**Figure 54D**), like *CDC20* or *KPNA2*.

To functionally evaluate the impact of *LEF1* KD in primary CLL cell proliferation, LEF1 *KD* was induced in CLL cells (n=6). At day 3 after CRISPR, even though LEF1 levels were considerably decreased, no differences in cell viability were found between NTC and LEF1 KD cells (**Figure 54E-F**). In KD cells, LEF1 high (non-edited cells) and LEF1 low (*LEF1* KD cells) gates for CLL populations were defined using the NTC cells (**Figure 54G**). Then, I determined the Ki67 levels within the two populations (**Figure 54H**). Accordingly, Ki67 levels were lower in cells with very low levels of LEF1, whereas in non-edited CLL cells, Ki67 protein levels were maintained high (**Figure 54H**). Altogether, the transcriptomic and functional evaluation indicate that LEF1 plays a role in driving CLL proliferation. However, the

higher LEF1 protein levels in U-CLL, as compared to M-CLL, may confer an additional proliferative push in the former subtype.

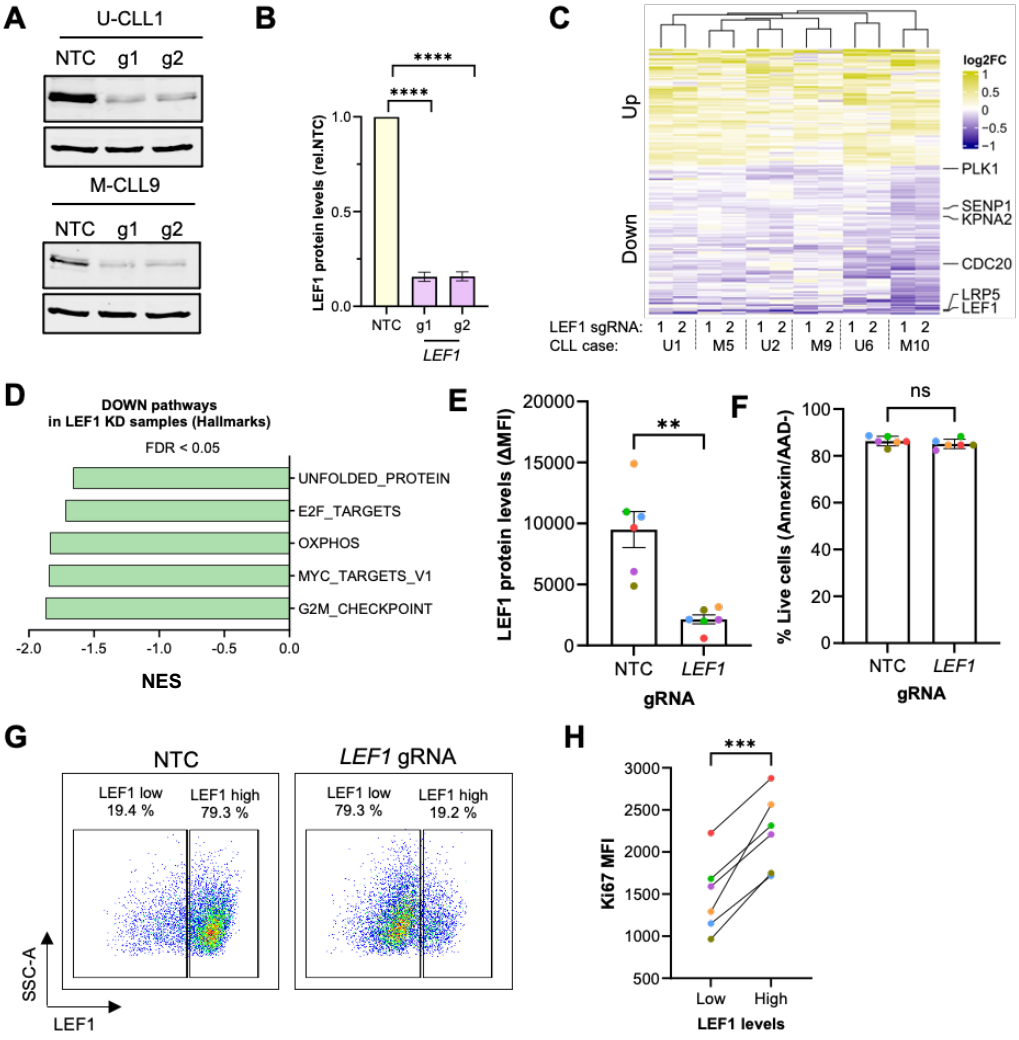


Figure 54. *LEF1* downregulation in primary CLL cells. A) LEF1 protein levels in CLL samples (1 U-CLL and 1 M-CLL) electroporated with NTC or *LEF1* sgRNA#1 and #2. β-Actin was used as a loading control. B) Quantification of LEF1 levels in all the samples used in this experiment (n=6). Unpaired t-test. C) Heatmap with the DE genes (p-val < 0.01) in *LEF1* KD cells (sg1 and sg2) plotted using log2FC of LEF1 KD versus NTC cells. D) GSEA of downregulated genes (FDR < 0.05) in *LEF1* KD cells identified by DESEq2. E) LEF1 levels at day 3 after LEF1 CRISPR in NTC and LEF1 cells (n=6). Paired t-test. F) Percentage of live cells in NTC and LEF1 KD samples at day 3 after CRISPR. Paired t-test. G) FACS plots show the gates of LEF1 low and LEF1 high in CLL cells electroporated with NTC and LEF1 gRNAs (day 3 after CRISPR). H) Ki67 protein levels in high and low LEF1 groups defined in CLL samples (n=6). Paired t-test.

2.6. The LEF1 interactome of CLL cells

To decipher the mechanisms behind the specific proliferative role of LEF1 in U-CLL, the "additional proliferative push", I investigated if a differential interactor partner, in addition to the identified differential DNA binding, could be playing a role. To evaluate this, I performed LEF1 nuclear IP followed by mass-spec in 2 M-CLL and 2 U-CLL cases upon *in vitro* expansion with MM1 stromal cells. The resultant interactors of LEF1 were kept if their log2FC protein abundance was >10 of LEF1 versus IgG control antibody and present in < 7 experiments from the Crapome database (321). Then, the final number of LEF1 interactors for M-CLL or U-CLL were defined by the common proteins found in the 2 cases profiled, respectively. Although the number of LEF1 partners was similar in U-CLL (n=105) and M-CLL (n=63), using the STRING database (291), I identified U-CLL cells showed a higher number of previously described protein-protein interactions, which was translated into a presence of significant higher enrichment of known protein networks (**Figure 55A-B**).

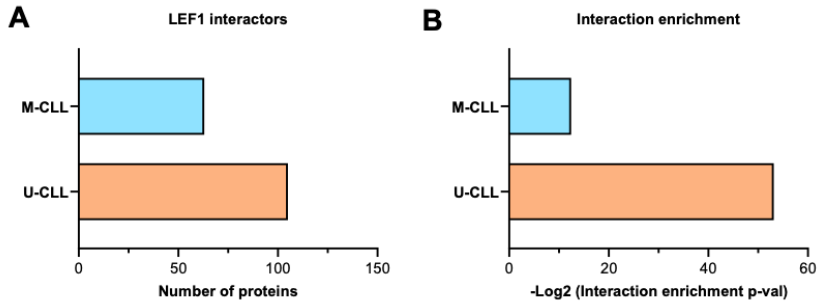


Figure 55. LEF1 interactors in primary CLL cells. A) Bar plot shows the number of protein interactors of LEF1 in M-CLL and U-CLL samples (n=2/subtype). B). Bar plot shows the interaction enrichment of LEF1 in M-CLL and U-CLL samples (n=2/subtype).

Remarkably, LEF1 interactors in U-CLLs were significantly linked to three protein complexes: nuclear pore structure, mRNA transcription/splicing and the β-catenin destruction complex (**Figure 56A**). The interaction of LEF1 with the β-catenin destruction complex suggests that LEF1 role in U-CLL cells might be

β-catenin independent. In contrast to this, no significant enrichment in specific complexes was found in M-CLL samples (**Figure 56B**).

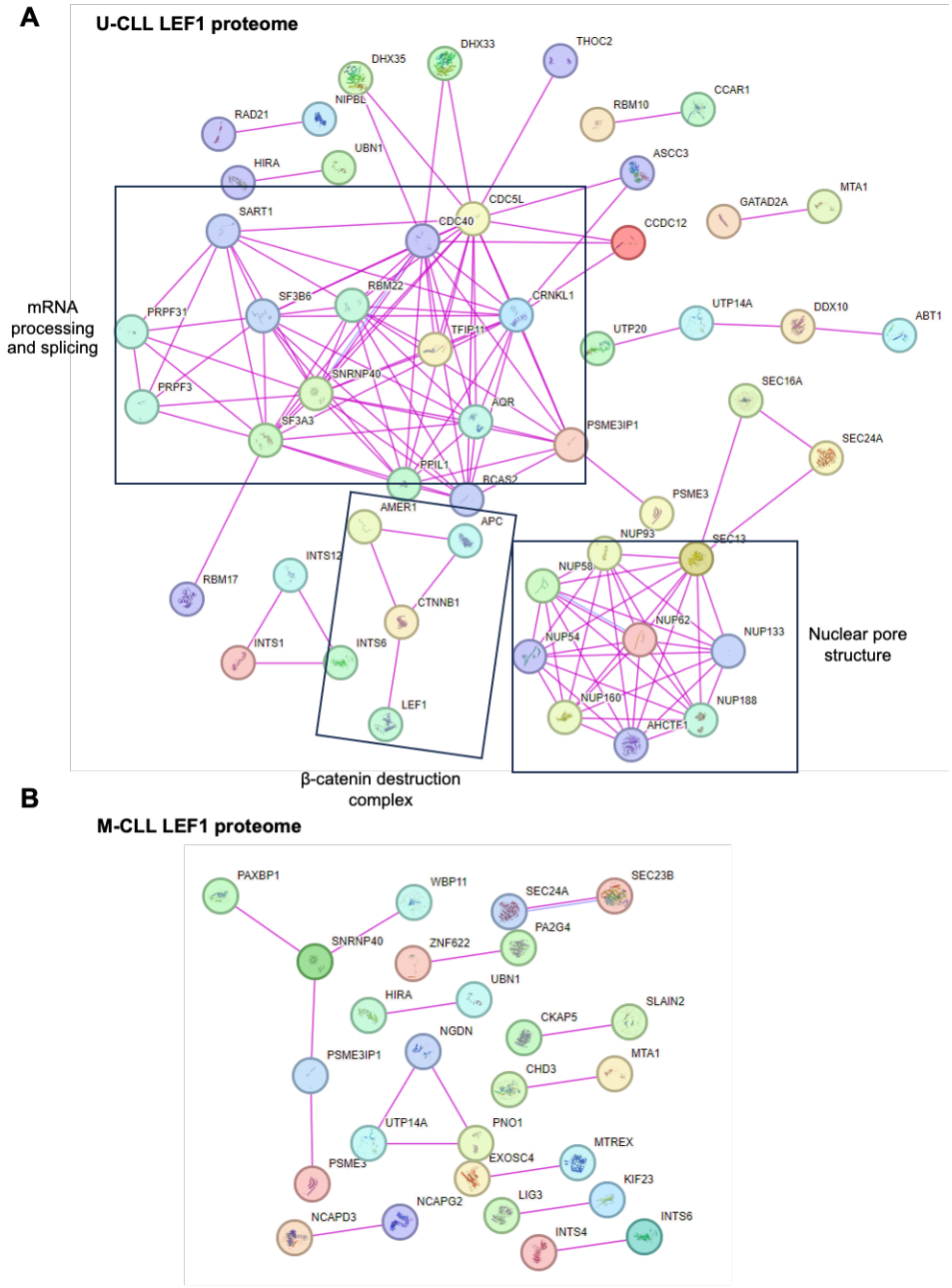
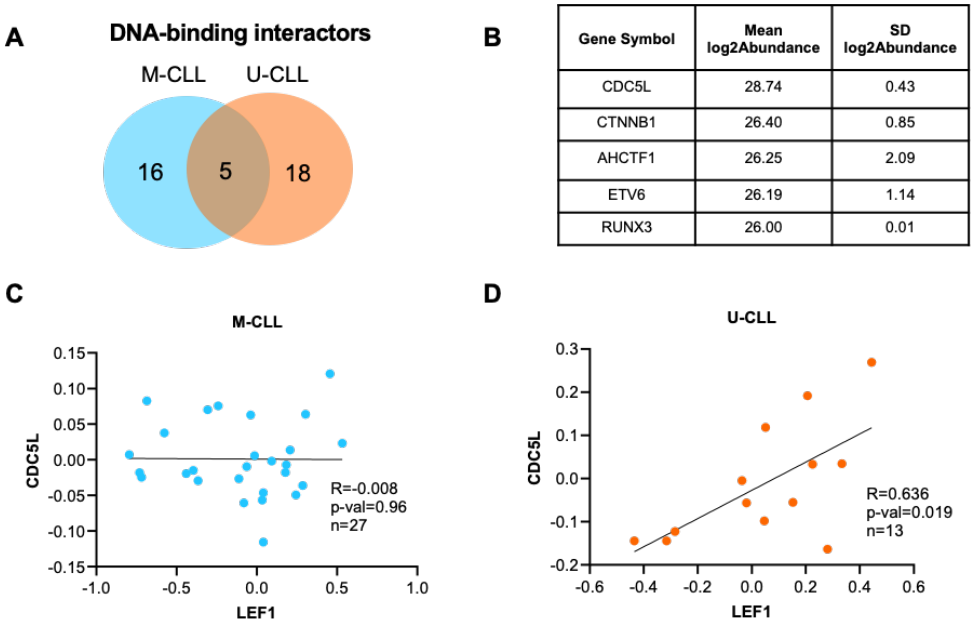


Figure 56. LEF1 interactors in primary CLL cells. Protein interactors and network interaction of LEF1 protein in A) U-CLL and B) M-CLL.

As my aim was to understand the mechanisms behind the proliferative push conferred by LEF1 DNA binding in U-CLLs, I reduced the list of LEF1 interactors to focus on DNA-binding proteins. As a result, I identified a similar number of DNA-binding interactors in U-CLL and M-CLL cells with little overlap between them (**Figure 57A**). Notably, the top U-CLL specific interacting protein was the cell division cycle 5-like (CDC5L) protein (**Figure 57B**). CDC5L protein can bind DNA to act as a transcriptional activator and, in addition, it is a core component of the PRP19/CDC5L complex, which is required for pre-RNA processing (322,323). It has been demonstrated that CDC5L can act as a positive regulator of cell cycle G2/M and cells lacking CDC5L ended up in mitotic catastrophe (324). CDC5L was also the only partner whose abundance positively correlated with LEF1 protein levels in U-CLL (**Figure 57D**), data from Herbst, 2022 (325), whereas there was no correlation between CDC5L and LEF1 protein levels in M-CLL samples (**Figure 57C**).



Gene Symbol	Mean log2Abundance	SD log2Abundance
CDC5L	28.74	0.43
CTNNB1	26.40	0.85
AHCTF1	26.25	2.09
ETV6	26.19	1.14
RUNX3	26.00	0.01

Figure 57. Specific DNA-binding interactors of LEF1 in U-CLL samples. A) Overlap of DNA-binding interactors of LEF1 found in M-CLL and U-CLL. DNA-binding interactors (TF) were selected if present at least two references (292–295). B) Top 5 of LEF1 DNA-binding interactors specific for U-CLL cases. C-D) Correlation between LEF1 and CDC5L in M-CLL (n=27) and U-CLL samples (n=13) from another independent study (325).

Concordantly, *CDC5L* mRNA levels are higher in U-CLL compared to M-CLL (**Figure 58A**), and increased *CDC5L* mRNA levels are associated to shorter TTFT not only in CLL as a whole but also within each CLL subtype, separately (**Figure 58B-C**).

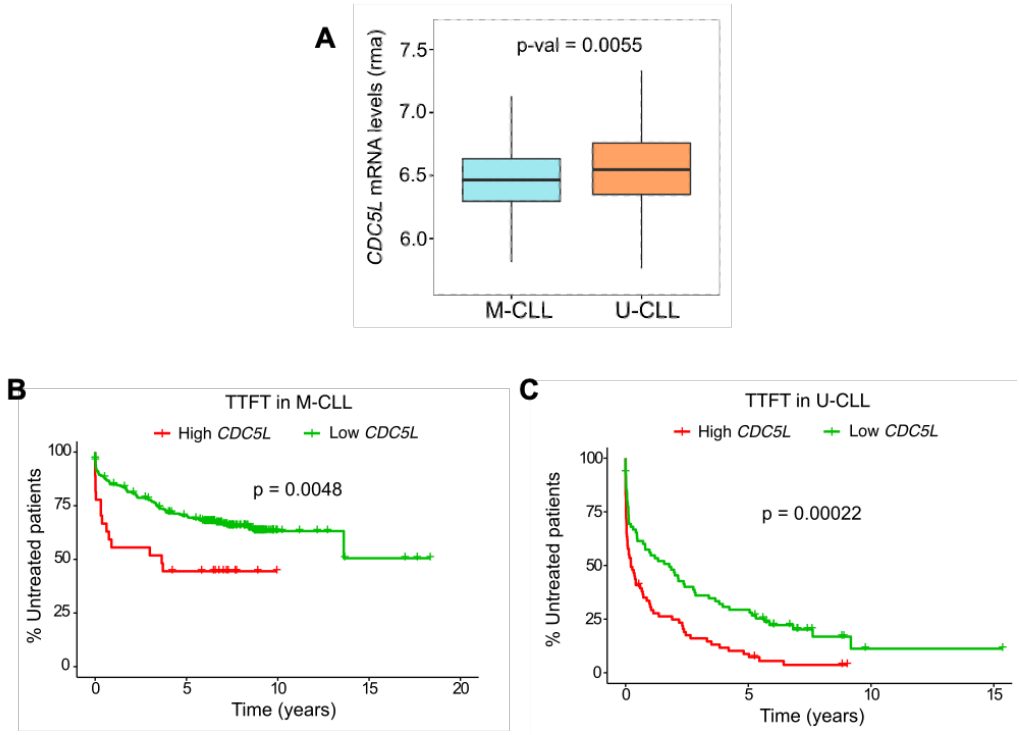


Figure 58. Higher *CDC5L* levels linked to U-CLL and poor prognosis. A) *CDC5L* mRNA levels in U-CLL (n=147) and M-CLL samples (n=256) obtained from microarray expression data (rma). Wilcoxon test. B-C) TTFT in patients with high (red) and low (green) levels of CDC5L in B) M-CLL and C) U-CLL cases.

I validated the LEF1:CDC5L interaction in U-CLLs by IP-western analysis in additional samples (**Figure 59A**). Unexpectedly, reverse nuclear IP with CDC5L antibody uncovered that CDC5L interacts with shorter LEF1isoforms in U-CLL cells (**Figure 59B**). There are three protein isoforms of LEF1 with a molecular weight within the range of 40-45 kDa in CLL cells: full-length (FL), isoform 6 (I6) and isoform 5 (I5) (**Figure 59C**). These three isoforms are considerably similar as they share a β-catenin binding domain, context-dependent regulatory region (CRD), DNA binding domain (HMG box) and nuclear localization signal (NLS). However,

LEF1-FL isoform contains an exon 6 located at the CRD domain, which is lost during alternative splicing in I6 and I5 isoforms. Furthermore, I6 has a different C-terminal end compared to LEF1-FL and I5. Remarkably, the molecular weight of these three isoforms coincided with the three protein bands of LEF1 present in CLL samples detected by total IP-western analysis (**Figure 59D**), where LEF1-I6 appeared to be the most abundant isoform in CLL cells. Furthermore, I validated the presence of LEF1-FL and LEF1-I6 after identifying specific peptide residues of these isoforms by PRM-mass-spec in all CLL samples tested (n=2/subtype) (**Figure 60A-B**). Nonetheless, I5 could not be detected due to lack of specific regions for this isoform, as it lacks the exon 6 like I6 but shares the C-terminal end with the FL isoform. Although it was not possible to obtain the 100% confirmation of I5 presence in CLL cells, I strongly believe I5 is the third band that we detected by western blot in CLL cells.

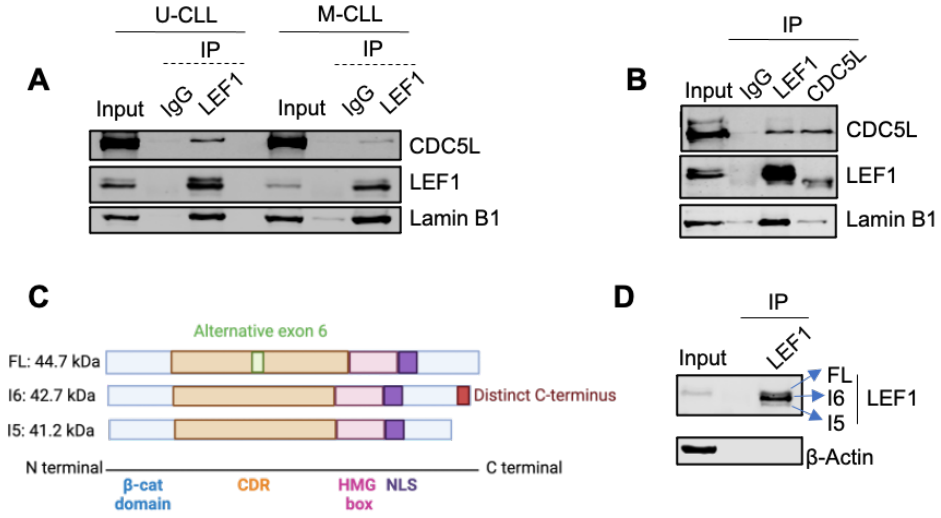


Figure 59. CDC5L interaction with LEF1 in primary U-CLL cells. A) Nuclear IP using IgG and LEF1 antibodies in a primary U-CLL and M-CLL case. Lamin B1 was used as a marker of the nuclear fraction. B) Nuclear IP using IgG, LEF1 and CDC5L antibodies in a primary U-CLL. C) Schematic representation of LEF1 isoforms: FL, I6 and I5. D) Total IP in a primary U-CLL sample using IgG and LEF1 antibodies. The three LEF1 isoforms are shown. β-Actin was used as a marker of the cytoplasmic fraction.

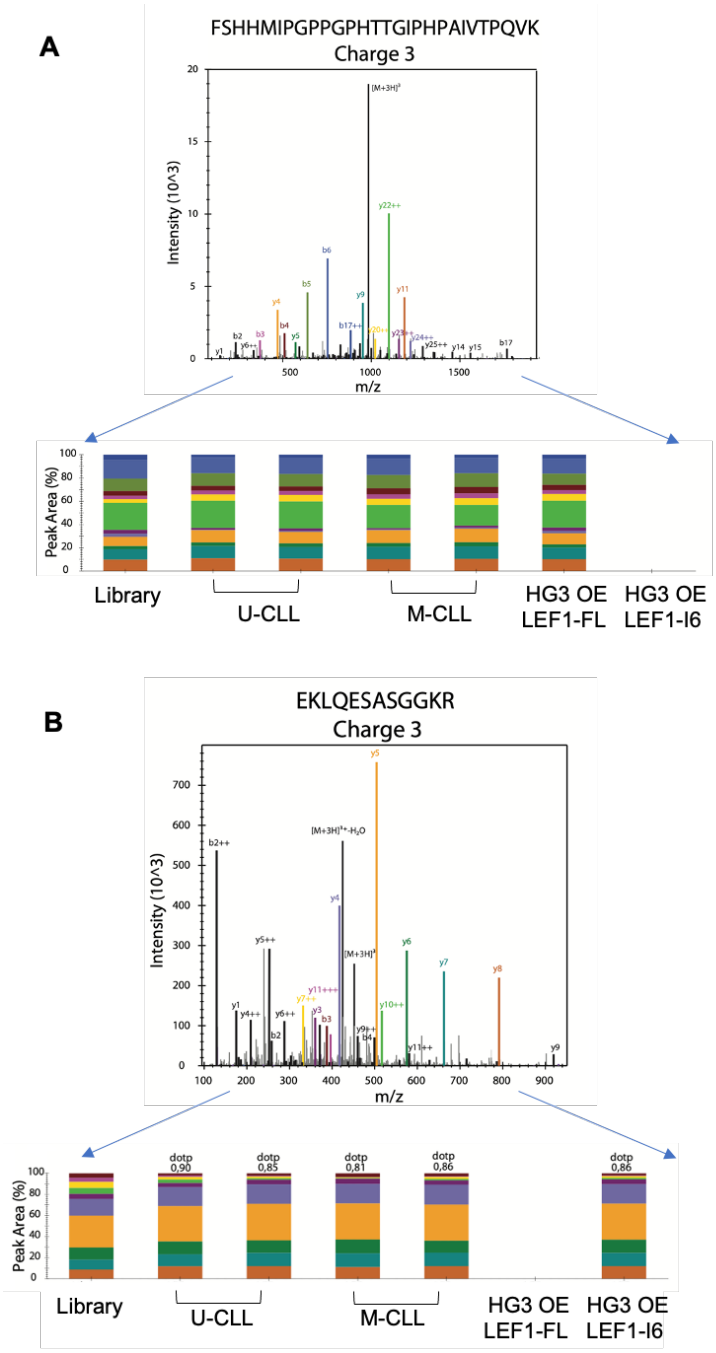


Figure 60. Identification of LEF1 isoforms in primary CLL samples. A-B) Unique peptides for A) FL and B) I6 were investigated in LEF1 nuclear digested samples of CLL. HG3 overexpressing (OE) LEF1-FL or LEF1-I6 were used as a positive and negative control for the specificity of each peptide identification.

Finally, to decipher which LEF1 isoform was interacting with CDC5L, I overexpressed the three different isoforms in HG3 cell line, which has very low expression of LEF1 (**Figure 61A**). Interestingly, nuclear CDC5L IP in HG3 cells revealed that I6 was the isoform interacting with CDC5L (**Figure 61B**).

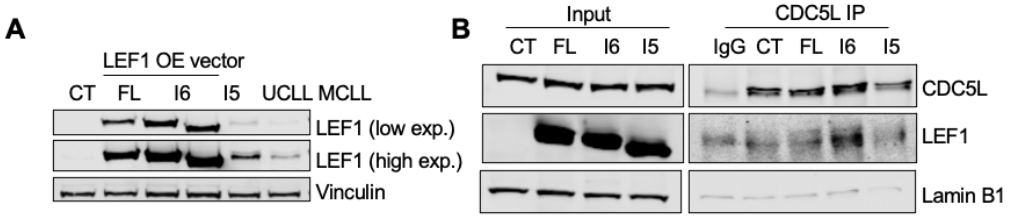


Figure 61. CDC5L interaction with LEF1 short isoforms. A) Western blot shows LEF1 protein in HG3 cell line transduced to overexpress the different isoforms of LEF1 and two primary CLL samples (U-CLL and M-CLL). Vinculin was used as a loading control. B) Nuclear IP using IgG and CDC5L antibodies in HG3-overexpressing LEF1 isoforms. Western blot shows the pull-down of CDC5L in all samples and of LEF1 only in those cells overexpressing I6.

In conclusion, I identified a specific interactor partner of LEF1 in U-CLL, CDC5L, which is known to be involved in the cell cycle control. Unexpectedly, CDC5L interacts with a specific LEF1 isoform that lacks the exon 6 expressed in the canonical LEF1 FL isoform.

2.7. *LEF1* exon 6 skipping in proliferative CLL cells

LEF1-FL has been primarily described to act as tumor promoting in solid tumors such as colorectal or pancreatic cancer (176,326,327). However, recent work has identified that the LEF1-FL isoform was linked to quiescence while the LEF1-I5 was associated with proliferation in neural progenitor cells (328). In addition, exon 6 of LEF1-FL has been connected to transcriptional repression of LEF1 target genes. Thus, I hypothesized that the expression of LEF1 isoforms missing exon 6 (Δexon 6) may also have a different role in CLL and contribute to the LEF1 pro-proliferative role identified in this cellular context. I first assessed the protein isoforms of LEF1 in unstimulated (from PB, quiescent) and stimulated CLL

cells (in culture for 6 days, proliferative) (n=6 U-CLL/6 M-CLL, paired samples). Unstimulated CLL cells showed mainly two bands that corresponded to LEF1-FL (upper band) and LEF1-Δexon6 (lower band) (**Figure 62A**). Interestingly, stimulated CLL cells, which were proliferating *in vitro*, had considerably reduced levels of LEF1-FL compared to unstimulated CLL cells. On the contrary, LEF1-Δexon 6 were maintained or slightly increased (**Figure 62A**). These results were confirmed by the ratio between Δexon 6/FL isoforms in unstimulated and stimulated CLL cells, which was significantly increased in the latter (**Figure 62B**).

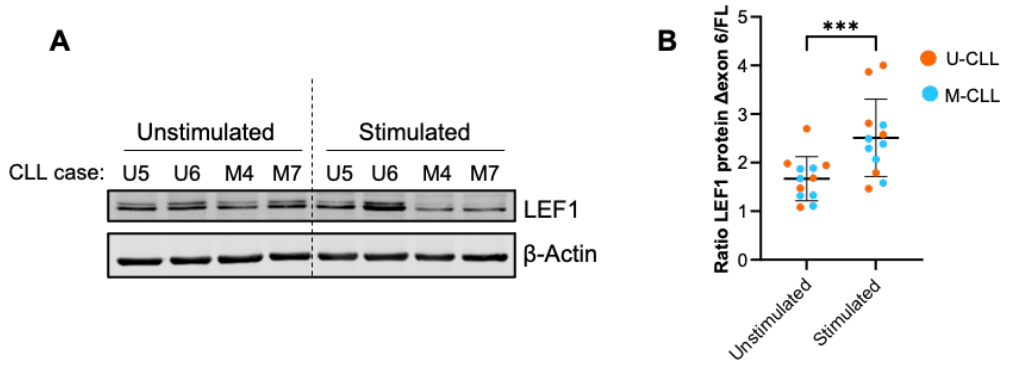


Figure 62. LEF1 isoform switching under proliferative conditions. A) Representative western blot showing LEF1 isoforms before and after stimulation (day 6 in culture with MM1 cell line). β-Actin was used as a loading control. B) Ratio of LEF1-Δexon 6 versus LEF1-FL isoforms in paired unstimulated and stimulated CLL samples (n=6/subtype). Paired t-test.

In mouse neurons/thymocytes and a human T-cell line (Jurkat), exon 6 inclusion in *LEF1* transcript depends on the expression and binding of CELF2 protein to sequences flanking exon 6 (170,329,330) (**Figure 63A**). Thus, CELF2 binding to *LEF1* transcript avoids exon 6 skipping and results in formation of the LEF1-FL isoform. Interestingly, *CELF2* mRNA is downregulated in LN-derived CLL cells compared to PB-derived CLL cells (**Figure 63B**). Similarly, CELF2 mRNA and protein levels were significantly decreased in stimulated CLL cells (n=8, **Figure 63C-E**), suggesting that the LEF1-FL isoform is reduced in CLL cells under proliferative conditions.

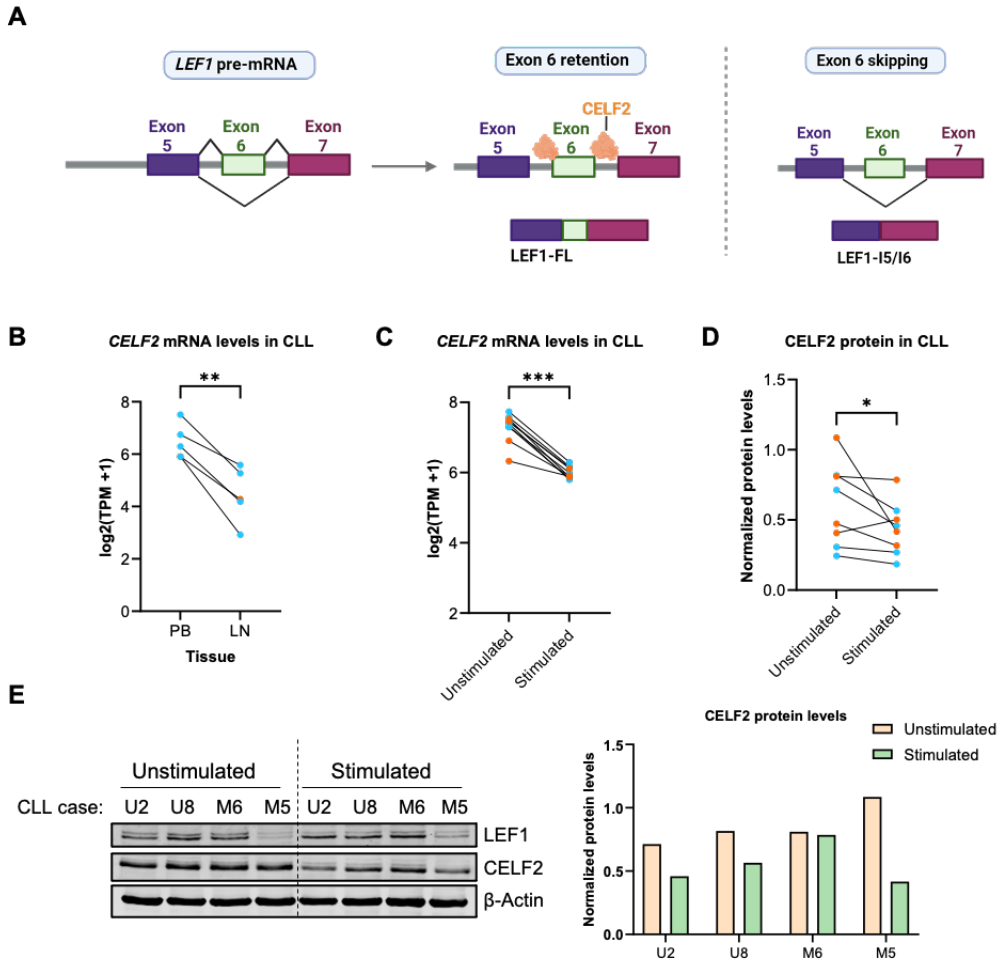


Figure 63. CELF2 expression in CLL under proliferative conditions. A) Schematic representation of *LEF1* exon 6 inclusion or skipping controlled by CELF2 binding. B) *CELF2* mRNA levels in paired PB and LN CLL samples (n=5). Paired t-test. C) *CELF2* mRNA levels in paired unstimulated and stimulated samples *in vitro* (n=4/subtype). D) CELF2 protein levels in paired unstimulated and stimulated samples *in vitro* (n=4/subtype). Wilcoxon matched-pairs signed rank test in C and D. E) Representative western blot of LEF1 and CELF2 levels before and after stimulation of CLL cells *in vitro*. Bar plot represents the quantification of CELF2 protein levels. CLL case: U (U-CLL) or M (M-CLL).

Importantly, M-CLL cases show higher mRNA levels of *CELF2* than U-CLL (**Figure 64A**). In line with this, high expression levels of *CELF2* are associated to better prognosis in CLL (**Figure 64B-C**), which reinforces the idea of LEF1-FL linked to a decreased CLL proliferation and more stable disease. In contrast, low

levels of *CELF2* are linked to a more aggressive disease, which would associate LEF1-Δexon 6 isoforms to proliferation. These data suggest that, under proliferative conditions, CLL cells favor LEF1 exon 6 skipping by *CELF2* downregulation that results in reduced protein levels of LEF1-FL.

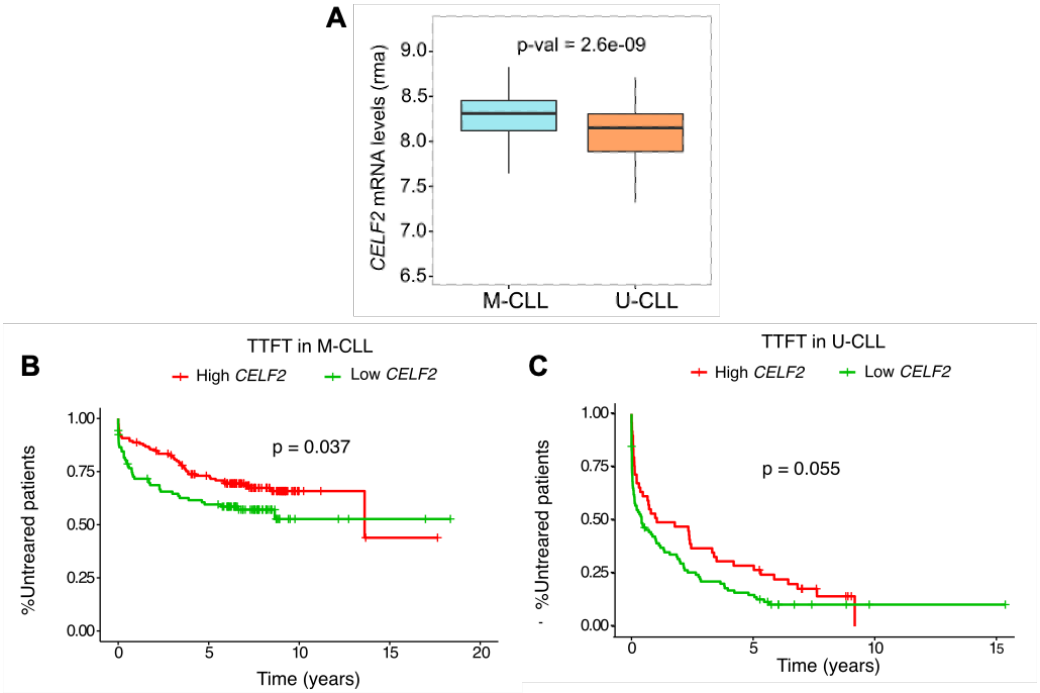


Figure 64. *CELF2* higher levels linked to M-CLL and better prognosis. A) *CELF2* mRNA levels in U-CLL (n=147) and M-CLL (n=256) samples obtained from microarray expression data (rma). Wilcoxon test. B-C) TTFT in patients with high (red) and low (green) levels of *CELF2* in B) M-CLL and C) U-CLL.

2.8. Effects of overexpressing different LEF1 isoforms in CLL cell lines

I aimed to further investigate the link between LEF1 isoforms and cell quiescence or proliferation. As HG3 and MEC1 CLL cell lines express very low levels of LEF1, they are suitable models to study the role of these isoforms. Therefore, CLL cell lines were transduced to overexpress one of the three LEF1 isoforms: FL, I6 and I5 (**Figure 65A**). Each isoform was labeled with a different fluorescent reporter protein, so that infected cell lines could be followed by flow cytometry. At day 6 after the lentiviral infection, cell lines were sorted by the expression of the reporter

protein/LEF1 isoform (**Figure 65B**). Then, RNA was extracted and RNA-seq was performed.

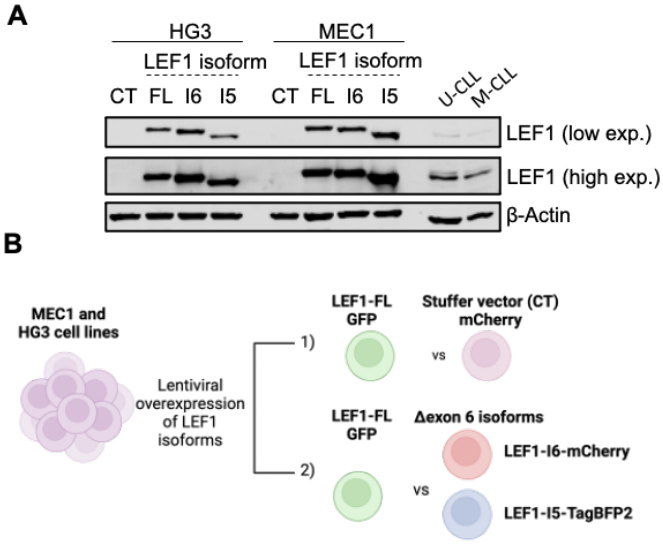


Figure 65. Overexpression of LEF1 isoforms in HG3 and MEC1 cell lines. A) Representative western blot showing overexpression of LEF1 in cell lines (HG3 and MEC1) along with endogenous LEF1 levels in CLL (U-CLL and M-CLL). B) Experimental design to study the phenotypical effects of LEF1 isoforms overexpression.

Firstly, I compared the transcriptional changes observed in cells overexpressing LEF1-FL by comparing them with control cells, which were transduced with lentiviral vector that had no transgene to overexpress (stuffer vector) (**Figure 66A**). There were 67 genes upregulated and 92 downregulated in LEF1-FL overexpressing CLL cells (log2FC > 0.5/ < -0.5 and -adj < 0.01) (**Figure 66B**). GSEA revealed that downregulated genes in LEF1-FL overexpressing cells were enriched in pathways controlling cell proliferation, such as *MYC* or *E2F* targets. These findings were also corroborated *in vitro*, as the follow-up of transduced cells, showed a gradual loss of LEF1-FL cells over time (**Figure 66C-D**). In contrast, the relative proportion of cells carrying the stuffer vector did not diminish. These results denote that LEF1-FL overexpression in CLL cell lines hindered the expression of genes involved in cell proliferation, inducing a quiescent phenotype, and, thus, conferred a proliferative disadvantage in comparison to control cells.

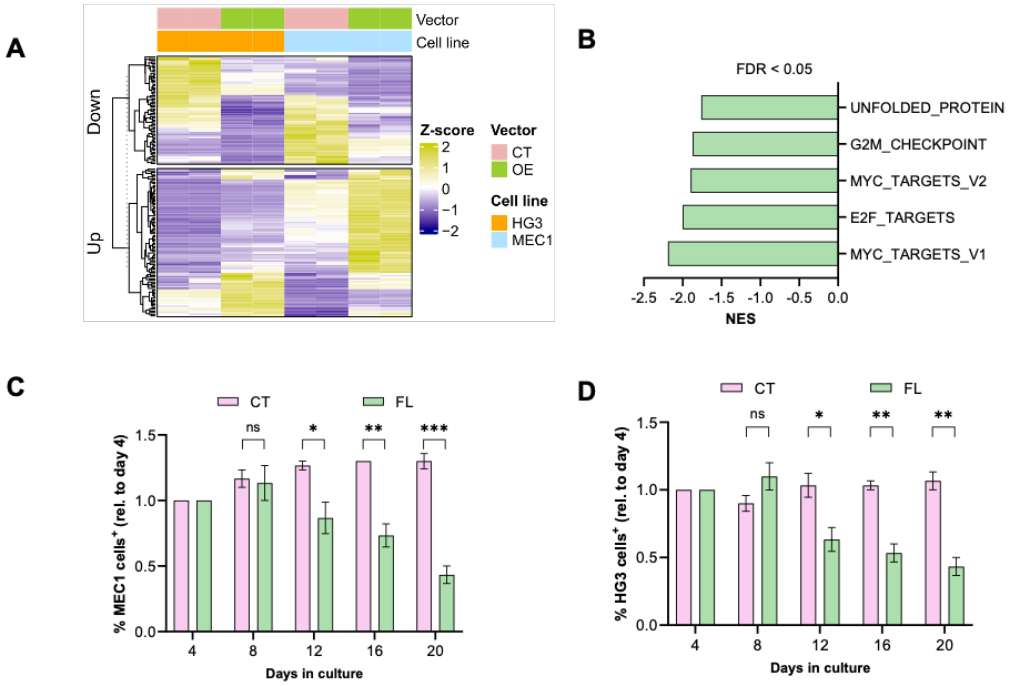


Figure 66. Effects of LEF1-FL isoform overexpression. A) Heatmap representing the DE genes in LEF1-FL overexpressing MEC1 and HG3 cells versus control cells (transduced with a stuffer/empty vector). B) GSEA (Hallmark database) of downregulated genes in LEF1-FL overexpressing cells (FDR < 0.05). C-D) Percentage of GFP+ cells (containing LEF1-FL or CT vector) over time (day 4-20 after infection) in C) MEC1 and D) HG3 cells (n=3/cell line). Unpaired t-test.

Next, I analyzed the effect of overexpressing LEF1-Δexon 6 isoforms (either I6 and I5) versus the LEF1-FL. PCA showed a clear separation of LEF-FL cells from I6/I5 cells, which, interestingly, were clustering together (**Figure 67A**). Differential expression analysis (log2FC > 0.5/ < -0.5 and -adj < 0.01) showed 304 genes upregulated and 251 genes downregulated in LEF1-Δexon 6 cells (**Figure 67B**). Accordingly, the upregulated genes were significantly enriched in pathways promoting cell proliferation (e.g., *MYC*/*E2F* targets and G2M checkpoint), which were the same ones observed downregulated by LEF1-FL overexpression (**Figure 67C-D**). Indeed, cell lines overexpressing LEF1-FL were lost more rapidly after infection in comparison to I6 and I5, which were maintained longer over time (**Figure 67E-F**).

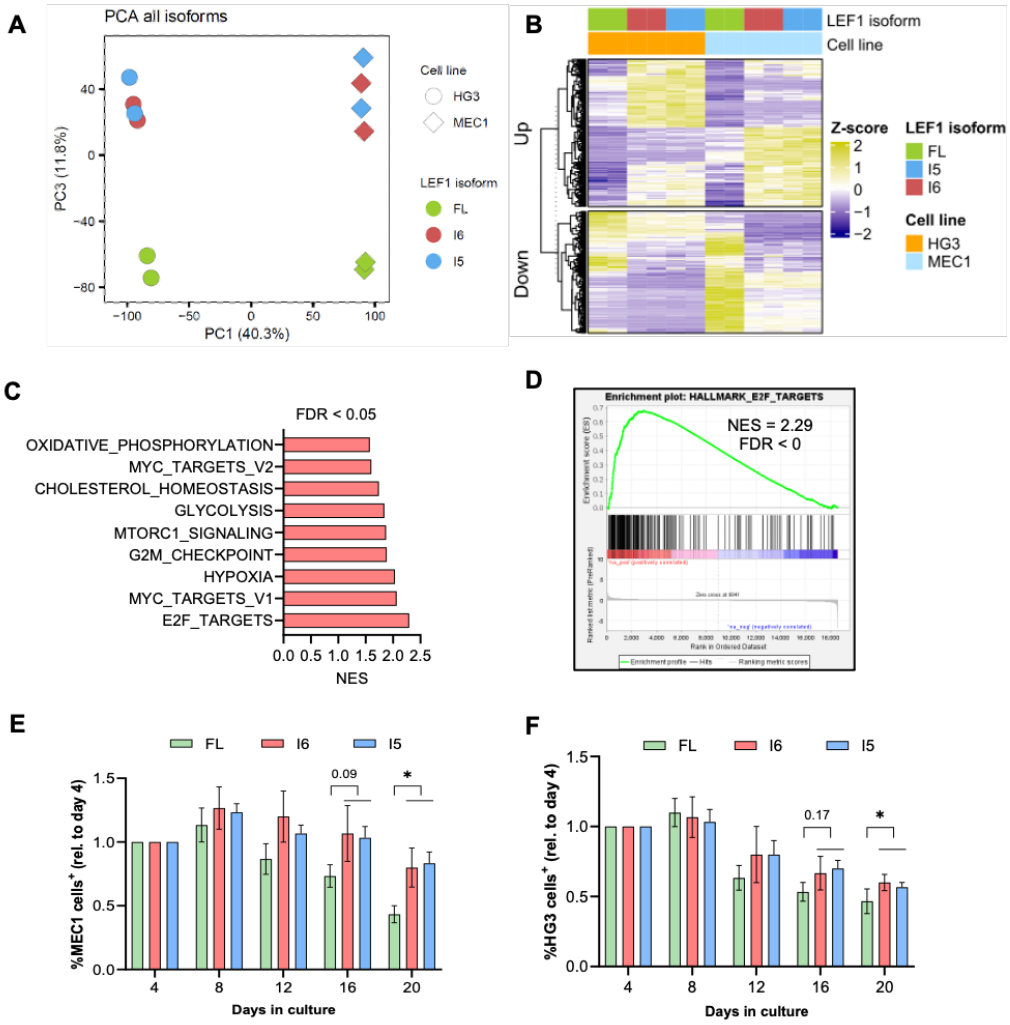


Figure 67. Effects of LEF1-I6 and I5 isoform overexpression versus FL. A) PCA of RNA-seq data of MEC1 and HG3 cells overexpressing LEF1 isoforms (FL, I5 and I6). B) Heatmap representing the DE genes in MEC1 and HG3 overexpressing LEF1-Δexon6 isoforms versus control LEF1-FL cells. C) GSEA (Hallmark database) of upregulated genes in LEF1-Δexon6 overexpressing cells compared to LEF1-FL (FDR < 0.05). D) Example of upregulated genes enriched in Hallmark_E2F_TARGETS. E-F) Percentage of GFP(LEF1-FL)/mCherry (I6)/BFP (I5) positive cells over time (day 4-20 after infection) in E) MEC1 and F) HG3 cells (n=3/cell line). Unpaired t-test.

To validate if LEF1-I6 and LEF1-I5 do confer a proliferative advantage compared to LEF1-FL cells, I performed competitive growth studies by mixing 1:1 population of 1) LEF1-FL + I6 and 2) LEF1-FL + I5 overexpressing cells (**Figure 68A-D**). Notably, in both conditions, especially in the MEC1 cell line (n=3), LEF1-

FL-GFP cells were reduced to almost a 50% by day 20, while cells overexpressing LEF1-I6-mCherry or LEF1-I5-BFP were slowly increasing over time, dominating the initial mixed population.

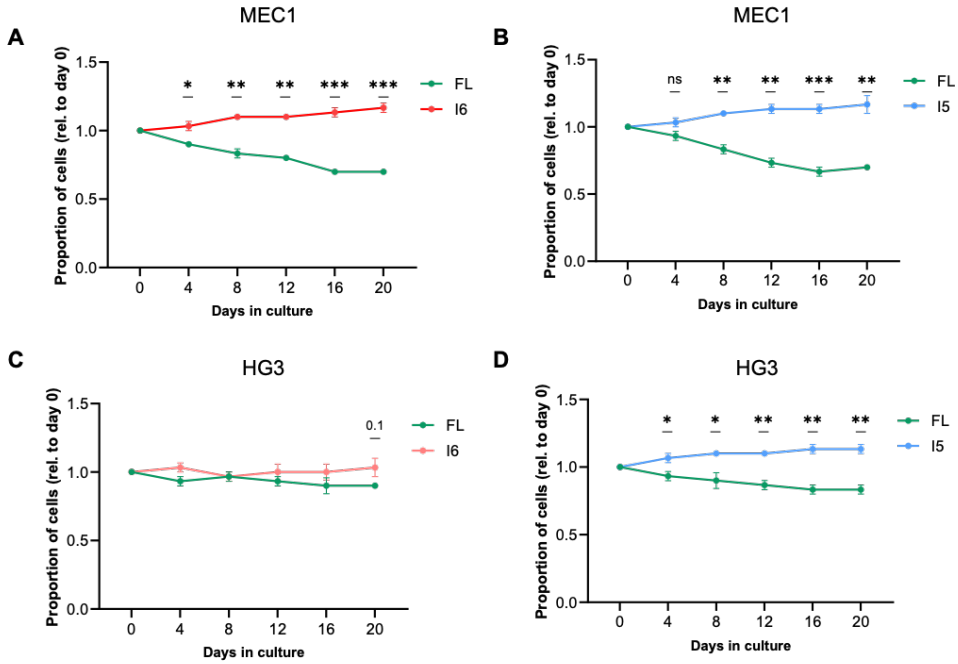


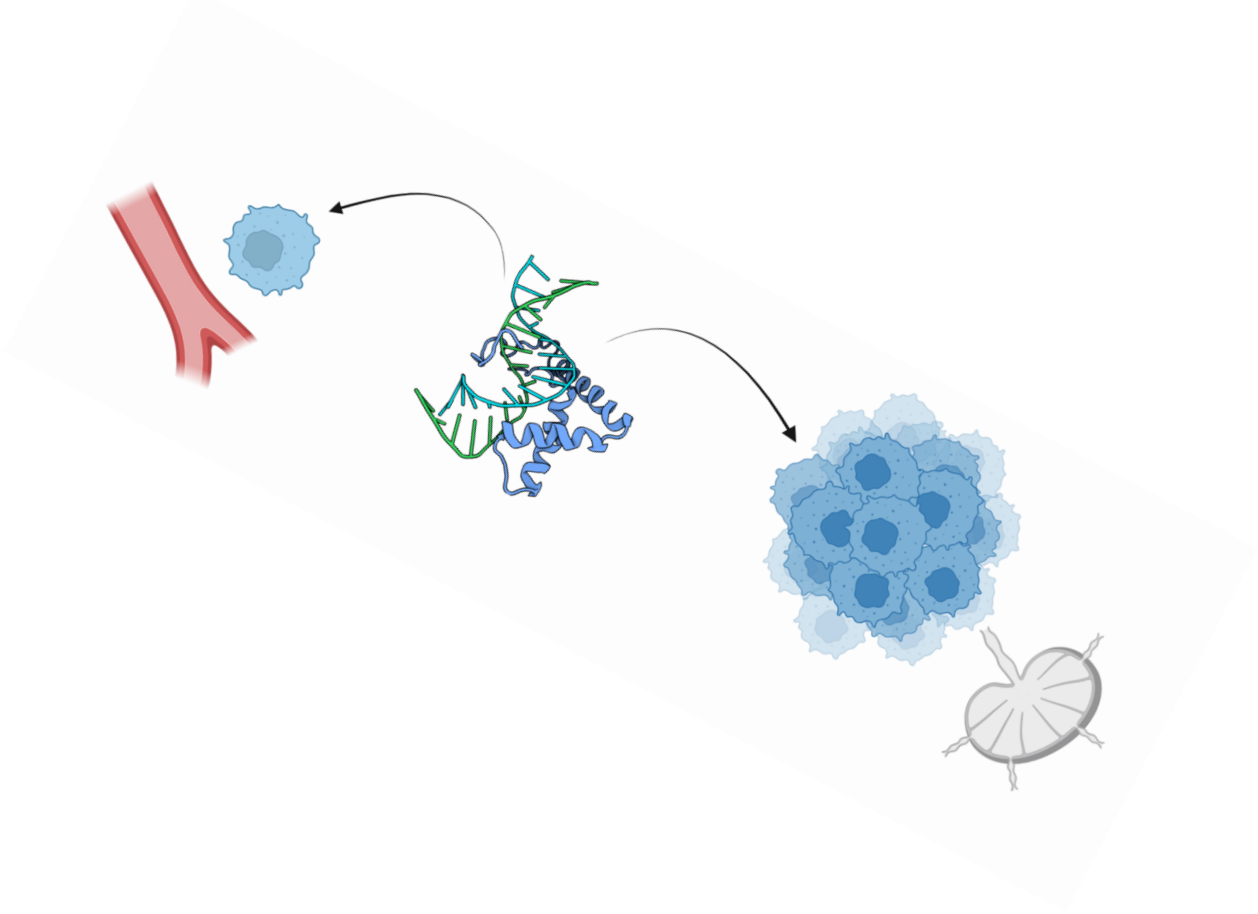
Figure 68. Competitive growth analysis between LEF1-Δexon6 and LEF1-FL. A & C) Follow-up of 1:1 mixed cells that overexpress LEF1-FL and LEF1-I6 in A) MEC1 and C) HG3. B & D) Follow-up of 1:1 mixed cells that overexpress LEF1-FL and LEF1-I5 in B) MEC1 and D) HG3. Each experiment was repeated 3 times in MEC1 and HG3 cell lines. Unpaired t-test.

In summary, my results indicate that LEF1-FL induces a pro-quiescent transcriptional profile and hinders cell expansion, while overexpression of both LEF1-Δexon6 isoforms generates a pro-proliferative transcriptional and phenotypical profile. Importantly, LEF1 I5 and I6 showed very similar transcriptional and phenotypical effects *in vitro*, suggesting the pro-proliferative role of LEF1 is mediated by the exon 6 skipping, which is shared by both isoforms.

3. Conclusions

1. LEF1 protein levels are higher in U-CLL due to increased protein stability.
2. *USP10* downregulation decreases LEF1 levels in M-CLL but not in U-CLL.
3. The difference in LEF1 protein levels mainly depends on the IGHV status, and not on the clinical aggressiveness of specific cases.
4. LEF1 binds to more regions in U-CLL than M-CLL, which are more accessible and open in U-CLL cells.
5. LEF1 target genes can be classified into common (shared by M-CLL and U-CLL) or U-CLL specific.
6. Common genes targeted by LEF1 are involved in lymphocyte survival and activation in response to microenvironmental stimuli.
7. Target genes specific to U-CLL are related to cell proliferation and are not present either in T cells, which also express high levels of LEF1.
8. The CDC5L cell cycle regulator interacts with LEF1 shorter isoforms (I6) in U-CLL cells.
9. CLL cells express three protein-coding isoforms: LEF1-FL, I6 and I5.
10. LEF1-FL is decreased in the proliferative fraction of patient-derived CLL cells.
11. Under proliferative conditions, there is a downregulation of *CELF2*, which leads to an increased exon 6 skipping of the LEF1 transcript, increasing LEF1-Δexon 6 isoforms and diminishing LEF1-FL isoform.
12. Overexpression of the LEF1-FL in CLL cell lines induces quiescence, while overexpression of the LEF1-Δexon 6 isoforms promote proliferation.

Discussion



1. *In vitro* modeling of CLL to study disease pathogenesis

Characterization of the MM1 cell culture system

Previous functional studies in CLL and this doctoral thesis have demonstrated how challenging is to model CLL *in vitro* or *in vivo*. CLL cells are characterized by being slowly proliferating cells that accumulate in PB in a resting state. Notably, CLL cells circulate between PB and LN, and actively proliferate only in the LN, where they receive pro-survival and pro-proliferative stimuli from the TME. The extreme genetic heterogeneity in CLL and the lack of a common genetic driver highlights the importance of the extrinsic signals from the TME to modulate cell behavior. In fact, the TME, especially T-cell stimuli, is fundamental in accelerating the expansion of CLL cells. For instance, U-CLL cells, which typically show a more proliferative phenotype, are less migratory and more adhesive than M-CLLs (331), which contributes into an enhanced retention in the LN, thereby prolonging tissue-based pro-proliferative signals (332). In this line, the extreme dependence of patient-derived CLL cells on the TME for their survival and proliferation results in spontaneous apoptosis when cells were cultured *in vitro*. For this reason, CLL cell lines in principle represent an attractive alternative to study CLL pathogenesis. However, the slowly proliferative profile of CLL cells makes the generation of CLL cell lines with intrinsic TME-independent survival and proliferation extremely difficult. For this reason, not only there are few CLL cells lines available, but also, they do not properly recapitulate many features observed in primary CLL cells. In fact, these cell lines were derived from patients with very aggressive or late-stage disease, which are less dependent on the TME and do not reflect the real spectrum of biological and clinical manifestations of CLL. Similarly, transgenic mouse models (e.g., Eμ-TCL1) display an aggressive variant of CLL-like disease, lacking the recurrent driver mutations found in primary CLL cells. Importantly, cell lines and transgenic mouse models of CLL lack the expression of

highly specific CLL markers, including LEF1. In addition, no successful patient-derived xenografts (PDX) have been established. Recently, few PDXs could be generated, but only from patient-derived Richter-transformed cells, which constitute an evolution of CLL into a high-grade lymphoma (333,334).

The lack of cellular models faithfully representing the key genetic and epigenetic events as well as the phenotypic features of CLL have reinforced the idea of using patient-derived material *in vitro* for functional studies. The study of CLL biology has led to the development of more sophisticated *in vitro* systems, based mostly on feeder cells, that try to mimic the TME found in the LN to sustain survival and proliferation of CLL cells. In this doctoral thesis, I cultured primary CLL cells together with the MM1 stromal cell line (266). Although this cell culture system induces a vigorous proliferation of CLL cells, I initially wondered whether it was faithfully mimicking LN-stimuli. MM1 cells provide CLL cells with NLC stimuli (BAFF) and T-cell stimuli (CD40L and IL-21). In the Study 1 of this thesis, I showed that this new *in vitro* system maintains cell viability and induces gradual activation and proliferation of cultured CLL cells, as it occurs in LN-derived CLL cells (296). Moreover, these phenotypical changes using surface markers in stimulated CLL cells were confirmed by transcriptomic analyses, which revealed an upregulation of genes involved in proliferation (*E2F, MYC*), DNA damage response and metabolic reprogramming (OXPHOS and mTORC). Concordantly, E2F and MYC pathways have been described as particularly enriched in LN-derived CLL cells (298). In short, all these results indicate that MM1 cell culture system is mimicking LN microenvironment. Thus, this *in vitro* system represents a useful strategy to understand the proliferative fraction of CLL cells, which, in the end, is the ultimate responsible for CLL expansion and progression.

However, the MM1 cell culture system also shows some limitations. First of all, it is time-dependent in terms of CLL identity and proliferation. CLL cells undergo a tremendous transcriptomic reconfiguration after being cultured with MM1 cells,

as shown in the large number of differentially expressed genes that I detected between stimulated and unstimulated cells. Remarkably, the more time they spend cultured *in vitro*, the more they transcriptionally deviate from unstimulated CLL cells (data not shown). For this reason, I tried to perform all the experiments in a time-frame of 6-8 days since thawing the primary cases. Secondly, there is a clonal expansion of those CLL cells responding to the proliferative stimuli whereas the non-responsive cells enter into apoptosis. Consequently, at the end of the experiments, I always had a very homogeneous activated and proliferative CLL population from each patient which reduced any transcriptional heterogeneity. present in unstimulated cells. Therefore, the *in vitro* system does not recapitulate the real situation in patients, in which the small proliferative fraction co-exists with resting CLL cells characterized by an anergic cell state (335). Moreover, the expansion of the CLL cells is time-limited, as it has been reported likewise by other 2D and 3D studies (336). Apparently, proliferating CLL cells show a limited number of cell divisions, and can be maintained *in vitro* for around 1-2 weeks. Further research is needed to determine which are the additional signals, apart from T-cell derived cytokines, required to sustain, for a longer time, a proliferative phenotype in primary CLL cells. In summary, co-cultured CLL cells show a more aggressive and homogeneous phenotype than original CLL samples, and show a time-limited cell expansion *in vitro*. Finally, the "well-being" of CLL cells *in vitro* completely depends on the state of MM1 cells. In other words, MM1 cells might express a varying amount of BAFF, CD40L and IL-21 depending on initial expansion and selection of these cells. Thus, if a batch of MM1 cells secretes less pro-survival and proliferative factors, CLL cells will have lower viability and reduced proliferation. In summary, there is less reproducibility when working with primary CLL cells than when growing CLL cell lines, which have a more stable behavior *in vitro*.

Development of gene inactivation strategies in primary CLL cells

The MM1 cell culture system enables the development of molecular biology techniques in primary CLL samples to study oncogenic mechanisms driving CLL, such as gene inactivation strategies. In my case, as my thesis mostly aimed at exploring the role of LEF1, I needed to inactivate or downregulate its expression in primary CLL cells. The development of gene editing methodologies in primary CLL cells has been hampered by the resistance of CLL to gene transfer methods (267). In the part 2 of the Study 1, I described all the specific steps needed to perform CRISPRi and standard CRISPR-Cas9 in patient-derived samples. Interestingly, CLL cells were receptive to gene transfer methods (lentiviral transduction or electroporation) when showing an activated and proliferative phenotype. To start with, I focused on the CRISPRi methodology, since it allows the selection of a pool of cells that contains both dCas9 and sgRNA to achieve silencing of the target gene. This was important, as primary CLL cells cannot grow as single clones *in vitro*, which is typically needed when generating KO clones in cell lines with the classic CRISPR-Cas9 editing approach. In fact, I tried to grow clones from one single CLL cell, following a previously published protocol that successfully achieved clonal expansions from a single B cell (337). Although each single CLL cell was in a well filled with CLL media and several interleukins (IL2/IL15, CD40L), there was no expansion of CLL cells while there was a growth of clones derived normal B cells present in the patient's sample. This indicates the importance of CLL cells interacting with each other for their survival *in vitro*.

CRISPRi was successfully optimized and carried out in CLL and MCL cell lines. Moreover, primary CLL cells were successfully transduced with the lentiviral vector encoding for sgRNA against LEF1. However, in the case of CRISPRi, the large size of dCas9-KRAB-ZIM3 (> 14 kb) made impossible to put this lentiviral vector into primary CLL cells, which are difficult-to-transfect. Indeed, it has been reported that plasmid DNA size modulates gene transfer efficiency, showing small DNA

molecules higher transduction efficiencies than large ones (338). Consequently, in spite of all the efforts, CRISPRi experiments in primary CLL samples were unsuccessful.

As an alternative, I applied electroporation-based CRISPR-Cas9 editing in primary CLL cells (274). In this case, stimulated CLL cells (in culture with MM1 cells for 2-3 days) were successfully electroporated and edited, and downregulation of the target gene was maintained over time. Notably, I could successfully target more than one gene at the same time. On the contrary, unstimulated CLL cells, which are in a quiescent state, were barely electroporated and no editing of the target gene could be achieved. Remarkably, this is the first transient CRISPR-mediated genome editing protocol in stimulated primary CLL cells, which expands previous efforts in cell lines (339,340). This finding highlights the importance of inducing a proliferative phenotype of CLL cells for efficient gene editing. Two strong points of the newly established protocol are: 1) there is no alteration in the viability of electroporated cells and 2) the action of the Cas9 is transient, as the complex formed by the Cas9 protein and gRNA is degraded within 48 hours after electroporation, reducing the toxicity of Cas9 cleavage and the risk of off-target effects. The latter point contrasts to lentiviral vectors, which are inserted into the genome of the host cells, conferring a constitutive expression of the Cas9 and gRNA, and increasing the probability of off-target effects. In conclusion, this robust and transient gene editing method paves the way to study the biological effects of driver genes. In this thesis, it has been used to study *LEF1*, but it could also be used to explore the impact frequent CLL genomic aberrations directly in patients' samples. Furthermore, this protocol overcomes the current dependency on cell lines or murine models that do not faithfully recapitulate the clinico-biological diversity of CLL.

Finally, the use of primary CLL cells for the CRISPR-mediated gene editing irremediably has some drawbacks. First, patient-derived CLL cells do not grow from

single clones. In consequence, I worked with a bulk population of CLL cells comprising both by edited cells and non-edited cells. Therefore, this protocol results in the downregulation of target gene expression (KD) instead of the complete target gene depletion (KO). Accordingly, there will always be traces of expression of the target gene that may hamper the detection of clear phenotypic and biological effects of this gene. Second, patient-derived material is limited. For this reason, it is not possible to perform CRISPR-library screenings, as there is not enough material to target many genes simultaneously. Thus, before applying the technique in patient-derived cells, it is essential to narrow down the list of potential candidates to few genes. In this sense, I used electroporation CRISPR-Cas9 based methodology to study LEF1 as a candidate driver of CLL.

2. The role of LEF1 protein abundance in CLL

High LEF1 protein levels in U-CLL samples do not correlate with mRNA levels

Expression of LEF1 is considered a hallmark of CLL, as it not expressed in other lymphoproliferative disorders (150). It is present in virtually all CLL samples as well as in MBL; the premalignant state preceding CLL. Additionally, any mature B cell subpopulation lacks expression of LEF1, and therefore, it is a *de novo* event in MBL/CLL cells. However, the functional role of aberrant LEF1 expression in CLL has not been thoroughly studied. In part, this is caused by the fact that LEF1 is not expressed in any of the widely used models to mechanistically study CLL pathogenesis, including cell lines and transgenic mouse model. In our RNA-seq data from patient samples, I detected similar expression levels between CLL and MBL samples, reinforcing the idea of LEF1 as an early driver in CLL pathogenesis (152). Similar to other studies working with RNA-seq in CLL (207,208), I noticed that LEF1 gene expression was stable across CLL samples, independently of the IGHV status. However, two publications report that high *LEF1* gene expression was associated with U-CLL cases, which typically show a more aggressive clinical course than M-

CLL cases (202,203). In these studies, *LEF1* expression was determined by RT-PCR, whereas, in our study and those with similar observations, LEF1 expression was assessed after performing RNA-seq in CLL samples. While both offer highly sensitive and reliable detection of expression levels, RT-PCR can only detect known sequences or certain transcripts depending on the designed primers. In contrast, RNA-seq provides high sensitivity to quantify all transcripts including rare variants. Therefore, RT-PCR might not detect certain transcripts of *LEF1* expressed in CLL samples.

Interestingly, the homogeneous pattern of *LEF1* gene expression in MBL and CLL did not correlate with the heterogeneous protein levels of LEF1 found in these samples. Surprisingly, LEF1 protein levels were significantly higher in U-CLL than in M-CLL or MBL (p-val < 0.001). In the clinical setting, LEF1 expression is typically assessed by IHQ in CLL samples obtained from LN biopsies (209). IHQ is a semi-quantitative method that can detect the presence of the LEF1 protein in the tissue and cellular level, but it is not sensitive enough to determine the absolute abundance of this protein. In addition, the majority of examined cases by IHQ were aggressive CLL cases that proliferate considerably in the infiltrated LN. Thus, it was almost impossible to detect any differences at the protein level with IHQ due to the limit of quantification of IHQ and the studied cases, which did not cover the clinical spectrum of the disease. Nonetheless, robust differences in LEF1 protein levels could be detected between U-CLL and M-CLL patients by using intracellular flow cytometry in PB samples. When using the appropriate fluorescence controls, intracellular flow cytometry provides quantitative reproducible measurements of LEF1 protein expression levels, which could potentially be used in the clinical setting. Interestingly, these results of higher LEF1 protein levels in U-CLL cells were validated by mass-spec data obtained from M-CLL and U-CLL samples (331). Furthermore, I observed that the higher LEF1 protein levels in the U-CLL subtype was basically linked to the cell of origin and not to clinical aggressiveness itself. I studied U-CLL cases with a more indolent clinical course (TTFT > 6 years), and they

still showed higher protein levels than aggressive M-CLLs (TTFT < 1 year). LEF1 is expressed at high levels in B-cell precursors whereas in mature B cells, from naive B cells onwards, LEF1 is silenced. Notably, U-CLL seems to derive from a more immature type B cell than M-CLL (341). Thus, it is tempting to speculate that higher LEF1 protein levels may simply reflect a more immature and undifferentiated state of the leukemic cells. In fact, when CLL cells were forced *in vitro* to differentiate into Ig-secreting cells, LEF1 expression decreased (342). However, this hypothesis might be wrong. Both U-CLL and M-CLL cells are known to be antigen experienced, and therefore, CLLs most likely arise from B cells that have reached the MBC stage through GC-dependent (in M-CLL) or independent ways (in U-CLL). Therefore, whether higher LEF1 expression levels are an aberrant feature acquired by U-CLL cells or whether it is somehow a feature related to the specific cell of origin that gave rise to U-CLL is still unknown.

To my knowledge, the lack of correlation between LEF1 mRNA and protein levels has never been described. However, in several cancers, there is increasing evidence that protein levels do not merely reflect the expression levels of their mRNAs, suggesting wide post-translational regulation of cancer proteomes (343,344). In consonance with this, Herbst and coworkers demonstrated that the overall correlation between protein abundance and the corresponding mRNA level was incredibly low (R=0.243) in CLL samples (325). In that work, they identified several proteomic profiles in CLL samples associated with clinical outcome, which did not correspond to a genetic or transcriptomic profile. Therefore, in the light of these findings, it is not unexpected that the higher LEF1 protein abundance found in U-CLL samples did not correspond to higher *LEF1* mRNA levels, suggesting that most likely LEF1 levels are modulated post-translationally in that CLL subgroup.

In line with the hypothesis posed above, in this thesis I demonstrated that indeed, the higher LEF1 protein abundance is a consequence of the increased protein stability of LEF1 in U-CLL samples as compared to M-CLL. In short, I

observed an impaired ubiquitin-mediated degradation of LEF1 through the proteasome in U-CLL cells. I thought that this was caused by the interaction of the deubiquitinase USP10 with LEF1 in CLL cells, as it happens with other family members of the Wnt pathway such as TCF4 and β-catenin (318–320). In fact, the downregulation of *USP10* decreased LEF1 protein levels in M-CLL but no in U-CLL cells. Remarkably, the loss of USP10 in U-CLL cells induced a compensatory mechanism to increase basal protein levels of LEF1. Thus, it seems LEF1 expression is extremely important for U-CLL cells and further research is needed to uncover the proteins that secure LEF1 protein synthesis and stability in U-CLL cells. Related to these observations, previous studies in CLL have identified some genes involved in protein synthesis and stability as potential drivers of the disease (117).

Higher LEF1 protein abundance associates with increased proliferation

The increased protein levels of LEF1 in U-CLL samples resulted in more extensive DNA binding of LEF1, detected by CUT&RUN, in the chromatin of U-CLL cells as compared to M-CLL cells. Remarkably, almost all LEF1 target genes in M-CLL were already included within the U-CLL subtype and were subsequently named as common genes. These common genes were enriched in pathways involved in lymphocyte activation, migration and response to microenvironment (TLR, cytokine signaling). In sharp contrast to these common genes, those genes bound by LEF1 exclusively in U-CLL were strongly enriched in cell cycle progression and proliferation. Thus, it seems that LEF1 participates in the survival and proliferation of all CLL cells, conferring the "CLLness" signature needed to promote the initial CLL growth. Then, the additional binding of LEF1 in U-CLL samples gives an extra proliferative push to these cells, thus contributing to the more aggressive phenotype of the U-CLL subtype. In summary, genome-wide binding sites of LEF1 in CLL cells indicate that increased LEF1 levels are involved in the proliferation of CLL cells.

Concordantly, LEF1 protein levels were increased in recent LN emigrants (proliferative fraction) compared to cells that have been unstimulated in PB for a longer time (resting fraction). The increased LEF1 protein levels in recent LN emigrants occurred in both subtypes, M-CLL and U-CLL, but only U-CLL cells conserved a higher protein abundance in the resting CLL fraction. This could be partially explained by the intrinsic increased protein stability of LEF1 in U-CLL cells, while M-CLL would require LN-stimuli to sustain high levels of LEF1 expression. Moreover, the increased LEF1 protein levels in U-CLL would facilitate the proliferative response to LN-stimuli, in contrast to M-CLL cells, which are typically less responsive to microenvironmental stimuli. Moreover, higher protein levels of LEF1 were also detected in stimulated CLL cells (i.e., proliferative) than in unstimulated CLL cells *in vitro.* Of note, this increased protein abundance in stimulated CLL cells was not detected at the mRNA level.

These observations were further validated after CRISPR-induced KD of *LEF1* in CLL samples. *LEF1* KD cells showed a downregulation of genes involved in proliferative pathways, and flow cytometry experiments showed that *LEF1*-edited cells had diminished protein levels of Ki67 as compared to non-edited cells. Importantly, Ki67 has been shown to positively correlate with LEF1 immunohistochemical staining (202,209) in CLL cells from LN biopsies and, in addition, LEF1 binding sites (derived from the CUT&RUN experiments) are found specifically in the promoter of *MKI67* in CLL and T cells. Until now, previous studies only associated LEF1 with CLL survival, but not with proliferation (152,345). Therefore, to my knowledge, this is the first time that LEF1 is mechanistically linked to the proliferation of CLL cells. In this context, it seems that LEF1 is important in the response of CLL to LN-stimuli. Thus, I postulate that samples with higher LEF1 protein levels, such as U-CLL, will respond earlier and more effectively to proliferative stimuli.

β-catenin-independent action of LEF1 in CLL cells

β-catenin has been defined as the main interacting partner of LEF1, in the context of WNT signaling pathway, in normal and tumor cells (177). In study 2, I uncovered the nuclear interactors of LEF1 in the context of U-CLL and M-CLL. Remarkably, I only detected β-catenin as LEF1 interacting partner in U-CLL samples. However, the interaction occurred inside the β-catenin destruction complex (346), suggesting the involvement of LEF1 in the degradation of β-catenin. This surprising interaction in U-CLL cells together with the lack of interaction in M-CLL indicate that the role of LEF1 is probably independent of β-catenin. Interestingly, previous studies have shown the lack of β-catenin activation and nuclear localization in primary CLL samples (209,211). For instance, nuclear staining of LEF1 was observed in virtually all cells from 100% (92/92) of LN biopsies from CLL cases, while 88% of these cases were negative for β-catenin nuclear staining (211). Moreover, Gutierrez and colleagues also reported that β-catenin protein levels were the same between CLL and mature B cells, indicating that the high expression of LEF1 in CLL had to be linked to other factors different from β-catenin (152). Altogether, these results suggest that the function of LEF1 in CLL might be β-catenin-independent.

To date, LEF1 has been reported to regulate transcription through the interaction with other co-factors such as ALY, ETS, ATF and Sp1 (170,347). Furthermore, LEF1 promoted the transcription of *E2F1*-target genes, by displacing the binding of histone deacetylase 1, in HEK293T and COS7 cells (348). Notably, in my work, *E2F*-target genes were downregulated after LEF1 downregulation in CLL cells. This is remarkable, as indicates that LEF1 can regulate proliferation independently of β-catenin.

Description of a new interactor of LEF1 in CLL involved in cell proliferation

The LEF1 interactome in U-CLL was considerably different from M-CLL, especially when looking at proteins involved in DNA-binding. Previous work has connected the two CLL subtypes to different protein composition (325,331). I identified CDC5L as the top interactor of LEF1 in U-CLL samples, and such interaction was not detected in M-CLL cells. These data initially suggested that the LEF1-CDC5L interaction was U-CLL specific. However, when validating this interaction by western blot, I could detect a weaker interaction between LEF1 and CDC5L in M-CLL as well. This suggests a dependence on protein levels: the higher levels of LEF1, the higher interaction with CDC5L.

CDC5L is a pre-mRNA splicing factor (322) that plays an essential role in mitosis, as depletion of CDC5L inhibits mitotic progression and eventually leads to mitotic catastrophe (323,324). In fact, I identified that high expression levels of *CDC5L* are associated with poor prognosis in CLL patients, suggesting that increased proliferation in CLL is related with higher *CDC5L* levels. Accordingly, overexpression of CDC5L is linked to worse outcome in solid tumors such as melanoma and osteosarcoma (349–351). Further research should decipher whether this potential proliferative role of the LEF1-CDC5L complex in CLL cells is mediated by DNA binding, as CDC5L can act as a transcriptional activator (352), or pre-mRNA splicing. However, it is tempting to speculate that the preferential binding of LEF1 to intronic regions in CLL genome could point towards a role of LEF1 in pre-mRNA splicing. In fact, a recent study has demonstrated that some transcription factors, among them LEF1, can bind DNA and RNA to regulate gene expression (353). Therefore, this reinforces the idea of LEF1 regulating the splicing of target genes in CLL cells.

In summary, it seems that higher levels of LEF1, typically found in U-CLL, interact with CDC5L, which may accelerate the splicing of genes involved in the G2-

M transition, and promote a more proliferative phenotype. Importantly, the interaction between CDC5L and LEF1 appears to occur only through shorter I6 of LEF1.

3. The role of alternative isoforms of LEF1 in CLL proliferation

Exon 6 controls proliferation of CLL cells

The most studied isoforms of LEF1 in the available literature are LEF1-FL, also known as canonical isoform, and the dnLEF1, which lacks the N-terminal β-catenin binding domain. In colon cancer cell lines, dnLEF1 competes with LEF1-FL and impairs the activation of β-catenin/LEF1 target genes (176,354). In line with this finding, it has been shown that AML stem cells, which show a great dependency on canonical WNT pathway for proliferation, express the LEF1-FL isoform while downregulating the expression of the dnLEF1 isoform (175). On the contrary, normal human HSCs and mature T cells express both isoforms, thus regulating proliferation in a context-dependent manner. Furthermore, out of the two best studied isoforms, CLL cells only express LEF1-FL (152), since the alternative promoter that generates dnLEF1 isoform, located within intron 2 of *LEF1*, is not active in these cells.

In CLL cells, a detailed observation of the Western blots indicates that LEF1 has multiple isoforms, which are derived from alternative splicing of the LEF1-FL transcript. In addition to LEF1-FL, I found that CLL cells express the I6 and I5 isoforms, both of which lack the exon 6 present in the FL isoform. As far as I am aware, these two shorter isoforms have never been described in the context of CLL. Unexpectedly, I demonstrated that the predominant isoform expressed in CLL cells is the I6 isoform. Interestingly, under proliferative conditions *in vitro*, all CLL cases, independently of the IGHV status, revealed a considerable decrease in the protein levels of LEF1-FL, while the expression of LEF1 isoforms lacking exon 6 (Δexon6, i.e. I5 and I6) was maintained or even increased. This finding suggests a role of exon

6 in the negative regulation of cell proliferation in CLL, as it was similarly reported in neural progenitors (328), where increased LEF1-FL was associated to a quiescent state of neural cells. In fact, exon 6 and the CRD, where exon 6 is located, have been associated with transcriptional repression of LEF1 target genes due to the binding of chromatin repressors to it (170,355). These findings were further supported by the overexpression of these three isoforms in CLL cell lines. Notably, LEF1-FL overexpression decreased cell proliferation while LEF1-I5/I6 did not. Actually, at the transcriptomic level, I observed that cell lines overexpressing the FL downregulated genes involved in cell cycle whereas those genes were upregulated upon LEF1-Δexon6 overexpression.

In short, LEF1-FL and LEF1-Δexon6 isoforms apparently target the same genes but have the ability of modulating proliferation in opposed ways. The presence of the exon 6 limits de proliferative role of LEF1-FL in CLL cells, most likely through recruitment of chromatin repressors that eventually downregulate the target genes involved in proliferation. In contrast, LEF1-Δexon6 isoforms can act as transcriptional activators of the target genes, promoting cell proliferation. In addition, as LEF1-I6 can more effectively interact with CDC5L through its different C-terminal end, I hypothesize that it can accelerate the G2/M transition by controlling the splicing of genes involved in this process.

CELF2 regulates *LEF1* exon 6 splicing

The available literature indicates that exon 6 splicing of the *LEF1* transcript is controlled by CELF2 protein in several types of human cells (328,329,356). In particular, the binding of CELF2 to the *LEF1* transcript causes the inclusion of exon 6 leading to the formation of LEF1-FL isoform. In developing T cells in the thymus (329), CELF2 protein levels increase as a result of an augmented transcription and mRNA stability, elevating thus LEF1-FL levels. This isoform promotes the transcription of the TCRα chain, which is essential for the TCR expression. Upon

stimulation, T cells from the leukemic cell line Jurkat also increase their levels of CELF2, favoring the expression of LEF1-FL (357). On the contrary, neural progenitors, under proliferative conditions, decrease CELF2 levels, favoring the expression of LEF1-I5 (328).

All these data suggest that *CELF2* transcription and stability are highly dependent on microenvironmental stimuli. In fact, I validated that CELF2 expression is downregulated in proliferating CLL cells (*in vitro* stimulated or the proliferative fraction of PB CLL cells, i.e., recent LN emigrants) compared to quiescent CLL cells (*in vitro* unstimulated or the resting fraction of PB CLL cells). Therefore, after certain amount of external pro-proliferative stimuli, *CELF2* is downregulated in CLL cells. Such downregulation results in diminished protein levels of LEF1-FL and augmented LEF1-Δexon6, promoting a more proliferative phenotype in CLL cells. However, further validation should be directly performed in LN-derived CLL samples to assess whether the diminished CELF2 mRNA and protein levels correlate with higher expression of LEF1-Δexon6 isoforms.

4. Dual role of LEF1 in CLL

A major finding of this doctoral thesis is the pathogenic role of LEF1 seems to depend both on its protein levels and the relative abundance of different isoforms. LEF1 is expressed in the early stages of CLL development, including the premalignant low-count and high-count MBL phases. While low count MBL rarely develops into CLL, high-count MBL progresses to overt CLL at a rate of just 1% per year (6). MBLs are strongly enriched in cases with mutated IGHV. Additionally, approximately one third of CLL cells, mostly M-CLL, remain stable over time in the absence of treatment. All these indolent cases express the LEF1 protein, but at lower levels than U-CLL cases, indicating that at the qualitative level the presence of this TF is essential for the survival of CLL cells (152), but it is not sufficient to induce proliferation *per se*. In addition to intrinsic factors, CLL proliferation is well-

known to be dependent on the interaction between CLL cells and the LN microenvironment. Such pro-proliferative cues induced by the TME are more pronounced in more aggressive CLLs (66,358) and U-CLL cells are overall more prone than M-CLLs to enter and being retained in the LN (331). In this context, the results of my thesis indicate that LEF1 seems to be modulated by the TME, not only in terms of overall protein levels but in the relative abundance of different isoforms. Under proliferative conditions (*in vitro* or in the LN), there is a relative increase of the LEF1-I6 isoform as compared to the LEF1-FL, which promotes CLL proliferation independently of the IGHV status. Moreover, the enhanced stability of LEF1 and, hence, increased overall protein levels are related to more extensive binding of LEF1 to genes involved in proliferation, which in turn confer additional proliferative capacity to U-CLL cells compared to M-CLL.

In conclusion, LEF1 seems to be a special kind of oncoprotein in CLL, as it seems to play a dual role in CLL pathogenesis (**Figure 69**). Baseline *de novo* expression levels of LEF1 are related to cell survival and lymphocyte activation and represent a very early event in CLL development, contributing to the steady-state phase of the disease. Further increased LEF1 levels in U-CLL seems to promote proliferation, which partially explains the more aggressive behavior of this CLL subtype. In particular, this LEF1-mediated proliferative function in U-CLL seems to rely on intrinsic and extrinsic factors. The intrinsic factor corresponds to the higher protein abundance of LEF1, whereas the extrinsic factor is related to a switch from the FL to the shorter isoforms, lacking exon 6, induced by the LN microenvironment. Such dual role of an oncogene in tumorigenesis is rare, but not unique to LEF1 in CLL. There are few additional examples described in the literature (359,360). For instance, the transforming growth factor β (TGF-β) induces apoptosis and inhibits proliferation in tumor cells in early phases, while in late sages shows pro-tumoral effects by modulating the TME and inducing epithelial mesenchymal transition, cell motility and metastasis (361,362). The findings derived from this thesis not only represent a significant contribution to our understanding of CLL biology, but also

may have future clinical implications. As LEF1 mediates both cell survival and proliferation in CLL, it may represent an attractive therapeutic target suitable for the entire clinical spectrum of CLL, including both indolent and progressive forms of the disease.

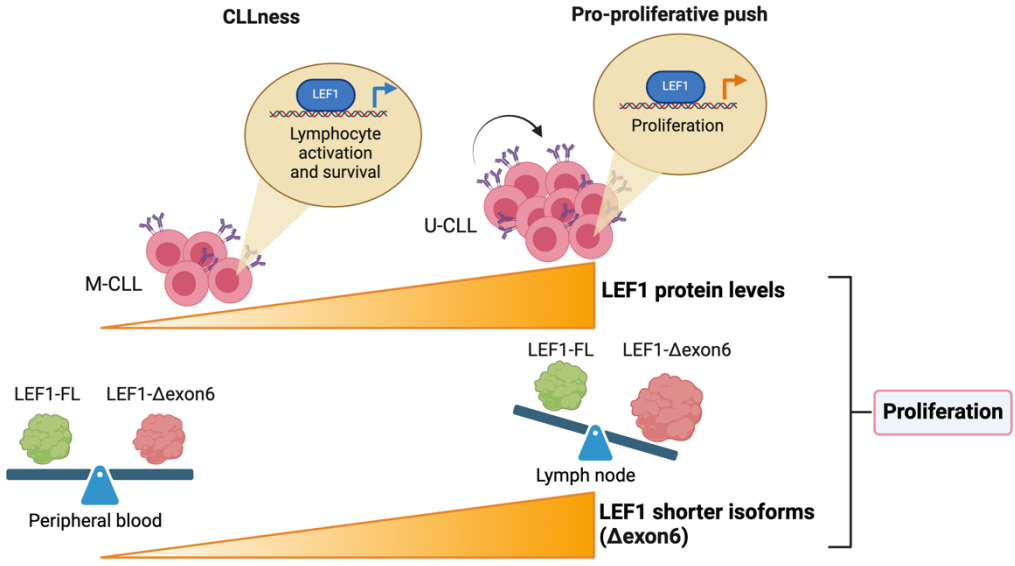
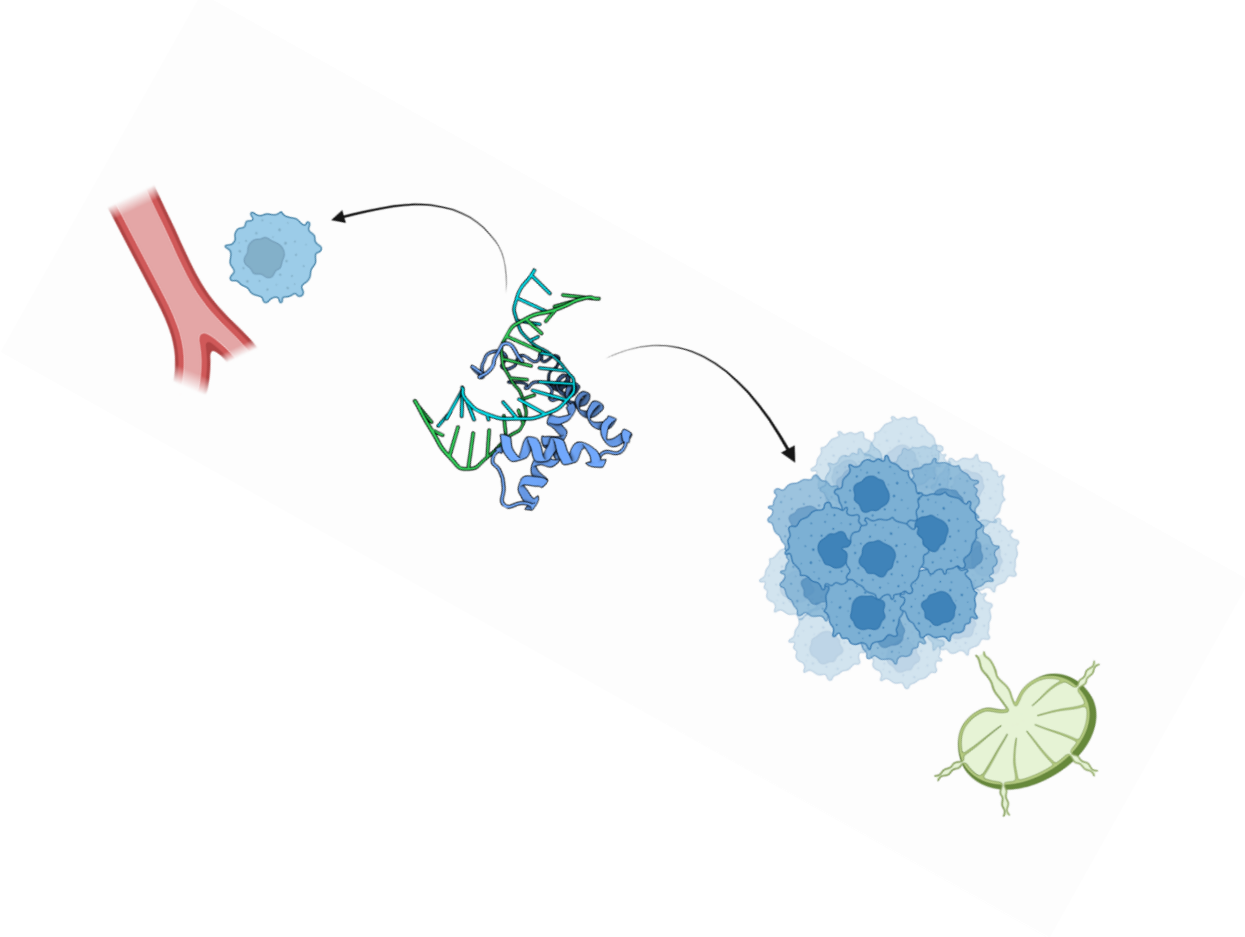


Figure 69. Graphical representation of the dual role of LEF1 in CLL. Created with Biorender.com.

General conclusions



This doctoral thesis is divided into two different studies, whose specific conclusions appear at the end of each respective chapter. Nevertheless, here I present the general conclusions that can be drawn from the doctoral thesis as a whole:

1. I have characterized the phenotypic and molecular effects of a new *in vitro* system to grow patient-derived CLL cells. This system constitutes a new model to study CLL pathogenesis, in particular to analyze proliferative phases of the disease.

2.. I have exploited the vigorous proliferation of CLL cells induced by the new culture system to develop an electroporation-based CRISPR-Cas9 method that achieves efficient gene editing in malignant B cells from primary CLL and MCL samples.

3. Although *LEF1* mRNA expression levels are increased at similar levels in U-CLL and M-CLL as compared to normal B cells, the more aggressive U-CLL subtype shows higher protein abundance due to increased protein stability.

4. Increased LEF1 protein levels in U-CLL seem to be associated with the cell of origin rather than with clinical aggressiveness itself, as aggressive M-CLLs do not show elevated LEF1 levels.

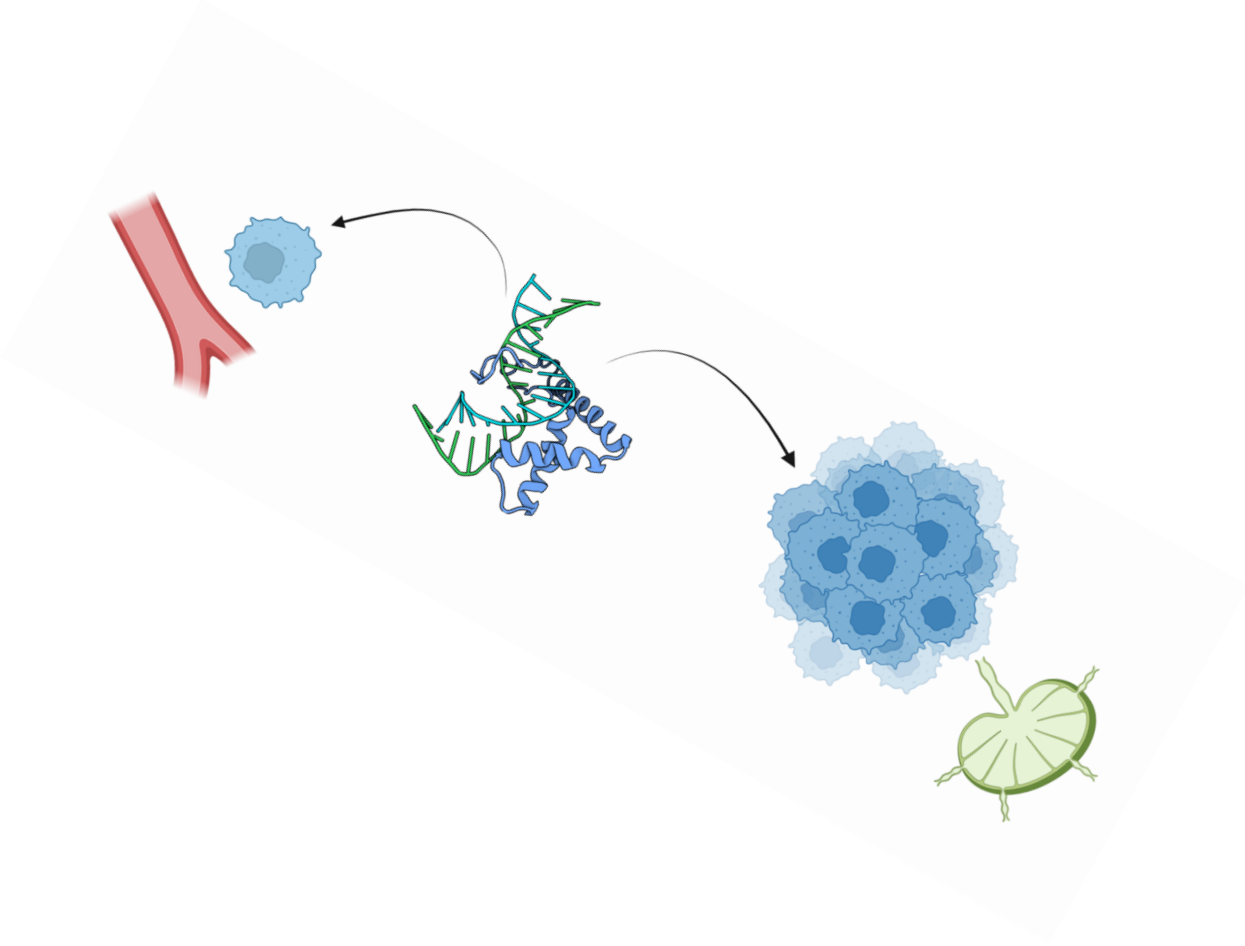
5. Low or intermediate LEF1 protein levels bind to genes involved in the response to microenvironmental signaling and lymphocyte activation, which seem to represent a sign of "CLLness" present in CLL regardless of the clinico-biological subtype. Remarkably, when LEF1 protein levels are further increased in U-CLL, it additionally binds to genes involved in cell cycle progression.

6. LEF1 levels are positively modulated by extrinsic stimuli promoting proliferation. Under LN-like conditions, the proliferative drive of LEF1 seems to be mediated by a shift from LEF1-FL to shorter isoforms lacking exon 6 in patient-derived CLL cells.

Remarkably, overexpression of LEF1-FL isoform induces quiescence, whereas shorter LEF1 isoforms promote proliferation in CLL cell lines.

Overall, the major conclusion of this doctoral thesis is that the oncogenic role of LEF1 in CLL seems to be two-fold depending on protein abundance and isoform expression. Baseline protein levels of LEF1 are associated with CLL as a whole, while increased protein levels in U-CLL, including a higher relative proportion of shorter LEF1 isoforms, drive CLL proliferation and a more aggressive clinical phenotype.

References



1. Kipps TJ, Stevenson FK, Wu CJ, Croce CM, Packham G, Wierda WG, et al. Chronic lymphocytic leukaemia. Nat Rev Dis Primers. 2017 Jan;3:16096.
2. Tse E, Kwong YL, Goh YT, Bee PC, Ng SC, Tan D, et al. Expert consensus on the management of chronic lymphocytic leukaemia in Asia. Clin Exp Med. 2023 Oct;23(6):2895–907.
3. Dillman RO, Beauregard JC, Lea JW, Green MR, Sobol RE, Royston I. Chronic lymphocytic leukemia and other chronic lymphoid proliferations: surface marker phenotypes and clinical correlations. J Clin Oncol. 1983 Mar;1(3):190–7.
4. Salem DA, Stetler-Stevenson M. Clinical Flow-Cytometric Testing in Chronic Lymphocytic Leukemia. Methods Mol Biol. 2019;2032:311–21.
5. DiGiuseppe JA, Borowitz MJ. Clinical utility of flow cytometry in the chronic lymphoid leukemias. Semin Oncol. 1998 Feb;25(1):6–10.
6. Strati P, Shanafelt TD. Monoclonal B-cell lymphocytosis and early-stage chronic lymphocytic leukemia: diagnosis, natural history, and risk stratification. Blood. 2015 Jul;126(4):454–62.
7. Damm F, Mylonas E, Cosson A, Yoshida K, Della Valle V, Mouly E, et al. Acquired initiating mutations in early hematopoietic cells of CLL patients. Cancer Discov. 2014 Sep;4(9):1088–101.
8. Shadman M. Diagnosis and Treatment of Chronic Lymphocytic Leukemia: A Review. JAMA. 2023 Mar;329 (11):918–32.
9. Douglas, MS. Richter Transformation: Clinical Manifestations, Evaluation, and Management. J Adv Pract Oncol. 2022 Jul;13(5):525–34.
10. Dighiero G, Maloum K, Desablens B, Cazin B, Navarro M, Leblay R, et al. Chlorambucil in indolent chronic lymphocytic leukemia. French Cooperative Group on Chronic Lymphocytic Leukemia. N Engl J Med. 1998 May;338(21):1506–14.
11. Hoechstetter MA, Busch R, Eichhorst B, Bühler A, Winkler D, Eckart MJ, et al. Early, risk-Adapted treatment with fludarabine in Binet stage A chronic lymphocytic leukemia patients: Results of the CLL1 trial of the German CLL study group. Leukemia. 2017 Dec; 31(12):2833–7.
12. Hampel PJ, Parikh SA. Chronic lymphocytic leukemia treatment algorithm 2022. Blood Cancer J. 2022 Nov;12(11):161.
13. Keating MJ, O'Brien S, Albitar M, Lerner S, Plunkett W, Giles F, et al. Early results of a chemoimmunotherapy regimen of fludarabine, cyclophosphamide, and rituximab as initial therapy for chronic lymphocytic leukemia. J Clin Oncol. 2005;23(18):4079–88.
14. Sengar M, Jain H, Rajendra A, Rengaraj K, Thorat J. Frontline Therapy of Chronic Lymphocytic Leukemia: Changing Treatment Paradigm. Curr Hematol Malig Rep. 2020 Jun;15(3):168-176.
15. Burger JA, Tedeschi A, Barr PM, Robak T, Owen C, Ghia P, et al. Ibrutinib as Initial Therapy for Patients with Chronic Lymphocytic Leukemia.N Eng J Med. 2015 Dec;373(25):2425–37.
16. Rastogi I, Jeon D, Moseman JE, Muralidhar A, Potluri HK, McNeel DG. Role of B cells as antigen presenting cells. Front Immunol. 2022 Sep;13:954936.
17. Dong Y, Pi X, Bartels-Burgahn F, Saltukoglu D, Liang Z, Yang J, et al. Structural principles of B cell antigen receptor assembly. Nature. 2022 Dec;612(7938):156–61.
18. Schroeder HW, Cavacini L. Structure and function of immunoglobulins. J Allergy Clin Immunol. 2010 Feb;125(2 Suppl 2):S41-52.
19. Mlynarczyk C, Fontán L, Melnick A. Germinal center-derived lymphomas: The darkest side of humoral immunity. Immunol Rev. 2019 Mar;288(1):214–39.
20. Rosenquist R, Ghia P, Hadzidimitriou A, Sutton LA, Agathangelidis A, Baliakas P, et al. Immunoglobulin gene sequence analysis in chronic lymphocytic leukemia: updated ERIC recommendations. Leukemia. 2017 Jul;31(7):1477–81.
21. Seifert M, Sellmann L, Bloehdorn J, Wein F, Stilgenbauer S, Dürig J, et al. Cellular origin and pathophysiology of chronic lymphocytic leukemia. J Exp Med. 2012 Nov;209(12):2183–98.
22. Darwiche W, Gubler B, Marolleau JP, Ghamlouch H. Chronic lymphocytic leukemia B-cell normal cellular counterpart: Clues from a functional perspective. Front Immunol. 2018 Apr; 9:683.
23. Chiorazzi N, Ferrarini M. Cellular origin(s) of chronic lymphocytic leukemia: cautionary notes and additional considerations and possibilities. Blood. 2011 Feb;117(6):1781–91.

24. Damle RN, Calissano C, Chiorazzi N. Chronic lymphocytic leukaemia: a disease of activated monoclonal B cells. Best Pract Res Clin Haematol. 2010 Mar;23(1):33–45.
25. Damle RN, Wasil T, Fais F, Ghiotto F, Valetto A, Allen SL, et al. Ig V gene mutation status and CD38 expression as novel prognostic indicators in chronic lymphocytic leukemia. Blood. 1999 Sep;94(6):1840–7.
26. Hamblin TJ, Davis Z, Gardiner A, Oscier DG, Stevenson FK. Unmutated Ig V(H) genes are associated with a more aggressive form of chronic lymphocytic leukemia. Blood. 1999 Sep;94(6):1848–54.
27. Chiorazzi N. Implications of new prognostic markers in chronic lymphocytic leukemia. Hematology Am Soc Hematol Educ Program. 2012;2012:76–87.
28. Rossi D, Terzi-di-Bergamo L, De Paoli L, Cerri M, Ghilardi G, Chiarenza A, et al. Molecular prediction of durable remission after first-line fludarabine-cyclophosphamide-rituximab in chronic lymphocytic leukemia. Blood. 2015 Oct;126(16):1921–4.
29. Fischer K, Bahlo J, Fink AM, Goede V, Herling CD, Cramer P, et al. Long-term remissions after FCR chemoimmunotherapy in previously untreated patients with CLL: updated results of the CLL8 trial. Blood. 2016;127(2):208–15.
30. Thompson PA, Tam CS, O'Brien SM, Wierda WG, Stingo F, Plunkett W, et al. Fludarabine, cyclophosphamide, and rituximab treatment achieves long-term disease-free survival in IGHV-mutated chronic lymphocytic leukemia. Blood. 2016 Jan;127(3):303–9.
31. Stamatopoulos K, Agathangelidis A, Rosenquist R, Ghia P. Antigen receptor stereotypy in chronic lymphocytic leukemia. Leukemia. 2017 Feb; 31(2):282–91.
32. Agathangelidis A, Darzentas N, Hadzidimitriou A, Brochet X, Murray F, Yan XJ, et al. Stereotyped B-cell receptors in one-third of chronic lymphocytic leukemia: a molecular classification with implications for targeted therapies. Blood. 2012 May;119(19):4467–75.
33. ten Hacken E, Gounari M, Ghia P, Burger JA. The importance of B cell receptor isotypes and stereotypes in chronic lymphocytic leukemia. Leukemia. 2019 Feb; 33(2):287–98.
34. Sonia Jaramillo, Andreas Agathangelidis, Christof Schneider, Jasmin Bahlo, Sandra Robrecht, Eugen Tausch, et al. Prognostic impact of prevalent chronic lymphocytic leukemia stereotyped subsets: analysis within prospective clinical trials of the German CLL Study Group (GCLLSG). Haematologica. 2020 Nov;105(11):2598–607.
35. Lanham S, Hamblin T, Oscier D, Ibbotson R, Stevenson F, Packham G. Differential signaling via surface IgM is associated with VH gene mutational status and CD38 expression in chronic lymphocytic leukemia. Blood. 2003 Feb;101(3):1087–93.
36. Deaglio S, Vaisitti T, Aydin S, Ferrero E, Malavasi F. In-tandem insight from basic science combined with clinical research: CD38 as both marker and key component of the pathogenetic network underlying chronic lymphocytic leukemia. Blood. 2006 Aug;108(4):1135–44.
37. Nolz JC, Tschumper RC, Pittner BT, Darce JR, Kay NE, Jelinek DF. ZAP-70 is expressed by a subset of normal human B-lymphocytes displaying an activated phenotype. Leukemia. 2005 Jun;19(6):1018–24.
38. Chiorazzi N, Ferrarini M. B cell chronic lymphocytic leukemia: Lessons learned from studies of the B cell antigen receptor. Annu Rev Immunol. 2003;21:841–94.
39. Hervé M, Xu K, Ng YS, Wardemann H, Albesiano E, Messmer BT, et al. Unmutated and mutated chronic lymphocytic leukemias derive from self-reactive B cell precursors despite expressing different antibody reactivity. J Clin Invest. 2005 Jun;115(6):1636–43.
40. Kulis M, Merkel A, Heath S, Queirós AC, Schuyler RP, Castellano G, et al. Whole-genome fingerprint of the DNA methylome during human B cell differentiation. Nat Genet. 2015 Jun;47(7):746–56.
41. Kulis M, Heath S, Bibikova M, Queirós AC, Navarro A, Clot G, et al. Epigenomic analysis detects widespread gene-body DNA hypomethylation in chronic lymphocytic leukemia. Nat Genet. 2012 Nov;44(11):1236–42.
42. Kulis M, Martin-Subero JI. Integrative epigenomics in chronic lymphocytic leukaemia: Biological insights and clinical applications. Br J Haematol. 2023 Feb;200(3):280–90.

43. Delgado J, Nadeu F, Colomer D, Campo E. Chronic lymphocytic leukemia: from molecular pathogenesis to novel therapeutic strategies. Haematologica. 2020 Sep;105(9):2205–17.
44. Stamatopoulos B, Smith T, Crompot E, Pieters K, Clifford R, Mraz M, et al. The Light Chain IgLV3-21 Defines a New Poor Prognostic Subgroup in Chronic Lymphocytic Leukemia: Results of a Multicenter Study. Clin Cancer Res. 2018 Oct;24(20):5048–57.
45. Nadeu F, Royo R, Clot G, Duran-Ferrer M, Navarro A, Martín S, et al. IGLV3-21R110 identifies an aggressive biological subtype of chronic lymphocytic leukemia with intermediate epigenetics. Blood. 2021 May;137(21):2935–46.
46. Nadeu F, Diaz-Navarro A, Delgado J, Puente XS, Campo E. Genomic and Epigenomic Alterations in Chronic Lymphocytic Leukemia. Annu Rev Pathol. 2020 Jan;15(1):149–77.
47. Queirós AC, Villamor N, Clot G, Martinez-Trillos A, Kulis M, Navarro A, et al. A B-cell epigenetic signature defines three biologic subgroups of chronic lymphocytic leukemia with clinical impact. Leukemia. 2015 Mar;29(3):598–605.
48. Bhoi S, Ljungström V, Baliakas P, Mattsson M, Smedby KE, Juliusson G, et al. Prognostic impact of epigenetic classification in chronic lymphocytic leukemia: The case of subset #2. Epigenetics. 2016 Jun;11(6):449–55.
49. Oakes CC, Seifert M, Assenov Y, Gu L, Przekopowitz M, Ruppert AS, et al. DNA methylation dynamics during B cell maturation underlie a continuum of disease phenotypes in chronic lymphocytic leukemia. Nat Genet. 2016 Mar;48(3):253–64.
50. Ghia P, Stamatopoulos K. In CLL, epigenetics also points to the BCR. Blood. 2021 May;137(21):2863–5.
51. Klein U, Tu Y, Stolovitzky GA, Mattioli M, Cattoretti G, Husson H, et al. Gene Expression Profiling of B Cell Chronic Lymphocytic Leukemia Reveals a Homogeneous Phenotype Related to Memory B Cells. J Exp Med. 2001 Dec;194(11):1625–38.
52. Rosenwald A, Alizadeh AA, Widhopf G, Simon R, Davis RE, Yu X, et al. Relation of Gene Expression Phenotype to Immunoglobulin Mutation Genotype in B Cell Chronic Lymphocytic Leukemia. J Exp Med. 2001 Dec; 194(11):1639–47.
53. Dal-Bo M, Bertoni F, Forconi F, Zucchetto A, Bomben R, Marasca R, et al. Intrinsic and extrinsic factors influencing the clinical course of B-cell chronic lymphocytic leukemia: prognostic markers with pathogenetic relevance. J Transl Med. 2009 Dec;7(1):76.
54. Smith LD, Minton AR, Blunt MD, Karydis LI, Dutton DA, Rogers-Broadway KR, et al. BCR signaling contributes to autophagy regulation in chronic lymphocytic leukemia. Leukemia. 2020 Feb;34(2):640–4.
55. Messmer BT, Messmer D, Allen SL, Kolitz JE, Kudalkar P, Cesar D, et al. In vivo measurements document the dynamic cellular kinetics of chronic lymphocytic leukemia B cells. J Clin Invest. 2005;115(3):755–64.
56. van Gent R, Kater AP, Otto SA, Jaspers A, Borghans JAM, Vrisekoop N, et al. In vivo dynamics of stable chronic lymphocytic leukemia inversely correlate with somatic hypermutation levels and suggest no major leukemic turnover in bone marrow. Cancer Res. 2008 Dec;68(24):10137–44.
57. Haselager M V., Kater AP, Eldering E. Proliferative Signals in Chronic Lymphocytic Leukemia; What Are We Missing? Front Oncol. 2020 Oct; 10:592205.
58. Herndon TM, Chen SS, Saba NS, Valdez J, Emson C, Gatmaitan M, et al. Direct in vivo evidence for increased proliferation of CLL cells in lymph nodes compared to bone marrow and peripheral blood. Leukemia. 2017 Jun;31(6):1340–7.
59. Stein H, Bonk A, Tolksdorf G, Lennert K, Rodt H, Gerdes J. Immunohistologic analysis of the organization of normal lymphoid tissue and non-Hodgkin's lymphomas. J Histochem Cytochem. 1980 Aug; 28(8):746–60.
60. Soma LA, Craig FE, Swerdlow SH. The proliferation center microenvironment and prognostic markers in chronic lymphocytic leukemia/small lymphocytic lymphoma. Hum Pathol. 2006 Feb;37(2):152–9.
61. Calissano C, Damle RN, Marsilio S, Yan XJ, Yancopoulos S, Hayes G, et al. Intraclonal complexity in chronic lymphocytic leukemia: fractions enriched in recently born/divided and older/quiescent cells. Mol Med. 2011;17(11-12):1374–82.

62. Caligaris-Cappio F, Bertilaccio MT, Scielzo C. How the microenvironment wires the natural history of chronic lymphocytic leukemia. Semin Cancer Biol. 2014 Feb;24:43–8.
63. Burger JA, Gribben JG. The microenvironment in chronic lymphocytic leukemia (CLL) and other B cell malignancies: Insight into disease biology and new targeted therapies. Semin Cancer Biol. 2014 Feb;24:71–81.
64. ten Hacken E, Burger JA. Microenvironment interactions and B-cell receptor signaling in Chronic Lymphocytic Leukemia: Implications for disease pathogenesis and treatment. Biochim Biophys Acta. 2016 Mar;1863(3):401–13.
65. Vlachonikola E, Stamatopoulos K, Chatzidimitriou A. T Cells in Chronic Lymphocytic Leukemia: A Two-Edged Sword. Front Immunol. 2021 Jan;11:612244.
66. Svanberg R, Janum S, Patten PEM, Ramsay AG, Niemann CU. Targeting the tumor microenvironment in chronic lymphocytic leukemia. Haematologica. 2021 Sep;106(9):2312–24.
67. Roessner PM, Seiffert M. T-cells in chronic lymphocytic leukemia: Guardians or drivers of disease? Leukemia. 2020 Aug;34(8):2012–24.
68. Os A, Bürgler S, Ribes AP, Funderud A, Wang D, Thompson KM, et al. Chronic Lymphocytic Leukemia Cells Are Activated and Proliferate in Response to Specific T Helper Cells. Cell Rep. 2013 Aug;4(3):566–77.
69. van Attekum MHA, van Bruggen JAC, Slinger E, Lebre MC, Reinen E, Kersting S, et al. CD40 signaling instructs chronic lymphocytic leukemia cells to attract monocytes via the CCR2 axis. Haematologica. 2017 Nov;102(12):2069–76.
70. Palma M, Gentilcore G, Heimersson K, Mozaffari F, Näsman-Glaser B, Young E, et al. T cells in chronic lymphocytic leukemia display dysregulated expression of immune checkpoints and activation markers. Haematologica. 2017 Mar;102(3):562–72.
71. Ramsay AG, Clear AJ, Fatah R, Gribben JG. Multiple inhibitory ligands induce impaired T-cell immunologic synapse function in chronic lymphocytic leukemia that can be blocked with lenalidomide: establishing a reversible immune evasion mechanism in human cancer. Blood. 2012 Aug;120(7):1412–21.
72. Riches JC, Davies JK, McClanahan F, Fatah R, Iqbal S, Agrawal S, et al. T cells from CLL patients exhibit features of T-cell exhaustion but retain capacity for cytokine production. Blood. 2013 Feb;121(9):1612–21.
73. Giannopoulos K, Schmitt M, Kowal M, Wlasiuk P, Bojarska-Junak A, Chen J, et al. Characterization of regulatory T cells in patients with B-cell chronic lymphocytic leukemia. Oncol Rep. 2008 Sep;20(3):677–82.
74. Kwok M, Oldreive C, Rawstron AC, Goel A, Papatzikas G, Jones RE, et al. Integrative analysis of spontaneous CLL regression highlights genetic and microenvironmental interdependency in CLL. Blood. 2020 Feb;135(6):411–28.
75. Tsukada N, Burger JA, Zvaifler NJ, Kipps TJ. Distinctive features of "nurselike" cells that differentiate in the context of chronic lymphocytic leukemia. Blood. 2002 Feb;99(3):1030–7.
76. Burger JA, Burger M, Kipps TJ. Chronic lymphocytic leukemia B cells express functional CXCR4 chemokine receptors that mediate spontaneous migration beneath bone marrow stromal cells. Blood. 1999 Dec;94(11):3658–67.
77. Ohata J, Zvaifler NJ, Nishio M, Boyle DL, Kalled SL, Carson DA, et al. Fibroblast-Like Synoviocytes of Mesenchymal Origin Express Functional B Cell-Activating Factor of the TNF Family in Response to Proinflammatory Cytokines. J Immunol. 2005 Jan;174(2):864–70.
78. Burger JA, Tsukada N, Burger M, Zvaifler NJ, Dell'Aquila M, Kipps TJ. Blood-derived nurse-like cells protect chronic lymphocytic leukemia B cells from spontaneous apoptosis through stromal cell-derived factor-1. Blood. 2000 Oct;96(8):2655–63.
79. Nishio M, Endo T, Tsukada N, Ohata J, Kitada S, Reed JC, et al. Nurselike cells express BAFF and APRIL, which can promote survival of chronic lymphocytic leukemia cells via a paracrine pathway distinct from that of SDF-1α. Blood. 2005 Aug;106(3):1012–20.
80. Jitschin R, Braun M, Büttner M, Dettmer-Wilde K, Bricks J, Berger J, et al. CLL-cells induce IDOhi CD14+HLA-DRlo myeloid-derived suppressor cells that inhibit T-cell responses and promote TRegs. Blood. 2014 Jul;124(5):750–60.

81. Alhakeem SS, McKenna MK, Oben KZ, Noothi SK, Rivas JR, Hildebrandt GC, et al. Chronic Lymphocytic Leukemia–Derived IL-10 Suppresses Antitumor Immunity. J Immunol. 2018 Jun;200(12):4180–9.
82. Smallwood DT, Apollonio B, Willimott S, Lezina L, Alharthi A, Ambrose AR, et al. Extracellular vesicles released by CD40/IL-4-stimulated CLL cells confer altered functional properties to CD4+ T cells. Blood. 2016 Jul;128(4):542–52.
83. Burger JA, Chiorazzi N. B cell receptor signaling in chronic lymphocytic leukemia. Trends in Immunol. 2013 Dec; 34(12):592–601.
84. Mazzarello AN, Gentner-Göbel E, Dühren-Von Minden M, Tarasenko TN, Nicolò A, Ferrer G, et al. B cell receptor isotypes differentially associate with cell signaling, kinetics, and outcome in chronic lymphocytic leukemia. J Clin Invest. 2022 Jan;132(2):e149308.
85. Dühren-von Minden M, Übelhart R, Schneider D, Wossning T, Bach MP, Buchner M, et al. Chronic lymphocytic leukaemia is driven by antigen-independent cell-autonomous signalling. Nature. 2012 Sep;489(7415):309–12.
86. Binder M, Müller F, Frick M, Wehr C, Simon F, Leistler B, et al. CLL B-cell receptors can recognize themselves: alternative epitopes and structural clues for autostimulatory mechanisms in CLL. Blood. 2013 Jan;121(1):239–41.
87. ten Hacken E, Scielzo C, Bertilaccio MTS, Scarfò L, Apollonio B, Barbaglio F, et al. Targeting the LYN/HS1 signaling axis in chronic lymphocytic leukemia. Blood. 2013 Mar;121(12):2264–73.
88. Herishanu Y, Katz BZ, Lipsky A, Wiestner A. Biology of chronic lymphocytic leukemia in different microenvironments. Hematol Oncol Clin North Am. 2013 Apr;27(2):173–206.
89. Petlickovski A, Laurenti L, Li X, Marietti S, Chiusolo P, Sica S, et al. Sustained signaling through the B-cell receptor induces Mcl-1 and promotes survival of chronic lymphocytic leukemia B cells. Blood. 2005 Jun;105(12):4820–7.
90. Krzysiek R, Lefèvre EA, Zou W, Foussat A, Bernard J, Portier A, et al. Antigen receptor engagement selectively induces macrophage inflammatory protein-1 alpha (MIP-1 alpha) and MIP-1 beta chemokine production in human B cells. J Immunol. 1999 Apr;162(8):4455–63.
91. Burger JA, Quiroga MP, Hartmann E, Bürkle A, Wierda WG, Keating MJ, et al. High-level expression of the T-cell chemokines CCL3 and CCL4 by chronic lymphocytic leukemia B cells in nurselike cell cocultures and after BCR stimulation. Blood. 2009 Mar;113(13):3050–8.
92. Packham G, Krysov S, Allen A, Savelyeva N, Steele AJ, Forconi F, et al. The outcome of B-cell receptor signaling in chronic lymphocytic leukemia: proliferation or anergy. Haematologica. 2014 Jul;99(7):1138–48.
93. Paggetti J, Moussay E. BCR engagement in CLL: when translation goes wrong. Blood. 2016 Jan;127(4):378–80.
94. Hoogeboom R, van Kesse KPM, Hochstenbach F, Wormhoudt TA, Reinten RJA, Wagner K, et al. A mutated B cell chronic lymphocytic leukemia subset that recognizes and responds to fungi. J Exp Med. 2013 Jan;210(1):59–70.
95. Kostareli E, Gounari M, Janus A, Murray F, Brochet X, Giudicelli V, et al. Antigen receptor stereotypy across B-cell lymphoproliferations: The case of IGHV4-59/IGKV3-20 receptors with rheumatoid factor activity. Leukemia. 2012 May;26(5):1127–31.
96. Apollonio B, Scielzo C, Bertilaccio MTS, ten Hacken E, Scarfò L, Ranghetti P, et al. Targeting B-cell anergy in chronic lymphocytic leukemia. Blood. 2013 May;121(19):3879–88.
97. Chu CC, Catera R, Zhang L, Didier S, Agagnina BM, Damle RN, et al. Many chronic lymphocytic leukemia antibodies recognize apoptotic cells with exposed nonmuscle myosin heavy chain IIA: implications for patient outcome and cell of origin. Blood. 2010 May;115(19):3907–15.
98. Catera R, Silverman GJ, Hatzi K, Seiler T, Didier S, Zhang L, et al. Chronic lymphocytic leukemia cells recognize conserved epitopes associated with apoptosis and oxidation. Mol Med. 2008 Nov;14(11–12):665–74.
99. Gounari M, Ntoufa S, Apollonio B, Papakonstantinou N, Ponzoni M, Chu CC, et al. Excessive antigen reactivity may underlie the clinical aggressiveness of chronic lymphocytic leukemia stereotyped subset #8. Blood. 2015 Jun;125(23):3580–7.

100. Chen L, Widhopf G, Huynh L, Rassenti L, Rai KR, Weiss A, et al. Expression of ZAP-70 is associated with increased B-cell receptor signaling in chronic lymphocytic leukemia. Blood. 2002 Dec;100(13):4609–14.
101. Crespo M, Bosch F, Villamor N, Bellosillo B, Colomer D, Rozman M, et al. ZAP-70 Expression as a Surrogate for Immunoglobulin-Variable-Region Mutations in Chronic Lymphocytic Leukemia. N Engl J Med. 2003 May;348(18): 1764–75.
102. Del Principe MI, Del Poeta G, Buccisano F, Maurillo L, Venditti A, Zucchetto A, et al. Clinical significance of ZAP-70 protein expression in B-cell chronic lymphocytic leukemia. Blood. 2006 Aug;108(3):853–61.
103. Rassenti LZ, Huynh L, Toy TL, Chen L, Keating MJ, Gribben JG, et al. ZAP-70 Compared with Immunoglobulin Heavy-Chain Gene Mutation Status as a Predictor of Disease Progression in Chronic Lymphocytic Leukemia. N Engl J Med. 2004 Aug;351(9):893–901.
104. Chen L, Apgar J, Huynh L, Dicker F, Giago-McGahan T, Rassenti L, et al. ZAP-70 directly enhances IgM signaling in chronic lymphocytic leukemia. Blood. 2005 Mar;105(5):2036–41.
105. Richardson SJ, Matthews C, Catherwood MA, Alexander HD, Carey BS, Farrugia J, et al. ZAP-70 expression is associated with enhanced ability to respond to migratory and survival signals in B-cell chronic lymphocytic leukemia (B-CLL). Blood. 2006 May;107(9):3584–92.
106. Minici C, Gounari M, Übelhart R, Scarfò L, Dühren-von Minden M, Schneider D, et al. Distinct homotypic B-cell receptor interactions shape the outcome of chronic lymphocytic leukaemia. Nat Commun. 2017 Jun;8;15746.
107. Iacovelli S, Hug E, Bennardo S, Duehren-von Minden M, Gobessi S, Rinaldi A, et al. Two types of BCR interactions are positively selected during leukemia development in the Eμ-TCL1 transgenic mouse model of CLL. Blood. 2015 Mar;125(10):1578–88.
108. Döhner H, Stilgenbauer S, Benner A, Leupolt E, Kröber A, Bullinger L, et al. Genomic Aberrations and Survival in Chronic Lymphocytic Leukemia. N Engl J Med. 2000 Dec;343(26):1910–6.
109. Puiggros A, Blanco G, Espinet B. Genetic abnormalities in chronic lymphocytic leukemia: where we are and where we go. Biomed Res Int. 2014;2014:435983.
110. Klein U, Lia M, Crespo M, Siegel R, Shen Q, Mo T, et al. The DLEU2/miR-15a/16-1 Cluster Controls B Cell Proliferation and Its Deletion Leads to Chronic Lymphocytic Leukemia. Cancer Cell. 2010 Jan;17(1):28–40.
111. Zenz T, Eichhorst B, Busch R, Denzel T, Häbe S, Winkler D, et al. TP53 mutation and survival in chronic lymphocytic leukemia. J Clin Oncol. 2010 Oct;28(29):4473–9.
112. Stankovic T, Skowronska A. The role of ATM mutations and 11q deletions in disease progression in chronic lymphocytic leukemia. Leuk Lymphoma. 2014 Jun;55(6):1227–39.
113. Döhner H, Stilgenbauer S, James MR, Benner A, Weilguni T, Bentz M, et al. 11q deletions identify a new subset of B-cell chronic lymphocytic leukemia characterized by extensive nodal involvement and inferior prognosis. Blood. 1997 Apr;89(7):2516–22.
114. Abruzzo L V., Herling CD, Calin GA, Oakes C, Barron LL, Banks HE, et al. Trisomy 12 chronic lymphocytic leukemia expresses a unique set of activated and targetable pathways. Haematologica. 2018 Dec;103(12):2069–78.
115. Puente XS, Beà S, Valdés-Mas R, Villamor N, Gutiérrez-Abril J, Martín-Subero JI, et al. Non-coding recurrent mutations in chronic lymphocytic leukaemia. Nature. 2015 Oct;526(7574):519–24.
116. Landau DA, Tausch E, Taylor-Weiner AN, Stewart C, Reiter JG, Bahlo J, et al. Mutations driving CLL and their evolution in progression and relapse. Nature. 2015 Oct;526(7574):525–30.
117. Knisbacher BA, Lin Z, Hahn CK, Nadeu F, Duran-Ferrer M, Stevenson KE, et al. Molecular map of chronic lymphocytic leukemia and its impact on outcome. Nat Genet. 2022 Nov;54(11):1664–74.
118. Nadeu F, Clot G, Delgado J, Martín-García D, Baumann T, Salaverria I, et al. Clinical impact of the subclonal architecture and mutational complexity in chronic lymphocytic leukemia. Leukemia. 2018 Mar;32(3):645–53.

119. Nadeu F, Delgado J, Royo C, Baumann T, Stankovic T, Pinyol M, et al. Clinical impact of clonal and subclonal TP53, SF3B1, BIRC3, NOTCH1, and ATM mutations in chronic lymphocytic leukemia. Blood. 2016;127(17):2122–30.
120. Lawrence MS, Stojanov P, Mermel CH, Robinson JT, Garraway LA, Golub TR, et al. Discovery and saturation analysis of cancer genes across 21 tumour types. Nature. 2014 Jan;505(7484):495–501.
121. Mehrmohamadi M, Sepehri MH, Nazer N, Norouzi MR. A Comparative Overview of Epigenomic Profiling Methods. Front Cell Dev Biol. 2021 Jul 22;9:714687.
122. Luger K, Dechassa ML, Tremethick DJ. New insights into nucleosome and chromatin structure: An ordered state or a disordered affair? Nat Rev Mol Cell Biol. 2012 Jun;13(7);436–47.
123. Millán-Zambrano G, Burton A, Bannister AJ, Schneider R. Histone post-translational modifications — cause and consequence of genome function. Nat Rev Genet. 2022 Sep;23(9):563–80.
124. Protacio RU, Li G, Lowary PT, Widom J. Effects of histone tail domains on the rate of transcriptional elongation through a nucleosome. Mol Cell Biol. 2000 Dec;20(23):8866–78.
125. Cosgrove MS, Boeke JD, Wolberger C. Regulated nucleosome mobility and the histone code. Nat Struct Mol Biol. 2004 Nov;11(11):1037–43.
126. Lawrence M, Daujat S, Schneider R. Lateral Thinking: How Histone Modifications Regulate Gene Expression. Trends Genet. 2016 Jan;32(1):42–56.
127. Furey TS. ChIP-seq and beyond: New and improved methodologies to detect and characterize protein-DNA interactions. Nat Rev Genet. 2012 Dec;13(12):840–52.
128. Mikkelsen TS, Ku M, Jaffe DB, Issac B, Lieberman E, Giannoukos G, et al. Genome-wide maps of chromatin state in pluripotent and lineage-committed cells. Nature. 2007 Aug;448(7153):553–60.
129. Ernst J, Kellis M. ChromHMM: Automating chromatin-state discovery and characterization. Nat Methods. 2012 Feb;9(3):215–6.
130. Ernst J, Kheradpour P, Mikkelsen TS, Shoresh N, Ward LD, Epstein CB, et al. Mapping and analysis of chromatin state dynamics in nine human cell types. Nature. 2011 May;473(7345):43–9.
131. Klemm SL, Shipony Z, Greenleaf WJ. Chromatin accessibility and the regulatory epigenome. Nat Rev Genet; 2019 Apr;20(4):207–20.
132. Buenrostro JD, Giresi PG, Zaba LC, Chang HY, Greenleaf WJ. Transposition of native chromatin for fast and sensitive epigenomic profiling of open chromatin, DNA-binding proteins and nucleosome position. Nat Methods. 2013 Dec;10(12):1213–8.
133. Corces MR, Buenrostro JD, Wu B, Greenside PG, Chan SM, Koenig JL, et al. Lineage-specific and single-cell chromatin accessibility charts human hematopoiesis and leukemia evolution. Nat Genet. 2016 Oct;48(10):1193–203.
134. Dogan N, Wu W, Morrissey CS, Chen KB, Stonestrom A, Long M, et al. Occupancy by key transcription factors is a more accurate predictor of enhancer activity than histone modifications or chromatin accessibility. Epigenetics Chromatin. 2015 Apr;8:16.
135. Beekman R, Chapaprieta V, Russiñol N, Vilarrasa-Blasi R, Verdaguer-Dot N, Martens JHA, et al. The reference epigenome and regulatory chromatin landscape of chronic lymphocytic leukemia. Nat Med. 2018 Jun;24(6):868–80.
136. Scherer M, Schmidt F, Lazareva O, Walter J, Baumbach J, Schulz MH, et al. Machine learning for deciphering cell heterogeneity and gene regulation. Nat Comput Sci. 2021 Mar;1(3):183–91.
137. Brettingham-Moore KH, Taberlay PC, Holloway AF. Interplay between transcription factors and the epigenome: Insight from the role of RUNX1 in leukemia. Front Immunol. 2015 Sep;6:449.
138. Wilson S, Filipp FV. A network of epigenomic and transcriptional cooperation encompassing an epigenomic master regulator in cancer. NPJ Syst Biol Appl. 2018 Dec;4:24.
139. Mansisidor AR, Risca VI. Chromatin accessibility: methods, mechanisms, and biological insights. Nucleus. 2022 Dec;13(1):238–78.
140. Zaret KS, Carroll JS. Pioneer transcription factors: establishing competence for gene expression. Genes Dev. 2011 Nov;25(21):2227–41.

141. Lemma RB, Fleischer T, Martinsen E, Ledsaak M, Kristensen V, Eskeland R, et al. Pioneer transcription factors are associated with the modulation of DNA methylation patterns across cancers. Epigenetics Chromatin. 2022 Apr;15(1):13.
142. Hagman J, Lukin K. Early B-cell factor "pioneers" the way for B-cell development. Trends Immunol. 2005 Sep;26(9):455–61.
143. Boller S, Grosschedl R. The regulatory network of B-cell differentiation: a focused view of early B-cell factor 1 function. Immunol Rev. 2014 Sep;261(1):102–15.
144. Skene PJ, Henikoff JG, Henikoff S. Targeted in situ genome-wide profiling with high efficiency for low cell numbers. Nat Protoc. 2018 May;13(5):1006–19.
145. Rendeiro AF, Schmidl C, Strefford JC, Walewska R, Davis Z, Farlik M, et al. Chromatin accessibility maps of chronic lymphocytic leukaemia identify subtype-specific epigenome signatures and transcription regulatory networks. Nat Commun. 2016 Jun 27;7:11938.
146. Ott CJ, Federation AJ, Schwartz LS, Kasar S, Klitgaard JL, Lenci R, et al. Enhancer Architecture and Essential Core Regulatory Circuitry of Chronic Lymphocytic Leukemia. Cancer Cell. 2018 Dec;34(6):982-995.e7.
147. Mallm J, Iskar M, Ishaque N, Klett LC, Kugler SJ, Muino JM, et al. Linking aberrant chromatin features in chronic lymphocytic leukemia to transcription factor networks. Mol Syst Biol. 2019 May;15(5):e8339.
148. Pastore A, Gaiti F, Lu SX, Brand RM, Kulm S, Chaligne R, et al. Corrupted coordination of epigenetic modifications leads to diverging chromatin states and transcriptional heterogeneity in CLL. Nat Commun. 2019 Dec;10(1):1874.
149. Vilarrasa-Blasi R, Soler-Vila P, Verdaguer-Dot N, Russiñol N, Di Stefano M, Chapaprieta V, et al. Dynamics of genome architecture and chromatin function during human B cell differentiation and neoplastic transformation. Nat Commun. 2021 Jan;12(1):651.
150. Navarro A, Clot G, Martínez-Trillos A, Pinyol M, Jares P, González-Farré B, et al. Improved classification of leukemic B-cell lymphoproliferative disorders using a transcriptional and genetic classifier. Haematologica. 2017 Sep;102(9): e360–3.
151. Speedy HE, Beekman R, Chapaprieta V, Orlando G, Law PJ, Martín-García D, et al. Insight into genetic predisposition to chronic lymphocytic leukemia from integrative epigenomics. Nat Commun. 2019 Aug;10(1):3615.
152. Gutierrez A, Tschumper RC, Wu X, Shanafelt TD, Eckel-Passow J, Huddleston PM, et al. LEF-1 is a prosurvival factor in chronic lymphocytic leukemia and is expressed in the preleukemic state of monoclonal B-cell lymphocytosis. Blood. 2010 Oct;116(16):2975–83.
153. Wolf C, Garding A, Filarsky K, Bahlo J, Robrecht S, Becker N, et al. NFATC1 activation by DNA hypomethylation in chronic lymphocytic leukemia correlates with clinical staging and can be inhibited by ibrutinib. Int J Cancer. 2018 Jan;142(2):322–33.
154. Hrckulak D, Kolar M, Strnad H, Korinek V. TCF/LEF transcription factors: An update from the internet resources. Cancers (Basel). 2016 Jul;8(7):70.
155. Cadigan KM, Waterman ML. TCF/LEFs and Wnt signaling in the nucleus. Cold Spring Harb Perspect Biol. 2012 Nov;4(11):a007906.
156. Clevers H. Wnt/β-Catenin Signaling in Development and Disease. Cell. 2006 Nov; 127(3):469–80.
157. Janovská P, Bryja V. Wnt signalling pathways in chronic lymphocytic leukaemia and B-cell lymphomas. Br J Pharmacol. 2017 Dec;174(24):4701–15.
158. MacDonald BT, Tamai K, He X. Wnt/β-Catenin Signaling: Components, Mechanisms, and Diseases. Dev Cell. 2009 Jul; 17(1):9–26.
159. Green JL, Kuntz SG, Sternberg PW. Ror receptor tyrosine kinases: orphans no more. Trends Cell Biol. 2008 Nov;18(11):536–44.
160. Reyes M, Flores T, Betancur D, Peña-Oyarzún D, Torres VA. Wnt/β-Catenin Signaling in Oral Carcinogenesis. Int J Mol Sci. 2020 Jun;21(13):4682.
161. Liu J, Xiao Q, Xiao J, Niu C, Li Y, Zhang X, et al. Wnt/β-catenin signalling: function, biological mechanisms, and therapeutic opportunities. Signal Transduct Target Ther. 2022 Jan;7(1):3.
162. Seifert JRK, Mlodzik M. Frizzled/PCP signalling: A conserved mechanism regulating cell polarity and directed motility. Nat Rev Genet. 2007 Feb;8(2):126–38.

163. Kaucká M, Plevová K, Pavlová Š, Janovská P, Mishra A, Verner J, et al. The Planar Cell Polarity Pathway Drives Pathogenesis of Chronic Lymphocytic Leukemia by the Regulation of B-Lymphocyte Migration. Cancer Res. 2013 Mar;73(5):1491–501.
164. Urbanek KD, Stilgenbauer S, Mertens D. To β or Not to β: How Important Is β-Catenin Dependent and Independent WNT Signaling in CLL? Cancers (Basel). 2022 Dec;15(1):194.
165. Van Beest M, Dooijes D, Van De Wetering M, Kjaerulff S, Bonvin A, Nielsen O, et al. Sequence-specific high mobility group box factors recognize 10-12-base pair minor groove motifs. J Biol Chem. 2000 Sep;275(35):27266–73.
166. Haynes TL, Thomas MB, Dusing MR, Valerius MT, Potter SS, Wiginton DA. An enhancer LEF-1/TCF-1 site is essential for insertion site-independent transgene expression in thymus. Nucleic Acids Res. 1996 Dec;24(24):5034-44.
167. Giese K, Kingsley C, Kirshner JR, Grosschedl R. Assembly and function of a TCR alpha enhancer complex is dependent on LEF-1-induced DNA bending and multiple protein-protein interactions. Genes Dev. 1995 Apr;9(8):995–1008.
168. Eastman Q, Grosschedl R. Regulation of LEF-1/TCF transcription factors by Wnt and other signals. Curr Opin Cell Biol. 1999 Apr;11(2):233–40.
169. Carlsson P, Waterman ML, Jones KA. The hLEF/TCF-1 alpha HMG protein contains a context-dependent transcriptional activation domain that induces the TCR alpha enhancer in T cells. Genes Dev. 1993 Dec;7(12a):2418–30.
170. Arce L, Yokoyama NN, Waterman ML. Diversity of LEF/TCF action in development and disease. Oncogene. 2006 Dec; 25(57):7492–504.
171. Love JJ, Li X, Case DA, Giese K, Grosschedl R, Wright PE. Structural basis for DNA bending by the architectural transcription factor LEF-1. Nature. 1995 Aug;376(6543):791–5.
172. Atcha FA, Syed A, Wu B, Hoverter NP, Yokoyama NN, Ting JHT, et al. A Unique DNA Binding Domain Converts T-Cell Factors into Strong Wnt Effectors. Mol Cell Biol. 2007 Dec;27(23):8352–63.
173. Mao CD, Byers SW. Cell-Context Dependent TCF/LEF Expression and Function: Alternative Tales of Repression, De-Repression and Activation Potentials. Crit Rev Eukaryot Gene Expr. 2011;21(3):207–36.
174. Hovanes K, Li TWH, Waterman ML. The human LEF-1 gene contains a promoter preferentially active in lymphocytes and encodes multiple isoforms derived from alternative splicing. Nucleic Acids Res. 2000 May;28(9):1994–2003.
175. Yokoyama NN, Pate KT, Sprowl S, Waterman ML. A role for YY1 in repression of dominant negative LEF-1 expression in colon cancer. Nucleic Acids Res. 2010 Oct;38(19):6375–88.
176. Hovanes K, Li TWH, Munguia JE, Truong T, Milovanovic T, Lawrence Marsh J, et al. β-catenin–sensitive isoforms of lymphoid enhancer factor-1 are selectively expressed in colon cancer. Nat Genet. 2001 May;28(1):53–7.
177. Staal FJT, Sen JM. The canonical Wnt signaling pathway plays an important role in lymphopoiesis and hematopoiesis. European Journal of Immunology. 2008 Jul;38(7):1788–94.
178. Luis TC, Ichii M, Brugman MH, Kincade P, Staal FJT. Wnt signaling strength regulates normal hematopoiesis and its deregulation is involved in leukemia development. Leukemia. 2012 Mar;26(3):414–21.
179. Reya T, Duncan AW, Ailles L, Domen J, Scherer DC, Willert K, et al. A role for Wnt signalling in self-renewal of haematopoietic stem cells. Nature. 2003 May;423(6938):409–14.
180. Edmaier KE, Stahnke K, Vegi N, Mulaw M, Ihme S, Scheffold A, et al. Expression of the lymphoid enhancer factor 1 is required for normal hematopoietic stem and progenitor cell function. Leukemia. 2014 Jan;28(1):227–30.
181. Skokowa J, Cario G, Uenalan M, Schambach A, Germeshausen M, Battmer K, et al. LEF-1 is crucial for neutrophil granulocytopoiesis and its expression is severely reduced in congenital neutropenia. Nat Med. 2006 Oct;12(10):1191–7.
182. Steinke FC, Xue HH. From inception to output, Tcf1 and Lef1 safeguard development of T cells and innate immune cells. Immunol Res. 2014 Aug;59(1–3):45–55.

183. Choi YS, Gullicksrud JA, Xing S, Zeng Z, Shan Q, Li F, et al. LEF-1 and TCF-1 orchestrate TFH differentiation by regulating differentiation circuits upstream of the transcriptional repressor Bcl6. Nat Immunol. 2015 Sep;16(9):980–90.
184. Okamura RM, Sigvardsson M, Galceran J, Verbeek S, Clevers H, Grosschedl R. Redundant regulation of T cell differentiation and TCRalpha gene expression by the transcription factors LEF-1 and TCF-1. Immunity. 1998 Jan;8(1):11–20.
185. Steinke FC, Yu S, Zhou X, He B, Yang W, Zhou B, et al. TCF-1 and LEF-1 act upstream of Th-POK to promote the CD4+ T cell fate and interact with Runx3 to silence Cd4 in CD8+ T cells. Nat Immunol. 2014 Jul;15(7):646–56.
186. Shan Q, Li X, Chen X, Zeng Z, Zhu S, Gai K, et al. Tcf1 and Lef1 provide constant supervision to mature CD8+ T cell identity and function by organizing genomic architecture. Nat Commun. 2021 Oct;12 (1):5863.
187. Xing S, Gai K, Li X, Shao P, Zeng Z, Zhao X, et al. Tcf1 and Lef1 are required for the immunosuppressive function of regulatory T cells. J Exp Med. 2019 Apr;216(4):847–66.
188. Reya T, O'Riordan M, Okamura R, Devaney E, Willert K, Nusse R, et al. Wnt signaling regulates B lymphocyte proliferation through a LEF-1 dependent mechanism. Immunity. 2000 Jul;13(1):15–24.
189. Li Y, Wang L, Zhang M, Melamed J, Liu X, Reiter R, et al. LEF1 in Androgen-Independent Prostate Cancer: Regulation of Androgen Receptor Expression, Prostate Cancer Growth, and Invasion. Cancer Res. 2009 Apr;69(8):3332–8.
190. Nguyen DX, Chiang AC, Zhang XHF, Kim JY, Kris MG, Ladanyi M, et al. WNT/TCF signaling through LEF1 and HOXB9 mediates lung adenocarcinoma metastasis. Cell. 2009 Jul;138(1):51–62.
191. Markowitz SD, Bertagnolli MM. Molecular origins of cancer: Molecular basis of colorectal cancer. N Engl J Med. 2009 Dec;361(25):2449–60.
192. Heino S, Fang S, Lähde M, Högström J, Nassiri S, Campbell A, et al. Lef1 restricts ectopic crypt formation and tumor cell growth in intestinal adenomas. Sci Adv. 2021 Nov;7(47).
193. Wang WJ, Yao Y, Jiang LL, Hu TH, Ma JQ, Liao ZJ, et al. Knockdown of Lymphoid Enhancer factor 1 Inhibits Colon Cancer Progression In vitro and In vivo. PLoS One. 2013 Oct;8(10):e76596.
194. Xiao L, Zhang C, Li X, Jia C, Chen L, Yuan Y, et al. LEF1 Enhances the Progression of Colonic Adenocarcinoma via Remodeling the Cell Motility Associated Structures. Int J Mol Sci. 2021 Oct;22(19):10870.
195. Yang X, Liu H, Ye T, Ye Z. High expression of LEF1 correlates with poor prognosis in solid tumors, but not blood tumors: a meta-analysis. Biosci Rep. 2020 Sep;40(9):BSR20202520.
196. Kühnl A, Gökbuget N, Kaiser M, Schlee C, Stroux A, Burmeister T, et al. Overexpression of LEF1 predicts unfavorable outcome in adult patients with B-precursor acute lymphoblastic leukemia. Blood. 2011 Dec;118(24):6362–7.
197. Simon M, Grandage VL, Linch DC, Khwaja A. Constitutive activation of the Wnt/β-catenin signalling pathway in acute myeloid leukaemia. Oncogene. 2005 Mar;24(14):2410–20.
198. Albano F, Zagaria A, Anelli L, Orsini P, Minervini CF, Impera L, et al. Lymphoid enhancer binding factor-1 (LEF1) expression as a prognostic factor in adult acute promyelocytic leukemia. Oncotarget. 2014 Feb;5(3):649–58.
199. Petropoulos K, Arseni N, Schessl C, Stadler CR, Rawat VPS, Deshpande AJ, et al. A novel role for Lef-1, a central transcription mediator of Wnt signaling, in leukemogenesis. J Exp Med. 2008 Mar;205(3):515–22.
200. Müller-Tidow C, Steffen B, Cauvet T, Tickenbrock L, Ji P, Diederichs S, et al. Translocation Products in Acute Myeloid Leukemia Activate the Wnt Signaling Pathway in Hematopoietic Cells. Mol Cell Biol. 2004 Apr;24(7):2890–904.
201. Metzeler KH, Heilmeier B, Edmaier KE, Rawat VPS, Dufour A, Döhner K, et al. High expression of lymphoid enhancer-binding factor-1 (LEF1) is a novel favorable prognostic factor in cytogenetically normal acute myeloid leukemia. Blood. 2012 Sep;120(10):2118–26.
202. Erdfelder F, Hertweck M, Filipovich A, Uhrmacher S, Kreuzer KA. High lymphoid enhancer-binding factor expression is associated with disease progression and poor prognosis in chronic lymphocytic leukemia. Hematol Rev. 2010;2(1):24–7.

203. Wu W, Zhu H, Fu Y, Shen W, Miao K, Hong M, et al. High LEF1 expression predicts adverse prognosis in chronic lymphocytic leukemia and may be targeted by ethacrynic acid. Oncotarget. 2016 Apr;7(16):21631–43.
204. Baskar S, Kwong KY, Hofer T, Levy JM, Kennedy MG, Lee E, et al. Unique Cell Surface Expression of Receptor Tyrosine Kinase ROR1 in Human B-Cell Chronic Lymphocytic Leukemia. Clinical Cancer Research. 2008 Jan;14(2):396–404.
205. Janovska P, Poppova L, Plevova K, Plesingerova H, Behal M, Kaucka M, et al. Autocrine signaling by Wnt-5a deregulates chemotaxis of leukemic cells and predicts clinical outcome in chronic lymphocytic leukemia. Clin Cancer Res. 2016;22(2):459–69.
206. Poppova L, Janovska P, Plevova K, Radova L, Plesingerova H, Borsky M, et al. Decreased WNT3 expression in chronic lymphocytic leukaemia is a hallmark of disease progression and identifies patients with worse prognosis in the subgroup with mutated IGHV. Br J Haematol. 2016;175(5):851–9.
207. Lütge A, Lu J, Hüllein J, Walther T, Sellner L, Wu B, et al. Subgroup-specific gene expression profiles and mixed epistasis in chronic lymphocytic leukemia. Haematologica. 2023 May;108(10):2664–76.
208. Carbo-Meix A, Guijarro F, Wang L, Grau M, Royo R, Frigola G, et al. BCL3 rearrangements in B-cell lymphoid neoplasms occur in two breakpoint clusters associated with different diseases. Haematologica. 2023 Aug;109(2):493–508.
209. Menter T, Dirnhofer S, Tzankov A. LEF1: A highly specific marker for the diagnosis of chronic lymphocytic B cell leukaemia/small lymphocytic B cell lymphoma. J Clin Pathol. 2015;68(6):473–8.
210. Menter T, Trivedi P, Ahmad R, Flora R, Dirnhofer S, Tzankov A, et al. Diagnostic Utility of Lymphoid Enhancer Binding Factor 1 Immunohistochemistry in Small B-Cell Lymphomas. Am J Clin Pathol. 2017 Mar; 147(3):292-300.
211. Tandon B, Peterson L, Gao J, Nelson B, Ma S, Rosen S, et al. Nuclear overexpression of lymphoid-enhancer-binding factor 1 identifies chronic lymphocytic leukemia/small lymphocytic lymphoma in small B-cell lymphomas. Mod Pathol. 2011 Nov;24(11):1433–43.
212. Ross DA, Kadesch T. The notch intracellular domain can function as a coactivator for LEF-1. Mol Cell Biol. 2001 Nov;21(22):7537–44.
213. Bruhn L, Munnerlyn A, Grosschedl R. ALY, a context-dependent coactivator of LEF-1 and AML-1, is required for TCRalpha enhancer function. Genes Dev. 1997 Mar;11(5):640–53.
214. Gutierrez A, Tschumper R, Shanafelt TD, Eckel-Passow J, Kay NE, Jelinek DF. Aberrant Regulation of the LEF-1 Locus in Monoclonal B Cell Lymphocytosis (MBL) and Chronic Lymphocytic Leukemia (CLL): A Possible Role for Epigenetic Regulation. Blood. 2009 Nov;114(22):669.
215. Liu P, Xu B, Shen W, Zhu H, Wu W, Fu Y, et al. Dysregulation of TNFα-induced necroptotic signaling in chronic lymphocytic leukemia: Suppression of CYLD gene by LEF1. Leukemia. 2012 Jun;26(6):1293–300.
216. Wu W, Zhu H, Fu Y, Shen W, Xu J, Miao K, et al. Clinical significance of down-regulated cylindromatosis gene in chronic lymphocytic leukemia. Leuk Lymphoma. 2014 Mar;55(3):588–94.
217. Mathis B, Lai Y, Qu C, Janicki J, Cui T. CYLD-Mediated Signaling and Diseases. Curr Drug Targets. 2015 Apr;16(4):284–94.
218. Bertilaccio MTS, Scielzo C, Simonetti G, Ten Hacken E, Apollonio B, Ghia P, et al. Xenograft models of chronic lymphocytic leukemia: Problems, pitfalls and future directions. Leukemia. 2013 Mar;27(3):534–40.
219. ten Hacken E, Wu CJ. Understanding CLL biology through mouse models of human genetics. Blood. 2021 Dec;138(25):2621–31.
220. Hertlein E, Beckwith KA, Lozanski G, Chen TL, Towns WH, Johnson AJ, et al. Characterization of a New Chronic Lymphocytic Leukemia Cell Line for Mechanistic In vitro and In vivo Studies Relevant to Disease. PLoS One. 2013 Oct;8(10):e76607.

221. Wendel-Hansen V, Sällström J, De Campos-Lima PO, Kjellström G, Sandlund A, Siegbahn A, et al. Epstein-Barr virus (EBV) can immortalize B-cll cells activated by cytokines. Leukemia. 1994 Mar;8(3):476–84.
222. Teramoto N, Gogolák P, Nagy N, Maeda A, Kvarnung K, Björkholm T, et al. Epstein-Barr virus-infected B-chronic lymphocyte leukemia cells express the virally encoded nuclear proteins but they do not enter the cell cycle. J Hum Virol. 2000 May-Jun;3(3):125–36.
223. Doyle MG, Catovsky D, Crawford DH. Infection of leukaemic B lymphocytes by Epstein Barr virus. Leukemia. 1993 Nov;7(11):1858–64.
224. Takada K, Yamamoto K, Osato T. Analysis of the Transformation of Human Lymphocytes by Epstein-Barr Virus. Intervirology. 1980;13(4):223–31.
225. Maeda A, Bandobashi K, Nagy N, Teramoto N, Gogolák P, Pokrovskaja K, et al. Epstein-barr virus can infect B-chronic lymphocytic leukemia cells but it does not orchestrate the cell cycle regulatory proteins. J Hum Virol. 2001;4(5):227–37.
226. Klein E, Nagy N. Restricted expression of EBV encoded proteins in in vitro infected CLL cells. Semin Cancer Biol. 2010 Dec; 20(6):410–5.
227. Klein E, Nagy N, Rasul AE. EBV genome carrying B lymphocytes that express the nuclear protein EBNA-2 but not LMP-1 Type IIb latency. Oncoimmunology. 2013 Feb;2(2):e23035.
228. Lanemo Myhrinder A, Hellqvist E, Bergh AC, Jansson M, Nilsson K, Hultman P, et al. Molecular characterization of neoplastic and normal "sister" lymphoblastoid B-cell lines from chronic lymphocytic leukemia. Leuk Lymphoma. 2013 Aug;54(8):1769–79.
229. Caligaris-Cappio F, Bergui L, Rege-Cambrin G, Tesio L, Migone N, Malavasi F. Phenotypic, cytogenetic and molecular characterization of a new B-chronic lymphocytic leukaemia (B-CLL) cell line. Leuk Res. 1987 Jan;11(7):579–88.
230. Stacchini A, Aragno M, Vallario A, Alfarano A, Circosta P, Gottardi D, et al. MEC1 and MEC2: two new cell lines derived from B-chronic lymphocytic leukaemia in prolymphocytoid transformation. Leuk Res. 1999 Feb;23(2):127-36.
231. Bichi R, Shinton SA, Martin ES, Koval A, Calin GA, Cesari R, et al. Human chronic lymphocytic leukemia modeled in mouse by targeted TCL1 expression. Proc Natl Acad Sci U S A. 2002 May;99(10):6955-60.
232. Herling M, Patel KA, Khalili J, Schlette E, Kobayashi R, Medeiros LJ, et al. TCL1 shows a regulated expression pattern in chronic lymphocytic leukemia that correlates with molecular subtypes and proliferative state. Leukemia. 2006 Feb;20(2):280–5.
233. Pekarsky Y, Palamarchuk A, Maximov V, Efanov A, Nazaryan N, Santanam U, et al. Tcl1 functions as a transcriptional regulator and is directly involved in the pathogenesis of CLL. Proc Natl Acad Sci U S A. 2008 Dec;105(50):19643–8.
234. Gaudio E, Spizzo R, Paduano F, Luo Z, Efanov A, Palamarchuk A, et al. Tcl1 interacts with Atm and enhances NF-κB activation in hematologic malignancies. Blood. 2012 Jan 5;119(1):180–7.
235. Simonetti G, Bertilaccio MTS, Ghia P, Klein U. Mouse models in the study of chronic lymphocytic leukemia pathogenesis and therapy. Blood. 2014 Aug; 124(7):1010–9.
236. Yin S, Gambe RG, Sun J, Martinez AZ, Cartun ZJ, Regis FFD, et al. A Murine Model of Chronic Lymphocytic Leukemia Based on B Cell-Restricted Expression of Sf3b1 Mutation and Atm Deletion. Cancer Cell. 2019 Feb;35(2):283-296.e5.
237. Lazarian G, Yin S, ten Hacken E, Sewastianik T, Uduman M, Font-Tello A, et al. A hotspot mutation in transcription factor IKZF3 drives B cell neoplasia via transcriptional dysregulation. Cancer Cell. 2021 Mar;39(3):380-393.e8.
238. Gutierrez C, Ouspenskaia T, Fu D, Waddicor P, Biran A, Liani A, et al. RPS15 and TP53 Co-Mutation Drives B Cell Malignancy through Altered Translation and MYC Activation in a Murine Model. Blood. 2020 Nov ;136(Supplement 1):28–9.
239. Greiner DL, Shultz LD, Yates J, Appel MC, Perdrizet G, Hesselton RM, et al. Improved Engraftment of Human Spleen Cells in NOD/LtSz-scid/scid Mice as Compared with C.B-1 7-scid/scid Mice. Am J Pathol. 1995 Apr;146(4);888-902.

240. Ito M, Hiramatsu H, Kobayashi K, Suzue K, Kawahata M, Hioki K, et al. NOD/SCID/γcnull mouse: An excellent recipient mouse model for engraftment of human cells. Blood. 2002 Nov;100(9):3175–82.
241. Dürig J, Ebeling P, Grabellus F, Sorg UR, Möllmann M, Schütt P, et al. A novel nonobese diabetic/severe combined immunodeficient xenograft model for chronic lymphocytic leukemia reflects important clinical characteristics of the disease. Cancer Res. 2007 Sep;67(18):8653–61.
242. Bagnara D, Kaufman MS, Calissano C, Marsilio S, Patten PEM, Simone R, et al. A novel adoptive transfer model of chronic lymphocytic leukemia suggests a key role for T lymphocytes in the disease. Blood. 2011 May;117(20):5463–72.
243. Herman SEM, Sun X, McAuley EM, Hsieh MM, Pittaluga S, Raffeld M, et al. Modeling tumor-host interactions of chronic lymphocytic leukemia in xenografted mice to study tumor biology and evaluate targeted therapy. Leukemia. 2013 Dec;27(12):2311–21.
244. Burger JA. Nurture versus Nature: The Microenvironment in Chronic Lymphocytic Leukemia. Hematology. 2011 Dec;2011(1):96–103.
245. Herman SEM, Wiestner A. Preclinical modeling of novel therapeutics in chronic lymphocytic leukemia: the tools of the trade. Semin Oncol. 2016 Apr;43(2):222–32.
246. Panayiotidis P, Jones D, Ganeshaguru K, Foroni L, Hoffbrand A V. Human bone marrow stromal cells prevent apoptosis and support the survival of chronic lymphocytic leukaemia cells in vitro. Br J Haematol. 1996;92(1):97–103.
247. Zupo S, Isnardi L, Megna M, Massara R, Malavasi F, Dono M, et al. CD38 expression distinguishes two groups of B-cell chronic lymphocytic leukemias with different responses to anti-IgM antibodies and propensity to apoptosis. Blood. 1996 Aug;88(4):1365–74.
248. Bernal A, Pastore RD, Asgary Z, Keller SA, Cesarman E, Liou HC, et al. Survival of leukemic B cells promoted by engagement of the antigen receptor. Blood. 2001 Nov;98(10):3050–7.
249. Guarini A, Chiaretti S, Tavolaro S, Maggio R, Peragine N, Citarella F, et al. BCR ligation induced by IgM stimulation results in gene expression and functional changes only in IgVH unmutated chronic lymphocytic leukemia (CLL) cells. Blood. 2008 Aug;112(3):782–92.
250. Jahrsdorfer B, Blackwell S, Weiner G. The effects of CpG ODN on CLL proliferation, apoptosis or phenotype could have an impact on its clinical utility. Leukemia. 2007 Nov;21(11):2354–5.
251. Chatzouli M, Ntoufa S, Papakonstantinou N, Chartomatsidou E, Anagnostopoulos A, Kollia P, et al. Heterogeneous Functional Effects of Concomitant B Cell Receptor and TLR Stimulation in Chronic Lymphocytic Leukemia with Mutated versus Unmutated Ig Genes. J Immunol. 2014 May;192(10):4518–24.
252. Hoferkova E, Kadakova S, Mraz M. In vitro and In vivo Models of CLL–T Cell Interactions: Implications for Drug Testing. Cancers (Basel). 2022 Jul;14(13):3087.
253. Ahearne MJ, Willimott S, Piñon L, Kennedy DB, Miall F, Dyer MJS, et al. Enhancement of CD154/IL4 proliferation by the T follicular helper (Tfh) cytokine, IL21 and increased numbers of circulating cells resembling Tfh cells in chronic lymphocytic leukaemia. Br J Haematol. 2013 Aug;162(3):360–70.
254. Long M, Beckwith K, Do P, Mundy BL, Gordon A, Lehman AM, et al. Ibrutinib treatment improves T cell number and function in CLL patients. Journal of Clinical Investigation. 2017 Aug;127(8):3052–64.
255. Ghamlouch H, Darwiche W, Hodroge A, Ouled-Haddou H, Dupont S, Singh AR, et al. Factors involved in CLL pathogenesis and cell survival are disrupted by differentiation of CLL B-cells into antibody-secreting cells. Oncotarget. 2015 Jul;6(21):18484–503.
256. Gricks CS, Zahrieh D, Zauls AJ, Gorgun G, Drandi D, Mauerer K, et al. Differential regulation of gene expression following CD40 activation of leukemic compared to healthy B cells. Blood. 2004 Dec;104(13):4002–9.
257. Néron S, Nadeau PJ, Darveau A, Leblanc JF. Tuning of CD40–CD154 Interactions in Human B-Lymphocyte Activation: A Broad Array of In vitro Models for a Complex In vivo Situation. Arch Immunol Ther Exp (Warsz). 2011 Feb 14;59(1):25–40.

258. Dancescu M, Rubio-Trujillo M, Biron G, Bron D, Delespesse G, Sarfati M. Interleukin 4 protects chronic lymphocytic leukemic B cells from death by apoptosis and upregulates Bcl-2 expression. J Exp Med. 1992 Nov;176(5):1319–26.
259. Willimott S, Baou M, Naresh K, Wagner SD. CD154 induces a switch in pro-survival Bcl-2 family members in chronic lymphocytic leukaemia. Br J Haematol. 2007 Sep;138(6):721–32.
260. Hamilton E, Pearce L, Morgan L, Robinson S, Ware V, Brennan P, et al. Mimicking the tumour microenvironment: Three different co-culture systems induce a similar phenotype but distinct proliferative signals in primary chronic lymphocytic leukaemia cells. Br J Haematol. 2012 Sep;158(5):589–99.
261. Tromp JM, Tonino SH, Elias JA, Jaspers A, Luijks DM, Kater AP, et al. Dichotomy in NF-B signaling and chemoresistance in immunoglobulin variable heavy-chain-mutated versus unmutated CLL cells upon CD40/TLR9 triggering. Oncogene. 2010 Sep;29(36):5071–82.
262. Schleiss C, Ilias W, Tahar O, Güler Y, Miguet L, Mayeur-Rousse C, et al. BCR-associated factors driving chronic lymphocytic leukemia cells proliferation ex vivo. Sci Rep. 2019 Jan;9(1):701.
263. Pascutti MF, Jak M, Tromp JM, Derks IAM, Remmerswaal EBM, Thijssen R, et al. IL-21 and CD40L signals from autologous T cells can induce antigen-independent proliferation of CLL cells. Blood. 2013 Oct;122(17):3010–9.
264. de Totero D, Capaia M, Fabbi M, Croce M, Meazza R, Cutrona G, et al. Heterogeneous expression and function of IL-21R and susceptibility to IL-21-mediated apoptosis in follicular lymphoma cells. Exp Hematol. 2010 May;38(5):373–83.
265. Caeser R, Di Re M, Krupka JA, Gao J, Lara-Chica M, Dias JML, et al. Genetic modification of primary human B cells to model high-grade lymphoma. Nat Commun. 2019 Oct;10(1):4543.
266. Mangolini M, Maiques-Diaz A, Charalampopoulou S, Gerhard-Hartmann E, Bloehdorn J, Moore A, et al. Viral transduction of primary human lymphoma B cells reveals mechanisms of NOTCH-mediated immune escape. Nat Commun. 2022 Oct 1;13(1):6220.
267. Seiffert M, Stilgenbauer S, Döhner H, Lichter P. Efficient nucleofection of primary human B cells and B-CLL cells induces apoptosis, which depends on the microenvironment and on the structure of transfected nucleic acids. Leukemia. 2007 Sep;21(9):1977–83.
268. Liu N, Hargreaves V V., Zhu Q, Kurland J V., Hong J, Kim W, et al. Direct Promoter Repression by BCL11A Controls the Fetal to Adult Hemoglobin Switch. Cell. 2018 Apr;173(2):430-442.e17.
269. Zhu Q, Liu N, Orkin SH, Yuan GC. CUT&RUNTools: a flexible pipeline for CUT&RUN processing and footprint analysis. Genome Biol. 2019 Sep;20(1):192.
270. Bailey TL, Machanick P. Inferring direct DNA binding from ChIP-seq. Nucleic Acids Res. 2012 Sep;40(17):e128.
271. Yu G, Wang LG, He QY. ChIPseeker: an R/Bioconductor package for ChIP peak annotation, comparison and visualization. Bioinformatics. 2015 Jul;31(14):2382–3.
272. Liberzon A, Birger C, Thorvaldsdóttir H, Ghandi M, Mesirov JP, Tamayo P. The Molecular Signatures Database (MSigDB) hallmark gene set collection. Cell Syst. 2015 Dec;1(6):417–25.
273. Pliatsika V, Rigoutsos I. "Off-Spotter": very fast and exhaustive enumeration of genomic lookalikes for designing CRISPR/Cas guide RNAs. Biol Direct. 2015;10(1):4.
274. Mateos-Jaimez J, Mangolini M, Vidal A, Kulis M, Colomer D, Campo E, et al. Robust CRISPR-Cas9 Genetic Editing of Primary Chronic Lymphocytic Leukemia and Mantle Cell Lymphoma Cells. Hemasphere. 2023 Jun;7(6):e909.
275. Wu CM, Roth TL, Baglaenko Y, Ferri DM, Brauer P, Zuniga-Pflucker JC, et al. Genetic engineering in primary human B cells with CRISPR-Cas9 ribonucleoproteins. J Immunol Methods. 2018 Jun;457:33–40.
276. Brinkman EK, Chen T, Amendola M, Van Steensel B. Easy quantitative assessment of genome editing by sequence trace decomposition. Nucleic Acids Res. 2014 Dec; 42(22):e168.
277. Wickham H. ggplot2: Elegant Graphics for Data Analysis. New York: Springer International Publishing; 2016.
278. Hothorn T, Zeileis A. Generalized maximally selected statistics. Biometrics. 2008 Dec;64(4):1263–9.

279. Therneau TM, Grambsch PM. Modeling Survival Data: Extending the Cox Model. New York: Springer International Publishing; 2000.
280. Kopylova E, Noé L, Touzet H. SortMeRNA: fast and accurate filtering of ribosomal RNAs in metatranscriptomic data. Bioinformatics. 2012 Dec;28(24):3211–7.
281. Bolger AM, Lohse M, Usadel B. Trimmomatic: a flexible trimmer for Illumina sequence data. Bioinformatics. 2014 Aug;30(15):2114–20.
282. Bray NL, Pimentel H, Melsted P, Pachter L. Near-optimal probabilistic RNA-seq quantification. Nat Biotechnol. 2016 May;34(5):525–7.
283. Love MI, Huber W, Anders S. Moderated estimation of fold change and dispersion for RNA-seq data with DESeq2. Genome Biol. 2014 Dec;15(12):550.
284. Zhu A, Ibrahim JG, Love MI. Heavy-tailed prior distributions for sequence count data: removing the noise and preserving large differences. Bioinformatics. 2019 Jun;35(12):2084–92.
285. Gu Z, Eils R, Schlesner M. Complex heatmaps reveal patterns and correlations in multidimensional genomic data. Bioinformatics. 2016 Sep;32(18):2847–9.
286. Subramanian A, Kuehn H, Gould J, Tamayo P, Mesirov JP. GSEA-P: a desktop application for Gene Set Enrichment Analysis. Bioinformatics. 2007 Dec;23(23):3251–3.
287. Chiva C, Olivella R, Borràs E, Espadas G, Pastor O, Solé A, et al. QCloud: A cloud-based quality control system for mass spectrometry-based proteomics laboratories. PLoS One. 2018;13(1):e0189209.
288. Perkins DN, Pappin DJ, Creasy DM, Cottrell JS. Probability-based protein identification by searching sequence databases using mass spectrometry data. Electrophoresis. 1999 Dec;20(18):3551–67.
289. Beer LA, Liu P, Ky B, Barnhart KT, Speicher DW. Efficient Quantitative Comparisons of Plasma Proteomes Using Label-Free Analysis with MaxQuant. Methods Mol Biol. 2017;1619:339-52.
290. MacLean B, Tomazela DM, Shulman N, Chambers M, Finney GL, Frewen B, et al. Skyline: an open source document editor for creating and analyzing targeted proteomics experiments. Bioinformatics. 2010 Apr;26(7):966–8.
291. Szklarczyk D, Gable AL, Nastou KC, Lyon D, Kirsch R, Pyysalo S, et al. The STRING database in 2021: customizable protein-protein networks, and functional characterization of user-uploaded gene/measurement sets. Nucleic Acids Res. 2021 Jan;49(D1):D605–12.
292. Lambert SA, Jolma A, Campitelli LF, Das PK, Yin Y, Albu M, et al. The Human Transcription Factors. Cell. 2018 Feb;172(4):650–65.
293. Vaquerizas JM, Kummerfeld SK, Teichmann SA, Luscombe NM. A census of human transcription factors: function, expression and evolution. Nat Rev Genet. 2009 Apr;10(4):252–63.
294. Wingender E, Schoeps T, Haubrock M, Dönitz J. TFClass: a classification of human transcription factors and their rodent orthologs. Nucleic Acids Res. 2015 Jan 28;43(D1):D97–102.
295. Weirauch MT, Yang A, Albu M, Cote AG, Montenegro-Montero A, Drewe P, et al. Determination and Inference of Eukaryotic Transcription Factor Sequence Specificity. Cell. 2014 Sep;158(6):1431–43.
296. Pasikowska M, Walsby E, Apollonio B, Cuthill K, Phillips E, Coulter E, et al. Phenotype and immune function of lymph node and peripheral blood CLL cells are linked to transendothelial migration. Blood. 2016 Jul;128(4):563–73.
297. Saba NS, Liu D, Herman SEM, Underbayev C, Tian X, Behrend D, et al. Pathogenic role of B-cell receptor signaling and canonical NF-κB activation in mantle cell lymphoma. Blood. 2016 Jul;128(1):82–92.
298. Herishanu Y, Pérez-Galán P, Liu D, Biancotto A, Pittaluga S, Vire B, et al. The lymph node microenvironment promotes B-cell receptor signaling, NF-κB activation, and tumor proliferation in chronic lymphocytic leukemia. Blood. 2011 Jan 13;117(2):563–74.
299. Asmamaw M, Zawdie B. Mechanism and Applications of CRISPR/Cas-9-Mediated Genome Editing. Biologics. 2021 Aug;15:353–61.

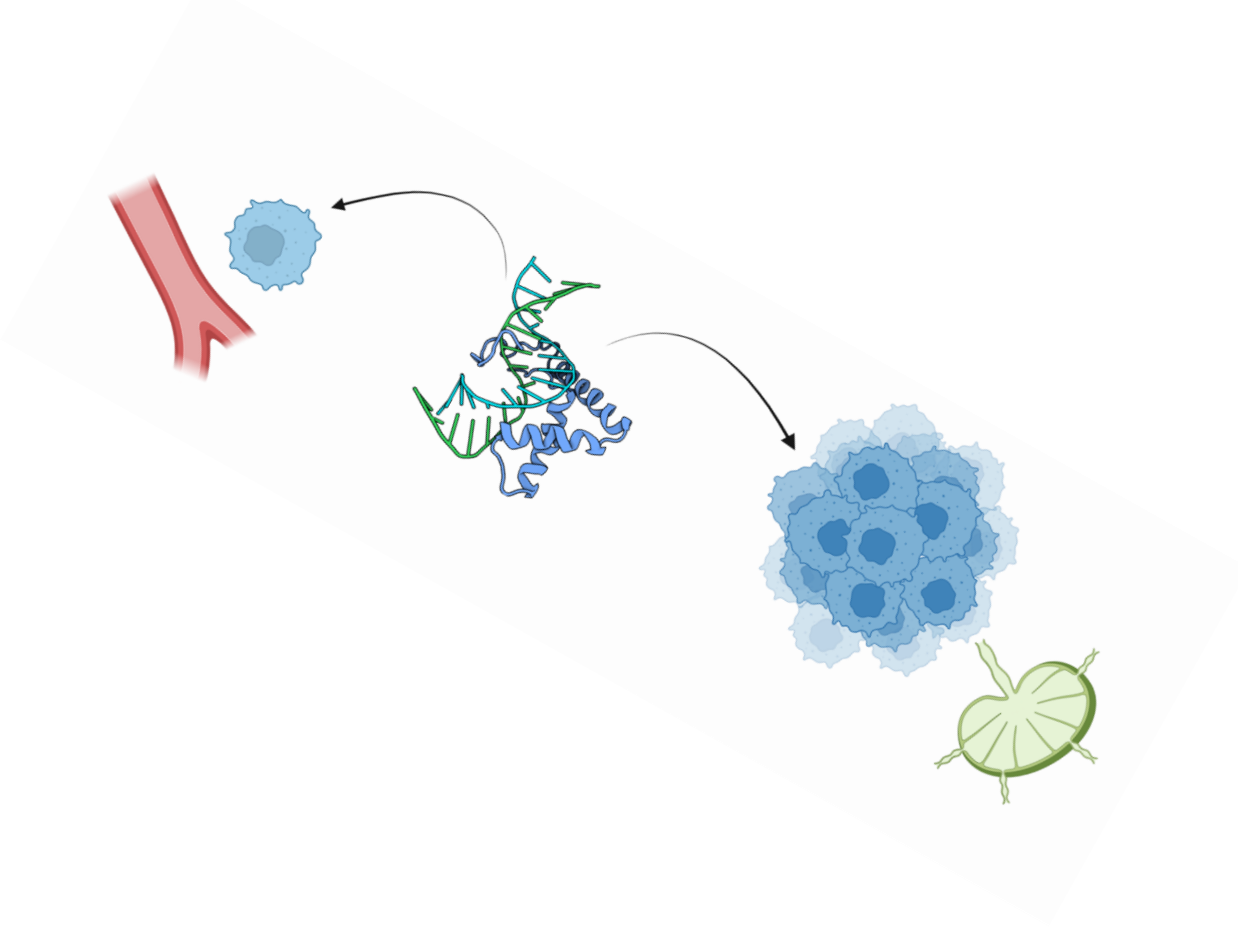
300. Giuliano CJ, Lin A, Girish V, Sheltzer JM. Generating Single Cell-Derived Knockout Clones in Mammalian Cells with CRISPR/Cas9. Curr Protoc Mol Biol. 2019 Sep;128(1):e100.
301. Nuñez JK, Chen J, Pommier GC, Cogan JZ, Replogle JM, Adriaens C, et al. Genome-wide programmable transcriptional memory by CRISPR-based epigenome editing. Cell. 2021 Apr;184(9):2503-2519.e17.
302. Qi LS, Larson MH, Gilbert LA, Doudna JA, Weissman JS, Arkin AP, et al. Repurposing CRISPR as an RNA-Guided Platform for Sequence-Specific Control of Gene Expression. Cell. 2013 Feb;152(5):1173–83.
303. Gilbert LA, Larson MH, Morsut L, Liu Z, Brar GA, Torres SE, et al. CRISPR-Mediated Modular RNA-Guided Regulation of Transcription in Eukaryotes. Cell. 2013 Jul;154(2):442–51.
304. Müller-Kuller U, Ackermann M, Kolodziej S, Brendel C, Fritsch J, Lachmann N, et al. A minimal ubiquitous chromatin opening element (UCOE) effectively prevents silencing of juxtaposed heterologous promoters by epigenetic remodeling in multipotent and pluripotent stem cells. Nucleic Acids Res. 2015 Feb;43(3):1577–92.
305. Williams S, Mustoe T, Mulcahy T, Griffiths M, Simpson D, Antoniou M, et al. CpG-island fragments from the HNRPA2B1/CBX3 genomic locus reduce silencing and enhance transgene expression from the hCMV promoter/enhancer in mammalian cells. BMC Biotechnol. 2005 Jun 3;5:17.
306. Sizer RE, White RJ. Use of ubiquitous chromatin opening elements (UCOE) as tools to maintain transgene expression in biotechnology. Comput Struct Biotechnol J. 2022 Dec;21:275–83.
307. Zhang F, Thornhill SI, Howe SJ, Ulaganathan M, Schambach A, Sinclair J, et al. Lentiviral vectors containing an enhancer-less ubiquitously acting chromatin opening element (UCOE) provide highly reproducible and stable transgene expression in hematopoietic cells. Blood. 2007 Sep;110(5):1448–57.
308. Alerasool N, Segal D, Lee H, Taipale M. An efficient KRAB domain for CRISPRi applications in human cells. Nat Methods. 2020 Nov;17(11):1093–6.
309. Klann TS, Black JB, Chellappan M, Safi A, Song L, Hilton IB, et al. CRISPR–Cas9 epigenome editing enables high-throughput screening for functional regulatory elements in the human genome. Nat Biotechnol. 2017 Jun 3;35(6):561–8.
310. Qin JY, Zhang L, Clift KL, Hulur I, Xiang AP, Ren BZ, et al. Systematic Comparison of Constitutive Promoters and the Doxycycline-Inducible Promoter. PLoS One. 2010 May;5(5):e10611.
311. Weintraub AS, Li CH, Zamudio A V., Sigova AA, Hannett NM, Day DS, et al. YY1 Is a Structural Regulator of Enhancer-Promoter Loops. Cell. 2017 Dec;171(7):1573-1588.e28.
312. Puente XS, Jares P, Campo E. Chronic lymphocytic leukemia and mantle cell lymphoma: crossroads of genetic and microenvironment interactions. Blood. 2018 May;131(21):2283–96.
313. Jordan ET, Collins M, Terefe J, Ugozzoli L, Rubio T. Optimizing electroporation conditions in primary and other difficult-to-transfect cells. J Biomol Tech. 2008 Dec;19(5):328–34.
314. Igawa T, Sato Y, Takata K, Fushimi S, Tamura M, Nakamura N, et al. Cyclin D2 is overexpressed in proliferation centers of chronic lymphocytic leukemia/small lymphocytic lymphoma. Cancer Sci. 2011 Nov;102(11):2103–7.
315. Decker T, Schneller F, Hipp S, Miething C, Jahn T, Duyster J, et al. Cell cycle progression of chronic lymphocytic leukemia cells is controlled by cyclin D2, cyclin D3, cyclin-dependent kinase (cdk) 4 and the cdk inhibitor p27. Leukemia. 2002 Mar;16(3):327–34.
316. Jelinek DF, Tschumper RC, Stolovitzky GA, Iturria SJ, Tu Y, Lepre J, et al. Identification of a global gene expression signature of B-chronic lymphocytic leukemia. Mol Cancer Res. 2003 Mar;1(5):346–61.
317. Lei H, Wang J, Hu J, Zhu Q, Wu Y. Deubiquitinases in hematological malignancies. Biomark Res. 2021 Aug;9(1):66.
318. Wang Y, Mao A, Liu J, Li P, Zheng S, Tong T, et al. USP10 strikes down β-catenin by dual-wielding deubiquitinase activity and phase separation potential. Cell Chem Biol. 2023 Nov;30(11):1436-1452.e10.

319. Guo K, Ma Z, Zhang Y, Han L, Shao C, Feng Y, et al. HDAC7 promotes NSCLC proliferation and metastasis via stabilization by deubiquitinase USP10 and activation of β-catenin-FGF18 pathway. J Exp Clin Cancer Res. 2022 Mar;41(1):91.
320. Yang JR, Lu YB, Su HX, Xiao Y, Pan Q, Su F, et al. USP10 promotes the progression of triple-negative breast cancer by enhancing the stability of TCF4 protein. Biochem Pharmacol. 2023 Dec;218:115864.
321. Mellacheruvu D, Wright Z, Couzens AL, Lambert JP, St-Denis NA, Li T, et al. The CRAPome: a contaminant repository for affinity purification–mass spectrometry data. Nat Methods. 2013 Aug;10(8):730–6.
322. Ajuh P, Kuster B, Panov K, Zomerdijk JC, Mann M, Lamond AI. Functional analysis of the human CDC5L complex and identification of its components by mass spectrometry. EMBO J. 2000 Dec;19(23):6569–81.
323. Boudrez A, Beullens M, Groenen P, Van Eynde A, Vulsteke V, Jagiello I, et al. NIPP1-mediated interaction of protein phosphatase-1 with CDC5L, a regulator of pre-mRNA splicing and mitotic entry. J Biol Chem. 2000 Aug;275(33):25411–7.
324. Mu R, Wang YB, Wu M, Yang Y, Song W, Li T, et al. Depletion of pre-mRNA splicing factor Cdc5L inhibits mitotic progression and triggers mitotic catastrophe. Cell Death Dis. 2014 Mar;5(3):e1151.
325. Herbst SA, Vesterlund M, Helmboldt AJ, Jafari R, Siavelis I, Stahl M, et al. Proteogenomics refines the molecular classification of chronic lymphocytic leukemia. Nat Commun. 2022 Oct;13(1):6226.
326. Wang SH, Nan KJ, Wang YC, Wang WJ, Tian T. The balance between two isoforms of LEF-1 regulates colon carcinoma growth. BMC Gastroenterol. 2012 May;12:53.
327. Jesse S, Koenig A, Ellenrieder V, Menke A. Lef-1 isoforms regulate different target genes and reduce cellular adhesion. Int J Cancer. 2010;126(5):1109–20.
328. García-Corzo L, Calatayud-Baselga I, Casares-Crespo L, Mora-Martínez C, Julián Escribano-Saiz J, Hortigüela R, et al. The transcription factor LEF1 interacts with NFIX and switches isoforms during adult hippocampal neural stem cell quiescence. Front Cell Dev Biol. 2022 Jul;10:912319.
329. Mallory MJ, Jackson J, Weber B, Chi A, Heyd F, Lynch KW. Signal- and Development-Dependent Alternative Splicing of LEF1 in T Cells Is Controlled by CELF2. Mol Cell Biol. 2011 Jun;31(11):2184–95.
330. Nagalski A, Irimia M, Szewczyk L, Ferran JL, Misztal K, Kuznicki J, et al. Postnatal isoform switch and protein localization of LEF1 and TCF7L2 transcription factors in cortical, thalamic, and mesencephalic regions of the adult mouse brain. Brain Struct Funct. 2013 Nov;218(6):1531–49.
331. Eagle GL, Zhuang J, Jenkins RE, Till KJ, Jithesh P V, Lin K, et al. Total proteome analysis identifies migration defects as a major pathogenetic factor in immunoglobulin heavy chain variable region (IGHV)-unmutated chronic lymphocytic leukemia. Mol Cell Proteomics. 2015 Apr;14(4):933–45.
332. Cuesta-Mateos C, Brown JR, Terrón F, Muñoz-Calleja C. Of Lymph Nodes and CLL Cells: Deciphering the Role of CCR7 in the Pathogenesis of CLL and Understanding Its Potential as Therapeutic Target. Front Immunol. 2021 Mar;12:662866.
333. Playa-Albinyana H, Arenas F, Royo R, Giró A, López-Oreja I, Aymerich M, et al. Chronic lymphocytic leukemia patient-derived xenografts recapitulate clonal evolution to Richter transformation. Leukemia. 2024 Mar;38(3):557–69.
334. Vaisitti T, Braggio E, Allan JN, Arruga F, Serra S, Zamò A, et al. Novel Richter Syndrome Xenograft Models to Study Genetic Architecture, Biology, and Therapy Responses. Cancer Res. 2018 Jul;78(13):3413–20.
335. Stevenson FK, Forconi F, Kipps TJ. Exploring the pathways to chronic lymphocytic leukemia. Blood. 2021 Sep;138(10):827–35.
336. Haselager M V, van Driel BF, Perelaer E, de Rooij D, Lashgari D, Loos R, et al. In vitro 3D Spheroid Culture System Displays Sustained T Cell-dependent CLL Proliferation and Survival. Hemasphere. 2023 Sep;7(9):e938.

337. Machado HE, Mitchell E, Øbro NF, Kübler K, Davies M, Leongamornlert D, et al. Diverse mutational landscapes in human lymphocytes. Nature. 2022 Aug;608(7924):724–32.
338. Sweeney NP, Vink CA. The impact of lentiviral vector genome size and producer cell genomic to gag-pol mRNA ratios on packaging efficiency and titre. Mol Ther Methods Clin Dev. 2021 Apr;21:574–84.
339. Quijada-Álamo M, Hernández-Sánchez M, Alonso-Pérez V, Rodríguez-Vicente AE, García-Tuñón I, Martín-Izquierdo M, et al. CRISPR/Cas9-generated models uncover therapeutic vulnerabilities of del(11q) CLL cells to dual BCR and PARP inhibition. Leukemia. 2020 Jun;34(6):1599–612.
340. Hernández-Sánchez M. CRISPR/Cas9 in Chronic Lymphocytic Leukemia. Encyclopedia. 2022 May;2(2):928–36.
341. Stevenson FK, Krysov S, Davies AJ, Steele AJ, Packham G. B-cell receptor signaling in chronic lymphocytic leukemia. Blood. 2011 Oct;118(16):4313–20.
342. Gutierrez A, Arendt BK, Tschumper RC, Kay NE, Zent CS. Differentiation of Chronic Lymphocytic Leukemia B Cells into Immunoglobulin Secreting Cells Decreases LEF-1 Expression. PLoS One. 2011;6(10):26056.
343. Zhang H, Liu T, Zhang Z, Payne SH, Zhang B, McDermott JE, et al. Integrated Proteogenomic Characterization of Human High-Grade Serous Ovarian Cancer. Cell. 2016 Jul;166(3):755–65.
344. Johansson HJ, Socciarelli F, Vacanti NM, Haugen MH, Zhu Y, Siavelis I, et al. Breast cancer quantitative proteome and proteogenomic landscape. Nat Commun. 2019 Apr;10(1):1600.
345. Gandhirajan RK, Staib PA, Minke K, Gehrke I, Plickert G, Schlösser A, et al. Small molecule inhibitors of Wnt/β-Catenin/Lef-1 Signaling induces apoptosis in chronic lymphocytic leukemia cells in vitro and in vivo. Neoplasia. 2010;12(4):326–35.
346. Stamos JL, Weis WI. The β-catenin destruction complex. Cold Spring Harb Perspect Biol. 2013 Jan;5(1):a007898.
347. Grumolato L, Liu G, Haremaki T, Mungamuri SK, Mong P, Akiri G, et al. β-Catenin-Independent Activation of TCF1/LEF1 in Human Hematopoietic Tumor Cells through Interaction with ATF2 Transcription Factors. PLoS Genet. 2013 Aug;9(8):e1003603.
348. Zhou F, Zhang L, Gong K, Lu G, Sheng B, Wang A, et al. LEF-1 activates the transcription of E2F1. Biochem Biophys Res Commun. 2008 Jan;365(1):149–53.
349. Gu Z, Zhang H, Li Y, Shen S, Yin X, Zhang W, et al. CDC5L drives FAH expression to promote metabolic reprogramming in melanoma. Oncotarget. 2017 Dec;8(69):114328–43.
350. Martin JW, Chilton-MacNeill S, Koti M, van Wijnen AJ, Squire JA, Zielenska M. Digital expression profiling identifies RUNX2, CDC5L, MDM2, RECQL4, and CDK4 as potential predictive biomarkers for neo-adjuvant chemotherapy response in paediatric osteosarcoma. PLoS One. 2014;9(5):e95843.
351. Lu XY, Lu Y, Zhao YJ, Jaeweon K, Kang J, Xiao-Nan L, et al. Cell cycle regulator gene CDC5L, a potential target for 6p12-p21 amplicon in osteosarcoma. Mol Cancer Res. 2008 Jun;6(6):937–46.
352. Li J, Zhang N, Zhang R, Sun L, Yu W, Guo W, et al. CDC5L Promotes hTERT Expression and Colorectal Tumor Growth. Cell Physiol Biochem. 2017;41(6):2475–88.
353. Oksuz O, Henninger JE, Warneford-Thomson R, Zheng MM, Erb H, Vancura A, et al. Transcription factors interact with RNA to regulate genes. Mol Cell. 2023;83(14):2449-63.e13.
354. Li TWH, Ting JHT, Yokoyama NN, Bernstein A, van de Wetering M, Waterman ML. Wnt Activation and Alternative Promoter Repression of LEF1 in Colon Cancer. Mol Cell Biol. 2006 Jul;26(14):5284–99.
355. Ghogomu SM, van Venrooy S, Ritthaler M, Wedlich D, Gradl D. HIC-5 Is a Novel Repressor of Lymphoid Enhancer Factor/T-cell Factor-driven Transcription. J Biol Chem. 2006 Jan;281(3):1755–64.
356. Ajith S, Gazzara MR, Cole BS, Shankarling G, Martinez NM, Mallory MJ, et al. Position-dependent activity of CELF2 in the regulation of splicing and implications for signal-responsive regulation in T cells. RNA Biol. 2016 Jun;13(6):569–81.

357. Mallory MJ, Allon SJ, Qiu J, Gazzara MR, Tapescu I, Martinez NM, et al. Induced transcription and stability of CELF2 mRNA drives widespread alternative splicing during T-cell signaling. Proc Natl Acad Sci U S A. 2015 Apr;112(17):E2139-48.
358. Deaglio S, Malavasi F. Chronic lymphocytic leukemia microenvironment: shifting the balance from apoptosis to proliferation. Haematologica. 2009 Jun;94(6):752–6.
359. Datta N, Chakraborty S, Basu M, Ghosh MK. Tumor Suppressors Having Oncogenic Functions: The Double Agents. Cells. 2020 Dec;10(1):46.
360. Aster JC, Pear WS, Blacklow SC. The Varied Roles of Notch in Cancer. Annu Rev Pathol. 2017 Jan;12(1):245–75.
361. Zhao H, Wei J, Sun J. Roles of TGF-β signaling pathway in tumor microenvironment and cancer therapy. Int Immunopharmacol. 2020 Dec;89(Pt B):107101.
362. Papageorgis P. TGF-β Signaling in Tumor Initiation, Epithelial-to-Mesenchymal Transition, and Metastasis. J Oncol. 2015 Mar;2015:587193.

Appendix



A

CLL case	IGHV status	IGHV % identity to germline	IGHV gene	Gender	Age at diagnosis	Color in figures
1	MUT	97.25	IGHV4-61	M	45	
2	MUT	89.58	IGHV3-30	M	60	
3	MUT	93.87	IGHV3-49	M	58	
4	MUT	97.19	IGHV4-34	F	64	
5	MUT	94.09	IGHV1-8	M	48	
6	UNMUT	100	IGHV1-69	F	59	
7	UNMUT	98.61	IGHV3-30	M	45	
8	UNMUT	100	IGHV1-2	M	62	

B

MCL case	IGHV status	IGHV % identity to germline	SOX11	Gender	Age at diagnosis	Color in figures
nnMCL1	MUT	95.14	Negative	M	75	
nnMCL2	MUT	97.22	Negative	M	80	
cMCL1	UNMUT	97.92	Positive	M	76	
cMCL2	UNMUT	99.65	Positive	M	43	

M = Male, F = Female
MUT = Mutated, UNMUT = Unmutated

Appendix Table 1. Patients' characteristics of samples used in the Study 1. A) CLL samples and B) MCL samples. All these samples were obtained from PB.

The rest of the supplementary data is available online in the published paper (274).

Case	Diagnosis	Age	Gender	IGHV status	% CD20+ CD5+	LEF1 ΔMFI	FISH
MBL1	High count MBL	56	M	MUT	41.1	2040.2	Del13q 27%
MBL2	High count MBL	38	F	MUT	66.6	1176.4	No alterations
MBL3	High count MBL	66	M	MUT	61.2	292.6	Tri12 25%
MBL4	High count MBL	69	F	MUT	75.5	2263.9	No alterations
MBL5	High count MBL	66	F	MUT	77.5	2141.2	Del13q 62%
MBL6	High count MBL	65	F	MUT	53.1	1053.2	No alterations
MBL7	High count MBL	78	F	MUT	30.1	2476.5	Del13q 94%
MBL8	High count MBL	54	M	MUT	57.6	2723.1	Del13q 30%
MBL9	High count MBL	76	F	MUT	49.5	3139.9	Del13q 85%
MBL10	High count MBL	72	M	MUT	40.4	655.4	Del13q 60%. Tri12 75%
MBL11	High count MBL	69	M	MUT	56	2192.5	Tri12 40%
MBL12	High count MBL	77	M	UNMUT	69.9	1409.9	Tri12 30%
MBL13	High count MBL	61	M	MUT	56.4	1791.6	Del13q 38%

M = Male, F = Female
MUT = Mutated, UNMUT = Unmutated
LEF1 ΔMFI = LEF1 protein levels measured by intracellular flow cytometry

Appendix Table 2. Patients' characteristics of MBL samples used in the Study 2. All samples are obtained from PB.

Case	Gender	Age at diagnosis	Binet stage	IGHV status	Epi group	% IGHV identity	LEF1 ΔMFI	TTFT (years)
M-CLL1	M	56	A	MUT	m-CLL	86.94	2240.6	9.5825
M-CLL2	F	62	A	MUT	m-CLL	94.79	2600.6	9.9329
M-CLL3	F	65	A	MUT	m-CLL	97.19	2566.9	8.7583
M-CLL4	M	71	A	MUT	m-CLL	92.28	2145.8	2.9021
M-CLL5	M	58	A	MUT	m-CLL	93.88	1337.4	9.5825
M-CLL6	F	43	A	MUT	m-CLL	90.62	1972.8	3.5181
M-CLL7	M	56	A	MUT	m-CLL	84.91	2039.6	3.8275
M-CLL8	F	49	A	MUT	m-CLL	92.98	3548.9	8.8925
M-CLL9	M	60	A	MUT	m-CLL	91.76	NA	8.6461
M-CLL10	M	45	C	MUT	i-CLL	97.19	3170.9	0.0411
M-CLL11	M	53	A	MUT	i-CLL	94.44	2793.9	1.9822
M-CLL12	M	37	A	MUT	i-CLL	96.53	2026.9	3.7070
M-CLL13	M	71	A	MUT	i-CLL	97.54	2188.9	1.7112
M-CLL14	F	73	A	MUT	i-CLL	95.62	3148.8	5.8426
M-CLL15	M	60	A	MUT	i-CLL	93.75	1415.8	1.7522
M-CLL16	M	48	B	MUT	i-CLL	94.1	2161.6	0.0411
M-CLL17	F	66	**B**	MUT	m-CLL	94.04	2782.9	0
M-CLL18	F	66	A	MUT	Unclassified	93.54	2374.9	0
M-CLL19	M	74	A	MUT	Unclassified	96.88	1408.2	0
M-CLL20	M	53	A	MUT	m-CLL	87.85	1845.6	0.0192
	Tri12	**Del13q**	**Del11q**	**Del17p**	**SF3B1 mutation**	**TP53 mutation**	**IGLV321 R110**	**Treament**
M-CLL1	WT	WT	WT	WT	WT	WT	No	No
M-CLL2	WT	Deletion	WT	Deletion	WT	WT	No	No
M-CLL3	WT	Deletion	WT	WT	WT	WT	No	No
M-CLL4	WT	Deletion	WT	WT	WT	WT	No	No
M-CLL5	WT	WT	WT	WT	WT	WT	No	No
M-CLL6	WT	Deletion	WT	WT	WT	WT	No	No
M-CLL7	WT	Deletion	WT	WT	WT	WT	No	Yes
M-CLL8	WT	Deletion	WT	WT	WT	WT	No	No
M-CLL9	WT	Deletion	WT	WT	WT	WT	No	Yes
M-CLL10	WT	Deletion	WT	WT	WT	WT	No	Yes
M-CLL11	WT	Deletion	WT	WT	WT	WT	No	No
M-CLL12	WT	Deletion	NA	NA	WT	WT	No	Yes
M-CLL13	WT	Deletion	WT	WT	Missense	WT	Yes	Yes
M-CLL14	WT	Deletion	WT	WT	WT	WT	Yes	Yes
M-CLL15	WT	Deletion	WT	WT	WT	WT	Yes	No
M-CLL16	WT	WT	WT	WT	WT	WT	No	Yes
M-CLL17	WT	Deletion	WT	WT	WT	WT	No	Yes
M-CLL18	WT	WT	WT	WT	WT	WT	No	Yes
M-CLL19	WT	WT	WT	WT	WT	WT	No	Yes
M-CLL20	WT	WT	WT	WT	WT	WT	No	Yes

M = Male, F = Female
MUT = Mutated, UNMUT = Unmutated
LEF1 ΔMFI = LEF1 protein levels measured by intracellular flow cytometry

Appendix Table 3. Patients' characteristics of M-CLL PB samples used in the Study 2.

Case	Gender	Age at diagnosis	Binet stage	IGHV status	Epi group	% IGHV identity	LEF1 ΔMFI	TTFT (years)
U-CLL1	F	59	A	UNMUT	n-CLL	100	3319.2	0.016
U-CLL2	M	62	A	UNMUT	n-CLL	100	3691.2	0.2081
U-CLL3	M	58	A	UNMUT	n-CLL	100	2481.2	0.0192
U-CLL4	M	56	A	UNMUT	n-CLL	100	3573.2	0.1013
U-CLL5	M	63	A	UNMUT	n-CLL	100	4075.5	0.3285
U-CLL6	M	61	A	UNMUT	n-CLL	100	3971.6	2.7351
U-CLL7	M	68	A	UNMUT	n-CLL	100	3059.1	0.5038
U-CLL8	M	70	A	UNMUT	n-CLL	100	2552.8	2.6420
U-CLL9	M	56	A	UNMUT	n-CLL	100	3116.8	1.1663
U-CLL10	M	54	A	UNMUT	n-CLL	98.98	3888.4	1.0404
U-CLL11	M	67	A	UNMUT	n-CLL	100	2270	0.1123
U-CLL12	M	46	A	UNMUT	i-CLL	98.61	4283.9	0.3066
U-CLL13	M	49	A	UNMUT	i-CLL	98.26	3083	0.4162
U-CLL14	M	70	B	UNMUT	i-CLL	99.55	3856.6	0
U-CLL15	M	46	B	UNMUT	i-CLL	98.61	2174.5	9.925
U-CLL16	F	52	A	UNMUT	i-CLL	99.31	2620.8	7.5948
U-CLL17	M	70	A	UNMUT	n-CLL	100	3885.8	7.6222
U-CLL18	F	71	A	UNMUT	n-CLL	100	4687.1	6.8255
U-CLL19	M	54	A	UNMUT	m-CLL	98.26	3712.4	7.4031

	Tri12	Del13q	Del11q	Del17p	SF3B1 mutation	TP53 mutation	IGLV321 R110	Treament
U-CLL1	WT	Deletion	WT	WT	WT	WT	No	Yes
U-CLL2	WT	WT	WT	WT	WT	WT	No	Yes
U-CLL3	WT	Deletion	WT	WT	WT	WT	No	Yes
U-CLL4	WT	WT	WT	WT	WT	WT	No	Yes
U-CLL5	WT	Deletion	WT	WT	Missense	WT	No	Yes
U-CLL6	WT	WT	WT	WT	WT	Missense	No	Yes
U-CLL7	WT	Deletion	WT	WT	WT	WT	No	Yes
U-CLL8	WT	Deletion	WT	WT	WT	WT	No	Yes
U-CLL9	WT	Deletion	WT	WT	Missense	WT	No	Yes
U-CLL10	WT	WT	WT	WT	WT	WT	No	Yes
U-CLL11	WT	WT	WT	WT	WT	WT	No	Yes
U-CLL12	WT	WT	WT	WT	WT	WT	No	Yes
U-CLL13	WT	WT	WT	WT	Missense	WT	Yes	Yes
U-CLL14	WT	Deletion	WT	WT	Splice_Site	WT	Yes	Yes
U-CLL15	WT	Deletion	WT	WT	WT	WT	Yes	Yes
U-CLL16	WT	Deletion	WT	WT	WT	WT	No	No
U-CLL17	WT	WT	WT	WT	WT	WT	No	Yes
U-CLL18	WT	Deletion	WT	WT	WT	WT	No	Yes
U-CLL19	WT	WT	WT	WT	WT	WT	No	Yes

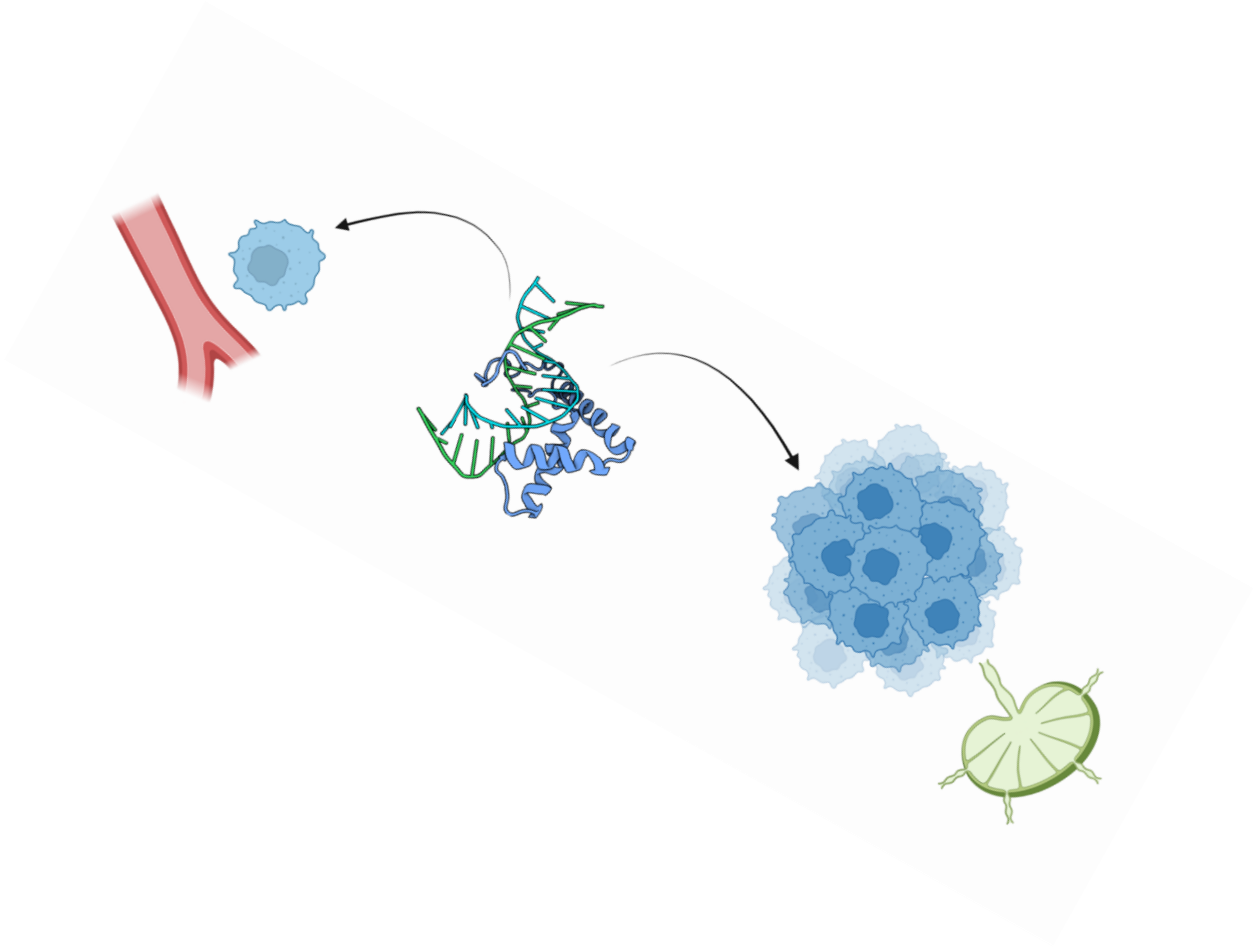
M = Male, F = Female
MUT = Mutated, UNMUT = Unmutated
LEF1 ΔMFI = LEF1 protein levels measured by intracellular flow cytometry

Appendix Table 4. Patients' characteristics of PB U-CLL samples used in the Study 2.

The rest of supplementary data derived from the Study 2, such as LEF1 CUT&RUN peak location, the complete list of LEF1 target genes or DE genes in the different experiments (e.g., *LEF1* KD vs WT cells) will be available online with the published article, but not in this doctoral thesis because of the large size of the tables.

.

Acknowledgments



Querido lector/a,

Has llegado a mi parte favorita de toda tesis: los agradecimientos. En mi caso, el doctorado ha sido una travesía con muchos momentos buenos y otros más sufridos y sombríos, algunos donde incluso sentía como el barco se hundía y me iba a marcar un Titanic. Sin embargo, después de casi 5 años, me encuentro punto de llegar a puerto. Esto no sería posible sin todas aquellas personas que, dentro y fuera del laboratorio, me han ayudado y acompañado. He escuchado, desde bien pequeña, lo importante que es saber compartir y trabajar en equipo. Saber sumar. Esta tesis es el reflejo más bonito de la enseñanza más básica que me dieron mis padres.

Gracias a mi director, Iñaki, por abrirme las puertas del grupo Epi, por confiar en mi para llevar a cabo tremendo proyecto. Gracias por anteponer siempre el bienestar de la persona a la productividad, por el ambiente tan bonito que tenemos en el grupo. Gracias por entender mi "internal thrive" y dejarme ser. Porque no hay nada más bonito que el hecho de que nadie te corte las alas. Gracias por tus charlas motivadoras y banales porque, aunque seas el jefe, siempre nos demuestras que eres como uno más del grupo. Espero que, después de todo este tiempo, se me haya pegado algo de tu magia y genialidad en la ciencia.

Gracias a mi directora, Alba, por ser mi maestra y faro en este viaje. Gracias por haber estado ahí en cada uno de los momentos de esta tesis. Por haberme escuchado, animado y reído conmigo. Porque, incluso en las noches de tormenta más oscuras, tu luz estaba ahí para guiarme y hacerme sentir que todo iría bien. He aprendido tantísimo de ti. No sabes cuánto valoro todo lo que me has enseñado y apoyado. Estoy segura que ésta es la primera de las muchas tesis que dirigirás.

Gracias a mi querida amiga Bea, por ser y estar. Me emociona y enorgullece tanto haber empezado y acabado este viaje contigo. Gracias por ser como una hermana para mí, por entenderme y escucharme en todo momento. Gracias por todo lo vivido. Porque he sabido que siempre, sin excepción, podía contar contigo para

charlar, tomarme un Chai latte o cualquier plan que tuviera en mente (como formatear esta tesis, por ejemplo). Para la posteridad, nos quedarán nuestros viajes a Nueva Orleans y Madrid con nuestras presentaciones orales y nuestras conversaciones infinitas. Sé que estaré en muchos más momentos de tu vida porque este vínculo no se va a romper, aunque estemos a 6000 km de distancia. Te quiero mucho, amiga.

Gracias Raúl, por ser tan buen amigo y compañero de trabajo. Porque nada más llegar, sin conocerme de nada, decidiste ayudarme en mi proyecto atascado y obraste tu magia. Desde entonces, el barco reflotó y pude volver a navegar sin mucha más complicación. Gracias por tu sentido del humor y por ser igual (o más cotilla que yo). Gracias porque, en este mundo, no es tan fácil encontrar una persona como tú, tan honesta y auténtica en la que poder confiar. Tengo la certeza de que la vida te depara grandes cosas porque, además de ser un genio, eres una buenísima persona.

Gracias Víctor por tu luz y alegría. Porque, desde que empezaste, el ambiente del grupo fue mejor todavía. Por elegir venir al trabajo y hacernos compañía cuando podrías haber teletrabajado mucho más. Por nuestras horas de charlas (científicas y no científicas) en el despacho con Raúl. No pierdas esa ilusión, esa curiosidad científica y esas ganas de comunicar que tienes. Ya verás como tu PhD será todo un éxito.

Gracias al resto de mis compañeros del grupo Epi. Anna, gràcies per la teva ajuda clau en el projecte i el teu somriure de cada dia. Marta K, gracias por ser el alma del Epi lab, por escucharme y darme ánimos siempre. Stella y Vicente, muchísimas gracias por vuestra paciencia, ayuda y consejo en todos los análisis bioinformáticos. Por intentar que saliera una bioinformática de provecho de esta científica de poyata sin remedio. Gracias Lucía y Martí, por vuestros consejos, charlas y buenas

palabras. Ha sido un placer pertenecer al grupo Biomedical Epigenomics estos 5 años. Me llevo buenísimos momentos con cada uno de vosotros.

Gracias al resto de mis amigos y compañeros del grupo Campo por todo lo compartido durante este tiempo. Especialment, vull mencionar al Dr Ferran Nadeu. Gràcies, amic, per acollir-me des d'un principi i haver estat sempre disponible per ajudes científiques, converses o Chai lattes amb xocolata (negra, sense discussió). Per la teva simpatia i modèstia. Per ser tan bona persona i amic. Perquè sempre he sabut que podia comptar amb tu. A la tornada de NY, em trobaré amb un gran PI.

Gràcies al grup de la Dolors i Patri per sempre donar-me la benvinguda a qualsevol dels seus plans. Gràcies, Heribert i Cèlia, per ser tan bons amics i per tot el que hem compartit dins i fora del lab durant tot aquest temps. Per cuidar i estimar tant al Ferran (i al seu +1 jeje). Espero seguir formant part de les vostres vides moltíssims anys més.

Gracias a mis amigos y familia porque son la clave para que yo haya llegado hasta aquí. Gracias a Lavinia e Irene porque, desde que nuestros caminos se juntaron en la carrera de biomedicina (hace ya 10 añitos), nunca más nos separamos. Gracias, amigas, por todo lo que hemos vivido y por todas las aventuras que nos quedan por vivir juntas.

Gracias a Nina y Tobby, los dos seres más puros y buenos que ha conocido este planeta, por vuestra compañía y amor incondicional.

Gracias a mi hermana, Laura, por ser mi mejor amiga y mi mayor animadora desde que tengo uso de razón. Por quererme y cuidarme siempre. Por ser la alegría de nuestra casa y hacerme reír tanto. Por ser mi mejor compañera de conciertos y helados. Porque siempre nos hemos tenido la una a la otra en todo momento. Recuerda que, aunque todo sea difícil, en los charcos saltaremos tú y yo. Sé que podré contar contigo siempre a pesar de que nos separen miles de kilómetros.

Aunque somos más de demostrarlo con hechos, quiero dejar por escrito lo mucho que te admiro, adoro y quiero, hermanita. Nunca olvides que eres una de las personas más fuertes que conozco. Siempre estaré ahí como tú lo has estado conmigo.

Gracias a mis padres, Elvira y José María, por darme el amor, cariño y los recursos para que yo llegara hasta aquí hoy. Porque habéis trabajado durísimo y os habéis sacrificado como nadie para que Laura y yo pudiéramos estudiar, seguir nuestros sueños y labrarnos un buen futuro. De vosotros aprendí lo importante que es la constancia, la perseverancia y el trabajo, pero, ante todo, la humildad y el ser buena persona. Vuestro amor y apoyo me ha ayudado a superar muchos obstáculos y a enfrentarme a mis miedos. Sin vosotros yo no sería nada. Os debo mi vida entera. Gracias porque no importa donde viva, si en Barcelona o Nueva York, mi casa, mi hogar, siempre seréis vosotros. Os quiero infinito. No sabéis lo afortunada que me siento de que la vida me diera estos padres.

Finalment, gràcies a l'amor de la meva vida, Ferran. M'has ajudat moltíssim en tot moment. Des del primer dia, vas perdre part del teu preciat i limitat temps en ensenyar-me a utilizar el citòmetre i a fer marcatges, sense perdre la paciència en cap segon. A part del suport experimental i els congressos que hem compartit junts, està el suport moral i amor que m'has donat durant aquest temps. Gràcies per la comprensió, per alliberar-me de qualsevol responsabilitat perquè em pugués dedicar al 100% a escriure la tesi i l'article. Per assecar-me les llàgrimes quan res no sortia i donar-me els ànims per no abandonar el vaixell. Per alegrar-te com ningú dels meus èxits i celebrar-los com si fossin teus. M'omple el cor haver pogut compartir tota aquesta experiència doctoral amb tu. Estic impacient per començar la nostra següent etapa com a companys de laboratori i de vida. Jo sóc feliç només d'imaginar tota una vida al teu costat, en poder passar cada estiu amb tu al mar o anar cada maig a la Cucanya. No hi ha suficients paraules per explicar tot el que has estat i suposes per mi. T'estimo mil.